**ROTTERDAM,**
THE NETHERLANDS

# THERMAL INTELLIGENCE

The Thermal Impacts of Urban Densification : A Using Deep Learning for climate assessments of urban development scenarios in Rotterdam

THERMAL COMFORT | NATURAL VENTILATION | SOLAR RADIATION | URBAN FORM



**Yilin Yang**
**6013686**

MSc Urbanism
Delft University of Technology

Date: November 2025 - June 2026

Delft University of Technology
Msc Architecture, Urbanism and Building Sciences, Urbanism track
Department of Urbanism

Title: Thermal Intelligence
Sub-title: The Thermal Impacts of Urban Densification : A Using Deep Learning for climate assessments of urban development scenarios in Rotterdam

Author:Yilin Yang | 6013686
Graduation Studio: City of the Future

First mentor: Daniela Maiullari
Assistant Professor Environmental Technology & Design
Faculty of Architecture and the Built Environment
Department of Urbanism

Second mentor: Aksel Ersoy
Assistant Professor/Section Coordinator in Urban Development Management
Faculty of Architecture and the Built Environment
Department of Urban Development Management

## Motivation

Growing up in Beijing, a city well known for its severe urban heat island effect, I have directly experienced how frequent summer heatwaves can reduce thermal comfort and limit the use of public spaces in everyday life. Extended periods of extreme heat not only affect physical comfort but also influence how people move, gather, and interact in the city. These experiences gradually shaped my interest in urban thermal environments and raised questions about how urban form and spatial configuration contribute to heat accumulation.

After moving to the Netherlands for my studies, I observed that although urban heat stress is generally less intense than in Beijing, Dutch cities are not immune to the problem. Ongoing densification and development pressures, particularly in city centres, indicate that urban heat issues may become more pronounced in the future. This contrast highlighted for me that urban heat is not limited to megacities, but is a broader spatial challenge that requires proactive planning responses.

In addition, I am strongly motivated by the rapid development of artificial intelligence and its growing influence on both everyday life and academic research. Urban systems are increasingly complex, involving large amounts of spatial, environmental, and socio-economic data that are difficult to fully capture through conventional analytical approaches. AI offers new possibilities for processing such complex datasets, identifying hidden spatial patterns, and supporting more systematic and efficient urban analysis.

Rather than viewing AI as a replacement for human judgment, I am interested in exploring how AI can function as a supportive research tool for urban researchers. By integrating AI into urban studies, it becomes possible to enhance the understanding of relationships between spatial form and environmental performance, reduce analytical uncertainty, and provide evidence-based insights that can inform planning and design processes. This motivation drives my interest in investigating how AI can be meaningfully applied within urban research to complement existing methods and expand the analytical capacity of urban planning practice.

Through this project, I aim to develop a basic understanding of machine learning and explore how it can be used as a tool in urban research. At the same time, the objective of this project focuses on investigating how heat-sensitive design strategies can be applied and integrated into the process of urban densification which will happen in several cities globally, in order to better respond to increasing thermal challenges in cities.

## Acknowledgments

I would like to sincerely thank my supervisors, Daniela Maiullari and Aksel Ersoy, for their continuous support and guidance throughout this project. Daniela introduced me to this research opportunity, which allowed me to further develop my interest in deep learning within the field of urban climate research. She also provided valuable academic opportunities, including support in academic writing and communication with the Municipality of Rotterdam. Throughout the project, both supervisors offered many constructive suggestions on academic writing, presentation, and research development, which significantly improved my academic expression and expanded my knowledge of thermal environment studies.

Besides, I would like to express my gratitude to the Municipality of Rotterdam for their support and for providing important data and materials that were essential to this research.

Finally, I would like to express my sincere gratitude to my parents for their continuous support, which allowed me to continue exploring my interests at TU Delft. I would also like to thank Yifei for helping me sharpen the project, patiently listening to my ideas and providing valuable suggestions throughout the process. I am equally grateful to my friends for their encouragement and various helpful advice.

## Abstract

Faced with a growing population, the Dutch government is promoting development plans to increase built density and accommodate the demand of new homes within existing urban areas. However, high-density developments are widely considered to exacerbate heat risks, causing health risks for vulnerable populations. Despite the known heat-related impacts on urban livability, effective methods are currently lacking at the municipal level for adopting heat-sensitive densification strategies while the high computational cost of existing simulation tools makes rapid assessment of multiple planning scenarios difficult. To address these challenges, the study addresses a densification case in Rotterdam and develops an AI-based methodology to quantify the thermal impact of increasing density within an existing urban area. The U-Net approach is used to estimate Tmrt and PET at a resolution of 1 m based on SOLWEIG-calculated data. This model reaches very high levels of precision ($R2 \approx 0.95$). It also allows rapid assessment of different scenarios while maintaining high resolution.

Nine densification scenarios with different floor space index and morphological configurations were tested through the U-Net model, showing that it can generate high speed prediction with high accuracy. The modelling results show that the morphological characteristics of the new buildings and street canyons, and the distribution of building masses lead to different levels of diurnal and nocturnal increase of temperature and thermal stress. On wider streets, densification through horizontal development contributes to higher Tmrt and PET compared to vertical development, as high-rise buildings cast more shade especially during the day. Besides, vertical development also exhibits less heat retention and foster better ventilation than horizontal development. In narrow streets, horizontal development has better shading and ventilation performance compared to vertical development. Although horizontal development slightly increases heat retention, the effect is minimal and can be reduced by the guiding airflow movements.

**Keywords:** CNN; U-Net; SOLWEIG; Mean radiant temperature (MRT); Physiological equivalent temperature (PET); Densification; Urban morphology

# CONTENT


GLOSSARY OF TERMS

**1. INTRODUCTION**
- 1.1 Global Warming Trend
- 1.2 Climate change in Europe
- 1.3 Warming Trend in Netherlands

**2. SITE CONDITION**
- 2.1 Rotterdam Exposure to Heat
- 2.2 Rotterdam Trend of Growth
- 2.3 Densification of Rotterdam

**3. RESEARCH UNDERPINNING**
- 3.1 Knowledge Gap
- · PROBLEM STATEMENT
- 3.2 Opportunity
- · RESEARCH QUESTIONS
- · METHODOLOGY FRAMEWORK

**4. FACTORS INFLUENCING OUTDOOR THERMAL ENVIRONMENT**
- 4.1 Introduction
- 4.2 Radiation and Temperature
- 4.3 Landcover
- 4.4 Urban Morphology
- 4.5 Blue-green Infrastructure
- 4.6 Materials and Albedo
- 4.7 Anthropogenic Activities
- 4.8 Summary

**5. METHODOLOGY**
- 5.1 Introduction
- 5.2 Introduction of UMEP
- 5.3 Selection of Thermal Assessment Indicators
- 5.4 Selection of Machine Learning Model
- 5.5 Methodology
- 5.6 Spatial Data Modelling
- 5.7 U-Net Model Structure
- 5.8 General Workflow

**6. MODEL EVALUATION AND REFLECTION**
- 6.1 MRT Model Performance Evaluation
- 6.2 PET Model Performance Evaluation
- 6.3 U-Net Model Reflection

**7. HEAT-SENSITIVE DESIGN EXPLORATION**
- 7.1 Design Site
- 7.2 Thermal Environment Comparison Before and After Densification
- 7.3 Spatial Scenarios Exploration
- 7.4 Building Morphology Exploration

**8. GUIDELINES**
- 8.1 Introduction
- 8.2 Urban Development Guidelines
- 8.3 Buildings Layout Guidelines
- 8.4 Additional Thermal Mitigation Guidelines

**9. CONCLUSION**
- 9.1 Answer of Research Question
- 9.2 Academic Relevance
- 9.3 Urbanism Relevance
- 9.4 U-Net Model
- 9.5 Thermal Environment Research
- 9.6 Transferability

**10. REFLECTION**
- 10.1 Personal Growth and Experience
- 10.2 Relationship Between Research and Design
- 10.3 Relation Between Urbanism
- 10.4 Value and Future Application of the Project

**11. REFERENCE**

**12. APPENDIX**

## Glossary of Terms

**Albedo:** The proportion of solar radiation reflected by a surface. Higher albedo means more reflection and less heat absorption.

**Anthropogenic Heat Release (AHR):** Heat released by human activities, such as traffic, air conditioning, and buildings.

**Blue-Green Infrastructure:** Blue-Green Infrastructure incorporates the integration of healthy soil, water and vegetation systems.

**Building Density:** The intensity of built structures in a given area, often related to floor space or building coverage.

**Convolutional Neural Network (CNN):** A type of deep learning model designed to process spatial data, such as images or raster data. It is widely used for pattern recognition and prediction tasks.

**Deep Learning (DL):** In machine learning, deep learning (DL) focuses on utilizing multilayered neural networks to perform tasks such as classification, regression, and representation learning.

**Evapotranspiration:** A cooling process where water evaporates from surfaces and plants, reducing air temperature.

**Floor Space Index (FSI):** A ratio of a building's total floor area (gross floor area) to the size of the piece of land upon which it is built. It is often used as one of the regulations in city planning along with the building-to-land ratio.

**Heatwave:** A period of abnormally hot weather. In the Netherlands, a heat wave is defined as a period of 5 consecutive days when the maximum air temperature is above 25 °C and during this period at least 3 days are above 30 °C.

**Landcover:** A physical material at the land surface of Earth. Land covers include flora, concrete, built structures, bare ground, and temporary water.

**Land Surface Temperature (LST):** An important variable within the Earth climate system. It describes processes such as the exchange of energy and water between the land surface and atmosphere, and influences the rate and timing of plant growth.

**Longwave Radiation:** Thermal radiation emitted by surfaces, especially at night after heat is stored during the day.

**Machine Learning (ML):** A field of study in artificial intelligence concerned with the development and study of statistical algorithms that can learn from data and generalize to unseen data, and thus perform tasks without being explicitly programmed.

**Mean Radiant Temperature (MRT):** The concept of mean radiant temperature (MRT) is used to quantify the exchange of radiant heat between human and their surrounding environment, with a view to understanding the influence of surface temperatures on personal comfort. Mean radiant temperature has been both qualitatively defined and quantitatively evaluated for both indoor and outdoor.

**Pedestrian Level:** The height at which people experience the environment, usually around 1.5–2 meters above ground.

**Physiological Equivalent Temperature (PET):** A biometeorological index defining thermal comfort as the air temperature (°C) in a standard, indoor setting where the human body's heat balance is maintained, resulting in the same core and skin temperatures as under complex, actual outdoor conditions.

**Shortwave Radiation:** Shortwave radiation is a radiant energy produced by the sun with wavelengths ranging from infrared through visible to ultraviolet. It is the main source of heat during the daytime.

**Sky View Factor (SVF):** An important variable to calculate local temperatures. It is the fraction of sky visible from the ground. The SVF depends on the height and density of the obstacles in the surroundings of a given location.

**SOLWEIG (Solar and LongWave Environmental Irradiance Geometry):** A model that simulates spatial variations of 3D radiation fluxes and the Tmrt in complex urban settings. It is also able to model spatial variations of shadow patterns.

**Street Canyon:** A place where the street is flanked by buildings on both sides creating a canyon-like environment.

**UMEP:** A climate service tool, designed for researchers and service providers, presented as a plugin for QGIS.

**U-Net:** A convolutional neural network that was developed for image segmentation. The network is based on a fully convolutional neural network whose architecture was modified and extended to work with fewer training images and to yield more precise segmentation.

**Wind Flow:** The movement and pattern of air in the urban environment, influenced by buildings and layout.

# 1. INTRODUCTION

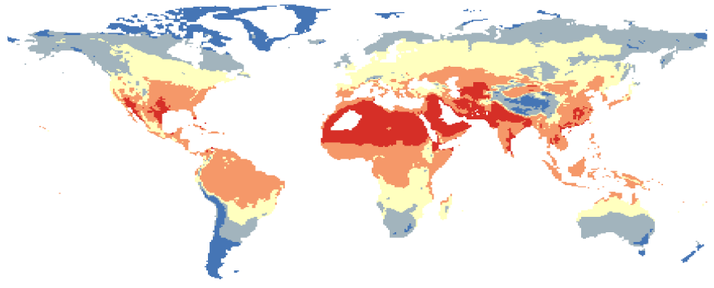
1.1 Global Warming Trend

1.2 Climate change in Europe

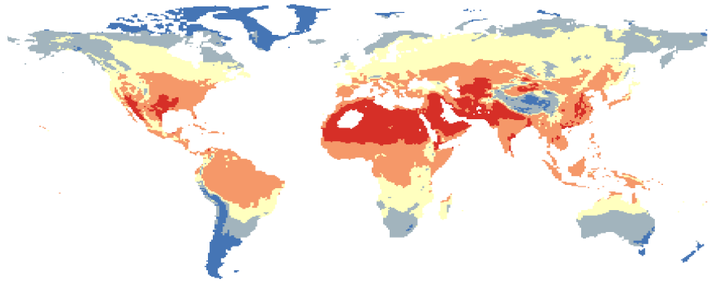
1.3 Warming Trend in Netherlands

## 1.1 Global Warming Trend

The continuous growth of global warming has become one of the most severe challenges for human in 21 century. According to the report by authoritative institutions, the maximum temperatures have broken the records persistently in the recent years among which 2024 was comfirmed as the warmest year on record. 2024 also became the first year with an average temperature clearly supassing 1.5°C above the preindustrial level (ECMWF, 2024). The frequency of extreme temperature events such as heat wave and droughts triggered by this sustain warming trend is also being increased, posing a rising threat to global ecosystems and human civilization.



Extreme average air temperature from 1981-2000



Extreme average air temperature from 2000-2025

**Figure 1.1:** World Temperature Growth 1981-2025 (Source: Arcgis Online)

Urban areas, on account of the high density of population, concentrated energy consumption and a large amount of low reflectivity and high heat storage surface materials, become an amplifier of climate change (Ramachandra et al., 2024). This effect leads to the internal urban temperatures exceeding the temperature of surrounding rural area, which is known as Urban Heat Island (UHI). When the heat island effect and global warming work together, making a multiplying effect on the extreme heat risks which directly impacts on public health, water resource management, and the stability of energy systems (Hasheim et al., 2025). For urban planners, UHI has been a significant challenge for climate change adaption and mitigation.

## 1.2 Climate change in Europe

Regional studies have indicated that Europe is one of the fastest warming areas in the world and its temperature is rising at approximately twice the global average rate. This trend is mainly because of several factors including changing weather patterns, reducing of air pollution and geography reason.

**Changing weather patterns:** Changes in atmospheric circulation lead to more frequent and intense heatwaves in Europe. The latest European State of the Climate report highlighted that the number of heat stress days is increasing in Europe, with 2024 seeing the second-highest number on record. The start of summer 2025 has already seen heatwaves across much of Europe.

**Reduced air pollution:** In the past, aerosol emissions in Europe had the capability to reduce the amount of solar radiation reaching the surface. However, since the 1980s, stricter air quality regulations have reduced the emission of aerosol across Europe. As a result, there is more solar radiation reaching to surfaces, and cloud cover is also reduced, both contributing to faster regional warming.

**Geography:** Parts of Europe extend into the Arctic –the fastest-warming region on Earth. (Copernicus, 2025). For European cities, this means the threshold of extreme heat risks will be lower rapidly, with a earlier time of appearance, longer time of duration and wider range of influence.

European cities are well-known by the historic and high-density urban context, intensifing the UHI effect. Dense streets and buildings cause the low Sky View Factor (SVF), which results in increased net heat retention within buildings and an increase of UHI (Dirkse et al., 2019). Second, the massive construction materials such as concrete, asphalt and bricks absorb and store large amounts of heat from both solar energy and human activities, forming gigantic thermal mass. Besides, the dense building layout and high buildings will create "urban canyon" effect, and this effectively hinders the airflow and ventilation within urban canopy layer, leading to the concentration of heat in the

city centers where the buildings and population are highly concentrated (Muniz-Gaal et al., 2020). As a result, having a better understanding of the relationship between quantifying urban configuration parameters (density, height and materials) and temperature is the precondition for developing an effective thermal adaptation plan.

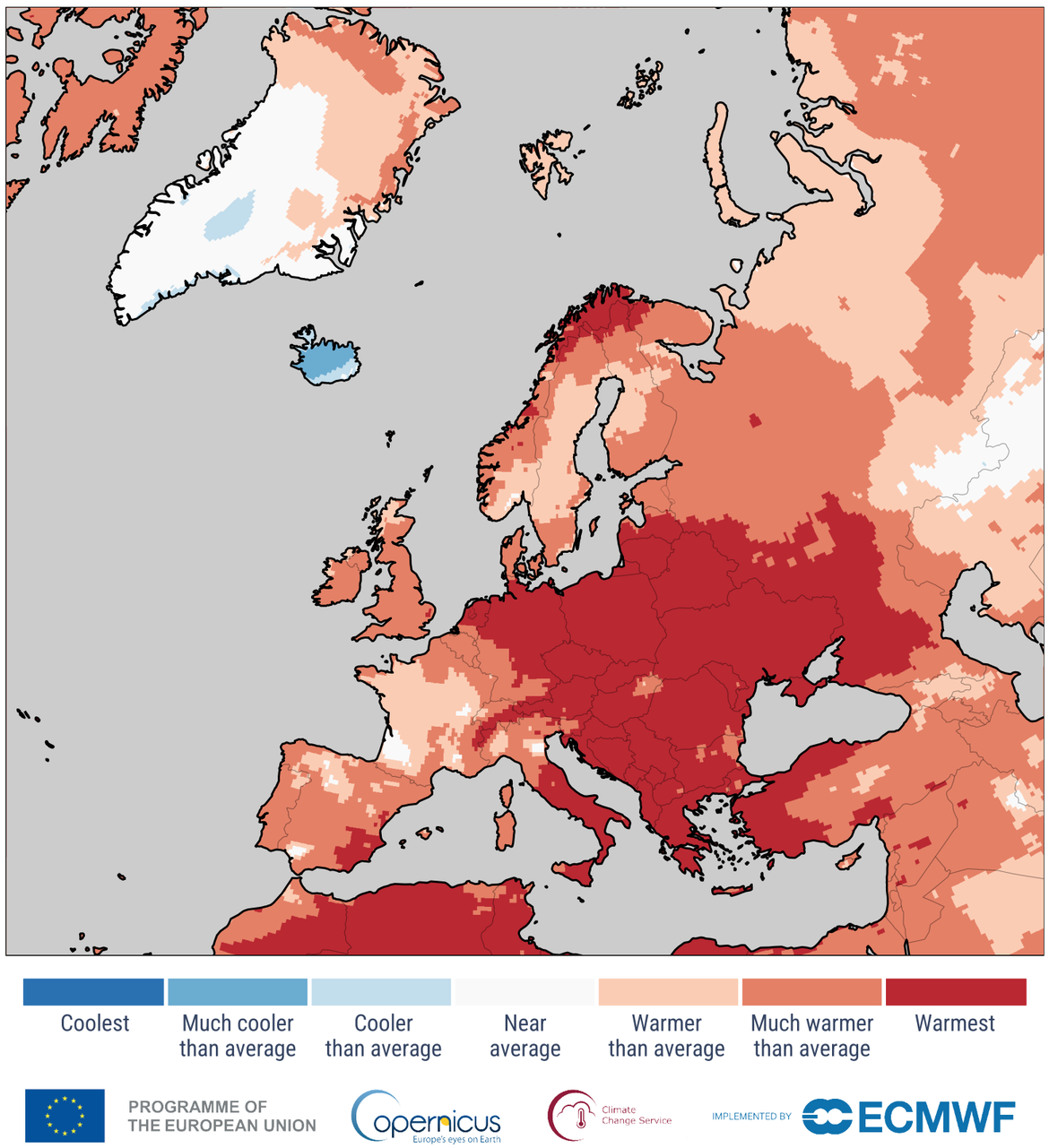



**Figure 1.2:** Anomalies and extremes in surface air temperature (Source: WMO)

## 1.3 Warming Trend in Netherlands

Situated in the western Europe, the Netherlands has a temperate maritime climate zone, having a mild climate in general. However, according to a new report from the Dutch Meteorological Institute (KNMI), the Netherlands is warming by 0.4 per cent every 10 years, which is significantly faster than the global average level. Since 1901, 32 times recorded heat waves have occurred mainly in the last 25 years. When it comes to the intensity, the annual warmest day is now on average 4 degrees warmer than in the year 1900. It is also important to mention that every official measurements refer mainly to suburb monitoring locations, meaning that the extreme temperature will be higher in the city. Figure 1.3 shows the Land Surface Temperature (LST) during heat wave on 15 August 2025. It can be noticed that the highest temperature is up to 49°C and the heat mainly occurs in the cities like Amsterdam, Rotterdam, Utrecht, etc.

The interaction between extreme heat and urban heat island pose severe conquences to Netherlands, primarily manifesting in the following four key areas:

**Health Risk for the Elderly and Vulnerable Groups:** The Netherlands National Institute for Public Health and the Environment (RIVM) estimates that by 2050, the number of annual deaths from heatstroke in Amsterdam will increase from 110 to approximately 250, depending on the climate

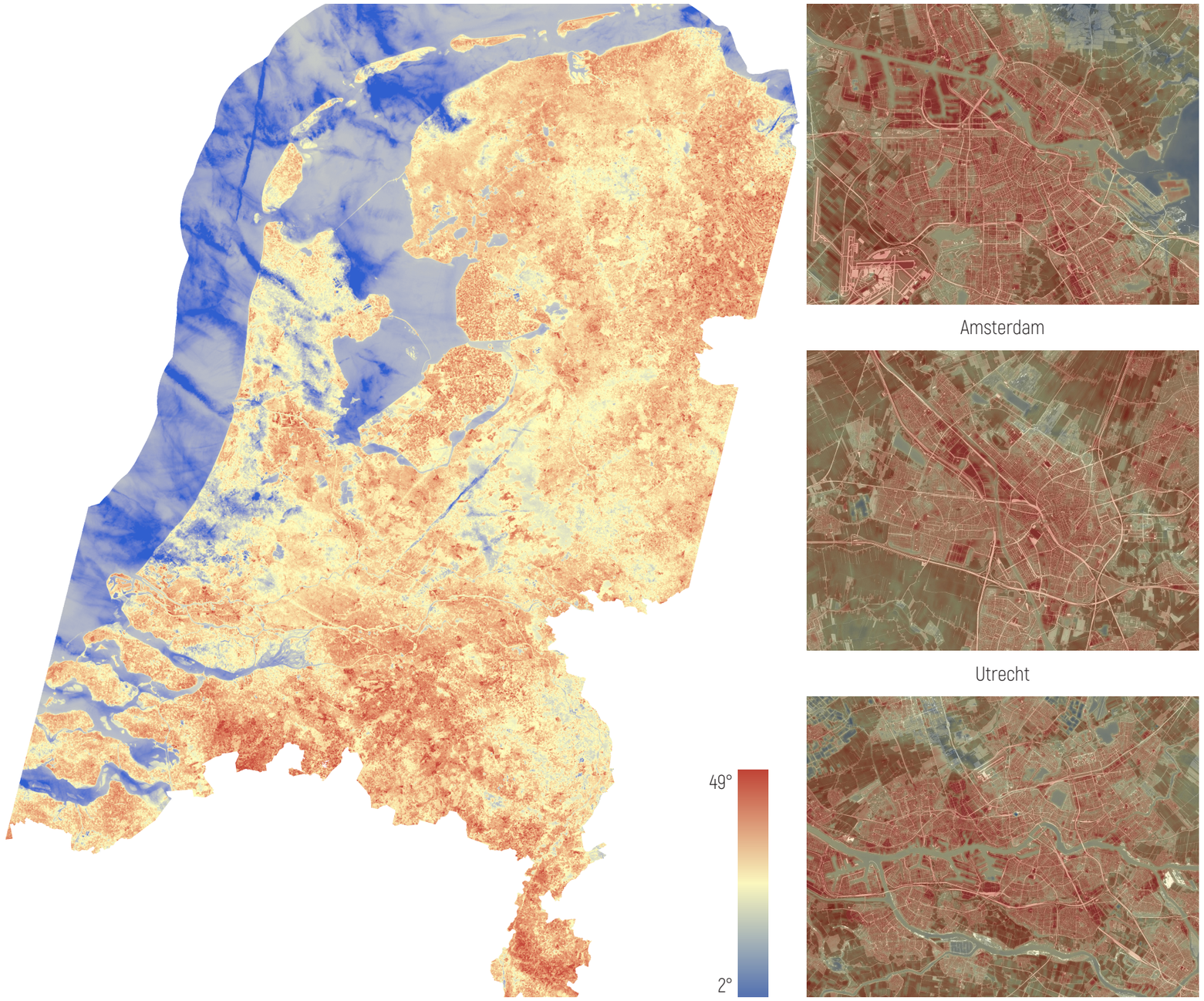



**Figure 1.3:** Land Surface Temperature NL, August 15, 2025 (Source: By Author)

scenario. Under low-temperature conditions, there is no significant difference in risk between different population groups. In addition to increasing the risk of death, high temperatures can also lead to increased disease incidence or decreased labor productivity. Studying the health effects of high temperatures is crucial in assessing the health impacts of climate change. (RIVM, 2025).

**Health Risk for the Outdoor Workers and Labour:**
Certain researches has found that the employers and employees notice the bad effects while working outside in high temperature, exposuring themselves to ultraviolet (UV) radiation, which causes several short-term and long-term negative effects on worker health and safety. For instance, decrease on workers' concentration increase the risks of working at public transportation, security, and working at heights. More seriously, sun exposure at work is associated with an increased risk of skin cancer (Nederlandse Arbeidsinspectie, 2024).

**Energy Consumption and Infrastructure Strain:**
In recent years, the proportion of households owning active cooling systems (such as air conditioners) has risen to 30%. Research by the Netherlands Organisation for Applied Scientific Research (TNO) indicates that household use of active cooling systems can lead to an increase in energy demand of 15% to 25%, This contradicts the Netherlands' energy transition strategy for achieving its emissions reduction targets. (Kuijer, 2024). UHI effect also amplifies this impact. Compared with rural weather data, the average cooling demand increase between 24-32% when using urban weather data, meaning urban warming phenomena greatly impact the overall energy demand (Maiullari, 2023).

**Natural Environment and Ecosystems:**
Droughts and heat waves are closely linked. High temperatures dry out the soil, leading to further increases in temperature. High temperatures also exacerbate the evaporation of surface water such as rivers and lakes, reducing vital freshwater sources for millions of people (Utrecht University, 2022). Temperature rises is also likely to enable many species to adapt or migrate, and sveral plants and animals are threatened with extinction in the Netherlands. Moreover, foodchain is also being disrupted by heat wave (Netherlands Environment Assessment Agency, 2025).

# 2. SITE CONDITION

2.1 Rotterdam as a Thermal Stress City

2.2 Rotterdam's Social Issues

2.3 Densification of Rotterdam

## 2.1 Rotterdam Exposure to Heat

As the biggest port city in the whole Europe, Rotterdam is well-known for its unique high-density urban form, making it become one of the most climate sensitive cities in the Netherland. Against the background of global warming, the extreme heat events in the second quarter of Rotterdam are becoming more frequent and intense. According to KNMI climate scenario predictions for the Netherlands, due to soil drying and more frequent east wind which brings warm dry air, summer warming will be stronger. Figure 2.1 and 2.2 show that Rotterdam's current number of summer days: 25 days, and its current number of days in heat wave: 4 days. Under future climate conditions in 2050 and 2100, these number of hot days will continue to rise, and there will be more heat wave under the highest scenario (Figure 2.3and 2.4).

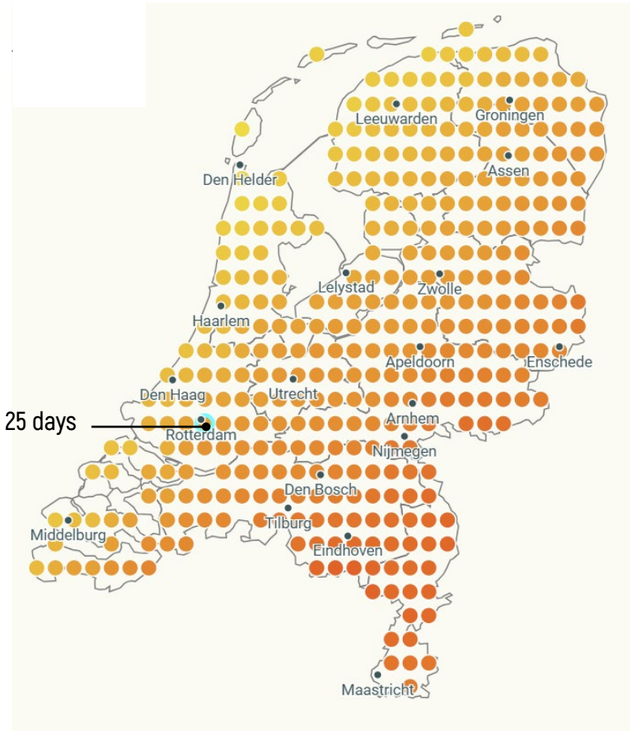



**Figure 2.1:** Number of Summer days in Rotterdam
(Source: https://www.klimaateffectatlas.nl)

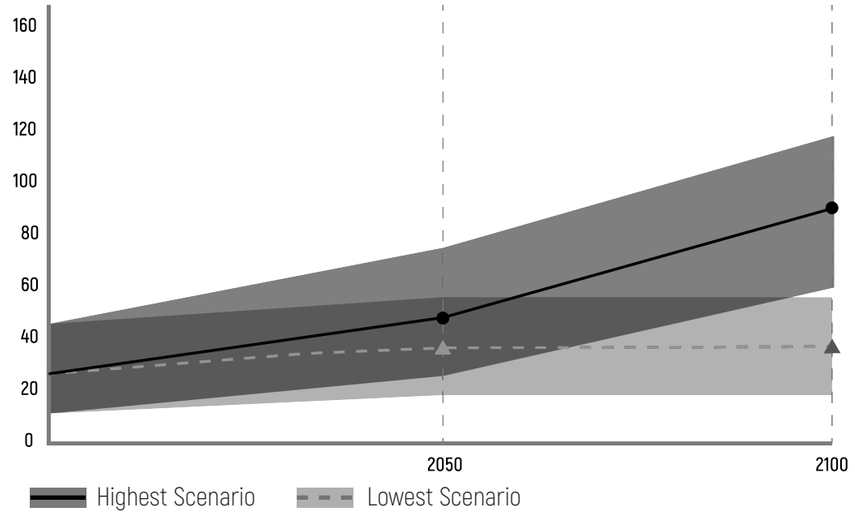



**Figure 2.3:** Prediction of Summer days in Rotterdam
(Source: https://www.klimaateffectatlas.nl)

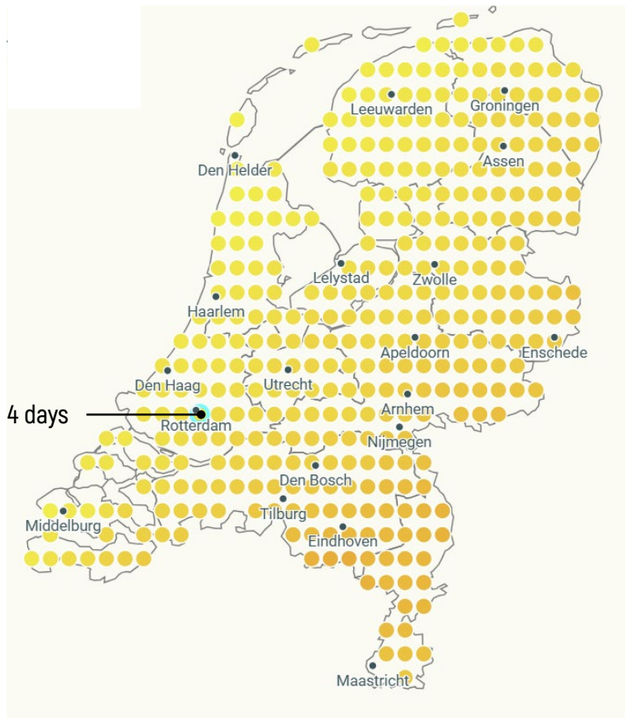



**Figure 2.2:** Number of days in Heat Wave in Rotterdam
(Source: https://www.klimaateffectatlas.nl)

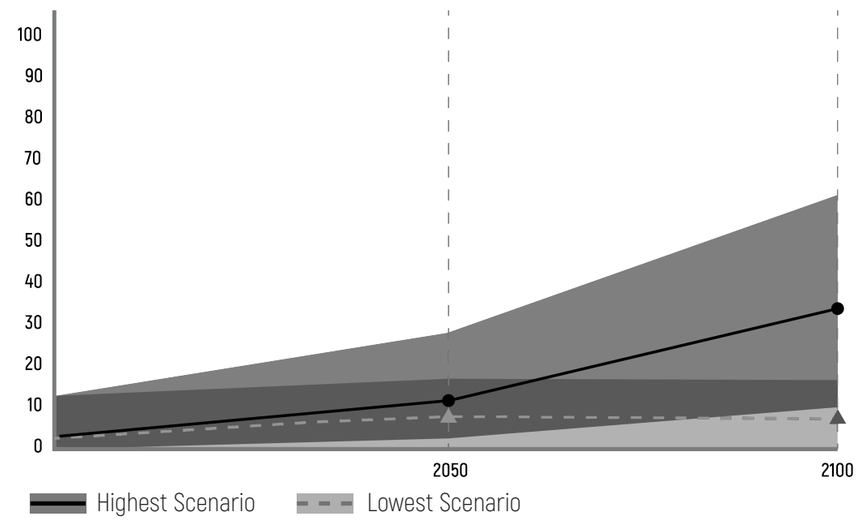



**Figure 2.4:** Prediction of days in Heat Wave in Rotterdam
(Source: https://www.klimaateffectatlas.nl)

## 2.2 Rotterdam Trend of Growth

Rotterdam, as the second largest city and a crucial European gateway, has encounted enormous pressure from housing market driven by complex population. On one hand, the total population continue to grow influenced by international migration and increased longevity. The Statistic Netherlands (CBS) predicts that urbanization will continue in major Dutch cities until 2040, while the population of Dutch Antilles, Turkish, Moroccan and Surinamese descent will continue to grow until 2050 (CBS, 2022). The Rotterdam's municipality has maken a goal of population growth, aiming to increase the population to 690,000 until 2035, in order to maintain economic development and urban vitality (Gemeente Rotterdam, 2018). On the other hand, the number of households increased to 8.37 million. Since the beginning of 2014, driven by population growth, aging, and increasing individualization, the number of households has increased by an average of 68,000 per year. By 2024, the number of households will reach 8.374 million. The average number of people per household will decrease from 2.18 in 2014 to 2.11 in 2024. According to Primos' 2024 projections, the average number of people per household will continue to decline in the coming years, reaching 2.06 by 2039. This trend is partly attributed to the increase in the number of single-person households (CBS, 2025).

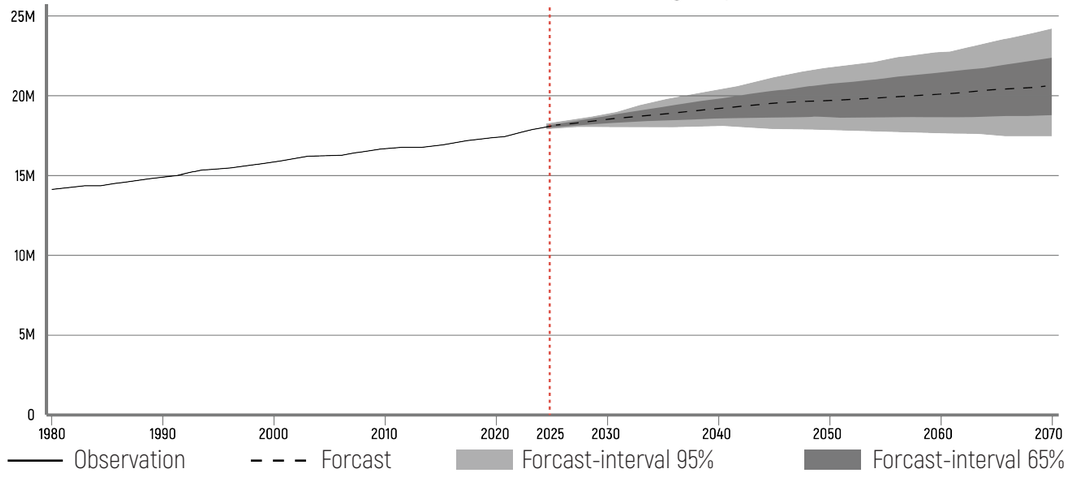



**Figure 2.5:** Prediction of Population Growth in Netherlands (Source: https://www.cbs.nl)

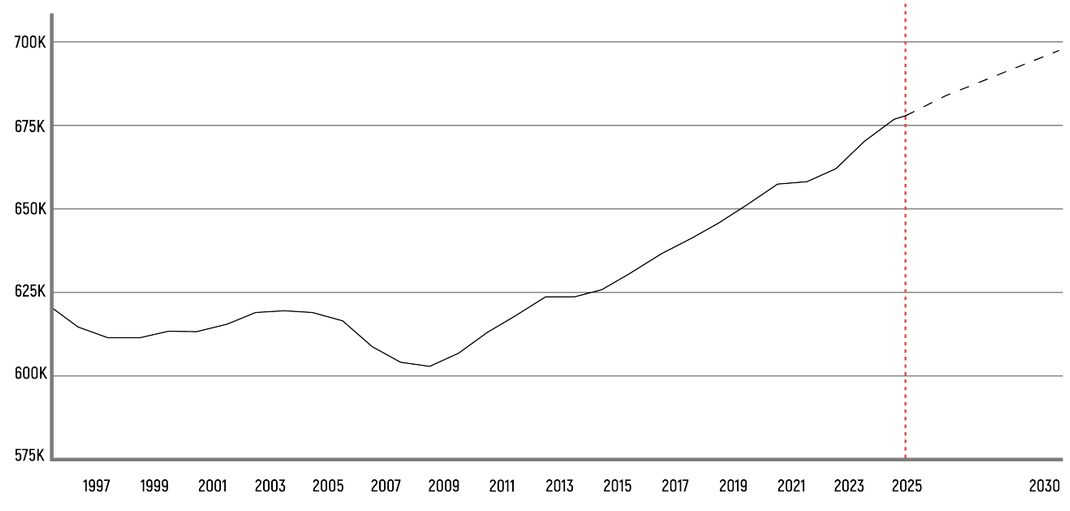



**Figure 2.6:** Population of Rotterdam in 2025 and Prediction in 2030 (Source: Based on https://allcharts.info/the-netherlands/municipality-rotterdam

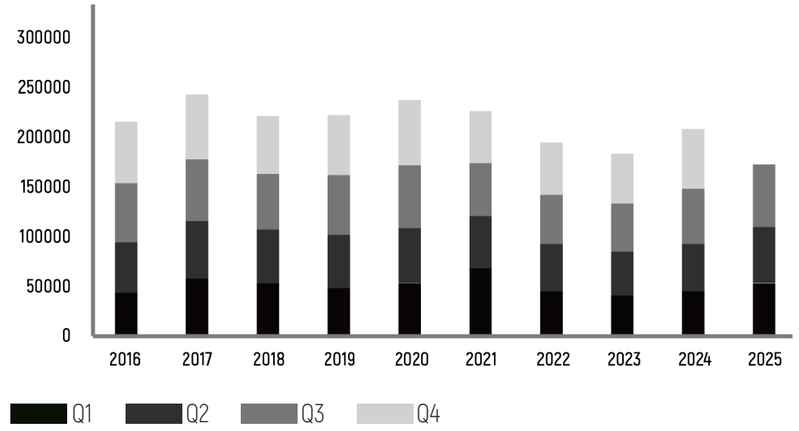



**Figure 2.7:** Number of Owner-occupied Dwellings Sold, Netherlands
(Source: https://www.globalpropertyguide.com/europe/netherlands/price-history)

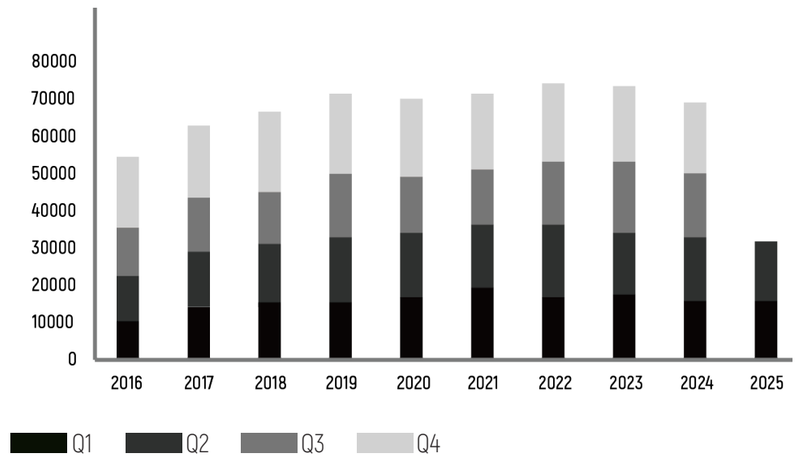



**Figure 2.8:** Number of Dwellings Completed, Netherlands
(Source: https://www.globalpropertyguide.com/europe/netherlands/price-history)

Population pressures are gradually evolving into an urgent macroeconomic challenge, threatening social housing equity. From 2023 to 2025, home sales increased year by year, with a record high of 171,468 owner-occupied homes sold in the first three quarters of 2025 alone, representing a 17.02% increase year-on-year (Figure 2.7). Meanwhile, the housing shortage has increased by 36,000 units recently, reaching approximately 436,000 units. The number of completed houses in Rotterdam witnesses a drop in recent three years. There are only around 67,000 new homes are built annually (Figure 2.8), while the number of new households reaches 85,000, creating a supply-demand imbalance and driving up housing prices (Bouwinvest, 2025). In 2024, Rotterdam built only 2,500 new homes, far below the city government's target of 3,500 to 4,000 new homes annually set in its "Housing Vision 2024." Rotterdam's new home construction is significantly lower than other major cities, while the number of homes actually demolished is much higher. Since 2012, Rotterdam's net housing stock has exceeded 3,500 units only twice, mainly achieved by subdividing existing residential buildings or converting office buildings into residential buildings (MERA25 Netherlands, 2025).

Several reasons cause this housing problem, involving the nitrogen crisis, a lack of building permits, tourism and the most important reason: lack of free space. In densely populated metropolises like Rotterdam, almost all urban land has already been developed (Figure 2.11). Furthermore, the Netherlands' Sustainable Urbanisation Ladder policy explicitly requires that urban development prioritize the use of existing built-up areas to protect the surrounding natural, agricultural, and hydrological landscapes. Therefore, new housing construction will be difficult to implement., making new housing construction difficult to implement.

As the four major cities (G4) in the Randstad serve as the primary engine for national economic growth, Rotterdam plays a important role in mitigating this national housing crisis.

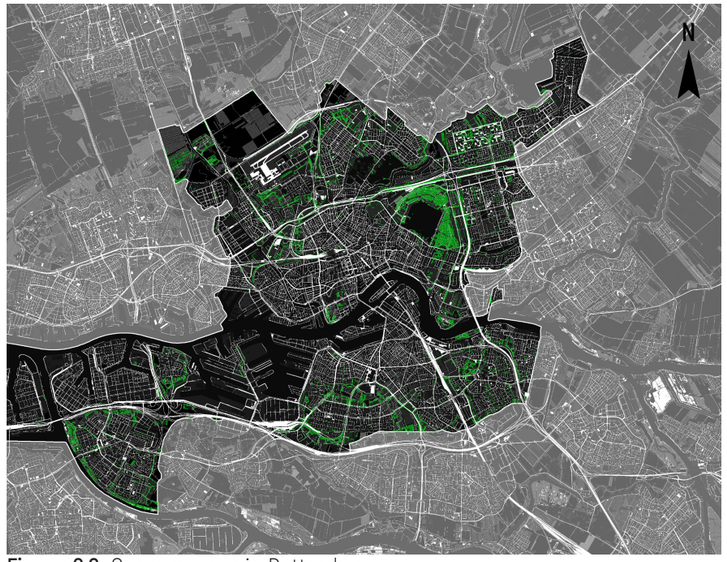



**Figure 2.9:** Green spaces in Rotterdam
(Source: By Author. Data from Open street Map)

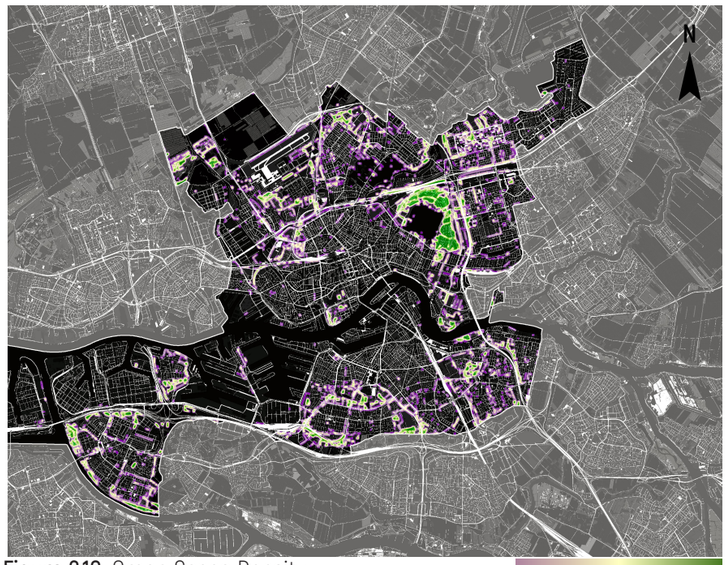



**Figure 2.10:** Green Space Density
(Source: By Author. Data from Open street Map)

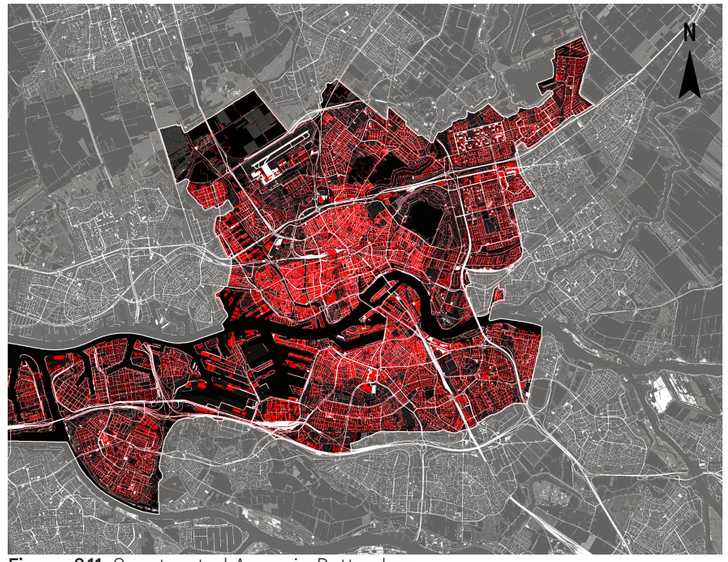



**Figure 2.11:** Constructed Areas in Rotterdam
(Source: By Author. Data from Open street Map)

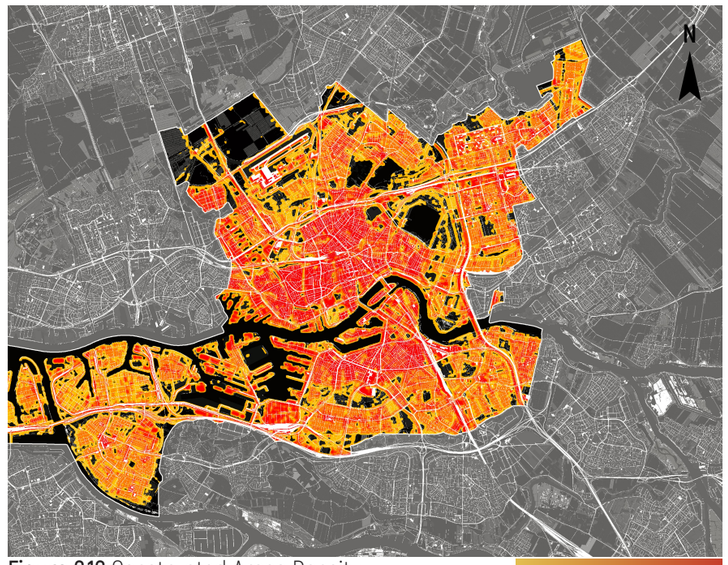



**Figure 2.12** Constructed Areas Density
(Source: By Author. Data from Open street Map)

## 2.3 Densification of Rotterdam

Given the aforementioned limitations, high-density urban development has become the only and irreplaceable strategic solution for achieving Rotterdam's population and housing goals. The government's solution is to build one million new homes by 2030 in the whole Netherlands, around 100,000 of them in Rotterdam. This is Rotterdam's densification, a response of the nation 1 million housing. Rotterdam's strategy for high-density urban development focuses on compact and sustainable urban development to address new demographic, economic, and environmental challenges (Beurden, 2013). The core of this new direction is Inward Growth, which means to improve landuse efficiency and building volume in the current urban areas to meet the need of continuously growing population and future urban functions. The future planning of Rotterdam will focus on reconfigure and make intensive use of internal resources, rather than searching areas by expanding current urban boundary.

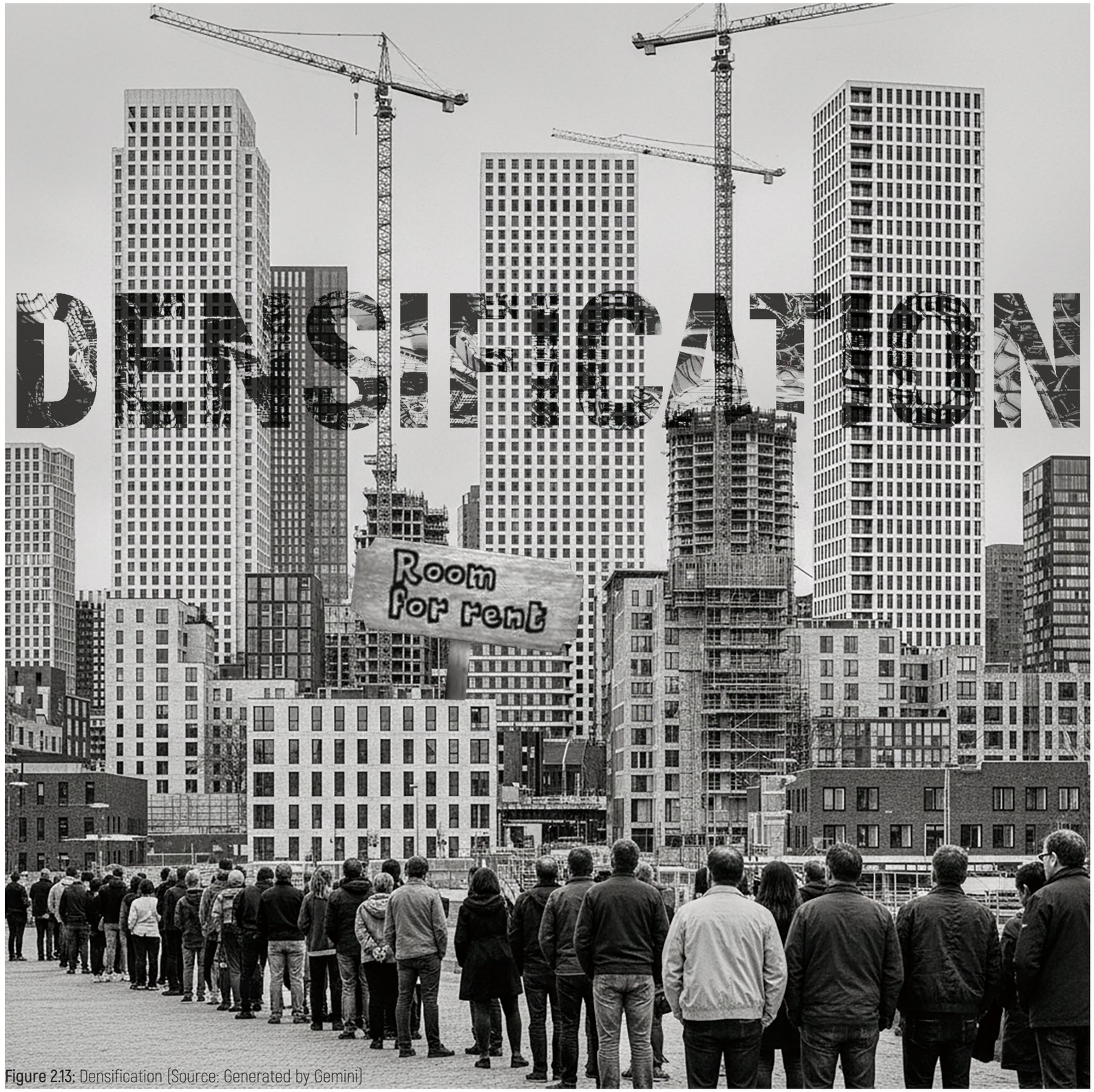



**Figure 2.13:** Densification (Source: Generated by Gemini)

The high-density implementation is mainly reflected in the following three aspects: Brownfield Redevelopment and Functional Transition, Infill Development and Vertical Growth and Transit-Oriented Development.

### Brownfield Redevelopment and Functional Transition:

This strategy aims to make intensive utilization of urban area through land reuse. Based on the research of Bezemer et al. (2022), the key to addressing inner-city brownfield issues lies not only in meeting consumer needs in terms of quantity, but also in improving quality by protecting cultural heritage and reducing urban sprawl (Nekkers, 2025).

### Infill Development and Vertical Growth:

Infill development refers to  utilizing available space between existing buildings to increase building density, and vertical growth allows developers to add floors above existing buildings, while promoting sustainable high-density development in urban areas. Residents often adopt this strategy in urban areas with diverse and discontinuous land use patterns (Attia et al., 2015).

### Demolition and Reconstruction for High-Rise:

Current low-rise buildings will be demolished and replaced with higher-density and taller buildings. While this technique is effective, it requires careful planning to minimize resident relocation and maintain sustainability (Alizadeh et al., 2025).

## 2.4 The Paradox of Densification and Heat Adaptation

Researcher have found that urban densification has been recognized as one of the main factors contributing to the outdoor thermal environment, which affects the microclimate and thermal comfort of urban areas (Jiang, 2025). The latest researches have adopted 3D spatial simulations. Wang et al. found that improper allocation of building height and density will exacerbate the heat risk in high-density cities. In addition, green space inequality will also occur while densification, and this inequality causes vulnerable populations encountered more severe heat stress (Ahmed et al., 2025).




**Figure 2.14:** Rotterdam and Hotterdam (Source: By Author and AI)

# 3. RESEARCH UNDERPINNING

3.1 Knowledge Gap

- PROBLEM STATEMENT

3.2 Opportunity

- RESEARCH QUESTIONS

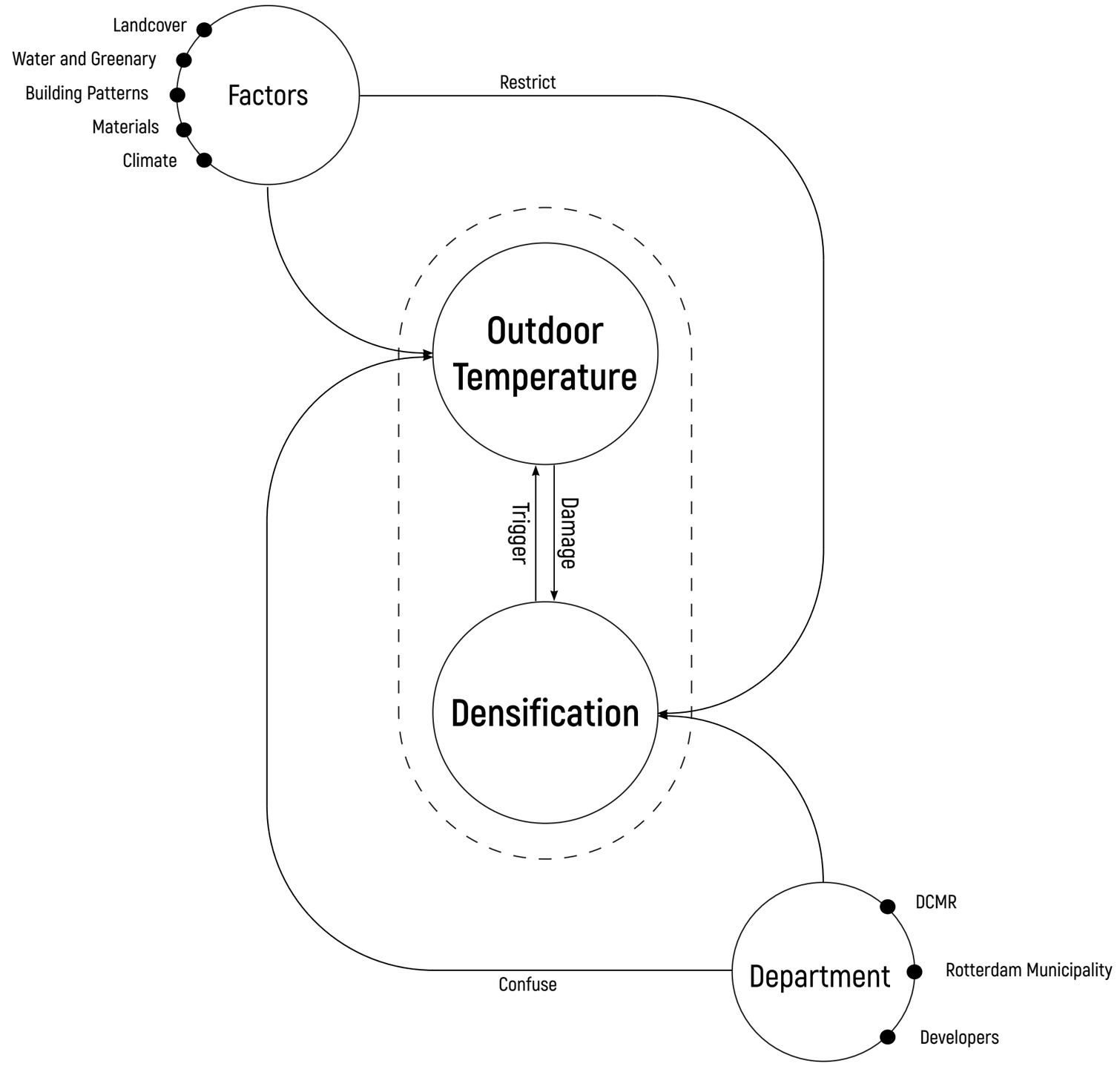
- METHODOLOGY FRAMEWORK

## 3.1 Knowledge Gap

Various complex factors drive the synergistic impacts of outdoor temperature on the built environment, which makes the temperature difficult to predict. Besides, many studies have shown that vegetations are one of the most effective ways to improve thermal comfort, but in the case of Rotterdam, the lack of opportunities to implement large-scale blue-green infrastructure or even vegetation implies that the urban form must be considered as an alternative solution to vegetation in the urban outdoor temperature mitigation process. Additionally, problems also occur from densification development processes. According to the Rotterdam municipality, despite municipality has recognized that the high-density urban area might increase the rate of heat retention, especially at pedestrian level, they still lack relevant heat-sensitive knowledge and experience while conducting densification, which may cause more serious climate consequences.

Widely use physical models, like ENVI-met and SOLWEIG, are applicable in simulating the urban thermal environment. They are considered to be time-consuming which makes it difficult to efficiently evaluate multiple design scenario.

As a consequence the results of densification processes from a thermal perspective is still unknown and lacks instruments that can facilitate assessments and inform decision making.



# PROBLEM STATEMENT

Along with the frequency and the intensity of extreme heat, cities around the world are encountering increasingly severe climate pressures. This warming issue grows even faster in Europe on account of changes in atmospheric circulation, reduction of air pollution and the extension of parts of Europe into Arctic region (ECMWF, 2025). In Netherlands, climate change has already imposed strongly effects.

According to KNMI, the annual mean temperature in Netherlands has increased by more than two degrees since 1906, which is almost twice as much as the 1.2°C increase in global mean temperature (KNMI, 2023), leading to a drier and hotter summer time in the future.

Rotterdam, as the second largest city in Netherland, is repeatedly regarded as one of the hottest cities on account of dense morphology, large industrial areas, limited green spaces and extensive hard surfaces. Peer-reviewed site measurement completed by Klok et al. in 2012 indicated that daytime temperature in Rotterdam is 10°C higher than non-urban areas. As a result, several consequences will be triggered such as the peak electricity demand and the raise of mortality and morbidity rate among vulnerable groups (Santamouris & Osmond, 2020).

However, the outdoor thermal environment in Rotterdam may witness a raise in the future. In recent years, due to population growth, Rotterdam's housing shortage has become increasingly severe. To address the housing needs of the growing population in the future, the Rotterdam municipality has decided to implement a densification process which will construct more skyscrapers and heighten the original residental buildings.This process will affect the release of heat radiation, causing outdoor temperatures in Rotterdam to rise. Although the Rotterdam municipality is aware that densification will cause a decresase to outdoor thermal comfort, they are still unclear about what standards should be provided for densification, and they also lack the necessary tools and knowledge to quantify the chances in temperatures within the urban canopy layer.

At the same time, microclimate and urban outdoor temperature will be impacted by change in urban configuration and composition, while there is still difficulty in modelling and computational expensive tools for design analysis of microclimate conditions created.

The general risk is that Rotterdam's densification is going to be conducted without effective standards or easy-to-use tools to assess the heat impacts of new buildings, which will likely result in an negetive effect on ourdoor thermal temperature, elevated heat-related health risks, and reduced environmental livability for vulnerable communities.

### 3.2 Opportunity

In recent years, with the rapid development of artificial intelligence, more and more AI technologies can be applied more maturely in urban planning and research, with machine learning and deep learning being among them. For urban developers and reseachers, AI has become a powerful tool to provide references or suggestions.

#### 3.2.1 Machine Learning and Deep Learning

Machine learning (ML) is a field of artificial intelligence which enables computers to identify patterns from data and make predictions without being explicitly programmed for every task. By learning relationships from existing datasets, machine learning models can be applied to estimate unknown outcomes. Deep learning (DL), a subset of machine learning, employs multi-layer artificial neural networks to automatically learn complex features and perform tasks such as classification, regression, and prediction.

#### 3.2.2 Machine Learning and Deep Learning on Heat Analysis

There are many types of triggering factors of high urban outdoor temperature, including landcover, urban morphology, water, plants, materials, human activities and climate factors, which make a lot of challenges in predict and modelling urban temperature in that the relationship between these factors and urban heat is usually non-linear, and spatial variability is also a major obstacle (Hoang, 2025). Current researches that comprehensively considers all explanatory factors affecting changes in land surface temperature also remains limited (Hoang, 2025).

Machine learning technology offers a promising solution to these challenges. In recent years, ensemble learning models, such as Extreme Gradient Boosting (XGBoost), LightGBM, and CatBoost have increasingly been applied on predict urban land surface temperature, because of the high results performance and accuracy (Mansourmoghadda, 2024). Hoang et al. showed that the LightGBM model achieved the lowest root mean square error (RMSE) on all datasets while predicting land surface temperature, which demonstrates that machine learning models can effectively identify factors influencing land surface temperature such as urban density and green space coverage (Hoang, 2025).

Although machine learning models have proven to be effective predictive methods, they still have limitations compared to deep learning models such as convolutional neural networks or long short-term memory networks, because machine learning models may limit their ability to capture certain complex spatiotemporal patterns in the dataset (Hoang, 2025).

Deep learning model like Convolutional Neural Network (CNN) has gradually attracted much attention because it has been shown that mid- and high-level abstract features can be extracted from raw images using interleaving convolutional layers and pooling layers (i.e., by spatially shrinking the feature maps layer by layer) (Zhu. 2017). Currently, deep learning has been widely used in classification and segmentation tasks, but the regression-based deep learning is also becoming popular, which make the estimation on data in enviornmental, urban and agricultural aspects more convenient (Kustura et al., 2025). Using Turin, Italy as a sample, Innocenti et al. used CNN to predict the city's highest temperature, achieving a mean absolute error (MAE) of 2.09°C at a resolution of 20 meters per pixel. Kustura et al. have also use CNN model trained by data from ECOSTRESS to predict land surface temperature. The result achieves the prediction with at least 80% pixel error within ±3°C. Beyond LST-focus studies, Briegel et al. in 2023 also used U-Net architecture to predict mean radiant temperature (MRT) based on spatial data derived from GIS, The model achieves an overall MAE of about 2.4 K. Moreover, this U-Net model is also capable of greatly improving computational efficiency, allowing for faster generation of MRT maps at high resolutions. In general, these studies show deep learning model has great potential to support climate adaptation strategies and enhance our understanding of the interaction between urban spatial types and climate (Kustura et al., 2025).

# RESEARCH QUESTIONS

The methodology framework of this project will be built on four sub-questions which is derived from the main research question.

In the first phase, according to the literature review of global warming, urban temperature and densification, problem statement will be raised and the conceptual framework is constructed. This framework will be used throughout the thesis and guides the analysis of how Rotterdam's densification can respond to increasing heat stress.

The second phase including geo-data analysis and a deep-learning prediction model development. Based on the literature review, temperature sensitive spatial and environment characteristics are assessed by GIS (SQ1), from which the result is going to be used in deep learning model training (SQ2). This is able to provide a simplified, efficient and relatively accurate product which not only can validate subsequent spatial designs, but also provide management with quantifiable tools (SQ4).

By using the model, the third phase tests respectively the heat corresponding to different spatial and building configurations (SQ3) and then translates the analysis and conclusion into practical guidelines. These guidelines support municipalities, land developers and design firms in evaluating and reducing thermal impacts (SQ4).

**Main Research Question**

**How could Rotterdam develop heat-sensitive densification strategies with the support of deep-learning technologies?**

**SQ 1**

What kinds of urban, environmental and morphological factors contribute to urban outdoor temperature?

**SQ 2**

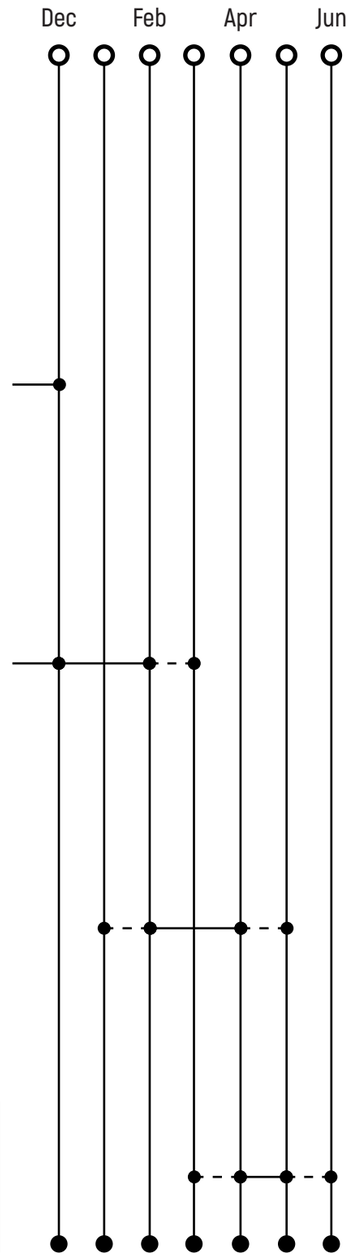
How can technology helps simplify and strengthen the prediction of urban outdoor temperature?

**SQ 3**

Which types of spatial configurations are most effective in reducing heat during both day and night in high density urban area in Rotterdam?

**SQ 4**

What guidelines can the municipality provide to developers to ensure a heat-sensitive densification?



# METHODOLOGY FRAMEWORK

## Problem Driven

Global Climate Warming

Urban Heat Intensification

Densification Pressure in Rotterdam

Governance & Knowledge Gap

## Research Questions

What kinds of urban, environmental and morphological factors contribute to urban outdoor temperature?

Literature Review + UMEP Study + GIS Analysis

How can technology helps simplify and strengthen the prediction of urban outdoor temperature?

GIS Analysis + Deep Learning + UMEP

Which types of spatial configurations are most effective on reducing heat during both day and night in high density urban area in Rotterdam?

Lead

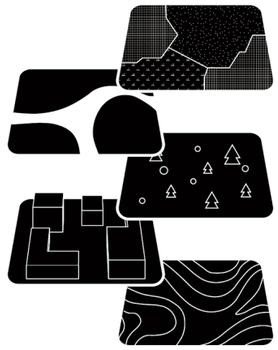
Parametric Design

Design Scenario

What guidelines can the municipality provide to developers to ensure a heat-sensitive densification?

Literature Review

## Expected Product



Training Dataset

Training

DL Model

Strengthen

Predict

Result

Guidelines

## Significance

### Scientific Contribution

- Thermal trade-offs of urban densification
- Morphology impacts on MRT and PET
- Deep-learning-assisted thermal prediction

### Planning & Design Relevance

- Heat-sensitive and morphology-based densification guidelines
- Rapid evaluation for design scenarios

### Policy & Governance

- Heat-risk spatial identification
- Evidence-based climate adaptation
- Thermal indicators for densification policies

### Society

- Reduce outdoor heat risk
- More climate-resilient cities
- Protection of vulnerable populations

# 4. FACTORS INFLUENCING OUTDOOR THERMAL ENVIRONMENT


4.1 Introduction

4.2 Radiation and Temperature

4.3 Landcover

4.4 Urban Morphology

4.5 Blue-green Infrastructure

4.6 Materials and Albedo

4.7 Anthropogenic Activities

4.8 Summary

## 4.1 Introduction

In this chapter, the major environmental and morphological elements that influence urban thermal environment will be explored. This includes radiation, landcover, urban morphology, wind environment, blue-green infrastructure, material properties and anthropogenic activities.

## 4.2 Radiation and Temperature

Radiation is fundamental element to all thermal processes on Earth. Shortwave radiation from the sun arrives reach the earth's surface. However, part of this radiation is scattered by particulates in the atmosphere, and another part is reflected by the surfaces (Oke, 1987; Wallenberg et al., 2020). When shortwave radiation is absorbed by urban materials, it is converted into heat energy and eventually emitted as longwave radiation, depending on the material albedo, heat capacity, and emissivity (Oke, 1987). Figure 4.1 shows the radiation mechanism.

**Direct shortwave radiation:** Shading plays an important role in determining the amount of solar radiation received (Lai et al., 2017). Buildings and hard objects create deep shade, while plant cover and semi-transparent objects create partial shades. Moreover, the angle of the sun's elevation changes the amount of radiation that the urban surface receives.

**Diffuse shortwave radiation:** Shortwave diffuse radiation occurs through the scattering effect created by various particles in the atmosphere that prevent solar rays from reaching the surface directly (Oke, 1987; Wallenberg et al., 2020).

**Reflected shortwave radiation:** The albedo of various urban surfaces affect the amount of solar raiation which is reflected back into air instead of being absorbed. (Morini et al., 2016).

**Longwave radiation:** Longwave radiation describes heat loss from surfaces in the form of infrared waves. Unlike shortwave radiation, longwave radiation intensity depends on the emission power and temperature of the emitting surface (Oke, 1987).

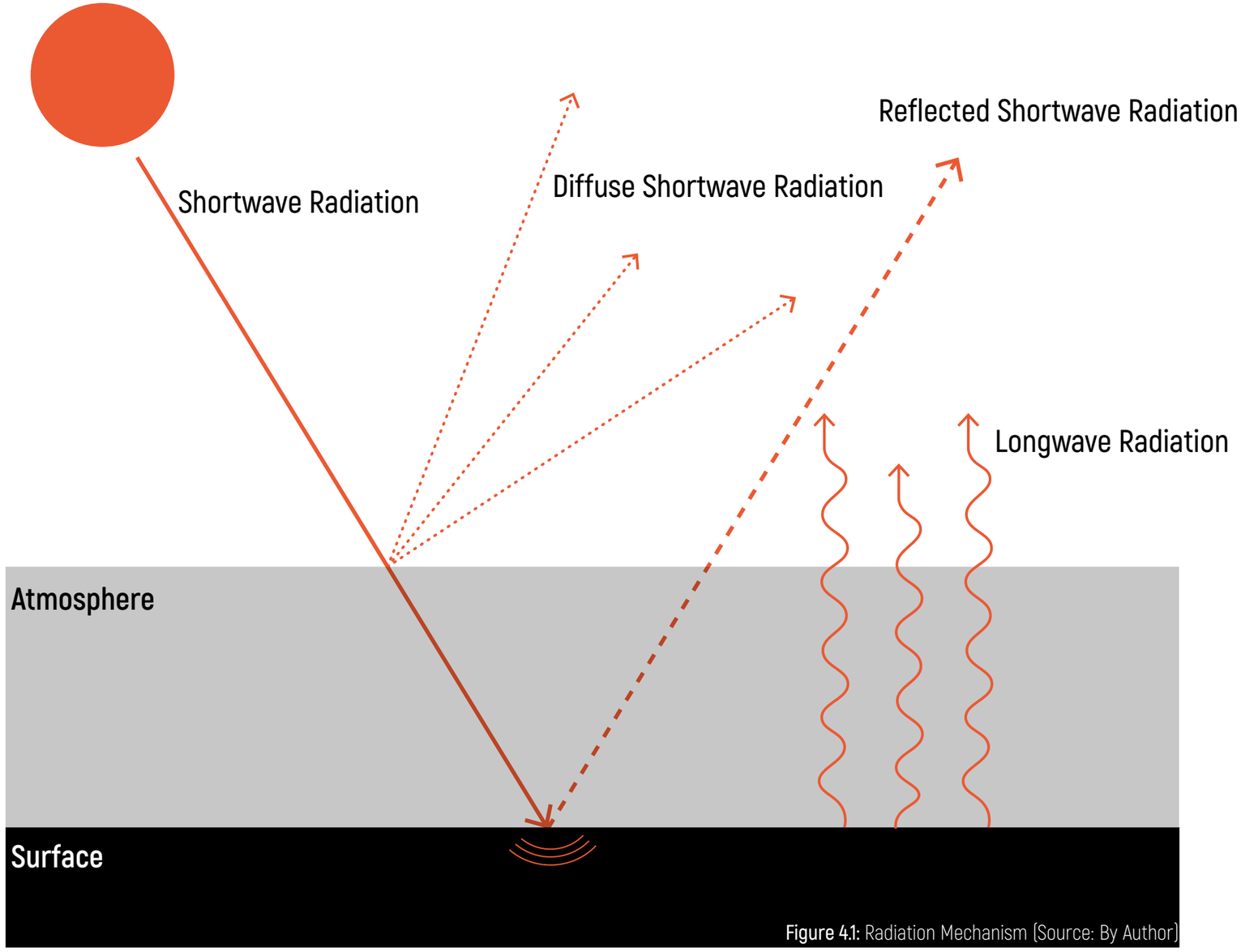



**Figure 4.1:** Radiation Mechanism (Source: By Author)

## 4.3 Landcover

Generally speaking, due to high building density and the characteristics of urban building materials and paving materials, heat is more easily retained in cities, which increases the city's heat risk, especially at night.

Figure 4.2 shows how landcover affect thermal environment in urban zones. The building surfaces, impermeable pavement like roads and railway, soil sealings, and bare lands have a tendency to absorb solar radiation and store the heat, which will emitted as longwave radiation during the night. On the contrary, water and vegetaion like forests and cultivated lands are highly reflective, and evapotranspiration occurs more in such areas, reducing net radiation and longwave radiation emission (Grimmond & Oke, 1999).

But harbors is an exception. Despite having water areas, due to industrial activity and impervious surfaces, more heat absorption occurs, which reduce the cooling effect of water, leading to more heat radiation. From Figure 4.3, the radiative heat is relatively high in Rotterdam harbor areas compared to other urban areas around it.

In general, the effects of landcover on urban outdoor temperature are primarily controlled by changes in surface radiation processes, such as solar radiation absorption, heat retention in the material, and the release of long-wave radiation.

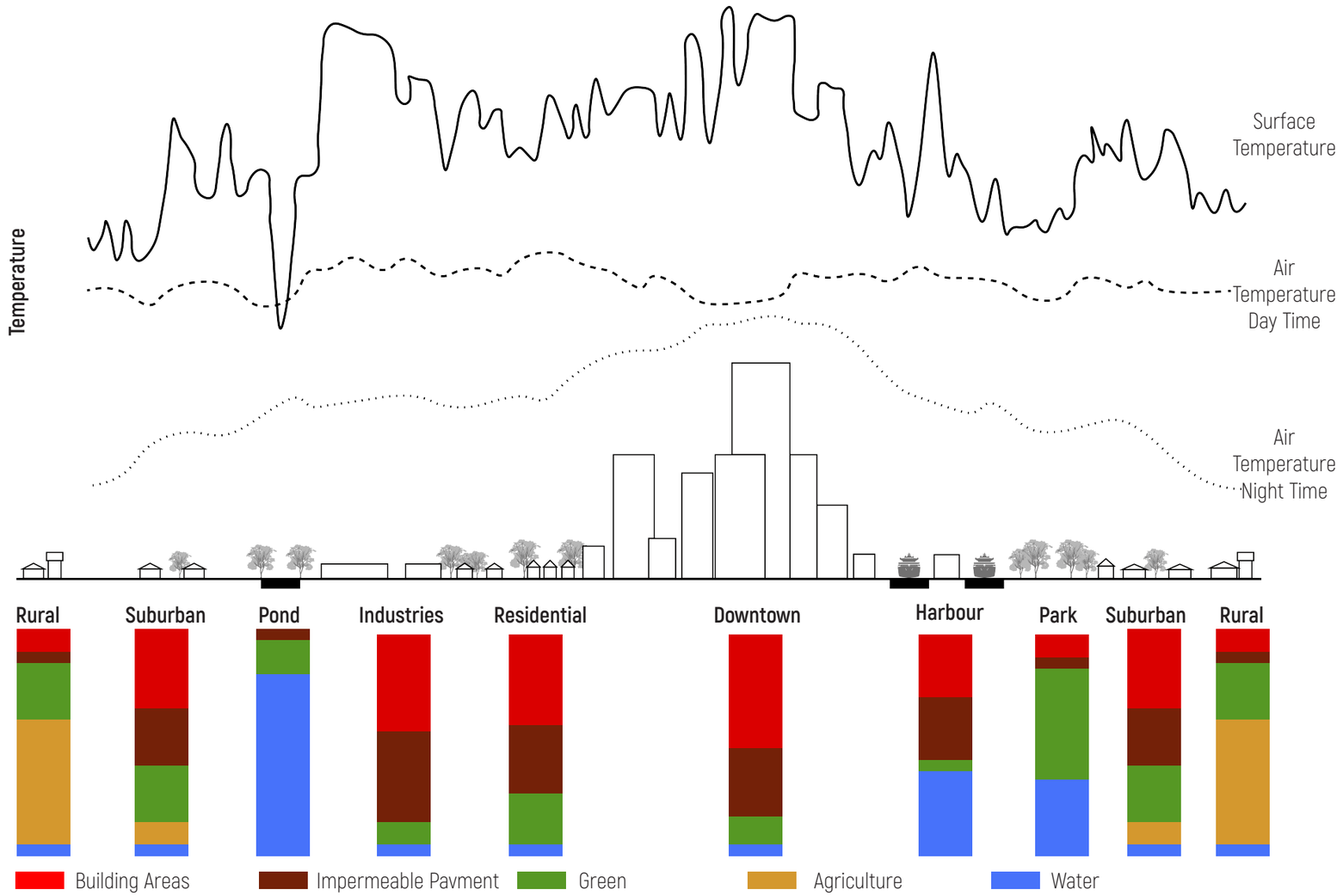



**Figure 4.2** Relation Between Landcover and temperature (Source: Modified from Voogt, (2004))

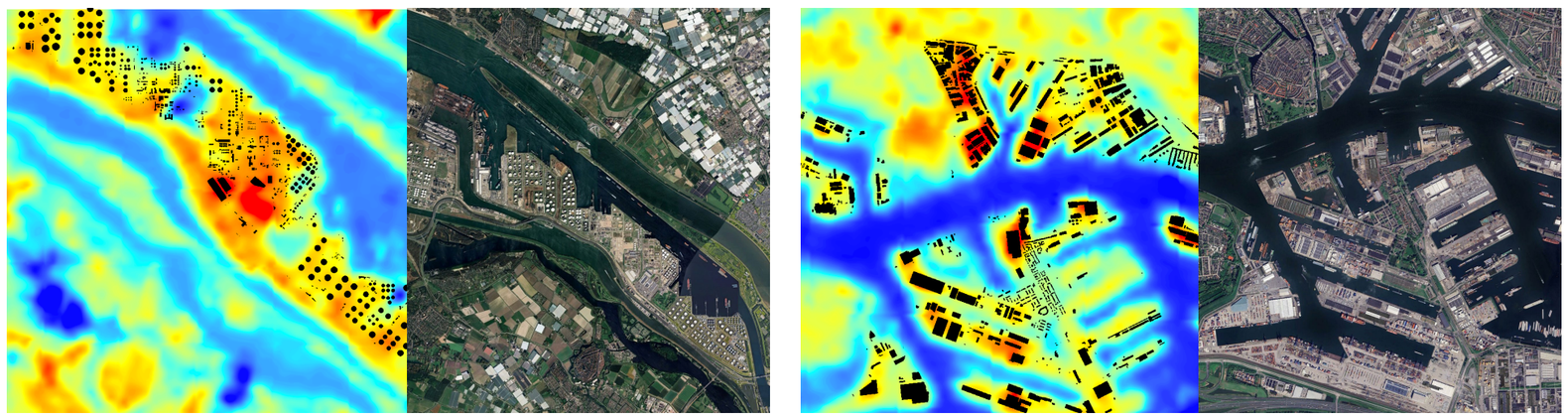


**Figure 4.3:** Land Surface Temperature of Harbours (Source: By Author. Data from USGS and Google Earth)

### 4.4 Urban Morphology

Urban morphology also has a devisive influence on the urban temperature. A research from Sobstyl et al., who analyzed 50 cities around the world, demonstrates urban morphology is able to explain the differences in urban temperature between different cities. The core mechanism by which urban morphology affects urban temperature lies in the changing efficiency of urban surfaces heat absorption during the day, and release of heat during the night. Urban morphology are mainly quantified using two geometric parameters: Building distribution Function and Sky View Factor (SVF). Their quantitative analysis showed that urban temperature is strongly negatively related with urban building cluster size, which means the higher the urban density and the smaller the building complex, the weaker the city's heat dissipation capacity and the higher the urban temperature.

#### 4.4.1 Building Distribution Function

Other researches also prove the same perspective. According to a research by He et al., the average building height (MBH) and the standard deviation of building height (BHSD) showed a negative correlation with temperature, while building density (BD) and building coverage Radio (BCR) showed the opposite (Figure 4.4). The Standard Deviation of Building Height (BHSD) is an important indicator used to quantify the degree of difference in building heights within a study area. From Figure 4.4, it can be noticed that when BHSD is less than 40, it shows a negative correlation with urban temperature. However, a higher BHSD does not necessarily mean a more significant cooling effect. The relationship between MBH and temperature is also non-linear. When MBH is less than 6m, an increase in building height will lead to a rise in temperature. When MBH is more than 6m, the temperature will drop due to the larger shadow that buildings provide (Wang et al., 2025). Besides, as for the building density, when the density is below 0.3, it helps to cool down, but once this threshold is exceeded, higher densities will lead to higher temperatures (Figure 4.4).
w

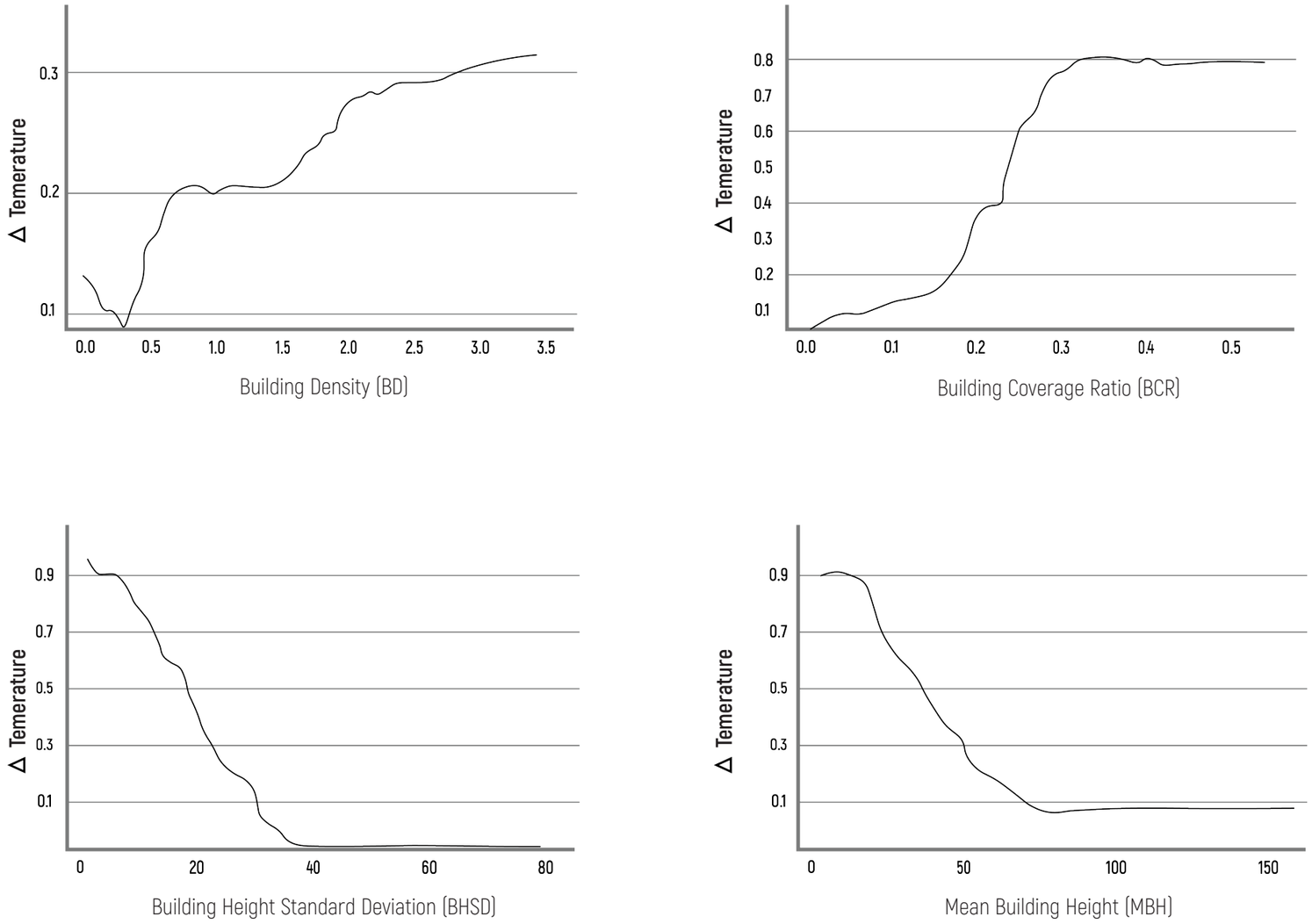



**Figure 4.4:** Relation Between Building distribution and temperature (Source: Modified from He et al. (2021))

### 4.4.2 Sky View Factor (SVF)

Sky View Factor is a comprehensive spatial result influenced by various urban morphology indicators, such as building height, building density, which is used for quantifying the degree to which urban surfaces including streets and rooftops are open to the sky in the surrounding environment (Figure 4.5). From physical aspect, SVF reflects the ability of a point to receive radiation from the sky, and it depends on the height of surrounding obstacle like trees and buildings. In the studies of urban temperature, SVF can represent as net radiation, which make it become a mechanism of urban temperature analysis, especially combining influence with factors like the diurnal temperature range, solar irradiance, wind speed, and vegetation fraction on UHI intensity (Dirksen et al, 2019).

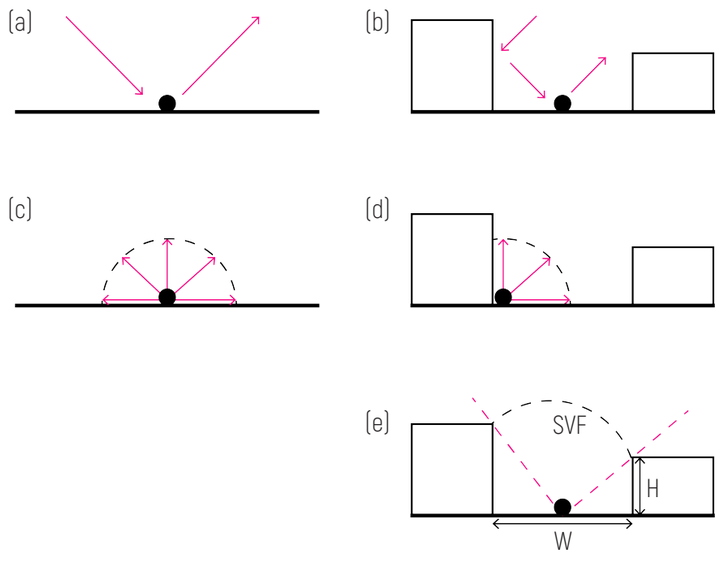



**Figure 4.5:** (a) Short wave radiation in an open field. (b) Short wave radiation in a street canyon. (c) Emission of long wave radiation in an open field. (d) Emission of long wave radiation in a street canyon. (e) SVF in a 2D street canyon; were W is the street width and H is the building height. (Source: Adapted from Urban Climate)

According to Lindberg and Grimmond (2010), the SVF formula is:

$$\mathbf{SVF}_a = \sum_{i=1}^{n} S_i \cdot \frac{2}{2\pi} \sin\left(\frac{\pi}{180}\right) \sin\left(\frac{\pi(2a_i - 1)}{2n}\right) \frac{360}{\Theta_i}$$

$SVF_a$ represents the sky view factor at a given location. $n$ is the total number of sky sectors considered in the azimuthal direction. $S_i$ is a binary visibility term indicating whether the sky is visible 1 or obstructed 0 in sector denotes the elevation angle of the sky sector, while $\Theta_i$ represents the azimuthal width of each sector. The trigonometric terms account for the spherical geometry of the sky hemisphere, ensuring that each sector contributes proportionally to the total visible sky area.

The relationship between SVF and urban heat is normally non-linear and complex. Chen et al. in 2021 have discovered the rationship between SVF and the land surface temperature (LST) (Figure 4.6). Their result shows the a positive correlation when SVF is larger than 0.3 and smaller than 0.9 and shows a negative correlation when SVF is less than 0.3 or larger than 0.9. This is because when SVF increases, open terrain absorbs more solar radiation, leading to an increase in ground temperature; when SVF is extremely low, the heat emitted by buildings is difficult to dissipate, causing a rise in temperature (Kim et al., 2022), (Kim et al., 2022).

Besides, Lyu et al. in 2019 have studied They explored the correlation between SVF and mean radiant temperature. Figure 4.7 show the relationship of SVF and MRT in the compacted high-rise area. The result has proven there is a strong relation between SVF and MRT, which shows a positive correlation. During the day, the correlation between SVF and MRT is affected by the size of building shadows: The correlation will be stranger while the shadows area is larger, (Lyu et al., 2019).

The impact of SVF on temperature varies in regions with different building heights and densities. Research found that the LST is higher when the average building height is 6 meters, and lower when the average building height is 21 meters. This may be because tall buildings also create a lot of shade, reducing the LST. Meanwhile, the SVF-LST relationship shows the greatest difference when the SVF value is between 0 and 0.4 (Figure 4.8).

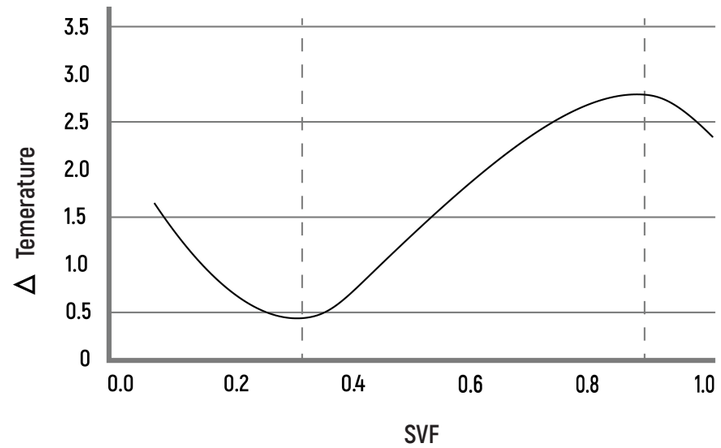



**Figure 4.6:** Relation Between SVF and Land Surface Temperature (Source: Adapted from Chen et al. (2021))

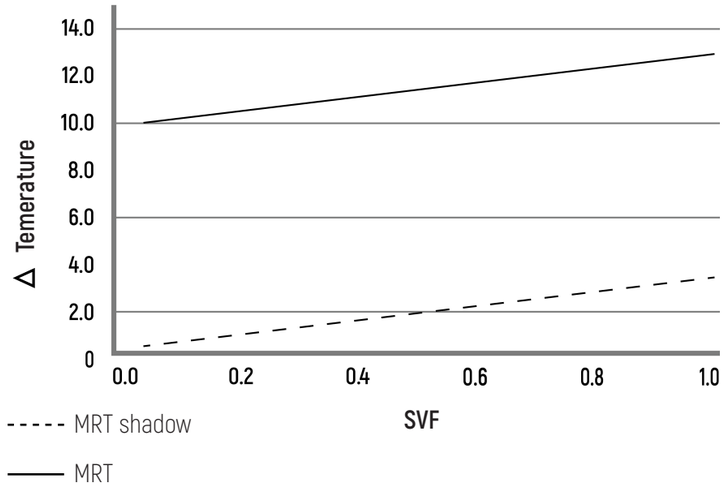



**Figure 4.7:** Relation Between SVF and Mean Radiant Temperature (Source: Adapted from Lyu et al., (2019))

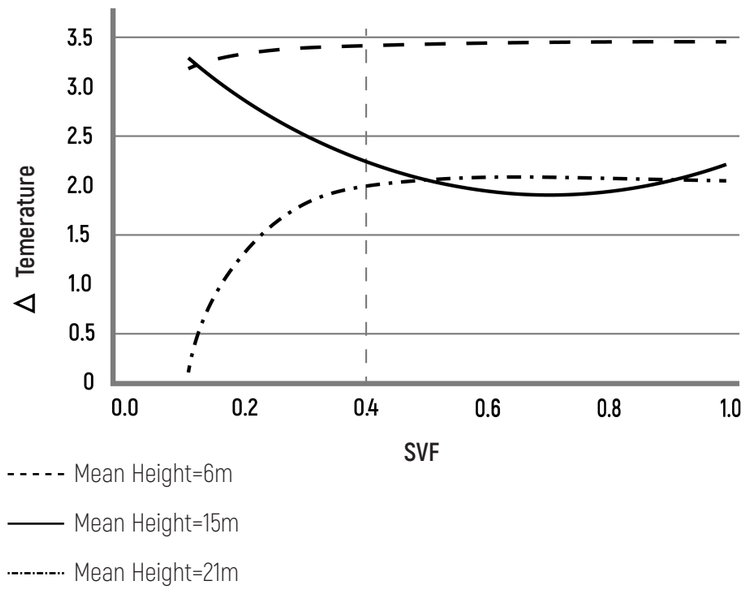



**Figure 4.8:** Relation Between SVF, building height and Temperature (Source: Adapted from Chen et al. (2021))

### 4.4.3 Wind Environment

Wind environment is another factor that affects urban outdoor temperature. Building height and street geometry are able to change the wind environment by creating street canyons, which will alter the wind speed and effciency of ventilation on pedestrian level (Figure 4.9). Previous studies have shown that High-rise buildings can introduce high wind speed at pedestrian level. When buildings are aligned with the prevailing wind direction, they can create a channel effect, locally accelerating wind speeds within a street canyon. Conversely, densely packed buildings can generate aerodynamic drag, reducing airflow in downstream areas (Kuo et al., 2020).

Wind speed plays an important role in urban thermal regulation and the Physiological Equivalent Temperature (PET) in that wind can enhance the heat exchange between human and the surrounding air. Several studies have quantified the impact of wind on PET. For instance, it was found that an increase in wind speed from 1 m/s to 2 m/s can lead to a reduction in PET by as much as 3.5 °C under direct solar radiation. Even in more severe cases, it was found that an increase in wind speed by as much as 2-2.5 m/s could lead to a reduction in PET by as much as 12 °C in hot urban environments (Müller et al., 2014). Additionally, it was found that the overall cooling potential of wind could be as high as 11-13 °C under calm and ventilated conditions (Roshan et al., 2020).

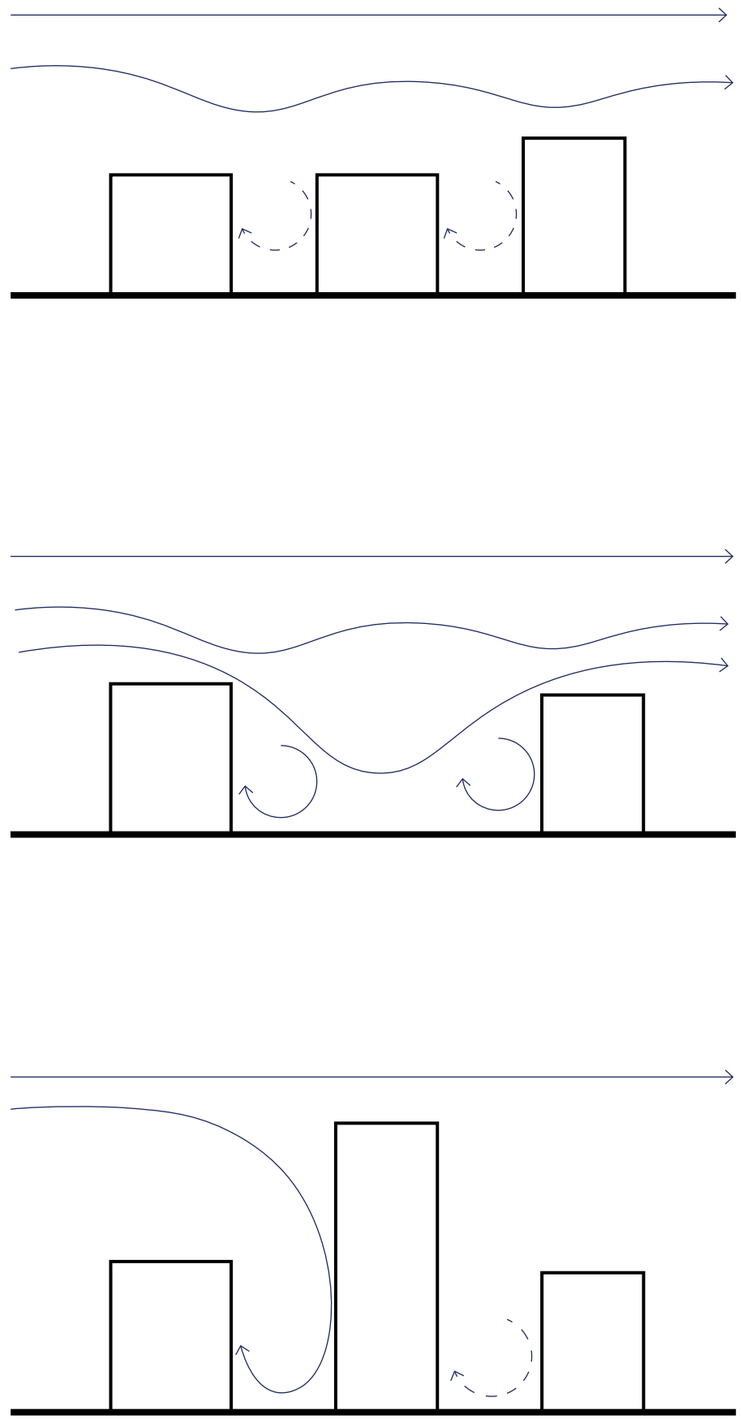


**Figure 4.9:** Urban Wind Environment (Source: By Author)

### 4.5 Blue-Green Infrastructure

It is well known that blue-green infrastructure (Green Spaces and Water Bodies) plays a significant role in mitigating the urban temperature in daytime. Their cooling effect is not limited to a certain boundary, but has a spillover effect that radiates to the surrounding areas (Gao et al., 2023) (Wu & Zhang, 2019). However, the cooling effect and the extent of influence differ between water bodies and green spaces. According to the research by Gao et al., the average cooling range of the green space to the surrounding area is 179.04 meters, with an average effective temperature drop of 0.96°C. In contrast, water bodies exhibit a more significant cooling effect. Based on the research by Wu et al., the maximum cooling distance for water bodies is appoximately 752 meters, at which point the temperature drop is approximately 2°C (Figure 4.10). Therefore, although both green spaces and water can effectively reduce urban temperatures within their own boundaries, water bodies, due to their higher specific heat capacity, can provide cooling services over longer distances and with greater spatial penetration.

Nevertheless, blue-green infrastructure does not always play an important role in cooling environment. In some circumstances, especially during nighttime, trees with large canopies could reduce the SVF, which prevents the release of longwave radiation, and blocks air circulation, leading to more heat retention (Wang et al., 2022). Likewise, small water areas cannot make any effcient impact on the thermal environment around them (Jacobs et al., 2020), while larger water bodies might even serve as a source of heat at night because of the higher specific heat capacity of water (Zeng et al., 2026).

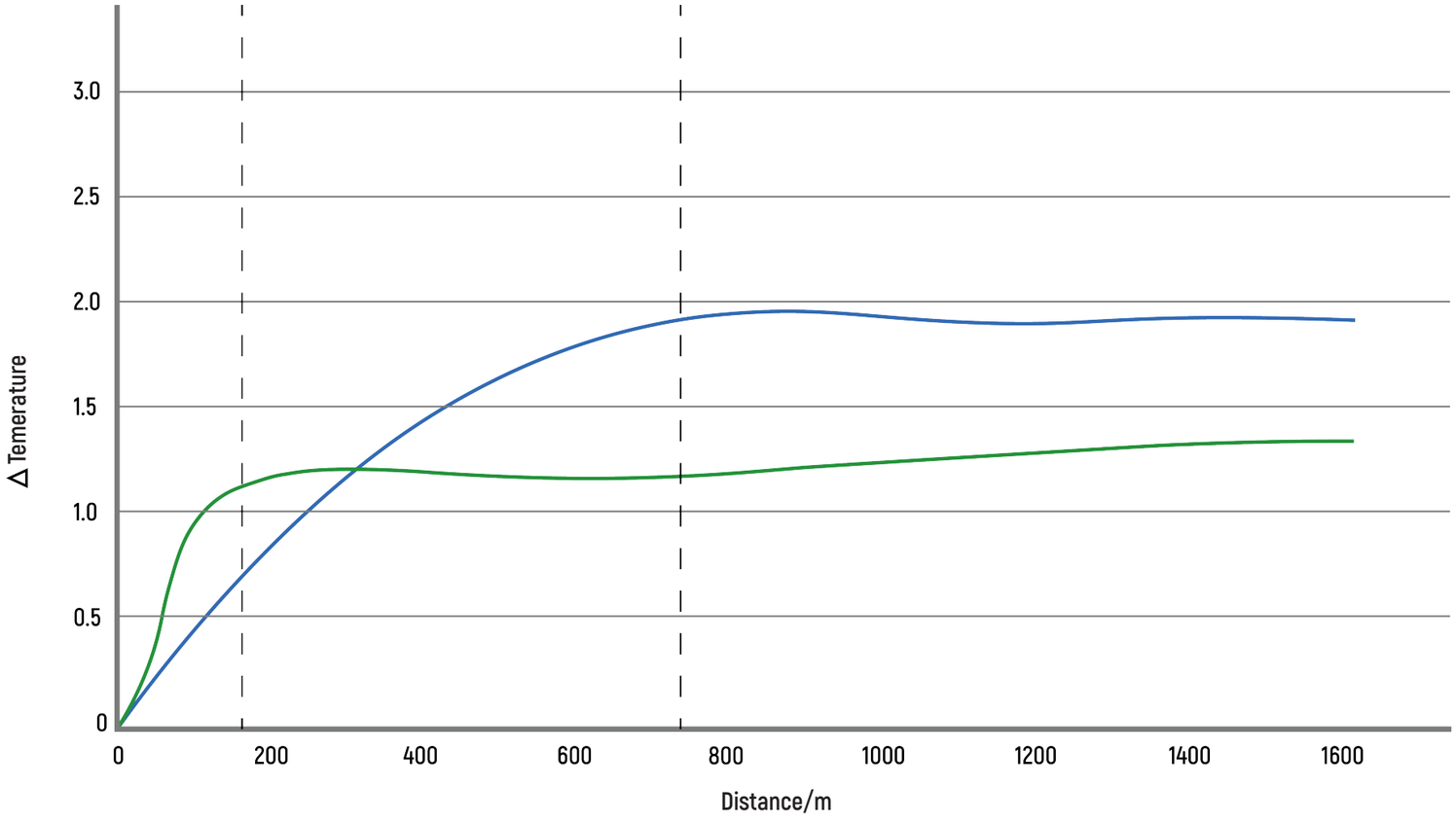



**Figure 4.10:** Relation Between Blue-green infrastructure and Temperature (Source: Adapted from Wu & Zhang. (2019))

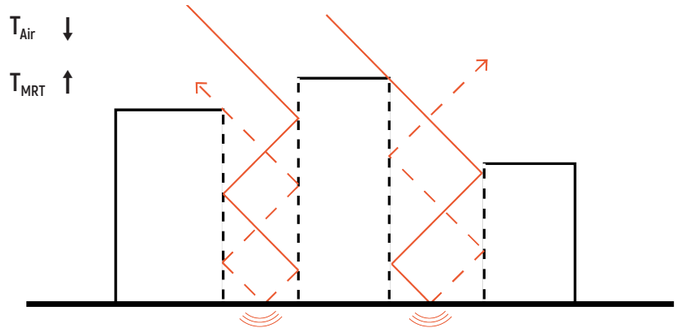
## 4.6 Materials and Albedo

Surface materials affect outdoor thermal environments mainly in terms of their radiative properties, especially surface albedo, which affects the fraction of shortwave radiation in urban canyons. Nevertheless, the effect of albedo on thermal conditions is highly dependent on urban morphology (Figure 4.11).

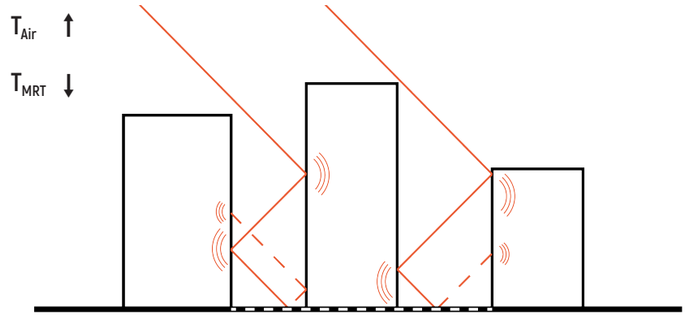
Yang and Li (2015) have shown that the fraction of incoming solar radiation to streets, walls, and roofs changes systematically with urban density. In low-density cases, horizontal street surfaces receive the largest amount of shortwave radiation, while in denser cases, a greater amount of radiation is intercepted by vertical façades as a result of reduced SVF and increased multiple reflections. This implies that the effectiveness of albedo modification is scale-dependent, with ground materials being more important in open urban morphologies and increasing importance of façade reflectivity in compact urban environments.

From the viewpoint of pedestrian thermal comfort, increasing surface albedo is not an effective measure to lower MRT. A simulation analysis of urban pavement surfaces indicated that increasing ground albedo lowered near-surface air temperature by as much as 0.5-1.0 °C but raised MRT by as much as 10.3 °C because of increased shortwave reflection to pedestrians.

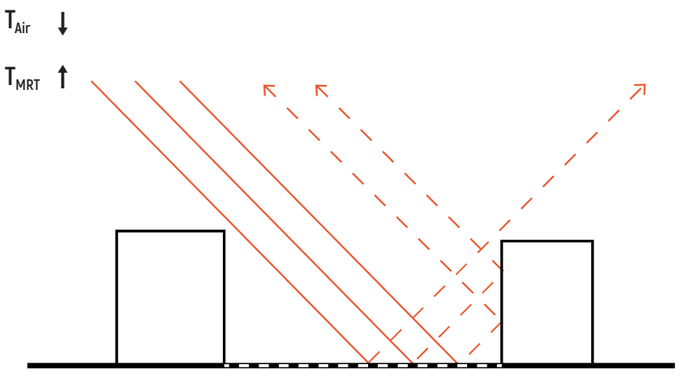
These results imply that material modifications should be assessed in terms of their effects on radiative transfer rather than being assessed solely on the basis of temperature reduction. In low-density areas, high-albedo ground materials could raise MRT by increasing reflected shortwave radiation, while in dense street canyons, the importance of facade reflectivity and shading geometry increases (Taleghani & Berardi, 2018).



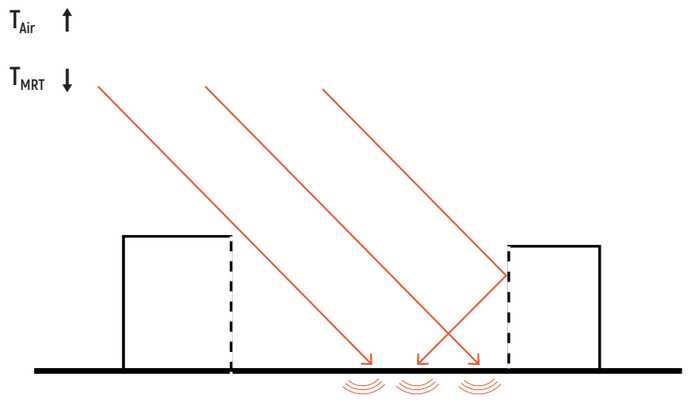

**High Density Area––Wall Albedo**



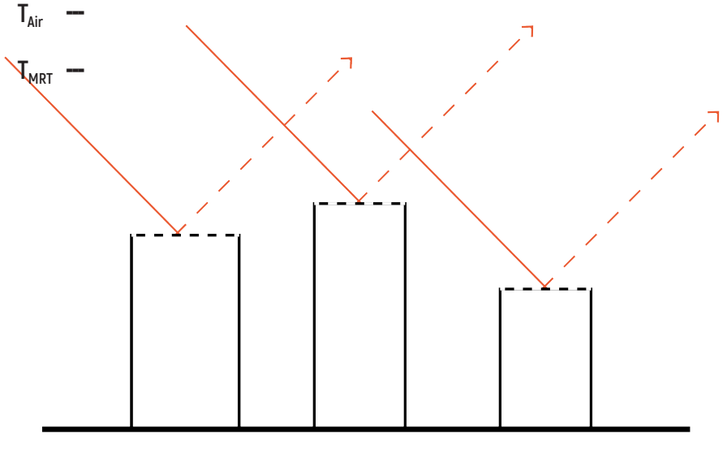

**High Density Area––Road Albedo**




**Low Density Area––Road Albedo**




**Low Density Area––Wall Albedo**




**High Density Area––Roof Albedo**

**Figure 4.11:** Relation Between Materials, Albedo and Temperature (Source: By author)

## 4.7 Anthropogenic Activities

Human activities in cities release a significant amount of anthropogenic heat into the atmosphere through various ways, including industrial, transportation, and cultural activities; this is known as anthropogenic heat release (AHR). In certain extend, AHR also triggers the urban warming effect (Cao et al., 2019). According to the study by Cao et al., compared with the normal situation of AHR, which contributes to air temperature ranged from 0.11°C to 0.36°C, doubling AHR results in a warming effect that is more than twice that of normal conditions, reaching a maximum of 0.71°C. The study further found that high-rise and medium-to-high-density building areas exhibited the most significant AHR heating effect, reflecting the combined effects of high population concentration, increased air conditioning energy consumption, and compact built-up environments.




**Figure x:** Heat from Industries (Source: Google)




**Figure 4.12:** Heat from Heavy Traffic (Source: Google)

### 4.8 Summary

The table 1 describes some of the crucial factors affecting the urban thermal environment and their association with physical elements like solar radiation, wind, and evaporation.

From the above explanation, it is evident that various factors influence the outdoor thermal environment, although their mechanism of influence are different and not all the factors may be controllable within the urban design progress.

In this study, urban morphology is selected as the dominated research variable. Due to the existing built-up conditions in the city center of Rotterdam, high economic costs and long implementation periods, the alteration of landcover on a large scale is practically restricted. Additionally, the implementation of more vegetation and water can also not be easily achieved on account of the limited space in Rotterdam city center.

As a result, the simulations primarily focus on morphological variations, while climatic conditions, blue-green infrastructure and material properties remain constant. Urban morphology and related landcover are systematically modified to examine their effects on thermal environment.

| Model Parameter | Solar Radiation | Wind | Evaporation | Variable Setting |
|---|---|---|---|---|
| Climate | ● | ● | ○ | Constant |
| Landcover | ● | ○ | ● | Variate |
| Urban Morphology | ● | ● | ○ | Variate |
| Blue-Green Infrastructure | ● | ○ | ● | Constant |
| Materials | ● | ○ | ○ | Constant |
| Human Activities | ○ | ○ | ○ | Constant |

**Table 1:** Parameter for SOLWEIG Calculation

# 5. DEEP LEARNING FRAMEWORK FOR THERAML PREDICTION

5.1 Introduction

5.2 Introduction of UMEP

5.3 Selection of Thermal Assessment Indicators

5.4 Selection of Machine Learning Model

5.5 Methodology

5.6 Spatial Data Modelling

5.7 U-Net Model Structure

5.8 General Workflow

## 5.1 Introduction

According to the sub-question 2, this chapter is trying to describe a general training method for deep learning model. For this purpose, the chapter fisrt describes a climate service tool, thermal assessment indicators and the type of deep learning model selected for the investigation and the methodology employed for the study

## 5.2 Introduction of UMEP

UMEP is a widely used plugin based on QGIS, mainly designed and used for urban climate analysis and environmental modeling (Lindberg et al., 2018). UMEP integrates a suite of tools that can assess urban thermal environment, radiation exchange, and microclimate processes using common spatial datasets. The core of UMEP is Solar and Long-wave Environmental Irradiance Geometry (SOLWEIG) model, which can estimating three-dimensional radiation flux and mean radiation temperature (MRT) in complex urban environments. The model only requires a few parameters including meteorological data like sun azimuth and air temperature, landcover, urban geometry data such as Digital Surface Model (DSM) and vegetation. Figure 5.1 shows the working process of SOLWEIG model.

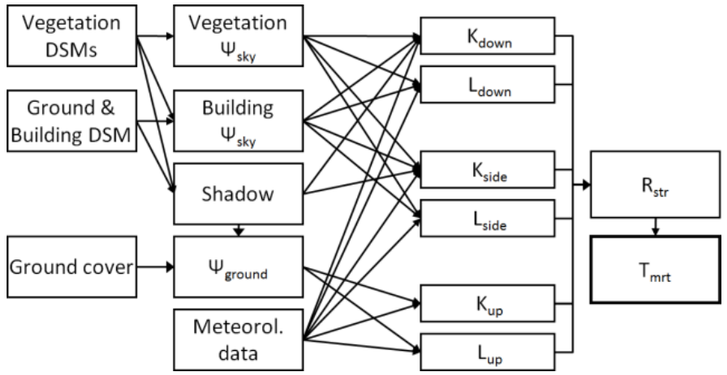



**Figure 5.1:** Overview of SOLWEI
(Source: https://umep-docs.readthedocs.io/projects/tutorial/en/latest/Tutorials/IntroductionToSolweig.html#id1)

## 5.3 Selection of Thermal Assessment Indicators

In the research of urban microclimate, it is important to choose a suitable temperature map as an indicator because it directly affects the practical value of the research. Currently, in academia, the following temperature maps are mainly used for research:

**Land Surface Temperature (LST):**

Land surface temperature refers to the temperature that can be felt when touching the land surface at a specific location (NASA). NASA and other international organizations have listed it as one of the most significant Earth system data records (King, 1999), which is usually utilized for the key indicator to land surface models for drought monitoring, soil moisture estimation, and evapotranspiration estimation (Hulley et al, 2019).

**Air Temperature:**

Air temperature refers to the temperature of the air in the immediate surroundings of the human body, which represents the environmental factors that determine the heat flow between the human body and the air" (Ahmad, 2016), directly affecting ecosystems, water resources and human activities (Mats et al., 2025).

**Mean Radiant Temperature (MRT):**

Mean radiant temperature is the sum of all shortwave and longwave radiation fluxes (including direct and reflected radiation) that the human body is exposed to. It is one of the most important meteorological parameters, affecting the human body's energy balance and thermal comfort (Thorsson et al, 2007).

**Physiological Equivalent Temperature (PET)**

PET is defined as the air temperature at which the human body's heat balance is in equilibrium with its core and skin temperatures in a typical indoor environment which without wind and solar radiation, the same temperature as the temperature under the complex outdoor conditions to be evaluated (Höppe, 1999).

Current research on the urban heat island effect is mainly based on land surface temperature (LST) because LST data is readily available and facilitates related experiments. However, LST does not reflect physiologically related human thermal comfort, or the situation of direct human exposure to high-temperature environments (Zhan et al., 2025). Therefore, this study will use MRT and PET of Rotterdam during heat waves as the core

indicator to train deep learning models. Since MRT reflects the overall radiation environment around pedestrians, while PET combines MRT with other meteorological indicators to characterize physiological heat harvesting in the human body.

### 5.4 Selection of Deep Learning Model

In this research, Convolutional Neural Networks (CNN) was selected because CNN can capture spatial patterns and make relation between local details. Rather than treating each sample as an independent feature, CNN integrates spatial information by convolution operations, which is different from traditional machine learning models like Random Forest and XGBoost. This is especially important while dealing with heat environment in that temperature distribution highly depends on landcover, spatial continuity and the surrounding environment.

Within the family of CNN model architecture, this research uses U-Net which follows an encoder-decoder structure with skip connections. U-Net can preserve both local details and large-scale spatial semantics in pixel-level regression tasks. Compared to standard CNN without skips connections or fully connected regression models, U-Net provides refined spatial consistency and robustness in heterogeneous urban environments, making it well suited for city-scale thermal mapping tasks.

### 5.5 Methodology

The methodology includes of four main steps. First, spatial and meteorological data are collected and processed to generate the raster inputs required for thermal simulations. Second, the UMEP framework, including the SOLWEIG and URock models, is applied to simulate MRT and PET under the heatwave scenario. Third, the calculated raster of MRT and PET are prepared to construct the deep learning training datasets, and deep learning models is trained based on the dataset. Finally, the trained models are used to evaluate different urban densification scenarios and analyse the influence of urban morphology on outdoor thermal conditions (Figure 5.2).

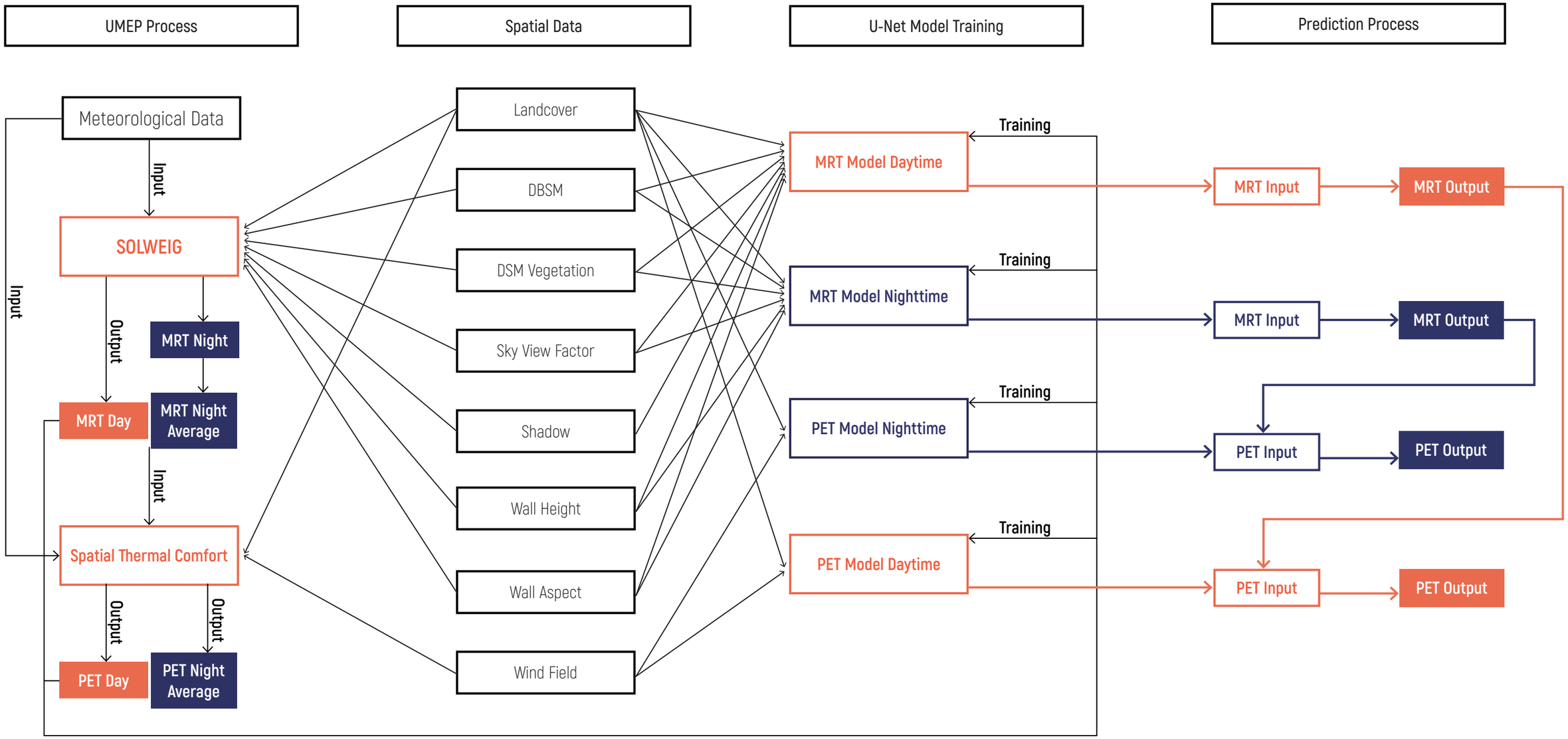



**Figure 5.2:** Methodology (Source: By author)

## 5.6 Spatial Data Modelling

### 5.6.1 Modelling Mean Radiant Temperature

In this research, the mean radiant temperature (MRT) is calculated through SOLWEIG model in UMEP by using spatial rasters with a resolution of 1 m, specifically using Landcover, Sky View Factor, Shadow, DSM Buildings, DSM Vegetaion, Wall Height and Wall Aspect. This process focuses on estimating the radiative flux of human feeling by simulating the exchanges of shortwave and longwave radiation in three-dimension urban environment. In addition, the model still requires meteorological data for calculations. The meteorological data obtaining from KNMI were selected based on the dates in Rotterdam during the heatwave, while avoiding cloudy or rainy days. Therefore, meteorological data from August 10th to August 14th, 2022, were used for MRT calculations. Specific data and model parameters are shown in the table 2.

| Model Parameter | Value |
|---|---|
| Emissivity | 0.95 (ground) |
| | 0.9 (walls) |
| Albedo | 0.15 (ground) |
| | 0.2 (walls) |
| Transmissivity | 3% |
| Trunk height | 25% of tree height |

**Table 2:** Parameter for SOLWEIG Calculation (Source: By author)

### 5.6.2 Modelling Physiological Equivalent Temperature

The Physiological Equivalent Temperature (PET) is calculated by using the Spatial Thermal Comfort (Spatial TC) plugin in the UMEP toolbox within QGIS. PET depends on various kinds of factors including MRT, air temperature, wind environment, relative humidity and centain anthropometric parameters like height, weight, clouthing, age and metabolic rate. MRT is simulated by SOLWEIG model and wind environment is simulated by URock model. These two data, along with meteorological data, will be input into Spatial TC to calculate PET temperature.

### 5.6.3 MRT GIS Data Acquisition and Processing

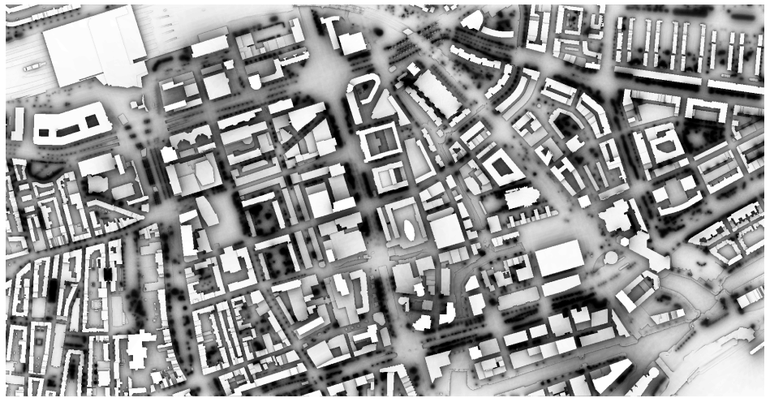
Landcover data is obtained from Basisregistratie Grootschalige Topografie (BGT), which provides the latest and the most precise information about the landcover in Netherlands. According to the instruction provided by Lindberg et al., the landcover data is reclassified into seven types: 1. Paved surfaces, 2. Buildings surfaces, 3. Evergreen trees, 4. Deciduous trees, 5. Grass, 6. Bare soil, 7. Water.

According to Lindberg and Gimmond, Sky View Factor represents the proportion of the radiation radiation exchanged (received or emitted) between a surface and the visible sky hemisphere. (Watson and Johnson 1987). SVF is a dimensionless measure between zero and one, representing completely obstructed or fully open areas, respectively. SVF calculated through UMEP plugin in QGIS, and the calculation requires DSM Buildiings and DSM vegetaion data which can be aquired from BGT and Rotterdam 3D.

Shadow, wall height and wall aspect using for SOLWEIG calculation are also made by UMEP based on DSM buildings and DSM vegetation.
These GIS spatial data are used for both SOLWEIG calculation and UNet training, and these rasters will uniformly aligned to the same spatial grid with a resolution of 1 m

For MRT training, the final dataset includes

Landcover, SVF, DSM buildings, DSM vegetation, wall height and wall aspect (Figure 5.3) . All these data are raster data and they were combined using the GIS Composite Bands function to create a complete training datasets.

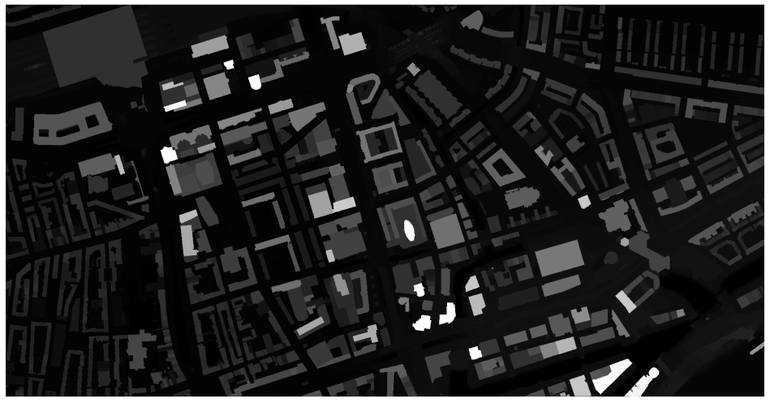


Sky View Factor

0 1



Shadow 8.10 h13.00 (Example) Shadow Trees Shadow Buildings



DBSM

-6.5m 129m



Wall Aspect

0° 360°



Landcover

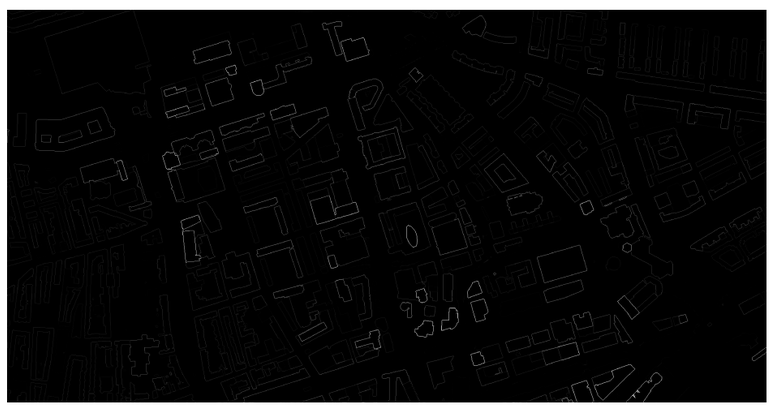
Roads Buildings

Water Green Spaces



DSM Vegetation

5m 25m



Wall Height

0m 129m

**Figure 5.3:** Training Dataset (Source: By author)

### 5.6.4 PET GIS Data Acquisition and Processing

Wind environment sitmulation of URock mainly requires buildings and vegetation outlines, which are provided in shapefile format. To ensure the accuracy of the wind simulation, the wind direction in URock is set according to the prevailing wind direction in Rotterdam. Based on meteorological observation, the direction of the wind in Rotterdam is generally southwest in both summers and winters (Tax, S, 2024). Thus, in the simulation by the UROCK model, the direction of the wind is set at 225°. Other parameters of URock is showed in the tabel 3. The final output raster resolution is 1m.

| URock Parameter | Value |
|---|---|
| Height of reference wind speed | 10m (KNMI) |
| Wind direction | 225° |
| Wind speed | 3m/s |
| Wind height | 1.5m |

**Table 3:** Parameters for URock Calculation (Source: By author)

For PET training, the final dataset includes Landcover, which is used to distinguish between building and street spaces, wind speed raster and MRT raster data from 12:00 to 16:00 on August 10th to 14th, 2022 generated by the SOLWEIG simulation (Figure 5.4).




**Figure 5.3:** Training Dataset (Source: By author)

## 5.7 U-Net model Design

### 5.7.1 Model Objective and Data Preparation

In temerate maritime cities like Rotterdam, the heat stress demonstrates a obvious iurnal rhythm variation instead of a constant daily intensity. The study examined the number of ambulance calls in Rotterdam during a heatwave, finding that the increases in ambulance calls occurred during midday (12.00-16.00) and evening (20.00-0.00) (Sirenko et al., 2026) (Thorsson et al., 2014). Based on the above conclusions, the main purpose of the model is to simulate and evaluate the MRT at a specific time under heat wave conditions.

To achieve this goal, four models will be trained to predict the MRT and PET during the day and the night, respectively. The daytime training dataset will cover spatial raster data and MRT raster data from 12:00 to 16:00 hourly on August 10th to August 14th, because during the daytime, MRT is dominantly affected by direct shortwave radiation, resulting in strong temporal variations depending on the position of the sun. Therefore, hourly training data are necessary to capture dynamic shadow patterns and peak radiative heating effects.

The nighttime model will be trained by using a nighttime averaged MRT raster and a nighttime average PET raster. At night, MRT is mainly affected by long-wave radiation exchange, and the temporal variation of MRT is generally smaller than that during the daytime. Hence, nighttime model based on the average MRT is used to determined

the region susceptible to heat storage. Besides, The spatial raster data for the nighttime training will not include the shadow raster.

### 5.7.2 U-Net model Structure

Based on the structure propound by Ronneberger et al. in 2015, the encoder consists of three downsampling layers, each of which includes two convolutional layers with ReLU activation and batch normalization, followed by max pooling. In order to capture more spatial information, the channel numbers of feature maps are gradually increased (64, 128, 256, 512). A bottleneck layer with 512 feature maps is also used to capture high-level spatial semantics. For the decoder, the convolutional layers are in reverse as the encoder, and skip connections are also instrduced to transfer more fine-scale spatial information to the reconstruction layer. The output layer is used for predicting single-channel continuous MRT values, which allow pixel-wise regression.

To introduce temporal forcing, the model takes in both solar geometry variables (solar altitude and azimuth angles) and daily maximum air temperature (Tmax) as additional inputs. Solar altitude and azimuth angles are transformed using sine and cosine functions to retain their cyclical nature, while Tmax is normalized to reflect the intensity of heat during extreme situations. These temporal features are then fed into a multilayer perceptron (MLP) to produce a 128-dimensional temporal embedding vector. After spatial broadcasting, the vector is concatenated with the bottleneck feature map and combined using a 1×1 convolution (Figure 6.1).

To ensure the model has high accuracy and good generalization ability, a block-based data segmentation strategy is employed to avoid spatial data leakage. This method segments the image into larger spatial blocks, and the image patches are divided into training or validation set randomly. In this case, spatially adjacent image patches will not appear in both the training and test sets simultaneously, ensuring a more realistic evaluation of the generalization performance of the model.

### 5.7.3 Training parameter settings

This U-Net model was built and executed in the Microsoft Visual Studio for Python programming environment. Each training sample consists of a 64 × 64 Pixel image, with an extraction stride of 30 pixels, making sure there will be an overlap of every training sample. The Nodata parts of rasters are filtered to avoid the comtamination of training dataset.

This model uses AdamW optimizer with an initial learning rate of $5 \times 10^{-4}$ and a weight decay rate of $1 \times 10^{-4}$, training for 15 epochs. The model also applied ReduceLROnPlateau learning rate scheduler. When the validation loss no longer improves, the learning rate is automatically reduced by 0.5 times, allowing the model to make more refined parameter tuning, enhancing the capability to characterize spatial temperature heterogeneity.

To quantify prediction performance, the model uses four metrics: Root Mean Squared Error (RMSE), Mean Absolute Error (MAE) and Coefficient of Determination ($R^2$):

Root Mean Squared Error (RMSE): RMSE is the square root of MSE, and it has the same unit as the predicted variable (for example, °C). As a result, it is easier to interpret the actual magnitude of the error.

$$\mathrm{RMSE} = \sqrt{\frac{\sum_{i=1}^{n} \left(y_i - \hat{y}_i\right)^2}{n}}$$

Mean Absolute Error (MAE): MAE represents the average absolute error between predicted and actual values. Compared to MSE/RMSE, MAE is less sensitive to extreme errors and better reflects the overall average deviation.

$$\mathrm{MAE} = \frac{1}{n} \sum_{i=1}^{n} \left| y_i - \hat{y}_i \right|$$

Coefficient of Determination ($R^2$) is used to assess the degree of fit between the predicted values and the reference data. It measures the model's ability to explain the variance of the value. The closer $R^2$ is to 1, the closer the model's predicted values are to the reference values.

$$R^2 = 1 - \frac{\sum_{i=1}^{n} \left(y_i - \hat{y}_i\right)^2}{\sum_{i=1}^{n} \left(y_i - \bar{y}\right)^2}$$

In these formula, $y_i$ represents the ground truth, $\hat{y}_i$ represents the prediction value, $n$ represents total number of samples, and $i$ represents sample index.

### 5.8 General Workflow

After the preparation of all the spatial raster datasets, MRT is simulated based on the SOLWEIG model using meteorological data (Table 4) Landcover, DBSM, DSM Vegetation, SVF, Wall Height and Wall Aspect for the period between 10 August and 14 August 2022. For day conditions, MRT are calculated for peak hours between 12:00 and 16:00, while for night conditions, MRT is calculated from 22:00 and 06:00.

Next, the nighttime MRT is processed using UMEP to calculate the average nighttime MRT.

Using the MRT data, PET is determined. For day conditions, PET are calculated using MRT, Meteorological data and Wind speed between 12:00 and 16:00. In addition, nighttime PET is determined using averaged nighttime MRT data to calculate PET.

The MRT and PET rasters and spatial rasters will be used to train 4 U-Net models: MRT Daytime model, MRT Nighttime model, PET Daytime model, PET Nighttime model,

For the prediction, 4 U-Net models are created to predict the outdoor thermal environment. Two models are used to predict the daytime MRT and PET during the afternoon period (12:00-16:00), while the other two models are used to predict the average nighttime MRT and PET.

To save computational time in the analysis of the thermal environment, firstly, the process starts by using the trained model in predicting the distribution of MRT based on the spatial datasets. After this, the predicted MRT will be used as another input in the prediction model of PET. In this way, the PET can be predicted in a very quick way without going through the full simulation process.

| Date | Max Air Temperature (°C) | Min Air Temperature (°C) | Max Solar Radiation Kdn (W/m$^2$) | Average Wind Speed (m/s) | Average Relative Humidity (%) |
|---|---|---|---|---|---|
| 8.10 | 28.8 | 14.4 | 802.78 | 3.3 | 59 |
| 8.11 | 31.1 | 15.8 | 802.78 | 3.2 | 56 |
| 8.12 | 31.4 | 16.6 | 791.67 | 3.0 | 55 |
| 8.13 | 31.2 | 15.5 | 802.78 | 2.7 | 49 |
| 8.14 | 31.1 | 16.7 | 791.67 | 2.3 | 54 |

**Table 4:** Daily Meteorological data for 10–14 August 2022. (Source: KNMI)

# 6. MODEL EVALUATION AND REFLECTION

6.1 MRT Model Performance  Evaluation

6.2 PET Model Performance  Evaluation

6.3 U-Net Model Reflection

## 6.1 MRT Model Performance Evaluation

Since the training set only included a small area around Rotterdam Central Station (Figure 6.2), the model could not generalize to areas outside this spatial range. Therefore, the validation set consisted of another area in Rotterdam city center (Figure 6.3), which was not included in the training set, to ensure that the model does not overfit to the Rotterdam central area during training. This study tests three different training strategies for U-Net model in predicting MRT during heatwave based on the U-Net structure (Figure 6.1).

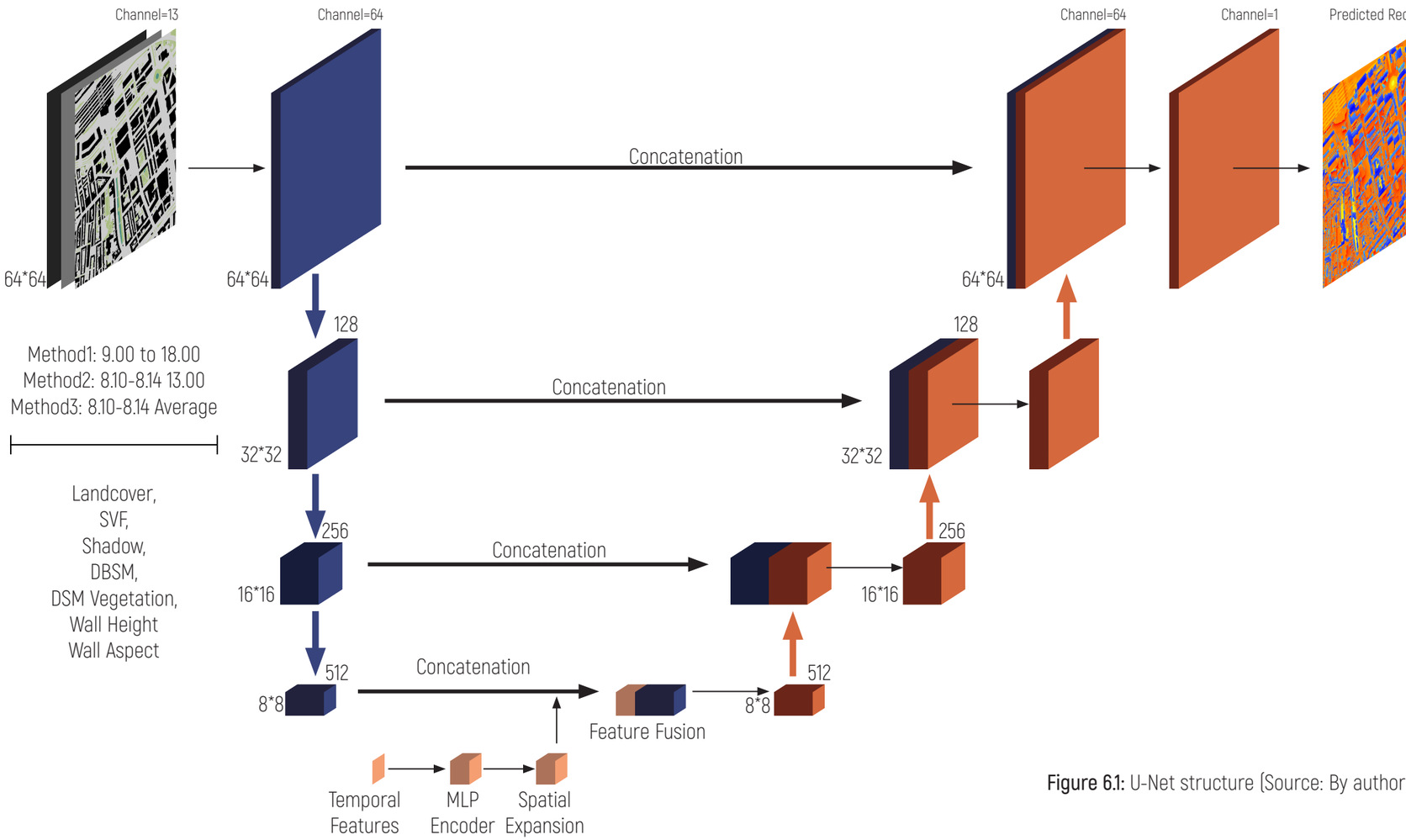



**Figure 6.1:** U-Net structure (Source: By author)



**Figure 6.2:** Training Area (Source: By author)



**Figure 6.3:** Testing Area (Source: By author)

The first method used MRT data from a single heatwave day, where the MRT data from 09:00 to 18:00 at hourly intervals was used, with the time of day being an additional parameter. As presented in the results, the model performs well in predicting MRT, with an MAE ranging from 1.20 to 1.64 °C, and an RMSE ranging from 2.08 to 3.27 °C, with an $R^2$ of 0.92 (Figure 6.2).

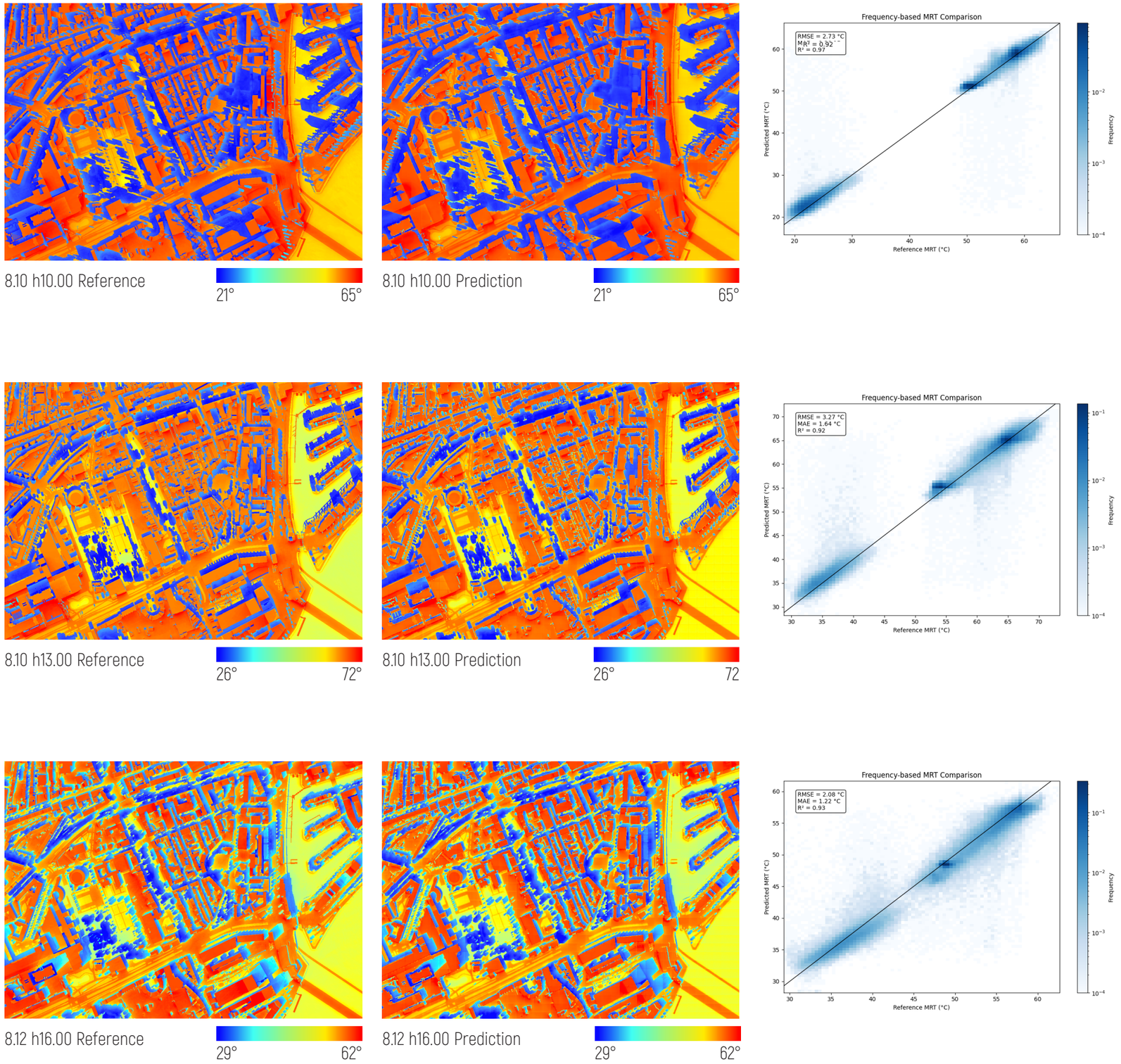
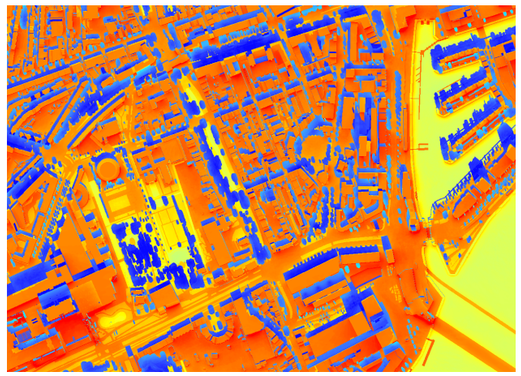


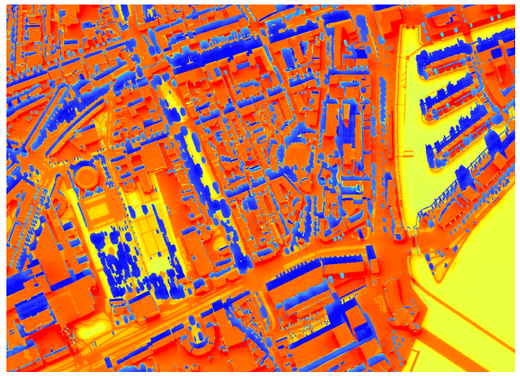

**Figure 6.2:** First Method Comparison (Source: By author)

The second method is based on predicting MRT at a specific time in the afternoon, where MRT data at the same hour (13.00) from August 10 to August 14 was used, with the daily maximum air temperature being an additional parameter. The results show the model performed well in predicting MRT, with an MAE of 1.77 °C, an RMSE of 3.52 °C, and an $R^2$ of 0.91. While using the same in testing the densification scenario, it gets an MAE of 1.82 °C, an RMSE of 4.02 °C, and an $R^2$ of 0.91, which represents a considerable drop in accuracy (Figure 6.3).



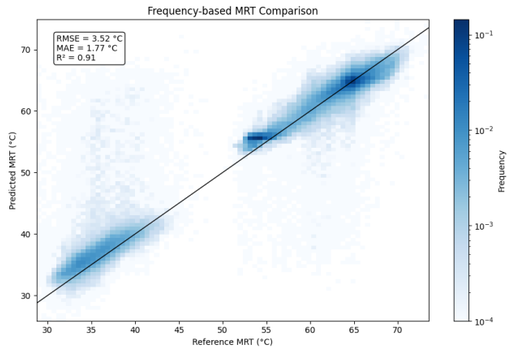
8.10 h13.00 Reference

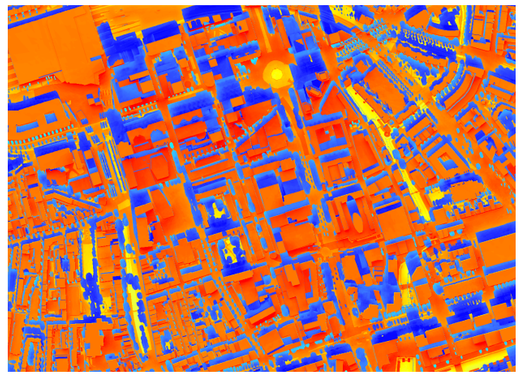


8.10 h13.00 Prediction

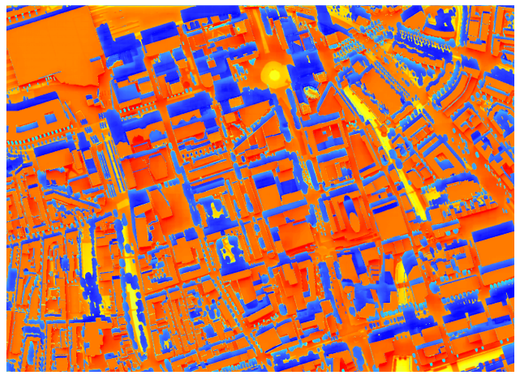


8.10 h13.00 Reference



8.10 h13.00 Prediction



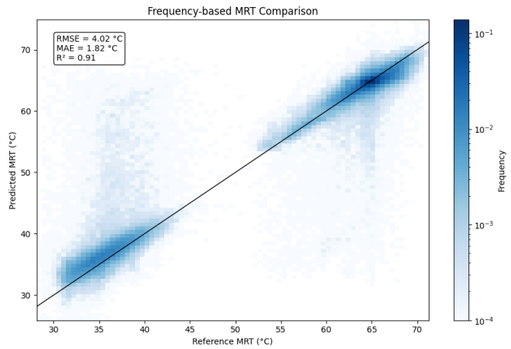
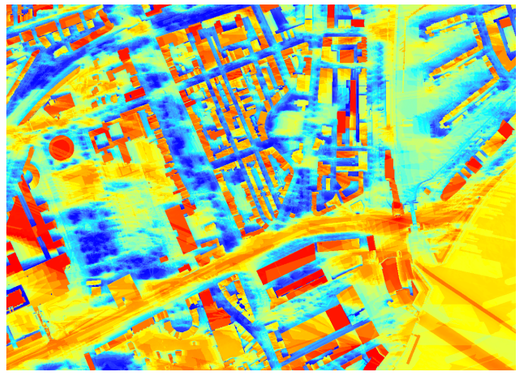
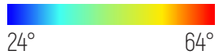



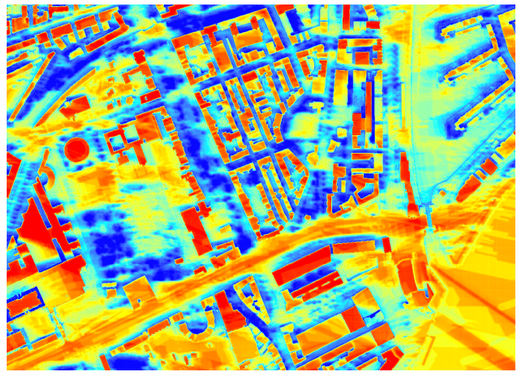

**Figure 6.3:** Second Method Comparison (Source: By author)

The third method uses the average MRT during the daytime and nighttime, calculated from the MRT data from August 10 to August 14, while introducing the daily maximum air temperature as an additional parameter. The model reaches an MAE of 2.22 °C, a RMSE of 2.78 °C, and a $R^2$ of 0.92 for the daytime MRT. For the nighttime MRT prediction, the results show an MAE of 0.09 °C, an RMSE of 0.18 °C, and an $R^2$ of 0.95 (Figure 6.4).

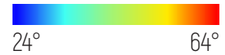


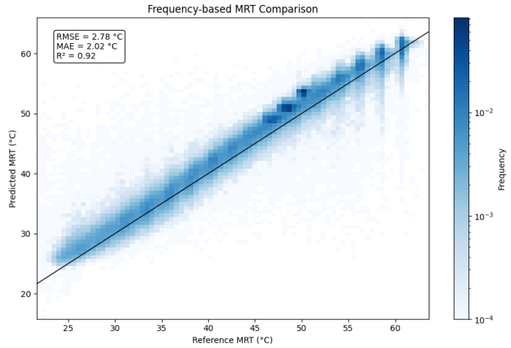
8.10 Day Average Reference

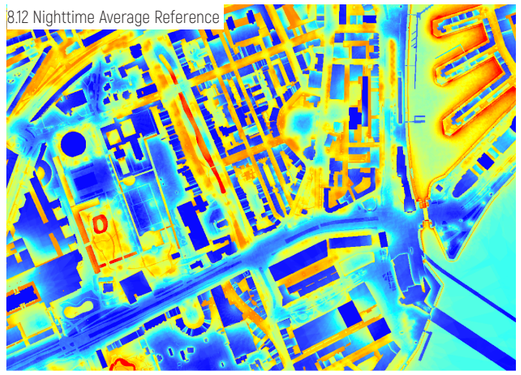


8.10 Day Average Prediction

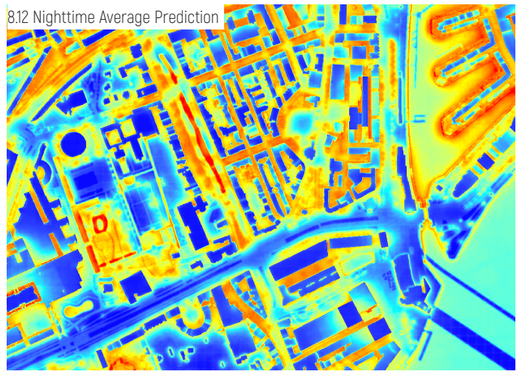



8.10 Night Average Reference




8.10 Night Average Prediction



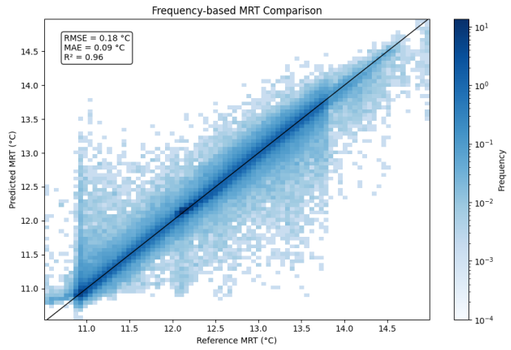




**Figure 6.4:** Third Method Comparison (Source: By author)

From the results, all three training methods exhibited high levels of accuracy in the experiment compared with other related research. For example, Briegel and colleagues achieved an MRT prediction accuracy with an $R^2$ of 0.92, and MAE within 2.4k. In addition, Zahra Rashtian and colleagues achieved a maximum MRT prediction accuracy with an $R^2$ of 0.93. The first technique performed marginally better compared to the second one. This could be attributed to the fact that it uses a bigger dataset for training purposes.

Likewise, good performance is also occured from the model trained on average nighttime MRT. This may be explained by the fact that the range of variation of nighttime MRT is relatively limited. The difference between the highest and lowest temperatures is generally within 5 °C, and the nighttime MRT is mainly dominated by longwave radiation, exhibiting smoother spatial and temporal variations, which makes the prediction task less complex. compared to daytime conditions.

### 6.1.1 Optimized Deep Learning modelling

The purpose of this study are to assess the high-density development scenario in Rotterdam under heatwave conditions in order to maximize both daytime cooling and nighttime heat retention. This can be realized through modeling under two different time zones – day and night.

For the daytime model, in order to achieve both accuracy and flexibility in the model, a combined approach to training was employed by mixing the first and second methods. Specifically, the model was employed by utilizing data from MRT between 12:00 and 18:00 from August 10 to August 14, which are the maximum heat stress hours. The time of day and daily maximum air temperature (Tmax) were also employed as additional inputs. The model has good predictive ability for the MRT in different times in a new test area, with MAE values of 1.02 and 1.51 °C, RMSE values of 1.84 and 3.20 °C, and $R^2$ values of 0.93 and 0.95. (Figure 6.5).

Furthermore, the final model is used for the prediction of the MRT in high-density development scenarios and was compared with the SOLWEIG results. The results show good fit of the models, with MAE values of 1.12 and 1.44 °C, RMSE values of 2.17 and 3.65 °C, and $R^2$ values of 0.93 and 0.95 (Figure 6.6).

For the nighttime the model will be trained using the third method, employing the average MRT data from the night of August 10th to 14th.

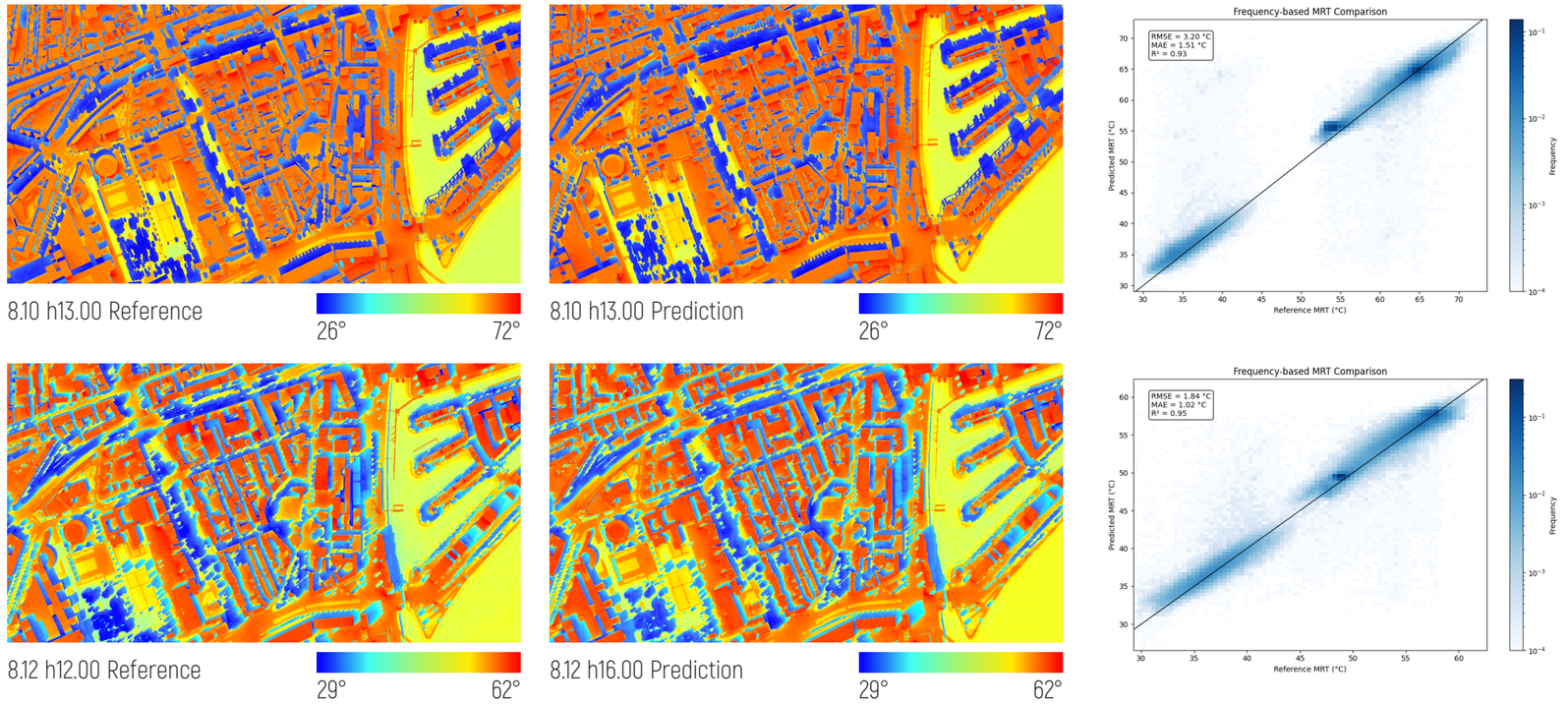



**Figure 6.5:** MRT Comparison (Source: By author)

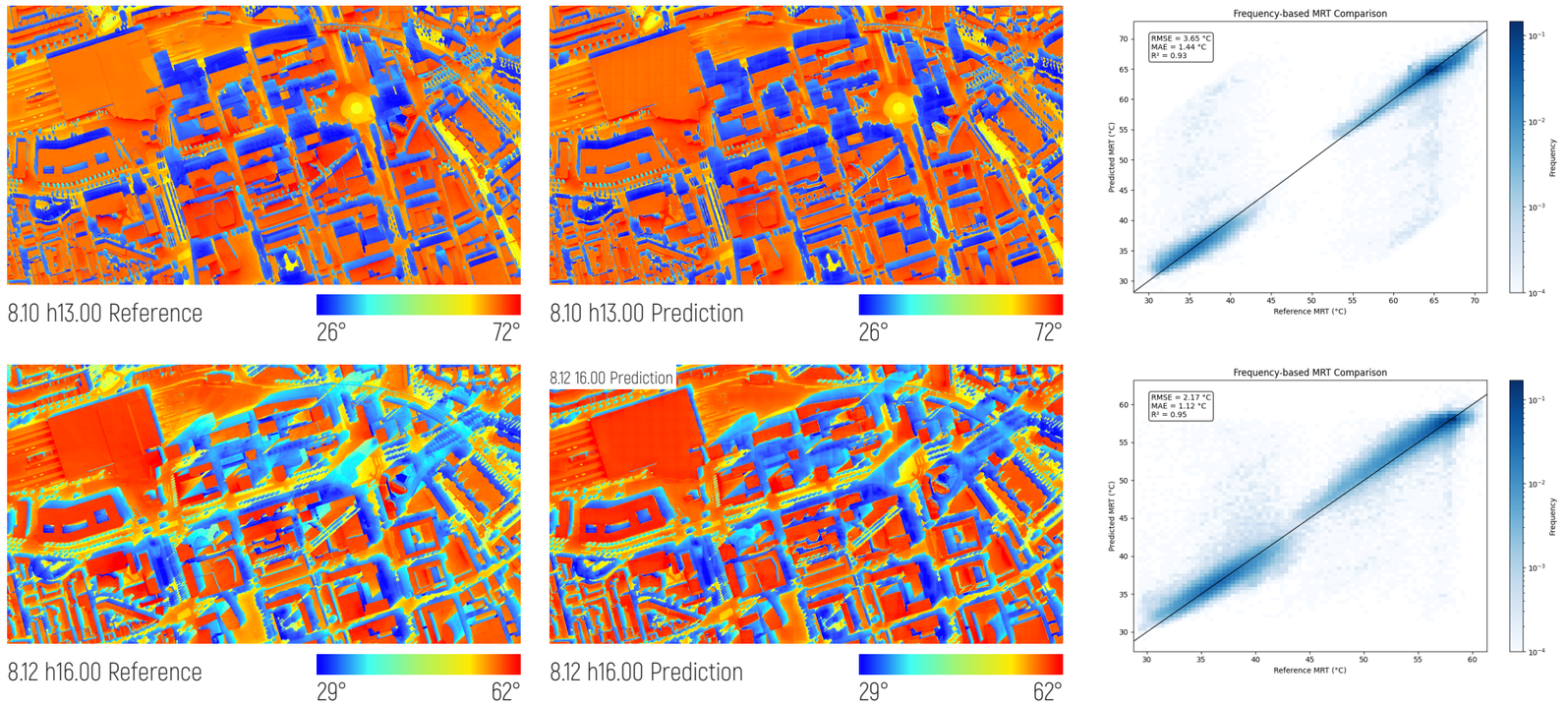


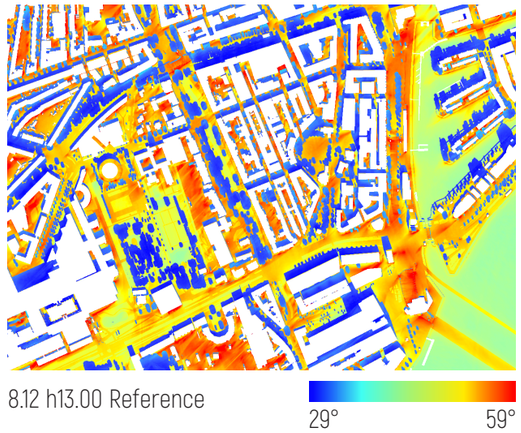

**Figure 6.6:** MRT Comparison Densification Scenario (Source: By

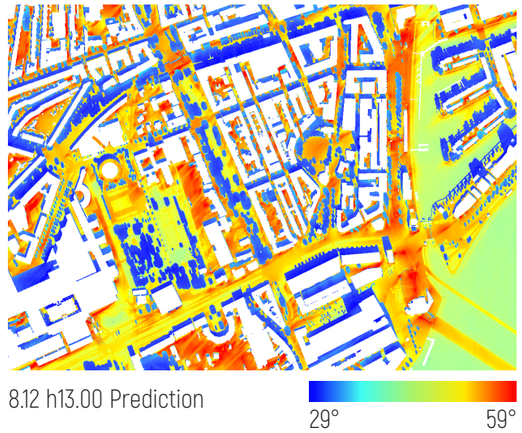
## 6.2 PET Model Performance Evaluation

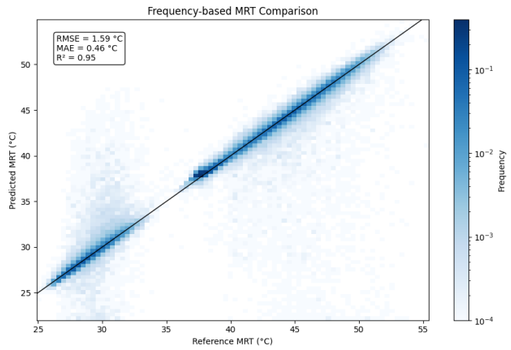
The PET model is trained based on the same strategies to that of the MRT model. For daytime, the training data consists of MRT data, land cover, and wind speed from 12:00 to 16:00 between August 10 and 14. For nighttime conditions, average MRT, land cover, and wind speed data are used over the same period.

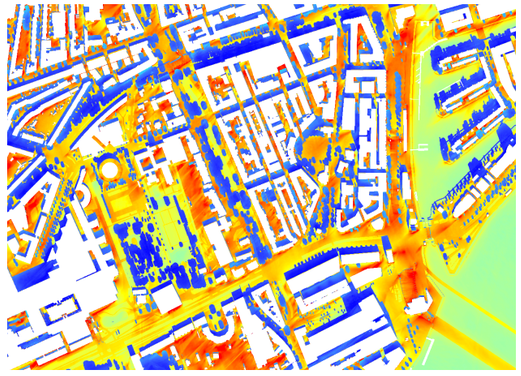
To test and examine the accuracy of the PET model, two different types of MRT data are utilized as model inputs: one is based on the SOLWEIG model, and the other is based on the U-Net model(Figure 6.7). When SOLWEIG data is utilized as an input to the PET model (e.g., August 10, 13:00), high accuracy is achieved with an MAE of 0.46°C, an RMSE of 1.59°C, and an $R^2$ of 0.95. When U-Net data is utilized, the errors are slightly increase (MAE of 0.93°C, RMSE of 1.99°C), while still maintaining high accuracy ($R^2$ of 0.91).

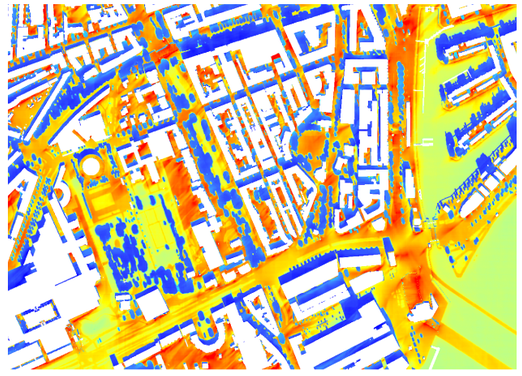
For nighttime conditions, when U-Net data is utilized, high accuracy is achieved with an MAE of 0.09°C, an RMSE of 0.15°C, and an $R^2$ of 0.95.

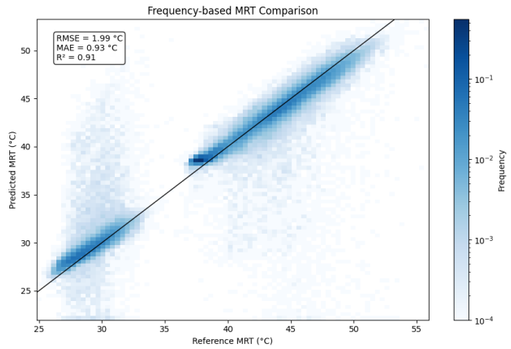


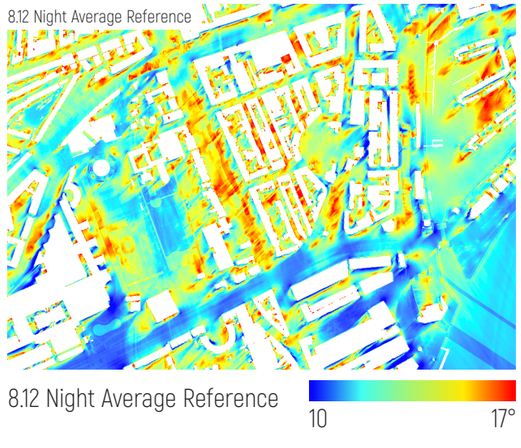



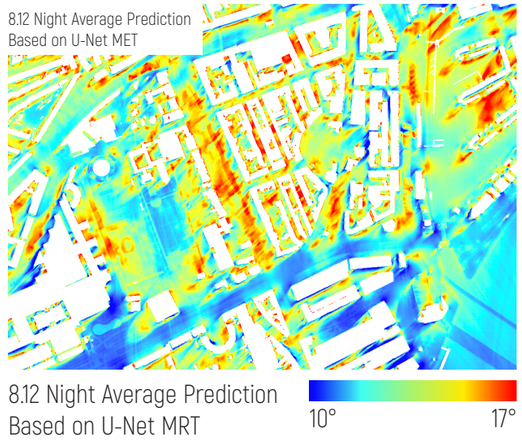



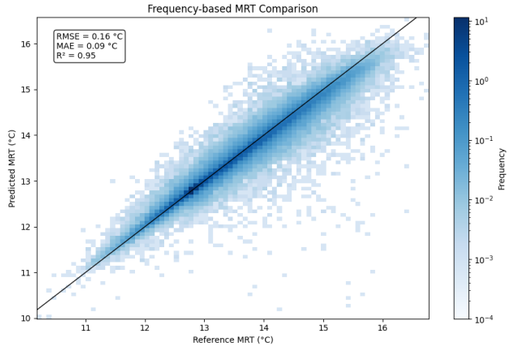




**Figure 6.7:** PET Comparison (Source: By author)

### 6.3 U-Net Model Reflection

Overall, these four U-Net models show good predictive performance and maintain good accuracy in preserving fine-scale spatial details. For instance, while forecasting MRT at 16:00, the U-Net model has the ability to infer updated surface temperatures under newly formed shading conditions based on previously learned surface thermal patterns. Even with minor differences between the results calculated by SOLWEIG, this still shows great spatial detail in modeling. The good performance of this model might be due to the fact that the prediction task is relatively clear and well-defined. The main spatial variables affecting MRT and PET, such as landcover, SVF, wind field, and shadow, are included in the training dataset. In comparison with Briegel et al. (2023), this study uses shadow raster input, which helps to avoid the weakness of low accuracy in complex shadow situations, especially in the high dense urban district.

In relation to the PET model performance, it can be seen that the accuracy is within a satisfactory range. Although the utilization of MRT predicted by the U-Net model increases the error, compared to the inputs calculated from the SOLWEIG model, the overall accuracy of the PET prediction is within an acceptable range. What is most important is that from the observation, the spatial patterns like wind field are still captured by the U-Net model.

Despite these positive results, there are still some weaknesses. Firstly, this model is specifically used under heatwave conditions. As a result, it is only efficient for extreme thermal situations. It would be difficult to apply this model to milder situations. Secondly, there is an increase in prediction error when this model is used for high-density development scenarios with building heights outside the training dataset (e.g., above 286 m). This indicates its weakness in unseen situations.

Despite these weaknesses, this model still presents good predictive results. More importantly, compared with SOLWEIG model results, this model reduces computation time significantly. This makes it an efficient tool for evaluating various urban planning scenarios.

# 7. HEAT-SENSITIVE DESIGN EXPLORATION

7.1 Design Site

7.2 Thermal Environment Comparison Before and After Densification

7.3 Spatial Scenarios Exploration

7.4 Building Morphology Exploration

## 7.1 Design site

According to Rotterdam municipality, the study area is situated in the RCD-XL district of Rotterdam (Figure 7.1) which has become one of the key areas for densification. In order to cope with the growing demand of housing requirement, several projects have been planning actively.

RCD-XL district is characterized by a concentration of new residential buildings and mixed-use developments such as Hofpleintoren (286 m), Weenatoren (158 m), CoolSingelTorens (143 m), Schiekadeblok (up to 200 m), Weena 70 (200 m and 150 m), Lumiere (155 m), and Treehouse (130 m) (Table 4).

Due to the scale and intensity of planning measures, the hofplein-RCD-XL area provides a representative example for the research of vertical heat-sensitive densification and heat exposure at the pedestrian scale because these planning projects significantly increased the site's original average building height, building density, and spatial enclosure.

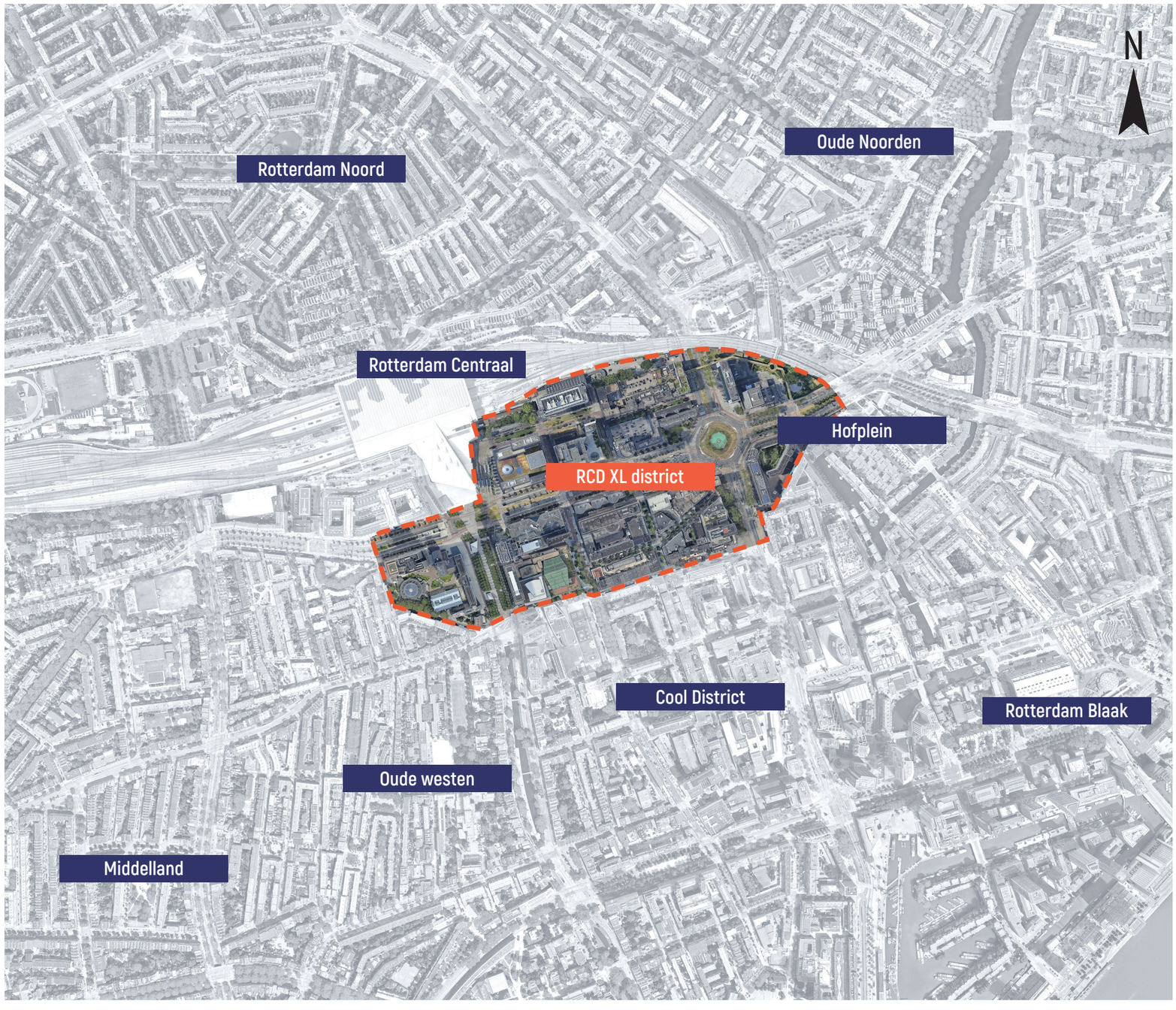



**Figure 7.1:** Research Location (Source: By Author)

The Floor Space Index (FSI) is a ratio of a building's total floor area to the size of the piece of land upon which it is built. It is often used as one of the regulations in city planning along with the building-to-land ratio. FSI reflects development intensity; a higher value indicates a higher development intensity in the region. FSI can be calculated according to the following formula. The present average FSI of the study area is estimated at 3.6, and the FSI of the proposed densification scenario provided by Rotterdam municipality is increased to approximately 5.8.

$$\mathrm{FSI} = \frac{\text{Total Floor Area}}{\text{Site Area}}$$

| District | Project | Tower | Height (m) |
|---|---|---|---|
| Stadsdriehoek | Post | Toren 1 | 155 |
| | Pompenburg | Toren 1 | 125 |
| | | Toren 2 | 115 |
| | | Toren 3 | 70 |
| | | Toren 4 | 70 |
| | Rise | Hofpleintoren | 286 |
| | | Weenatoren | 158 |
| | | Coolsingeltoren | 143 |
| CS-Kwartier | Treehouse | Toren 1 | 130 |
| | Schiekadeblok | Toren 1 | 200 |
| | | Toren 2 | 70 |
| | The Modernist | Toren Noord | 70 |
| | | Toren Zuid | 125 |
| Cool | Weena 70 | Toren 1 | 200 |
| | | Toren 2 | 150 |
| | Lumiere | Toren 1 | 155 |

**Table 4:** New Development of RCD-XL district (Source: Rotterdam Municipality)

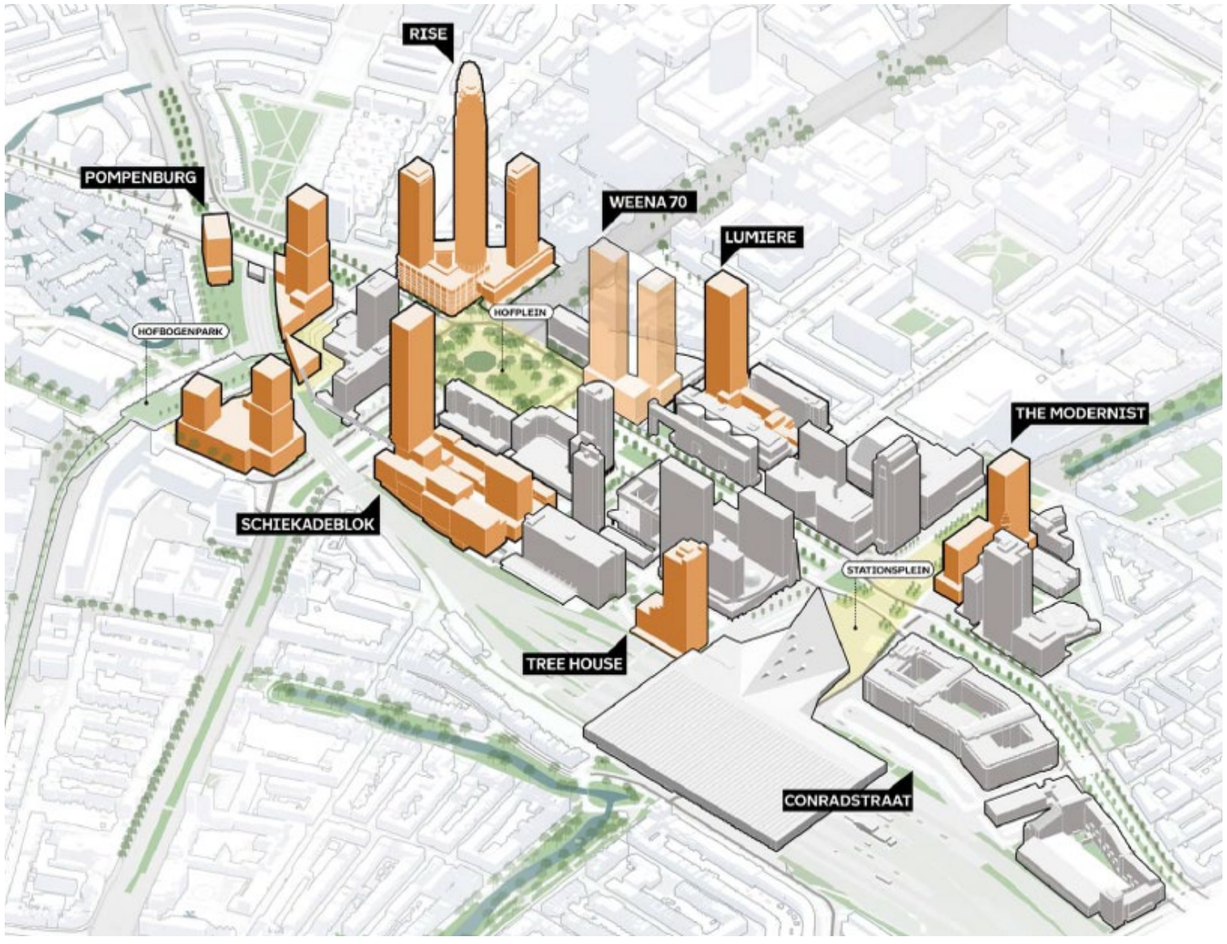



**Figure 7.2:** New Development of RCD-XL district (Source: Rotterdam Municipality)

## 7.2 Thermal Environment Comparison Before and After Densification

This study will compare the thermal environment of the densification scenarios and current situation based on MRT (Figure 7.3) and PET (Figure 7.4), using August 12 as an extreme example of heatwave conditions in the Netherlands. This assessment will be carried out for 13:00, 16:00, and nighttime, with 13:00 being an hour of minimum shade and 16:00 normally being the hottest hour in a day.

### 7.2.1 MRT Result

During the daytime, MRT experiences a drop after densification. Precisely speaking, at 13.00, the average MRT temperature on the street decreased by approximately 0.41°C. At 16.00, the average MRT temperature on the street decreased by approximately 1.48°C. The improvement is mainly because of the fact that the new high-rise buildings create more shading area on the street than previous buildings, which reduces effectively the impart of direct shortwave radiation on pedestrian areas.

During the nighttime, MRT increases slightly from observed. On average, the street MRT grows around 0.12°C. Although the overall change is slight, the temperature, however, rise more significantly in certain blocks, ranging from around 0.5°C to 1.4°C under windless conditions . This phenomenon can be explained by the reduce of SVF brought by densification, restricting the capablity to release

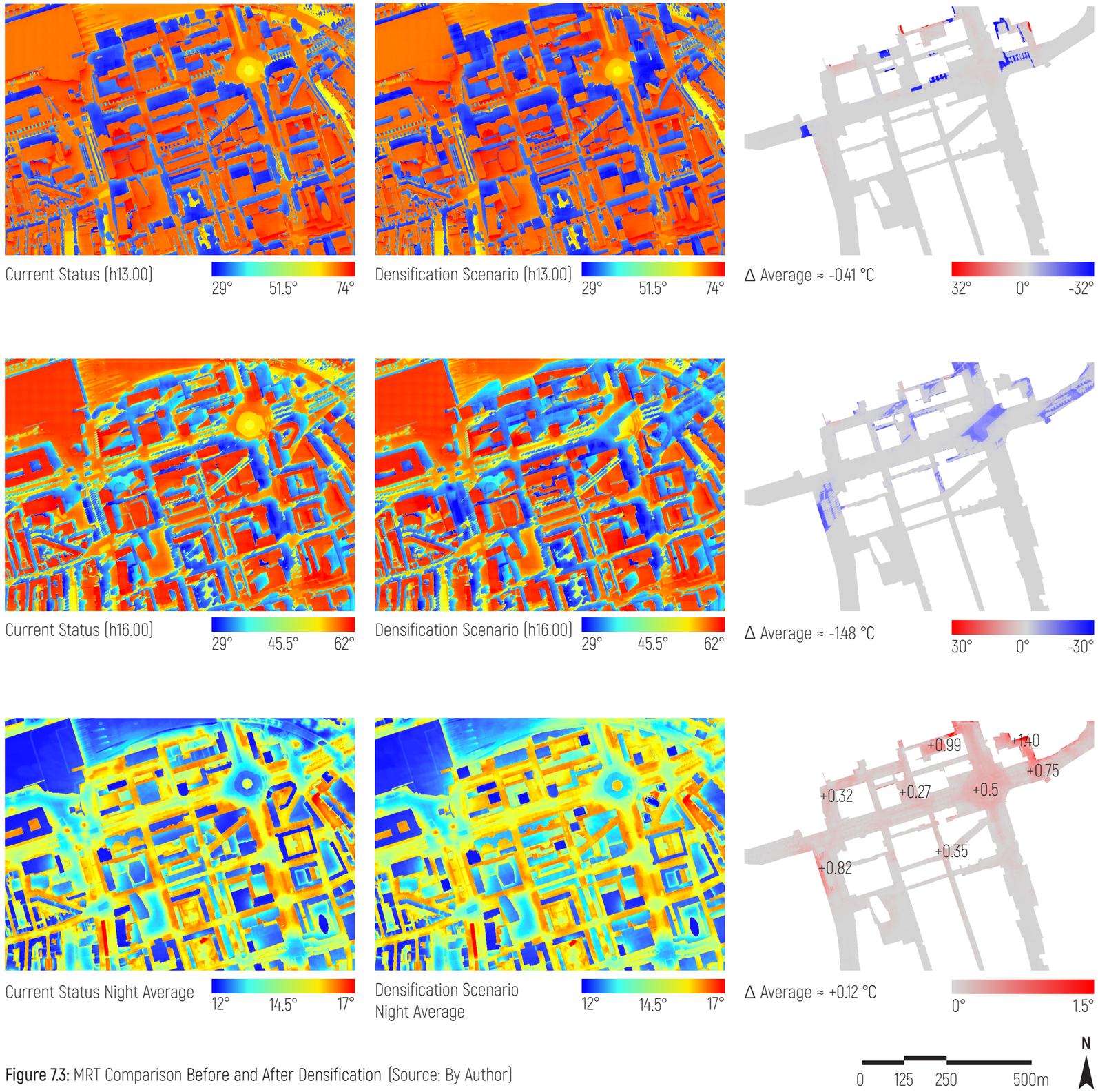



**Figure 7.3:** MRT Comparison Before and After Densification (Source: By Author)

longwave radiation into the sky, leading to the higher heat retention and higher MRT.

### 7.2.2 PET Result

As a result of the development of a number of high-rise buildings, the wind field is also affected. In certain areas, the wind speed is increased due to the street canyon effect of the high-rise buildings, while in some areas the wind speed was reduced due to the increased wind resistance. Nevertheless, the wind environment as a whole did not change significantly as a result of the densification.

During the day, solar radiation remains the major factor affecting the PET. Therefore, the increased shading effect resulting from the development of high-rise buildings had a significant effect on the PET. At 13:00 hours, the average street PET was reduced by 0.82°C as a result of the development. At 16:00 hours, the effect was more pronounced, with the average street PET reduced by 1.26°C.

At night, the effect of shortwave radiation is absent, and the dominant factors for the PET are air temperature, longwave radiation exchange, and wind speed. In comparison to daytime, the effect of wind speed is more prominent for determining human thermal comfort at night.

Changes in the pattern of airflow due to the incorporation of new high-rise buildings: Due to the formation of deeper street canyons,

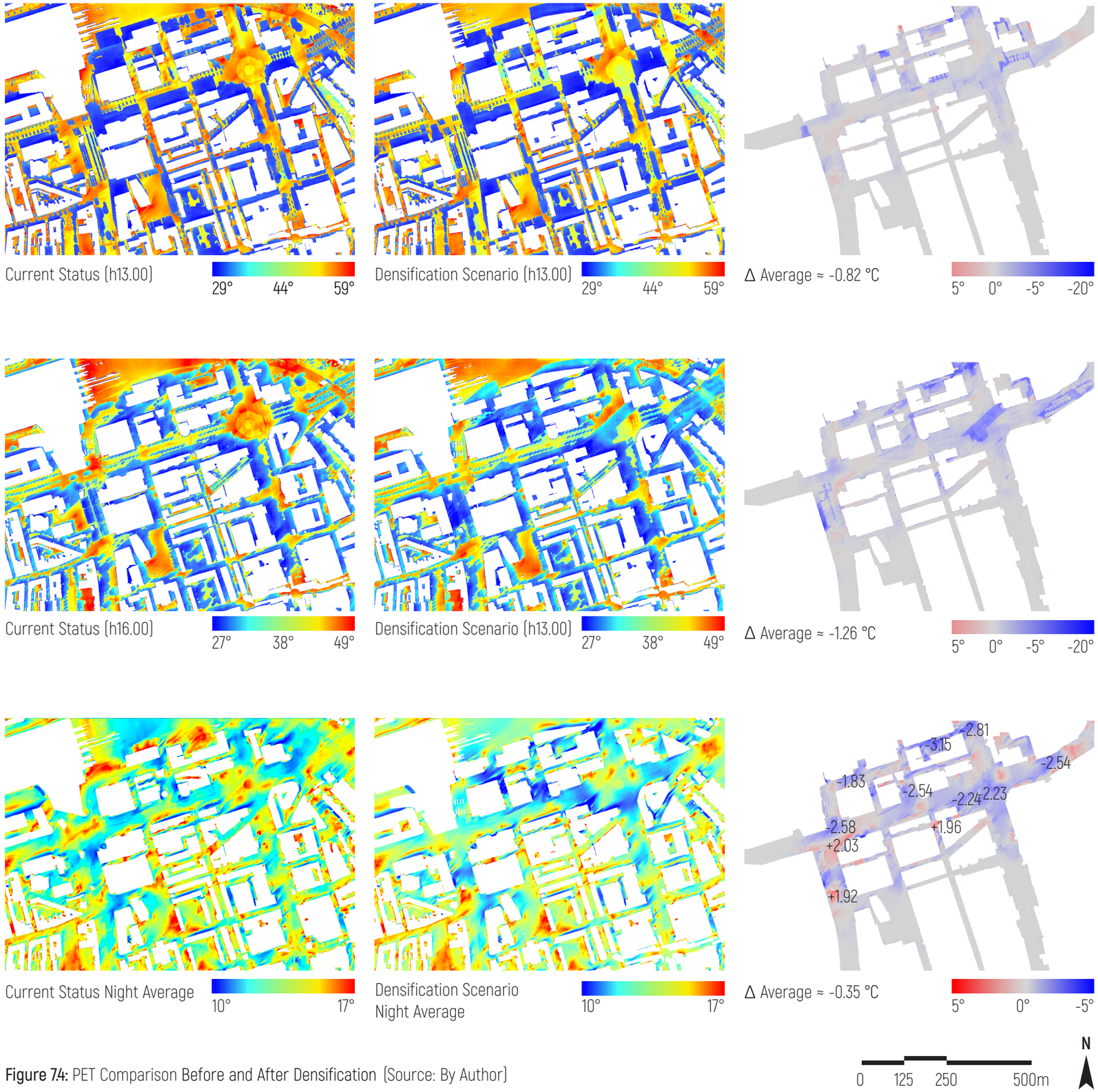



**Figure 7.4:** PET Comparison Before and After Densification (Source: By Author)

the wind speed increased in certain streets, whereas it decreased in other streets due to increased aerodynamic resistance. This shows that densification affects the wind environment at the micro-scale rather than changing the ventilation conditions uniformly.

On the other hand, under windy conditions, the average nighttime PET for the streets showed a slightly reduced value after densification by approximately 0.35°C. This is because of the wind speed is increase due to the deeper street canyons, which enhances the convective heat loss from the human body. At the same time, the increase in MRT because of reduced SVF has been offset by the decreasing in PET caused by the increasing wind speed.

### 7.2.3 Conclusion

In general, under the test condition, the increase in FSI results in an obvious drop in daytime thermal stress in that there will be more shading projected by buildings. During the windless nighttime, total changes in temperature will not be significant but there will be a local warming effect caused by the lower SVF which lead to the higher heat retention. For windy night-time periods, PET exhibits a moderate overall decrease, with more pronounced cooling in localized areas driven by enhanced windflow within deeper street canyons.

## 7.2 Design Logic

Although the cooling effect found in the Rotterdam densification scenario is promising, it does not mean that the effect of increased density always contributes to the outdoor thermal environment. Therefore, further research will be carried out to determine if the values of MRT and PET continue to decrease as the floor space index (FSI) increases. In addition, different densification strategies will be examined, including horizontal development, vertical development and a combination of both, in order to determine which can be the most beneficial to the urban outdoor thermal environment.

The floor space index (FSI) of the RCD XL district is currently at 3.6, and the Rotterdam municipality densified development plan has an FSI of 5.8. According to this information, this study aims to further investigate the effect of various urban spatial configurations in higher density conditions on the outdoor thermal environment, and compares it with the densification scenario from the Rotterdam Municipality.

In order to systematically study of the effect of densification on outdoor temperature, three major urban development strategies were utilized, including horizontal development, vertical development, and combining both strategies. These strategies are typical approaches to urban morphology in developing high-density areas.

The primary objective of the spatial design is to reduce daytime shortwave solar radiation, which is the primary driver of MRT during heat waves in day time. Therefore, shading strategies were prioritized (Lai et al., 2017). Accordingly, six spatial design schemes were included. These schemes are west side building layout for afternoon shading, south side building layout for solar obstruction during midday hours, non-central building placement for shadows to fall on the streets and not on the roofs, decentralized building layout for ventilation corridors and more evenly distributed shading, north-south tower orientation for reduced solar exposure on building facades, and tower placement on street intersections for maximum shading coverage. These spatial design schemes cover different arrangements of building volume and tower location within the study area.

Aside from the proposed densification strategy of increasing the FSI to 5.8, this study will test higher-density schemes, specifically increasing the FSI to 6.5 and 7.0, to explore the thermal performance of under the future higher-density layouts. These higher FSI scenarios are referenced from high-density cities such as New York and Hong Kong. For each FSI scheme, three urban development models and six design strategies were applied while keeping the FSI as a constant.

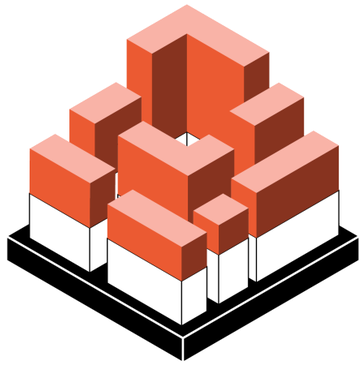
Figure 7.5 shows the design Logic of densification scenarios.

FSI = 3.6 Current

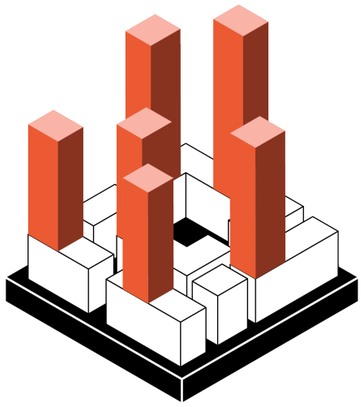
FSI = 5.8

FSI = 6.5

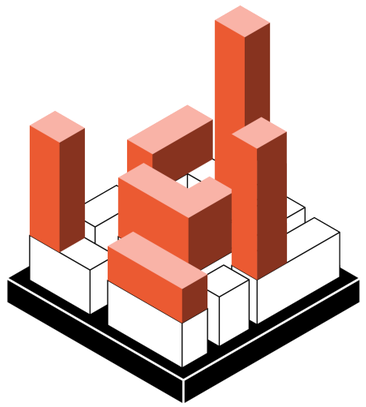
FSI = 7.0



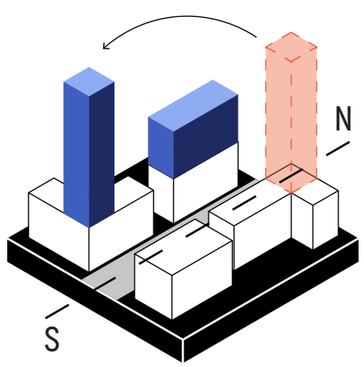
Horizontal Development



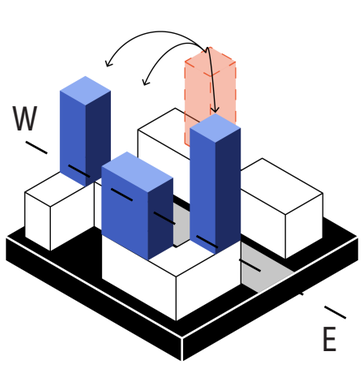
Vertical Development



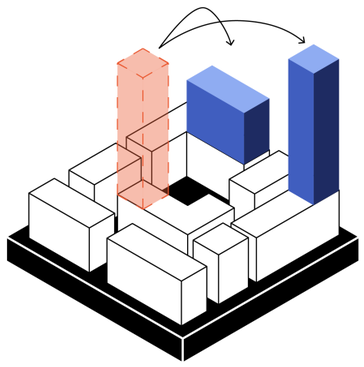
Combination



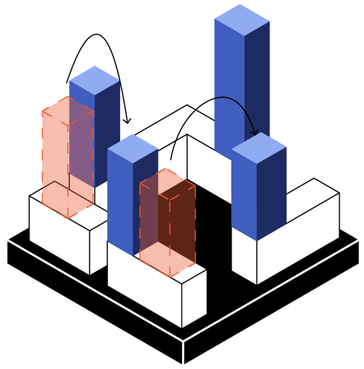

West-Side Building Layout



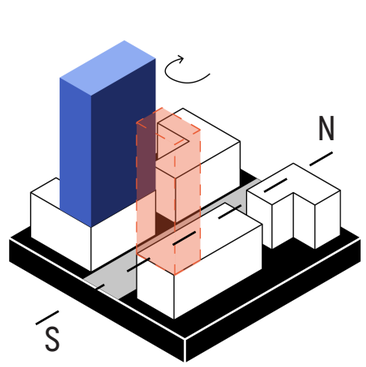

South-Side Building Layout



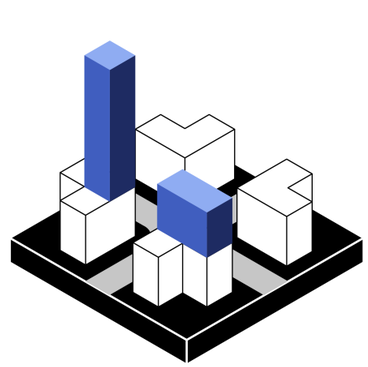
Avoid Central Placement



Decentralized Layout




North–South Tower Orientation



Towers at Street Intersection

**Figure 7.5:** Design Logic of Densification Scenarios. (Source: By Author)

## 7.3 Spatial Scenarios Exploration

### 7.3.1 FSI = 5.8 Horizontal Development

In Scenario 1, FSI is kept constant at 5.8. The high-rise towers in the original densification scenario are removed and replaced by increasing the height of podium buildings facing wider streets. Specifically, the building heights along the southern and western sides of the streets are increased to provide more shading coverage at the pedestrian level.

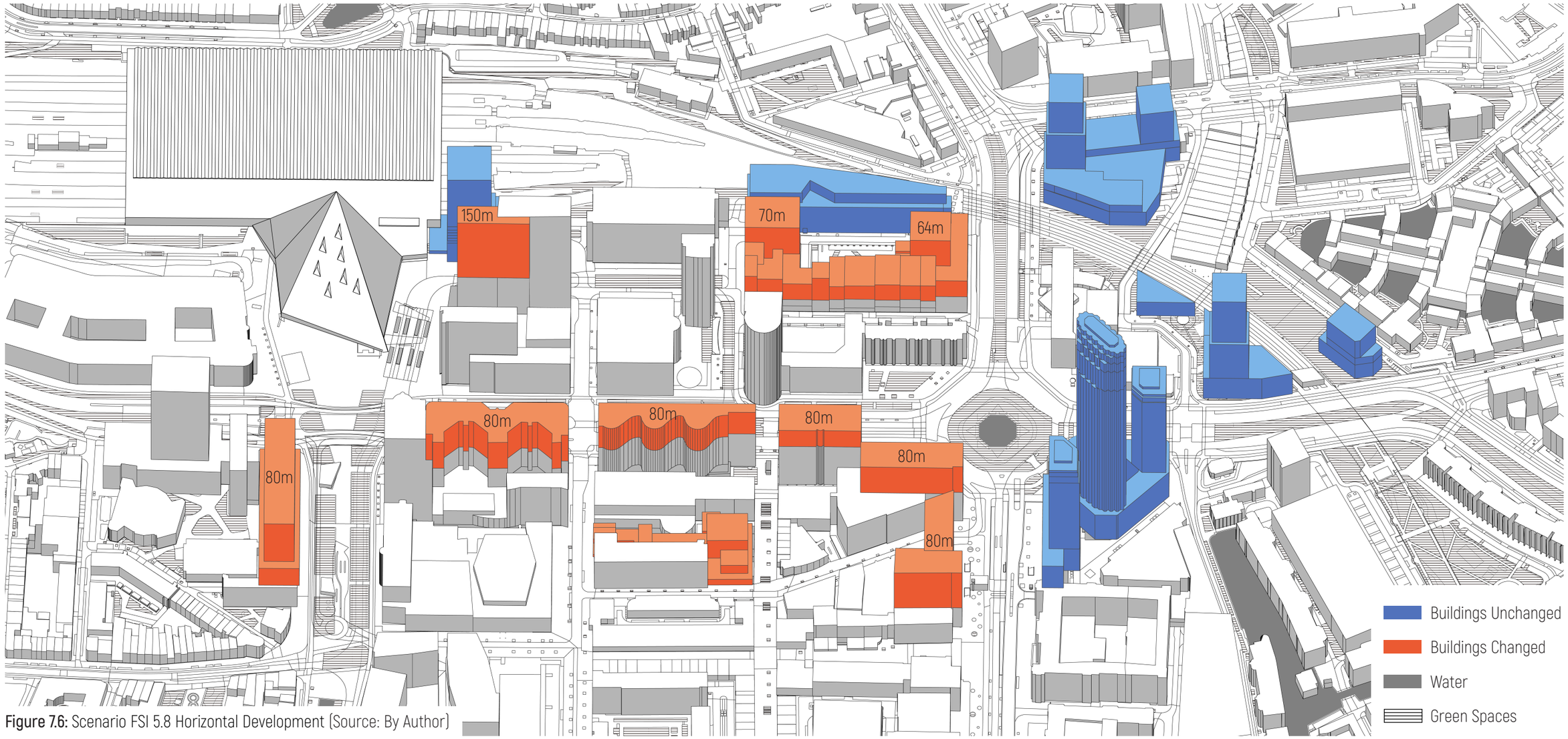



**Figure 7.6:** Scenario FSI 5.8 Horizontal Development (Source: By Author)

## MRT Result

For FSI 5.8, horizontal development results in more shading on the street level at 13:00. As a result, the MRT is reduced by an average of 1 °C compared with the original scenario. However, as time progresses to 16:00, as the solar altitude decreases and shadows become more directional, meaning that the horizontal development cannot make up for the loss of shading area provided by high-rise buildings. As a result, MRT increases in some areas, while on the street level, the average MRT remains unchanged.

Under windless nighttime conditions, the MRT slightly increases by 0.15 °C at certain points of the streets. At other points, however, MRT even drops as a result of the removal of high-rise buildings. In some narrow blocks, increased building height leads to more enclosed urban spaces and reduced sky view factor, resulting in localized MRT increases of up to 0.33 °C. In general, on average, MRT is almost unchanged.

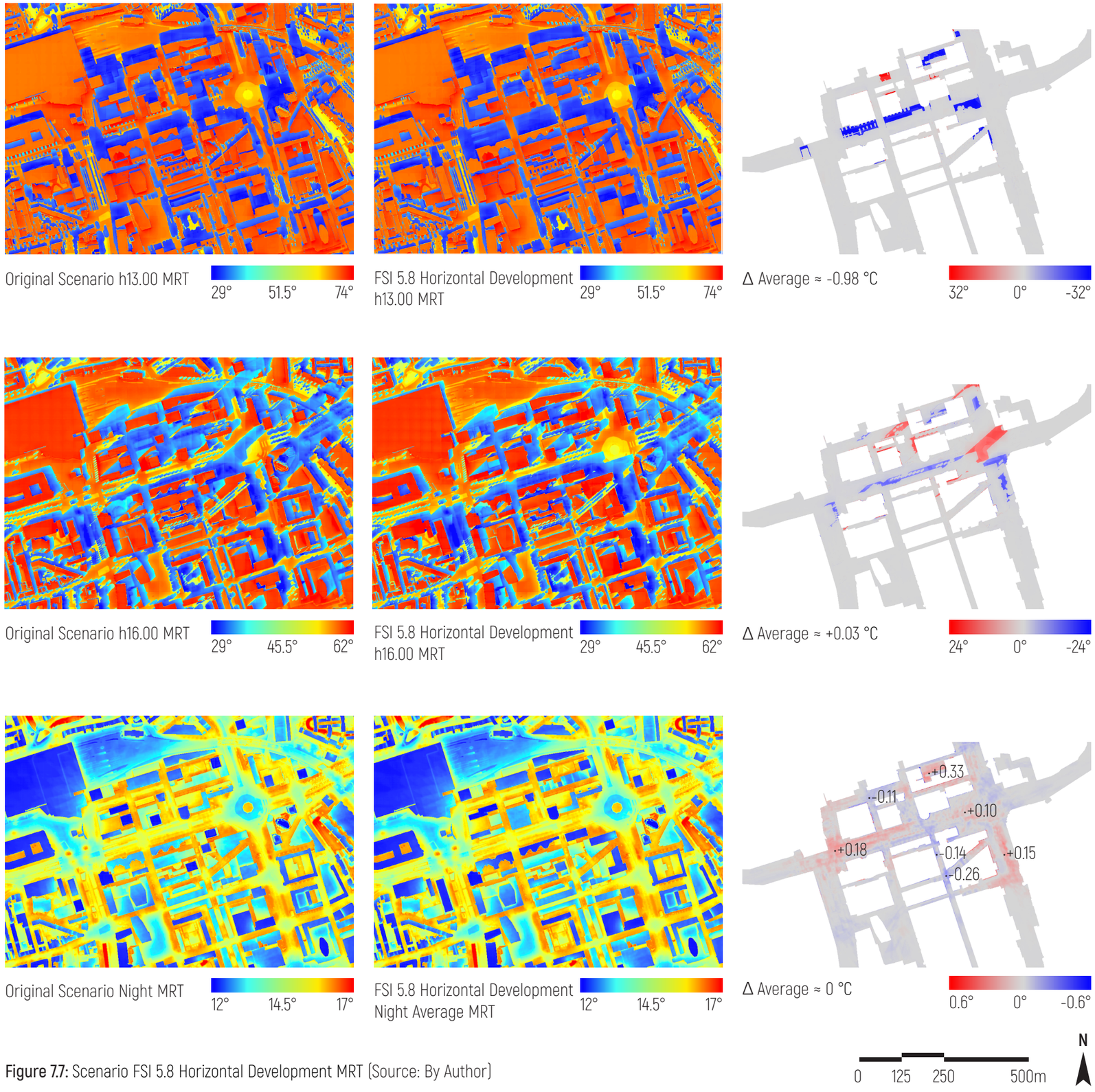



**Figure 7.7:** Scenario FSI 5.8 Horizontal Development MRT (Source: By Author)

## PET Result

At FSI 5.8, the effect of horizontal development on daytime PET is slight, as this is affected by both shading and wind conditions. At 13:00 hours, the average PET at street level decreases slightly by 0.17°C. However, at 16:00 hours, PET increases by 0.21°C. This is because the effect of shading, which is provided by the podiums, is dependent on time, and the effect of reduced wind speeds becomes more significant in the afternoons, thus offsetting the effect of reduced solar radiation.

At night, under windy conditions, PET is increased significantly. On wider streets and intersection areas, PET increases by 1.09 to 2.65°C. This is mainly attributed to the increased height of the podium, which obstructs airflow, thus reducing convective heat loss. However, the increased height of the podium also increases the wind speed on the same side of the street, resulting in a decrease in PET of approximately 2 °C compared to the original scenario.

In addition, along diagonal streets, the arrangement of higher podiums on both sides of the street creates wind corridors in the prevailing wind direction, resulting in increased wind flow and a reduction in PET by 1.84 °C.

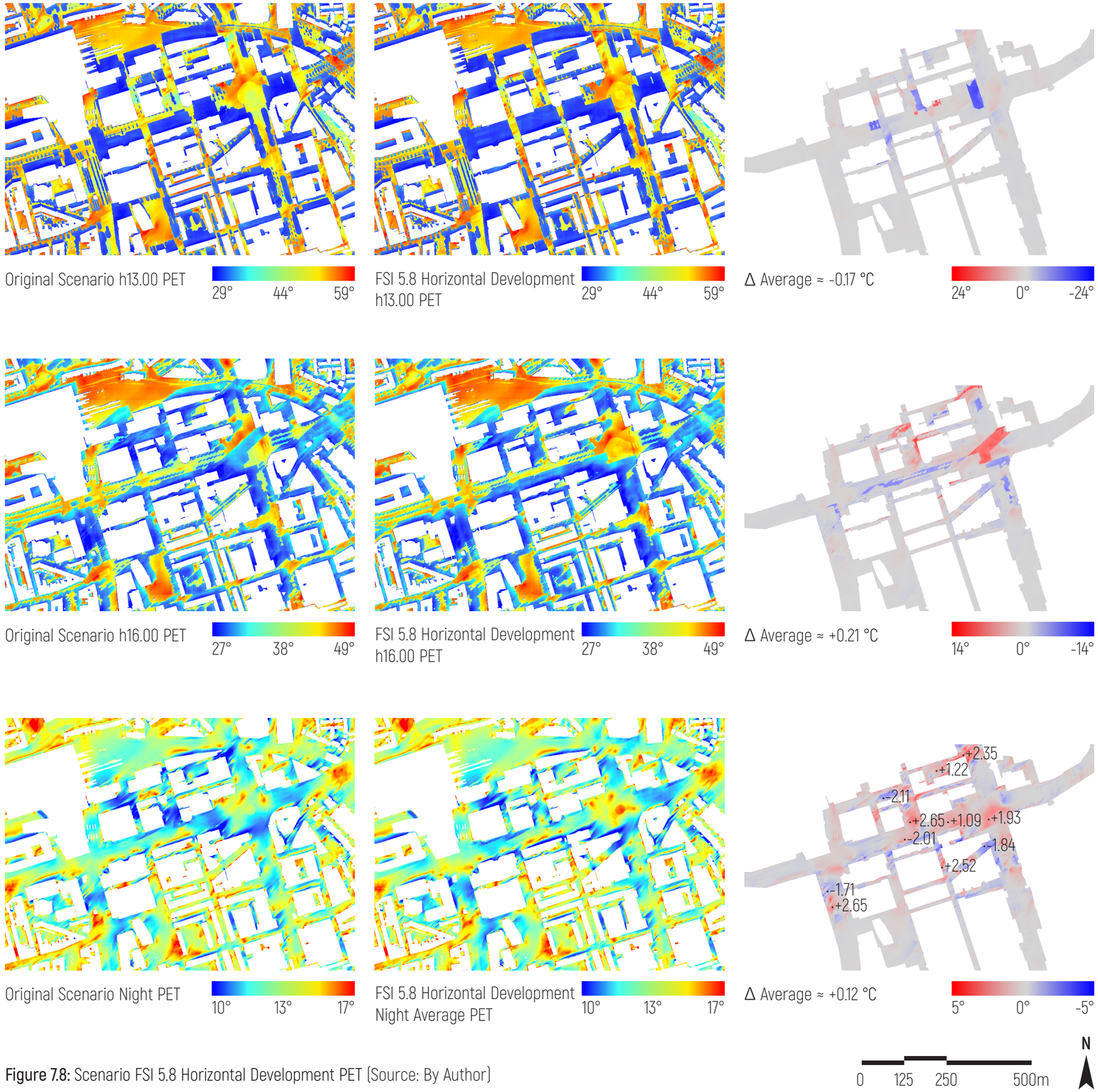



**Figure 7.8:** Scenario FSI 5.8 Horizontal Development PET (Source: By Author)

### 7.3.2 FSI = 5.8 Vertical Development

Under scenario 2, FSI is kept at 5.8. The main adjustment is relocated towers in the original plan. Some of those high-rise towers from the original densification scenario are moved closer to the wider streets, specifically on the southern and western sides. The propose of this is to maximize shading at street level by moving the towers into better shading positions.

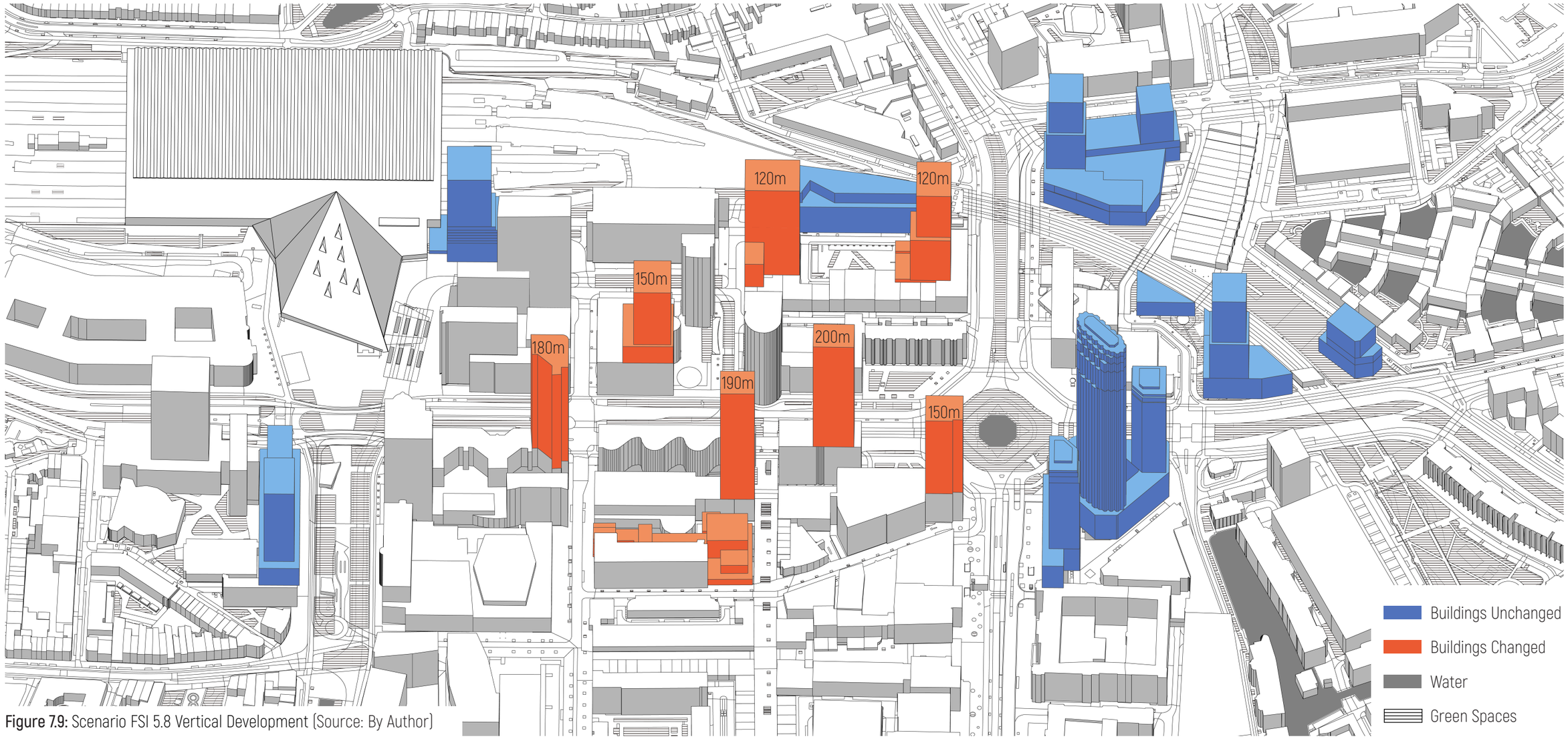



**Figure 7.9:** Scenario FSI 5.8 Vertical Development (Source: By Author)

## MRT Result

In FSI 5.8, changing the location of high-rise buildings results in a reduction of average street level MRT by 0.47 °C and 0.24 at 13:00 and 16:00 respectively compared to the original scenario. Although some areas become more exposed to solar radiation, a more balanced arrangement of high-rise buildings results in more efficient and widespread shading of streets.

Under windless nighttime conditions, slight increases in MRT are observed locally, particularly at intersections (up to 0.18 °C). However, at the overall street scale, MRT remains largely unchanged.

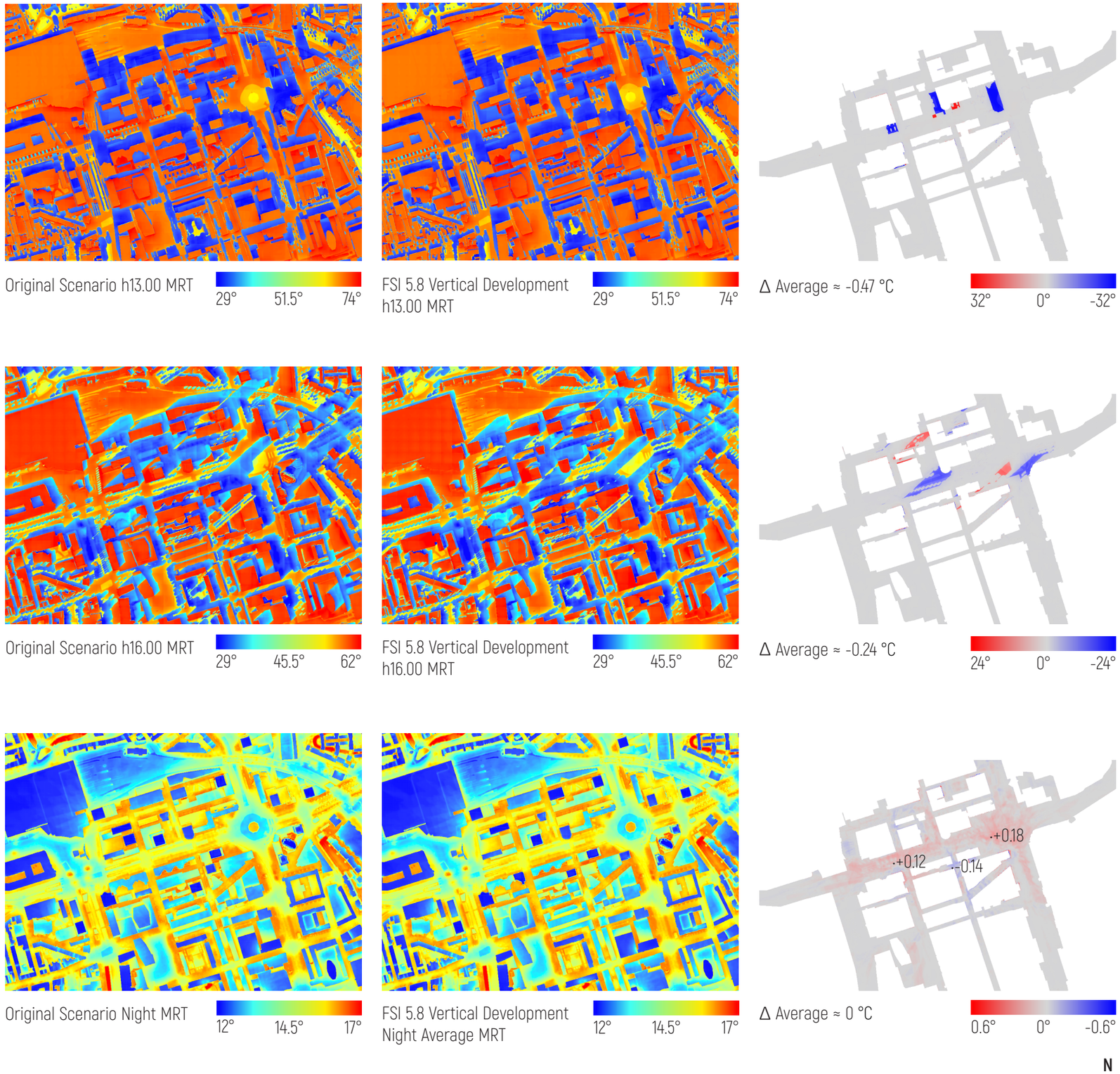



**Figure 7.10:** Scenario FSI 5.8 Vertical Development MRT (Source: By Author)

## PET Result

In FSI 5.8, the change in the location of high-rise buildings affects PET to a limited extent during the daytime, considering that PET is simultaneously affected by shading and wind conditions. At 13:00, the PET is reduced slightly on average by 0.15 °C, but this reduction is even smaller, around 0.06 °C, at 16:00 compared with the original scenario.

In windy nights, the PET changes in different areas are caused by the changes in wind speed resulting from the change in the location of high-rise buildings, but on the street level, the PET is almost unchanged.

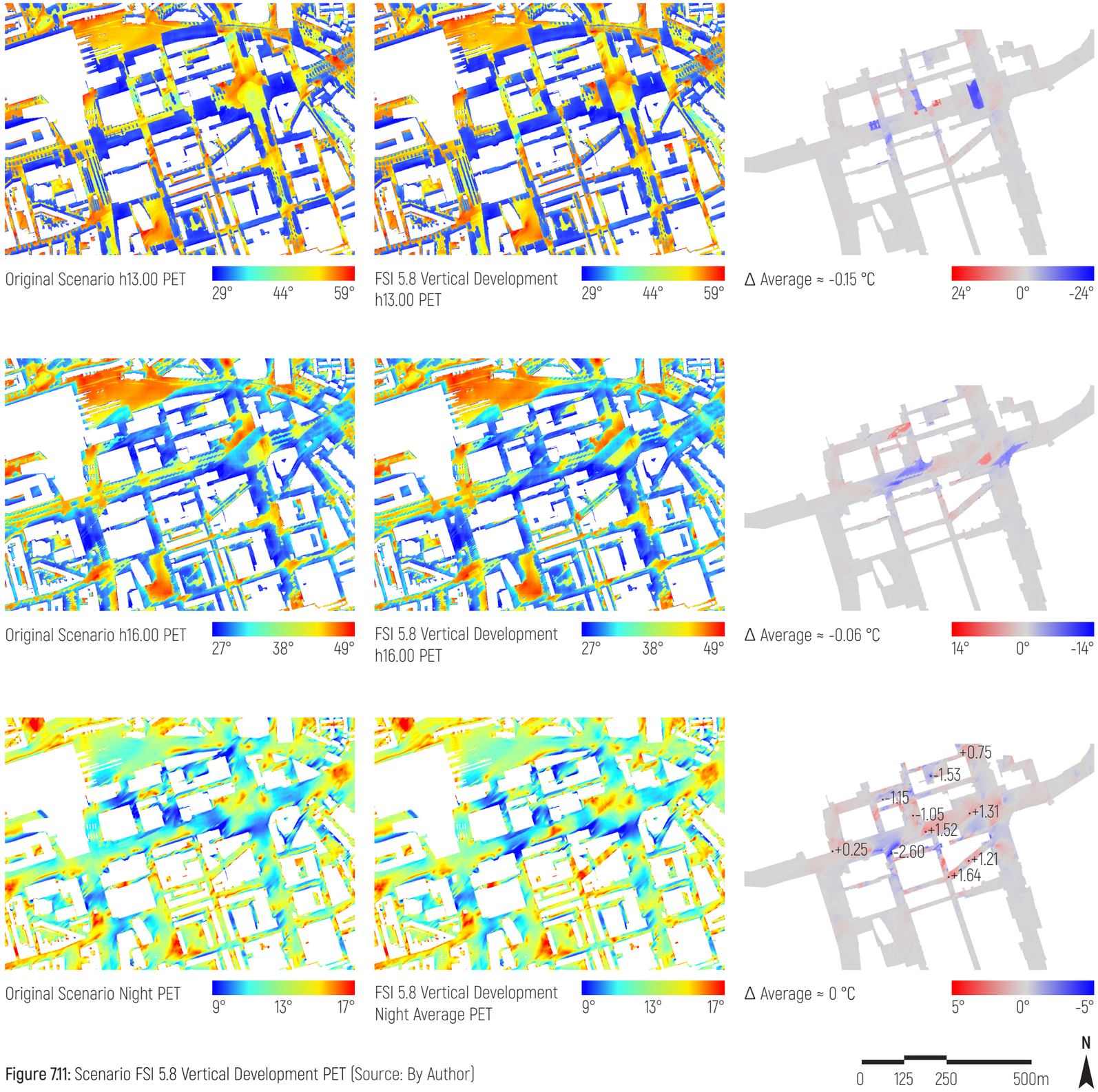



**Figure 7.11:** Scenario FSI 5.8 Vertical Development PET (Source: By Author)

### 7.3.3 FSI = 5.8 Combination

In Scenario 3, FSI is maintained at 5.8. This scenario integrates the strategies implemented in scenarios 1 and 2. Scenario 3 is achieved by removing some towers from the original scenario while increasing the height of podium buildings along the wider southern and western streets. Some towers are also shifted towards the intersection areas for better shading at the pedestrian level.

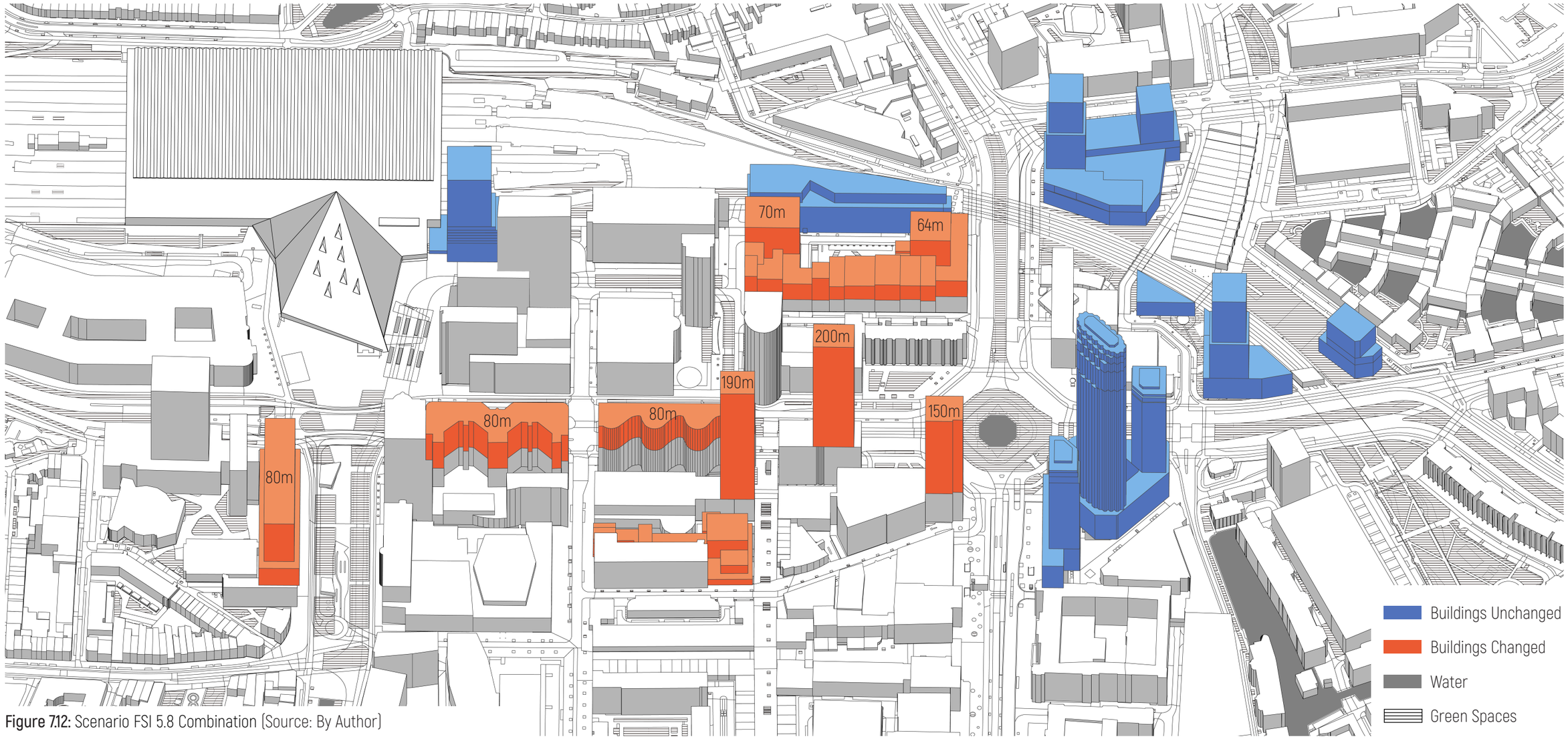
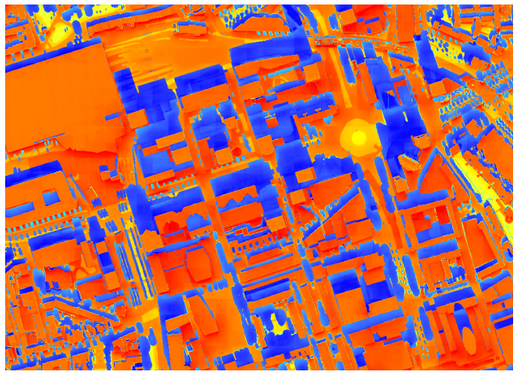



**Figure 7.12:** Scenario FSI 5.8 Combination (Source: By Author)

## MRT Result

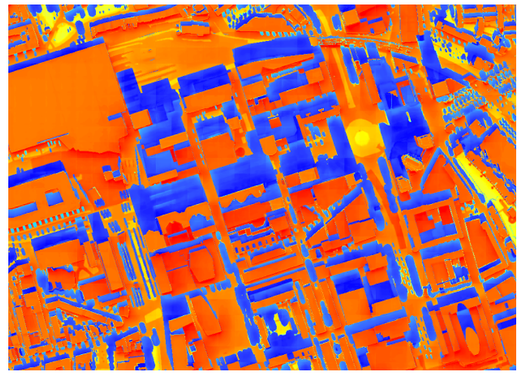
With FSI 5.8, the scenario of combining horizontal development and the vertical development lead to a decrease of 1 °C in average street level MRT at 13:00 hours, and 0.18 °C at 16:00 hours compared to the original scenario. This combines the advantages of both strategies, offering significant shading at mid-day from horizontal development and effective afternoon shading with the vertical development as the altitude of the sun reduces in the afternoon.

Under windless conditions at night, the total variations in MRT are still minimal. There are average increases of 0.18 °C along the street and 0.15 °C at intersections.



Original Scenario h13.00 MRT

29° 51.5° 74°



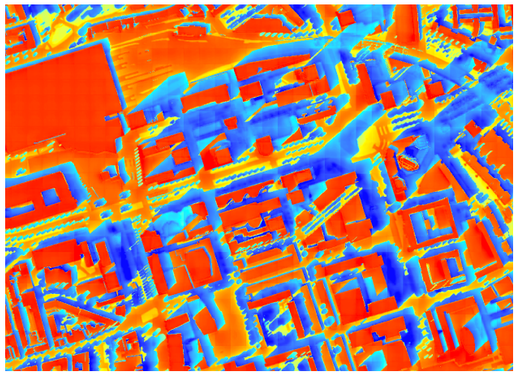
FSI 5.8 Combination h13.00 MRT

29° 51.5° 74°



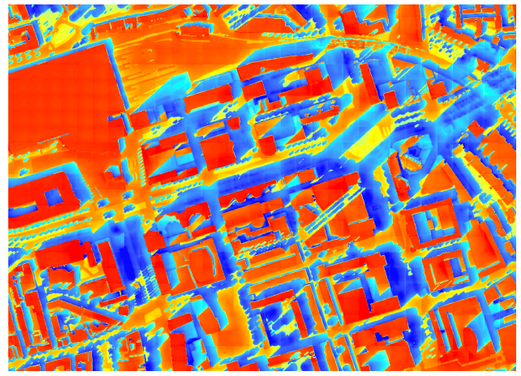
Δ Average ≈ -1.08 °C

32° 0° -32°



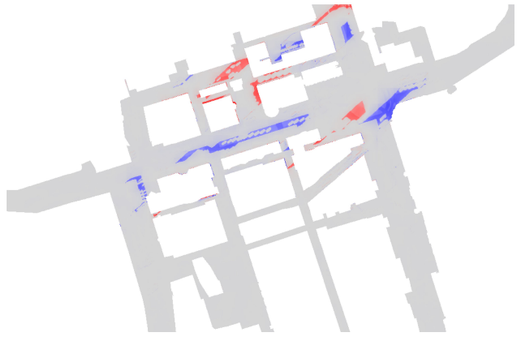
Original Scenario h16.00 MRT

29° 45.5° 62°



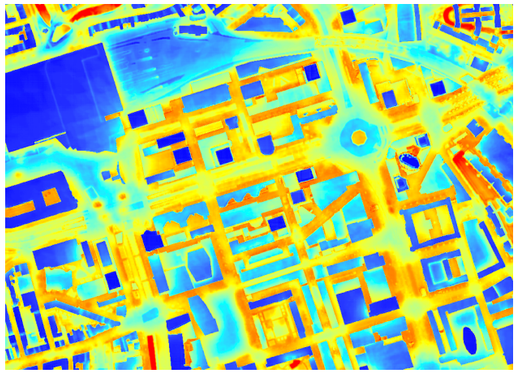
FSI 5.8 Combination h16.00 MRT

29° 45.5° 62°



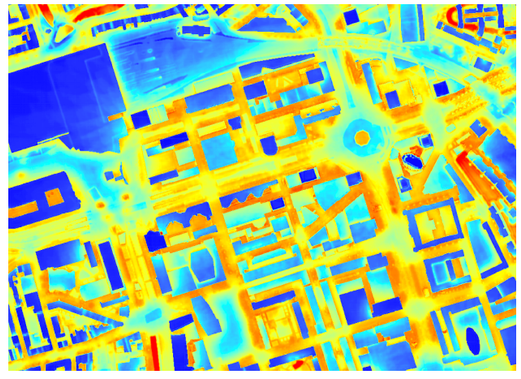
Δ Average ≈ -0.18 °C

24° 0° -24°



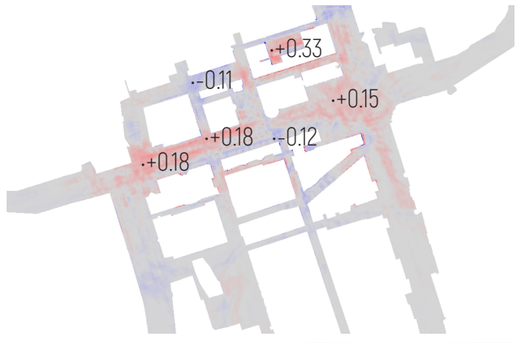
Original Scenario Night MRT

12° 14.5° 17°



FSI 5.8 Combination Night Average MRT

12° 14.5° 17°




Δ Average ≈ 0 °C

0.6° 0° -0.6°

0 125 250 500m

N

**Figure 7.13:** Scenario FSI 5.8 Combination MRT (Source: By Author)

## PET Result

In FSI 5.8, the combined strategy of horizontal development and vertical development indicates a limited impact on PET during the daytime, which is dominated by the combined influence of shading and wind effects. Compared to the original scenario, at 13:00, the average PET slightly decreases with a reduction of approximately 0.31 °C, while at 16:00, the PET remains almost unchanged, indicating that the relocation of high-rise towers alters the distribution of shading, leading to renewed solar exposure in some areas, while the cooling effect of shading is partially offset by changes in airflow.

During windy nights, PET demonstrates a strong spatial variation. For some areas, increased obstructions of podiums and towers result in a reduction of wind speeds, causing PET to increase locally by up to 2.8 °C. The vertical development, however, improves wind speeds by downwash effect, causing a cooling effect around 1.5 °C in other areas. Moreover, horizontal development creates deeper street canyon which enhances wind speeds along the edges of buildings, thus cooling PET in adjacent areas.

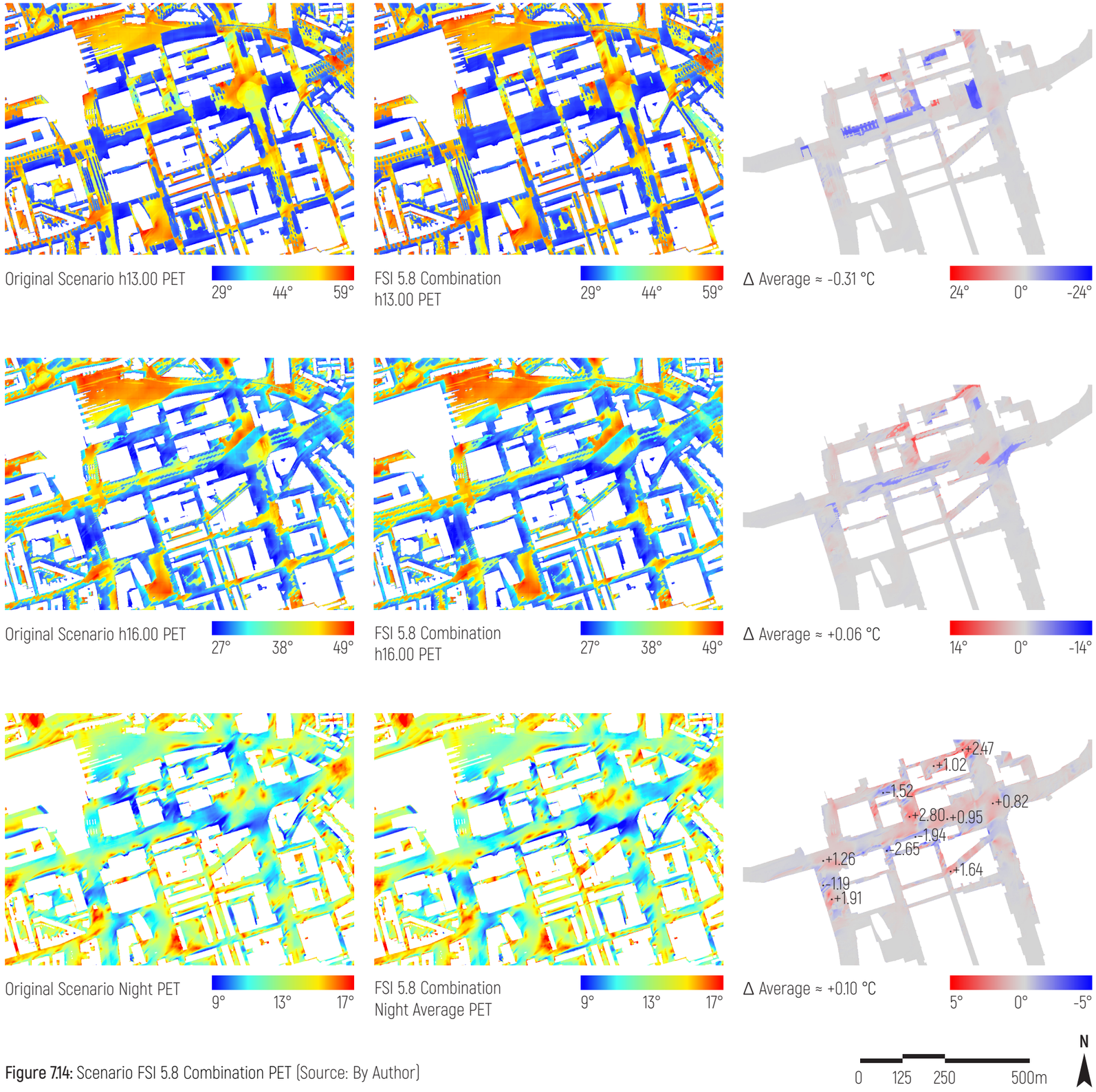



**Figure 7.14:** Scenario FSI 5.8 Combination PET (Source: By Author)

### 7.3.4 FSI = 6.5 Horizontal development

For Scenario 4, the FSI is increased to 6.5 based on the Scenario 1. In addition to increase the height podiums on the southern and western sides of wider streets, buildings' height is also increased on the northern side of wider streets and on the southern and western sides of some narrower streets.




**Figure 7.15:** Scenario FSI 6.5 Horizontal Development (Source: By Author)

## MRT Result

At FSI 6.5, compared with the original scenario, horizontal development can make a reduction of 1.29°C on average street level MRT by 13:00. At 16:00, compared to the horizontal development scenario under FSI 5.8, there is a further enhancement of the cooling effect, where there is an reduction of 0.4°C. This shows that higher density enhances the cooling effect by imporving the shading performance.

Under windless night time, because of increased FSI, the urban form becomes more enclosed, leading to a slight increase in nighttime MRT. For wider streets, the increase is less significant, with an increase of 0.18 to 0.25 °C. For narrower streets and alleys, there is a relatively larger increase in temperature, with MRT increasing by 0.35 to 0.55 °C. At intersection areas, MRT increases by 0.48 °C. This is more pronounced compared to the FSI 5.8 scenario.

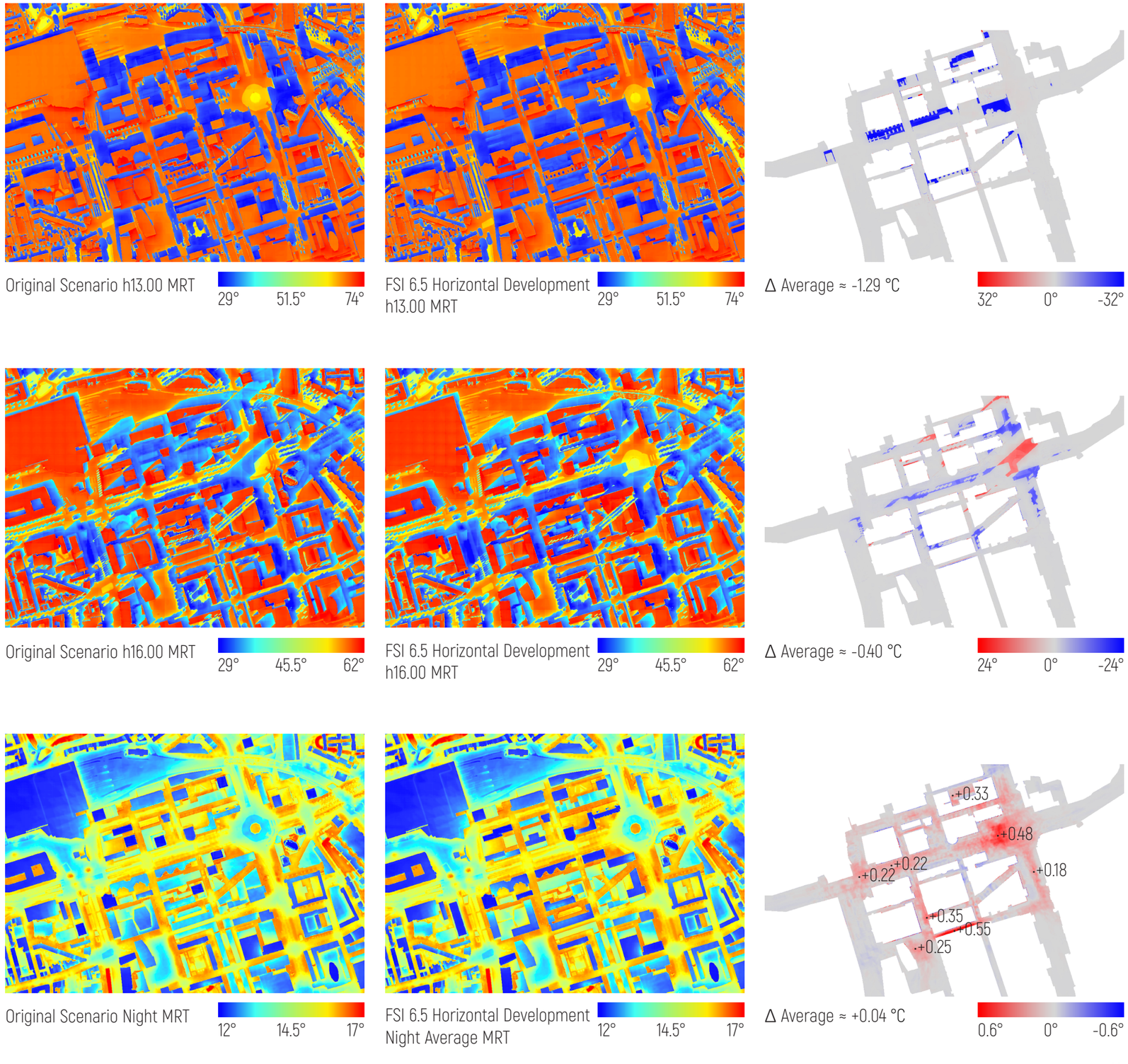



**Figure 7.16:** Scenario FSI 6.5 Horizontal Development MRT (Source: By Author)

## PET Result

At FSI 6.5, the horizontal development lead to a modest reduction on daytime PET, where the temperature is averagely reduced by 0.43 °C at 13:00 and 0.03 °C at 16:00 at the street level compared to the original scenario.

During windy nights, the PET is found to increase along the wider streets, where the higher podiums results in a more enclosed environment, thus suppressing the wind speeds. It is found that the PET is increased by 1.67 °C to 2.44 °C compared to the original scenario.

However, along the narrow streets, the PET is reduced by 2 °C, and it is due to the deeper street canyon.

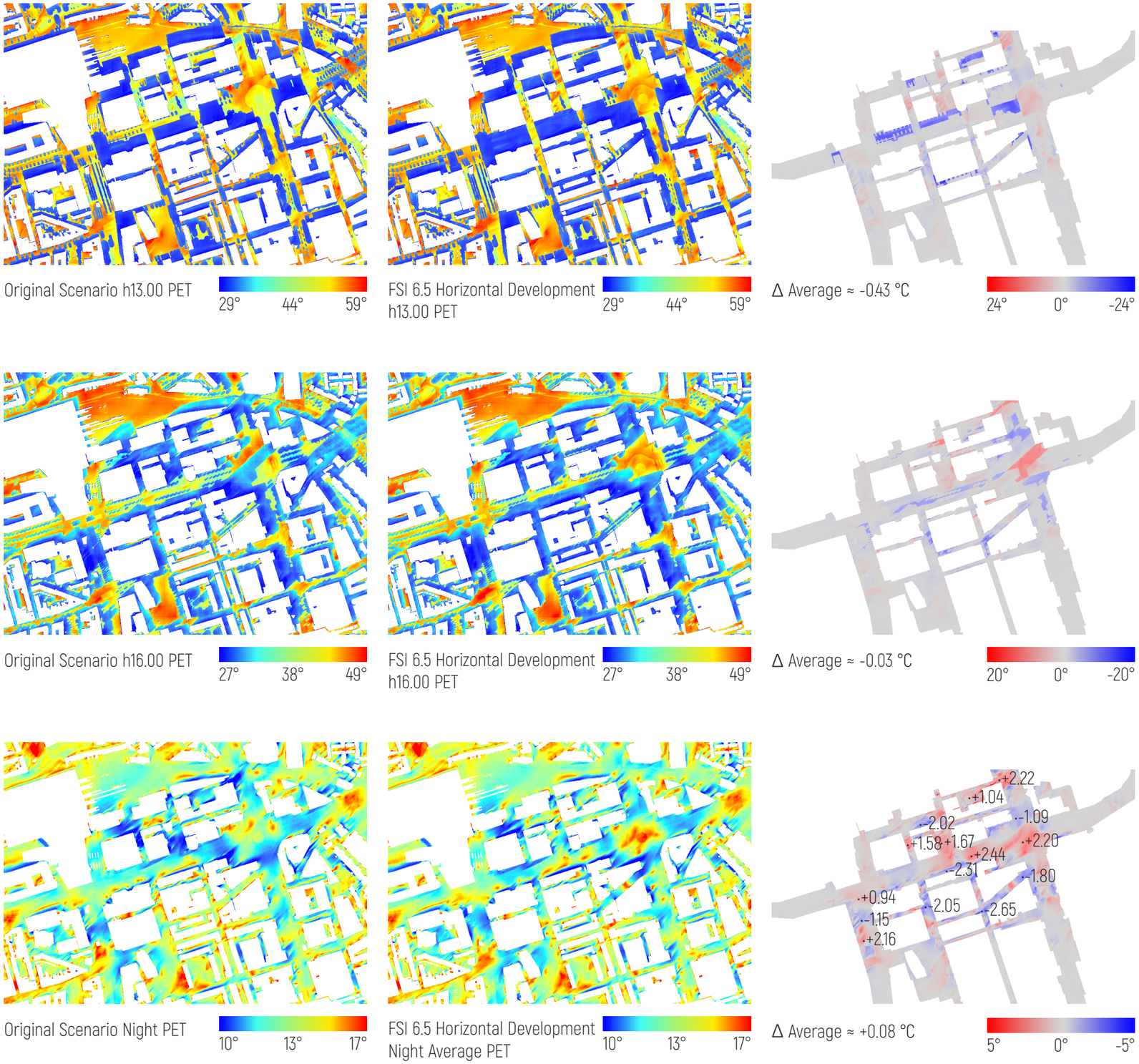



**Figure 7.17:** Scenario FSI 6.5 Horizontal Development PET (Source: By Author)

### 7.3.5 FSI = 6.5 Vertical Development

In Scenario 5, the FSI is increased to 6.5 based on Scenario 2. Apart from further increasing the height and adding new high-rise towers on the southern and western sides of the wider streets, vertical development is also conducted on the southern and western sides of some narrower streets. In addition, some podiums of the original scenario are replaced with high-rise towers.

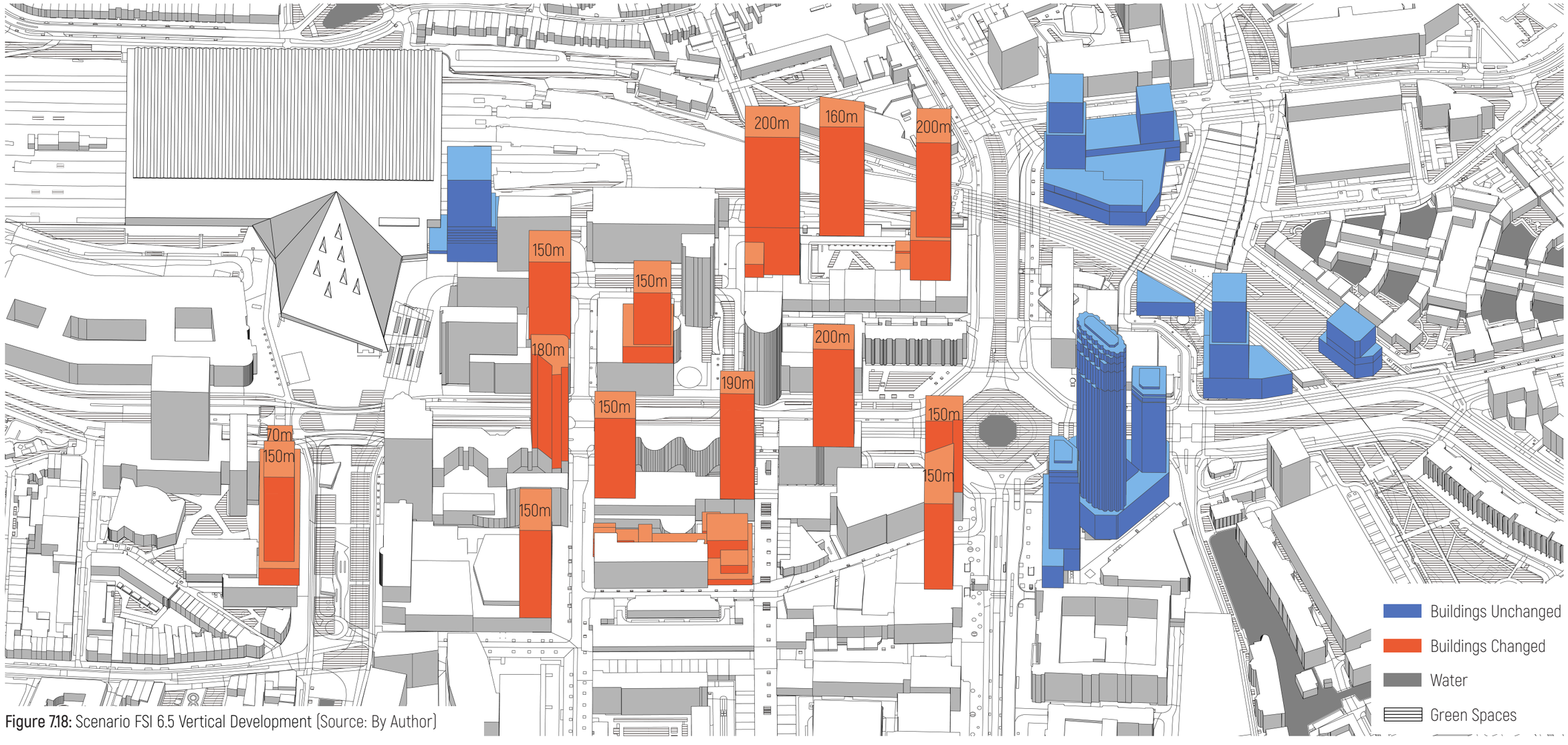



**Figure 7.18:** Scenario FSI 6.5 Vertical Development (Source: By Author)

## MRT Result

At FSI 6.5, changing the location of high-rise buildings and adding more buildings causes a reduction in average street-level MRT by 0.6 °C at 13:00 and 0.48 °C at 16:00. This is because of the increased number of buildings, which causes more continuous shading effects, thus creating a greater cooling effect compared to the FSI 5.8 scenario.

Under windless nighttime conditions, MRT increased slightly compared to the original scenario. On wider streets, the MRT increased by approximately 0.19 to 0.34°C, while on narrow streets and alleys, the increase remaines relatively small, at approximately 0.15°C, compared to the scenario of horizontal development at FSI 6.5. In the northern part, due to the replacement of a podium by the tower, the temperature reduces up to 0.75°C which is a considerable change.

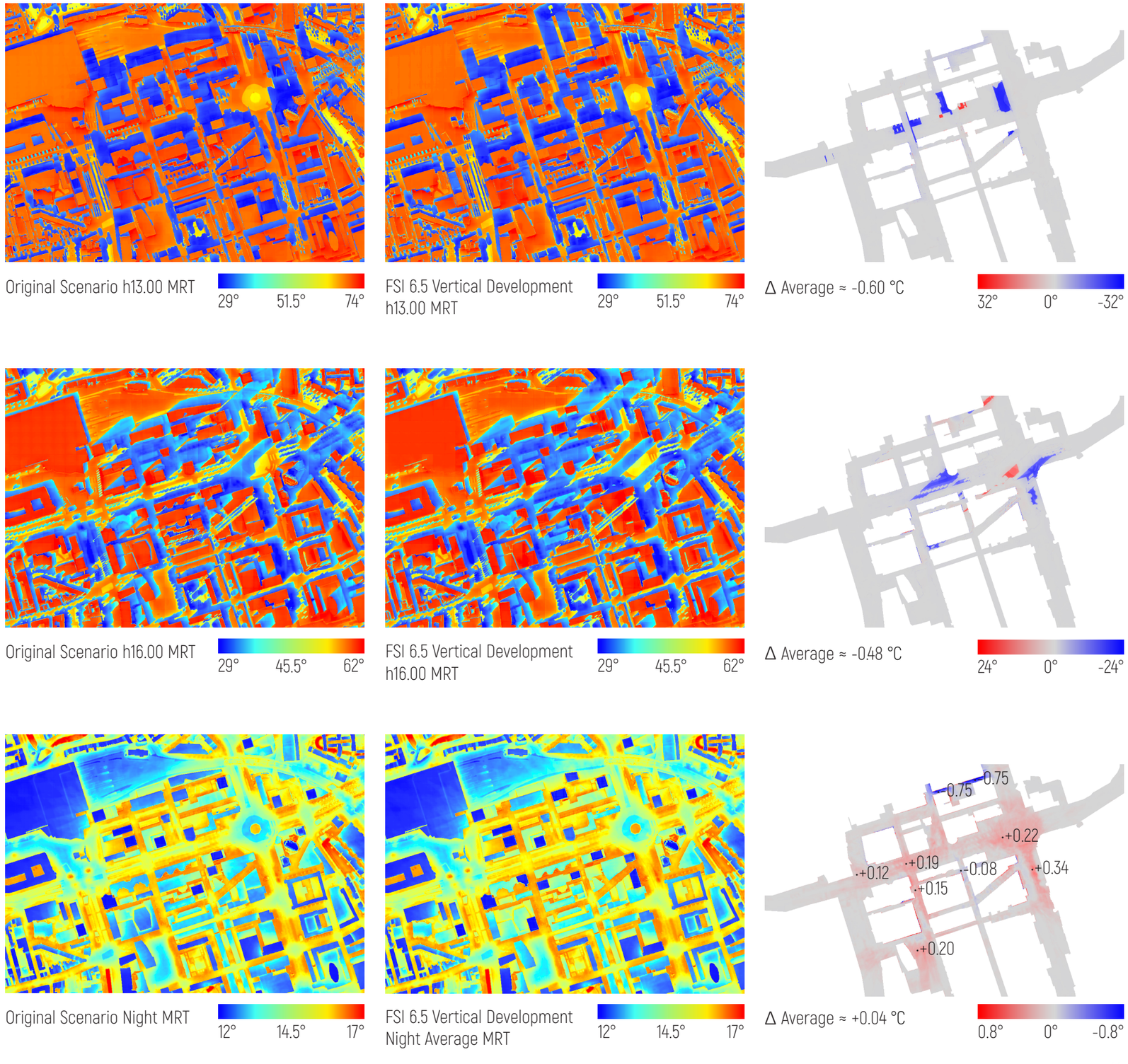



**Figure 7.19:** Scenario FSI 6.5 Vertical Development MRT (Source: By Author)

## PET Result

At FSI 6.5, vertical development causes a moderate decrease in daytime PET, with an average decrease of 0.39 °C at 13:00 and an average decrease of 0.27 °C at 16:00 at the street level compared to the original scenario.

Under windy nights, the change in tower layout causes localized increases and decreases in PET on wider streets, but these offset the effects of each other, resulting in less significant change in the overall street-level average. The vertical development also has a more neutral impact on windy nights when compared to the horizontal development scenario.

However, the addition of vertical development causes more significant local wind effects around high-rise towers, leading to larger decreases in PET. In some areas, the decrease in PET can be as high as 3 °C. The replacement of the podium by tower also leads to better ventilation, reducing PET around 2.74°C.

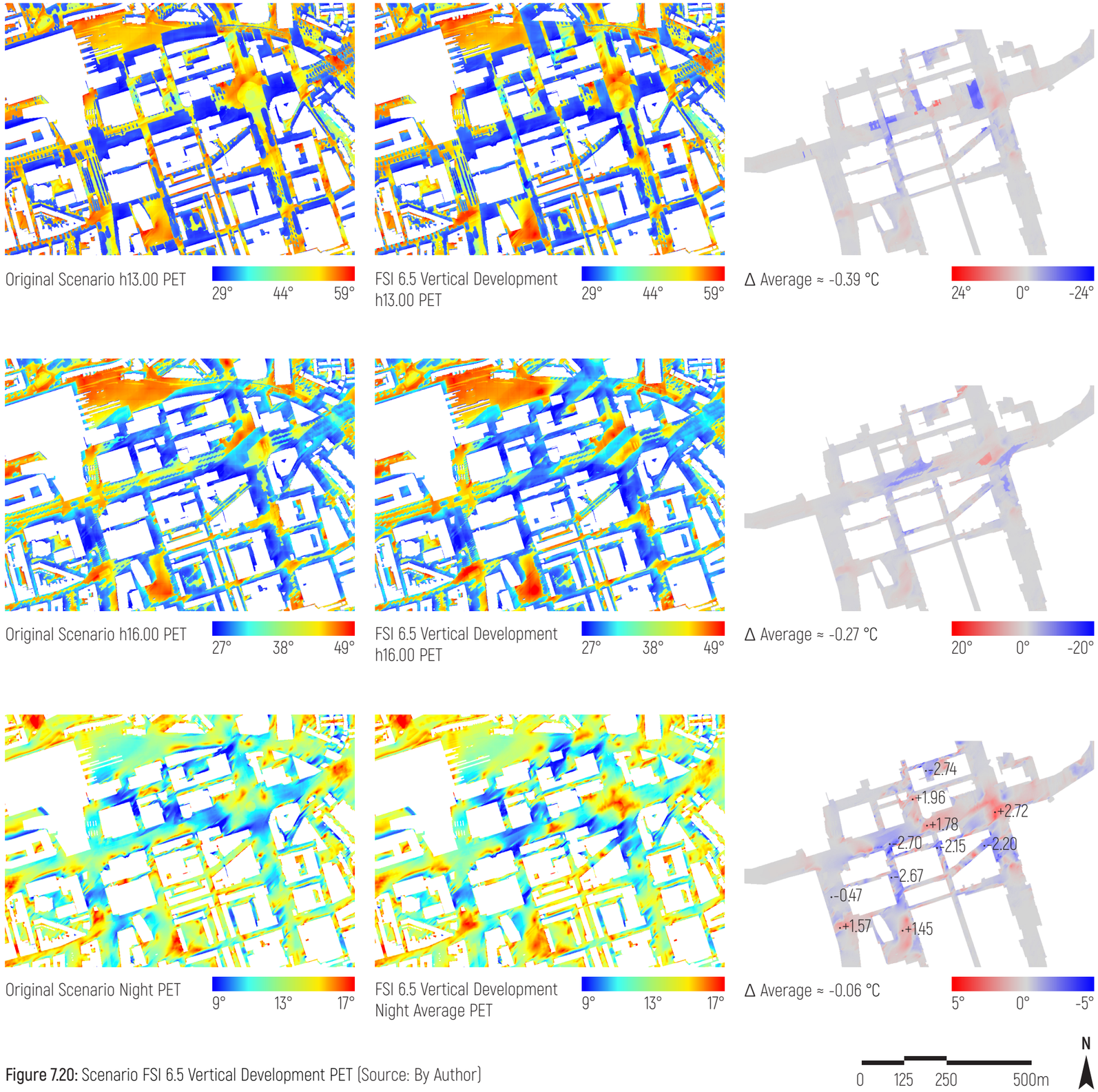



**Figure 7.20:** Scenario FSI 6.5 Vertical Development PET (Source: By Author)

### 7.3.6 FSI = 6.5 Combination

In Scenario 6, strategies from both Scenarios 4 and 5 are combined together. Podiums height is increased on the southern and western sides of wider street spaces, as well as adding more high-rise tower in intersection areas. Additionally, the height of podium on the southern and western sides of narrower streets are increased to improve the shading on the pedestrian.

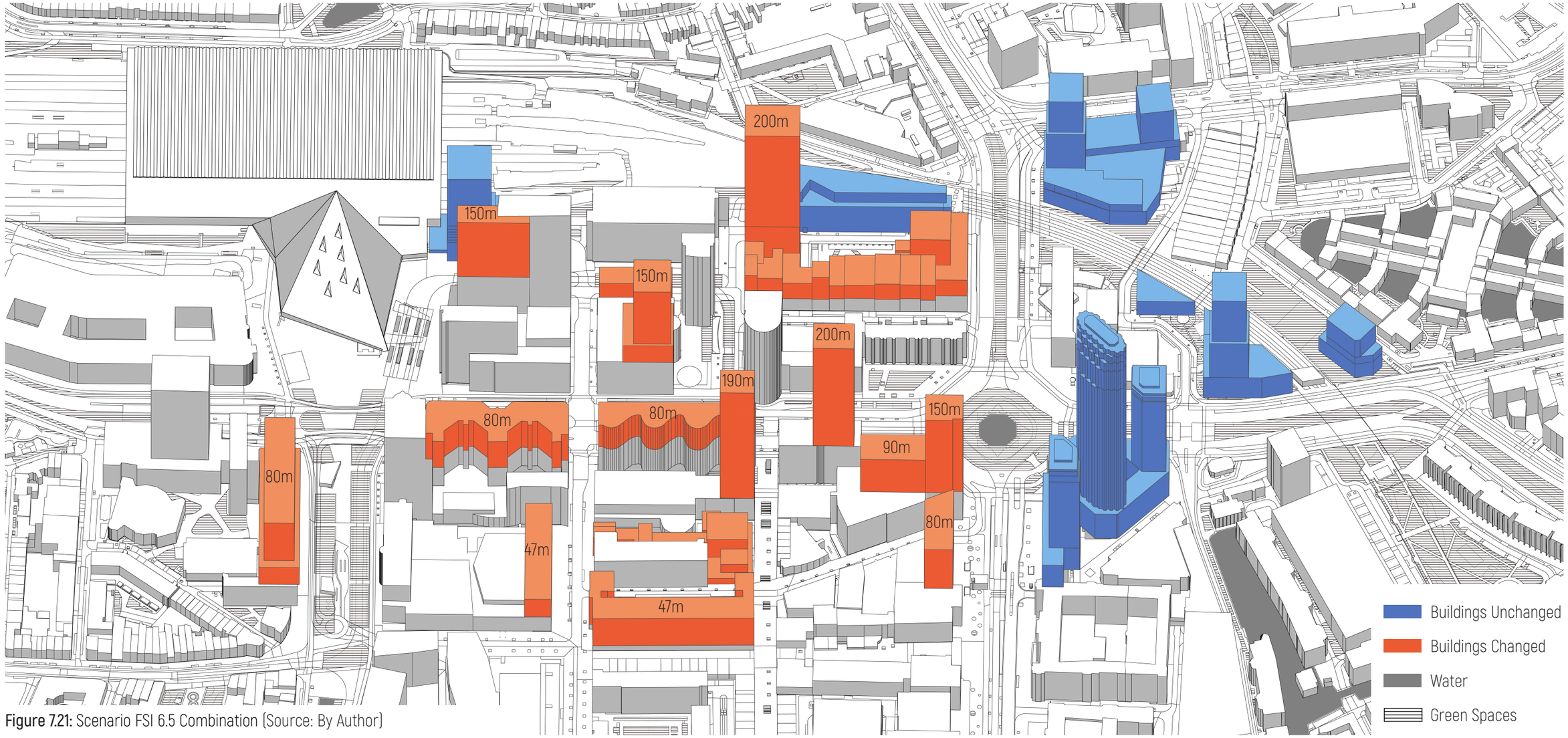
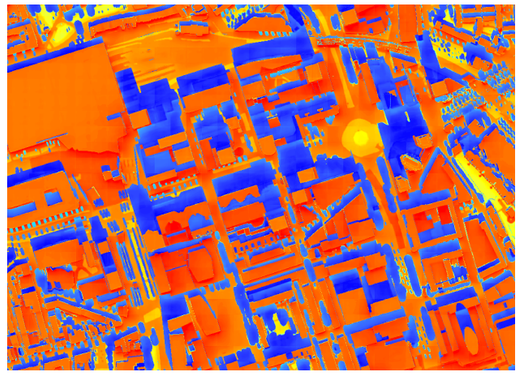



**Figure 7.21:** Scenario FSI 6.5 Combination (Source: By Author)

## MRT Result

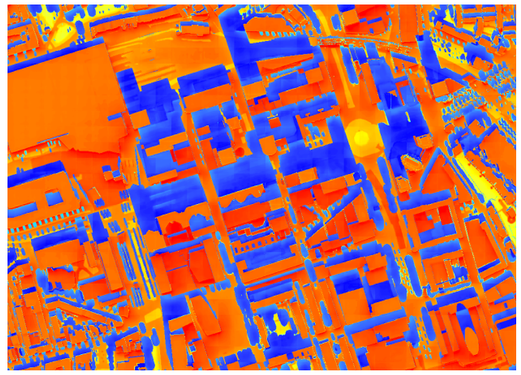
With FSI 6.5, horizontal development and the vertical development result in a significant drop in street-level MRT, recording a drop of 1.44 °C by 13:00 and 0.54 °C by 16:00. It is found that this configuration, which combines continuous shading from the horizontal development and extended shading from vertical development, has the strongest performance in daytime cooling among all scenarios.

On windless nights, the MRT temperature rose by approximately 0.25°C compared to the original scenario. However, the temperature increase is more pronounced in some narrow blocks or alleys, reaching as high as 0.5°C. Compared to the scenario with horizontal development (FSI=6.5), the temperature increase at intersections was smaller, only 0.27°C instead of 0.48°C, while other areas experienced similar increases. Compared to the scenario of vertical development (FSI=6.5), the temperature increase was slightly greater in narrow alleys.



Original Scenario h13.00 MRT

29° 51.5° 74°



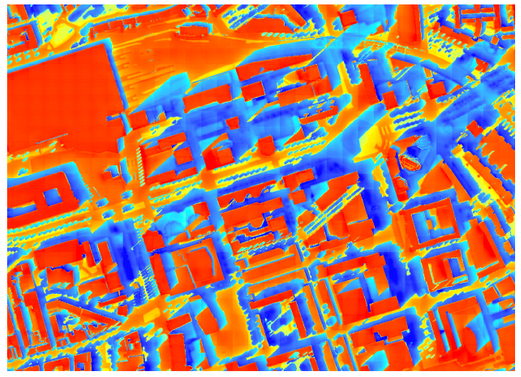
FSI 6.5 Combination h13.00 MRT

29° 51.5° 74°



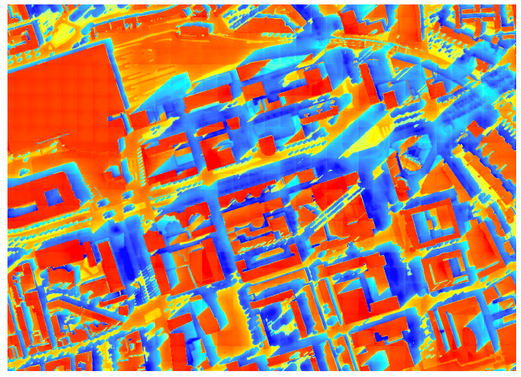
Δ Average ≈ -1.44 °C

32° 0° -32°



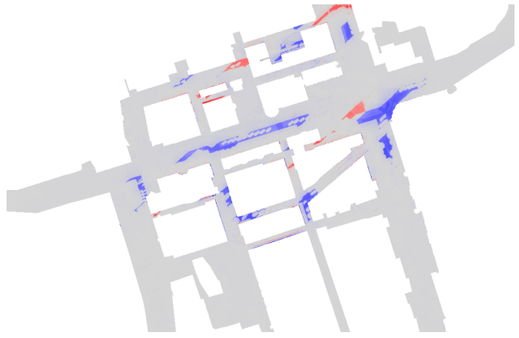
Original Scenario h16.00 MRT

29° 45.5° 62°



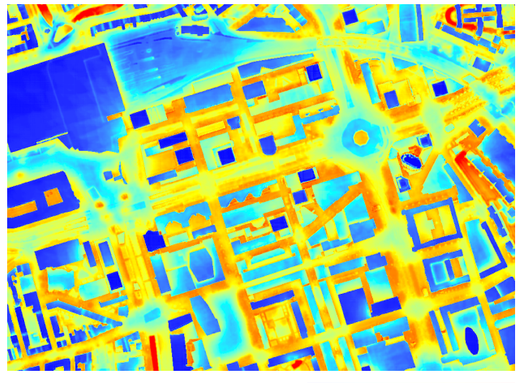
FSI 6.5 Combination h16.00 MRT

29° 45.5° 62°



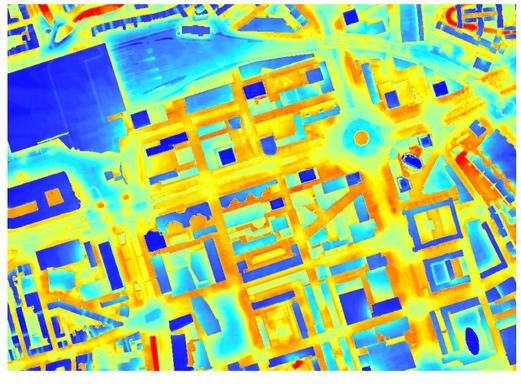
Δ Average ≈ -0.54 °C

24° 0° -24°



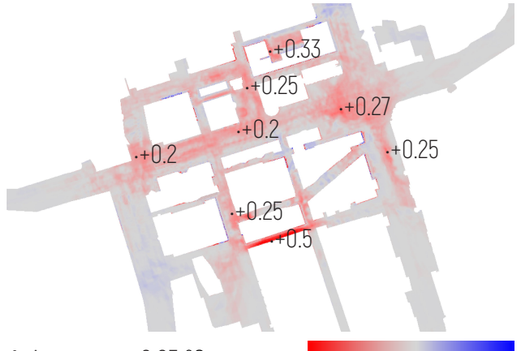
Original Scenario Night MRT

12° 14.5° 17°



FSI 6.5 Combination Night Average MRT

12° 14.5° 17°




Δ Average ≈ +0.03 °C

0.6° 0° -0.6°

0 125 250 500m

N

**Figure 7.22:** Scenario FSI 6.5 Combination MRT (Source: By Author)

## PET Result

For FSI 6.5, there is a decrease in daytime PET with the combination of horizontal and the implementation of high-rise buildings. Compared to the original scenario, there is a decrease in average street-level PET by 0.7°C at 13:00 and 0.27°C at 16:00. This shows that the combination is effective in minimizing thermal stress compared to horizontal development or vertical development.

For windy nights, the changes in PET on wider streets are small compared to the individual strategies. For areas with horizontal development, there is a localized acceleration of wind on the same side of the street, resulting in a decrease in PET.

There are significant spatial differences in PET. On wider streets, horizontal development does not have significant changes and the PET also increase in part of the streets (around 1.5°C). This may because the wind is blocked due to the height increase. On narrow streets, PET drops in certain areas about 2°C because of the deeper street canyon. Vertical development can increase wind speed on areas around high-rise buildings, causing PET reduce.

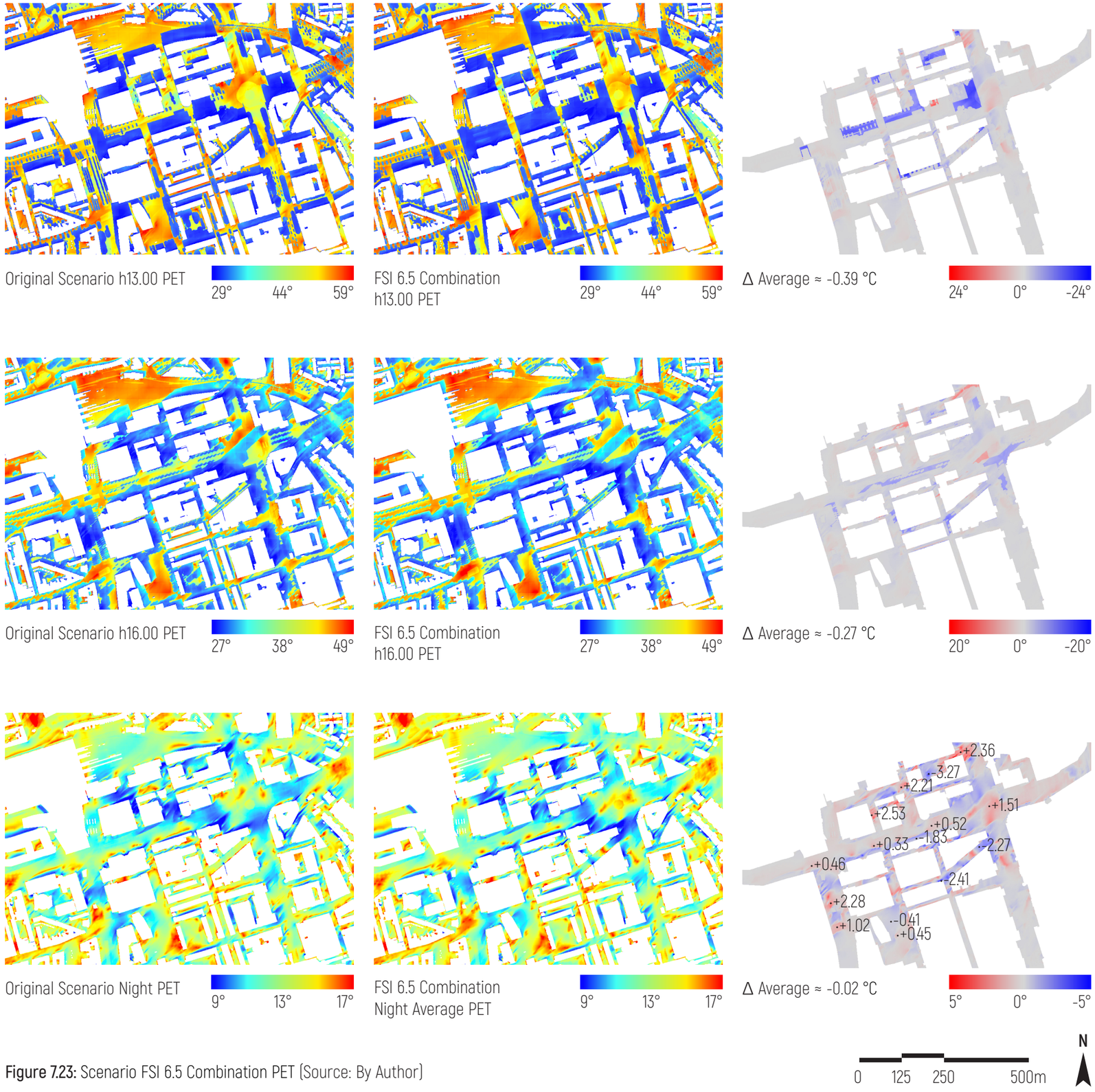



**Figure 7.23:** Scenario FSI 6.5 Combination PET (Source: By Author)

### 7.3.7 FSI =7.0 Horizontal Development

In Scenario 7, FSI density is increased to 7.0 which is an extreme density condition. This scenario build based on Scenario 4, where horizontal development are conducted on all sides of wider streets. Moreover, the podiums height on all sides of narrower streets are also elevated under high density conditions.




**Figure 7.24:** Scenario FSI 7.0 Horizontal Development (Source: By Author)

## MRT Result

At FSI 7.0, horizontal development yields a similar amount of daytime cooling as seen in FSI 6.5, with average street-level MRT reductions of around 1.29 °C at 13:00 and 0.57 °C at 16:00. This indicates that further increasing density does not lead to additional improvements in shading performance, suggesting a saturation of the cooling effect.

Under windless nights, the increases in MRT are seen to be more significant compared to lower-density scenarios. The narrow streets and alleys experience temperature increases of around 0.5°C due to the more enclosed urban form.

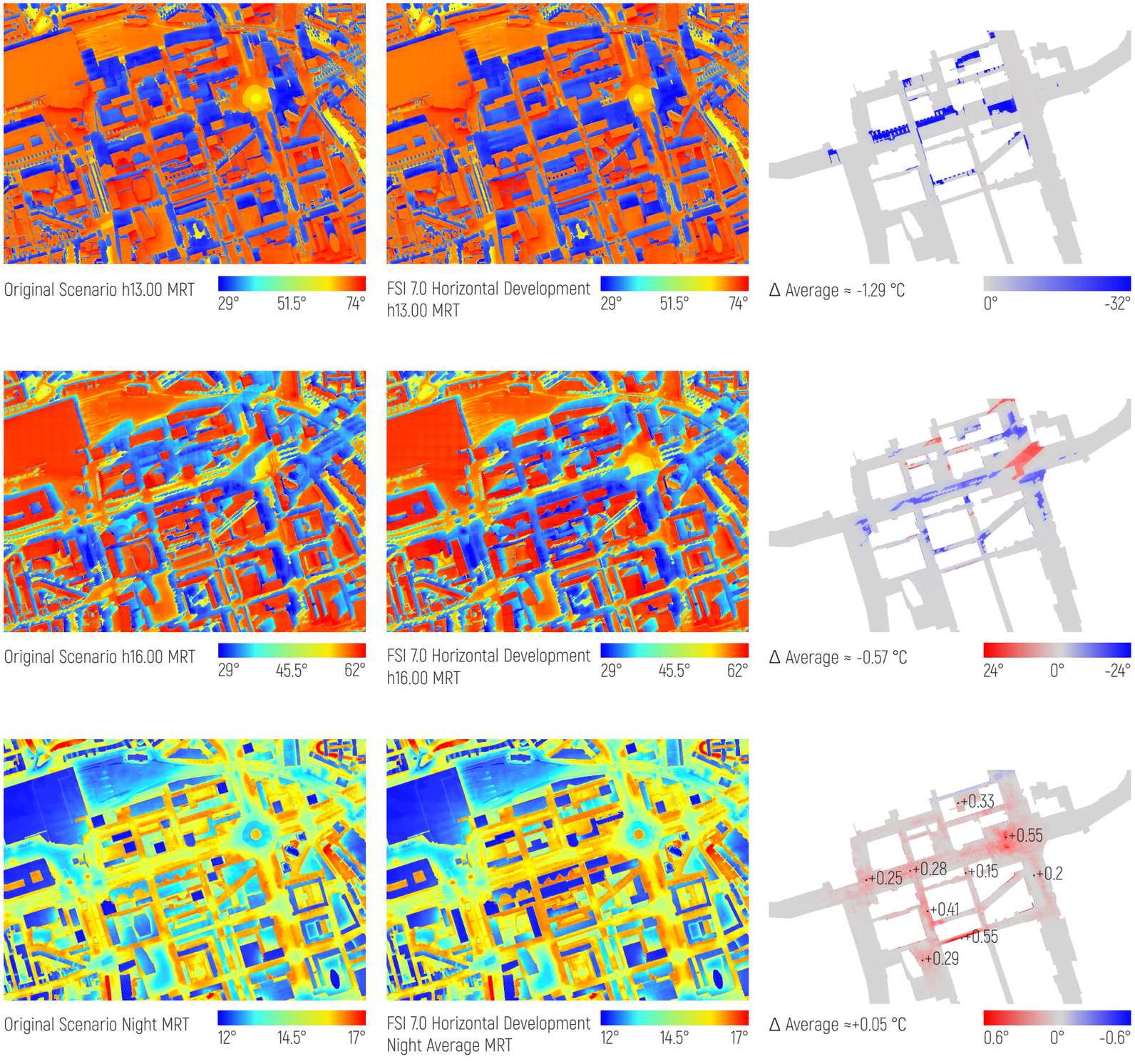



**Figure 7.25:** Scenario FSI 7.0 Horizontal Development MRT (Source: By Author)

## PET Result

At FSI 7, horizontal development has a considerable effect on the reduction of daytime PET. When compared with the original scenario, the average PET at the street level is reduced by approximately 0.56 °C at 13:00 and 0.16 °C at 16:00.

As mentioned in the previous section, on windy nights, PET on the wider streets increases due to the reduced airflow caused by the more enclosed built environment which increases by as much as 2.39 °C.

On narrower streets, there is a considerable reduction in PET. The increasing height of podiums deepens the street canyon which causes channeling effects. This enhances the wind speed at the street level. Hence, the PET is reduced by as much as 2.96 °C.

In addition, on diagonal streets, the further increase in height of the podium on both sides increases the wind corridor effect, resulting in increased airflow and a PET decrease of 2°C.

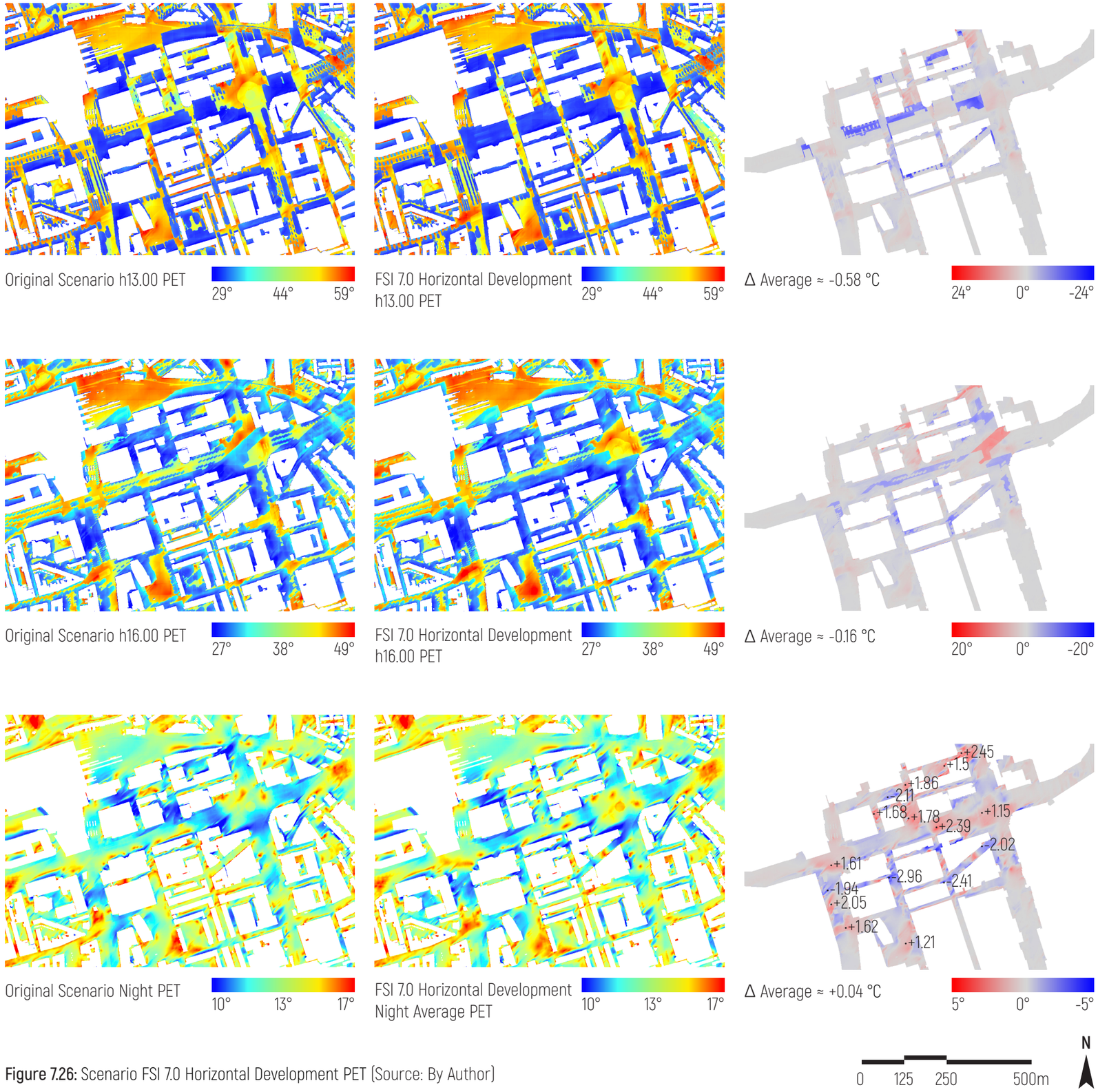



**Figure 7.26:** Scenario FSI 7.0 Horizontal Development PET (Source: By Author)

### 7.3.8 FSI =7.0 Vertical Development

In Scenario 8, the FSI is increased to 7.0 as an extreme density condition. Based on Scenario 5, the height of towers along wider streets is further increased, and additional towers are constructed to intensify vertical development. More high-rise towers are also constructed around narrower streets under higher density conditions.

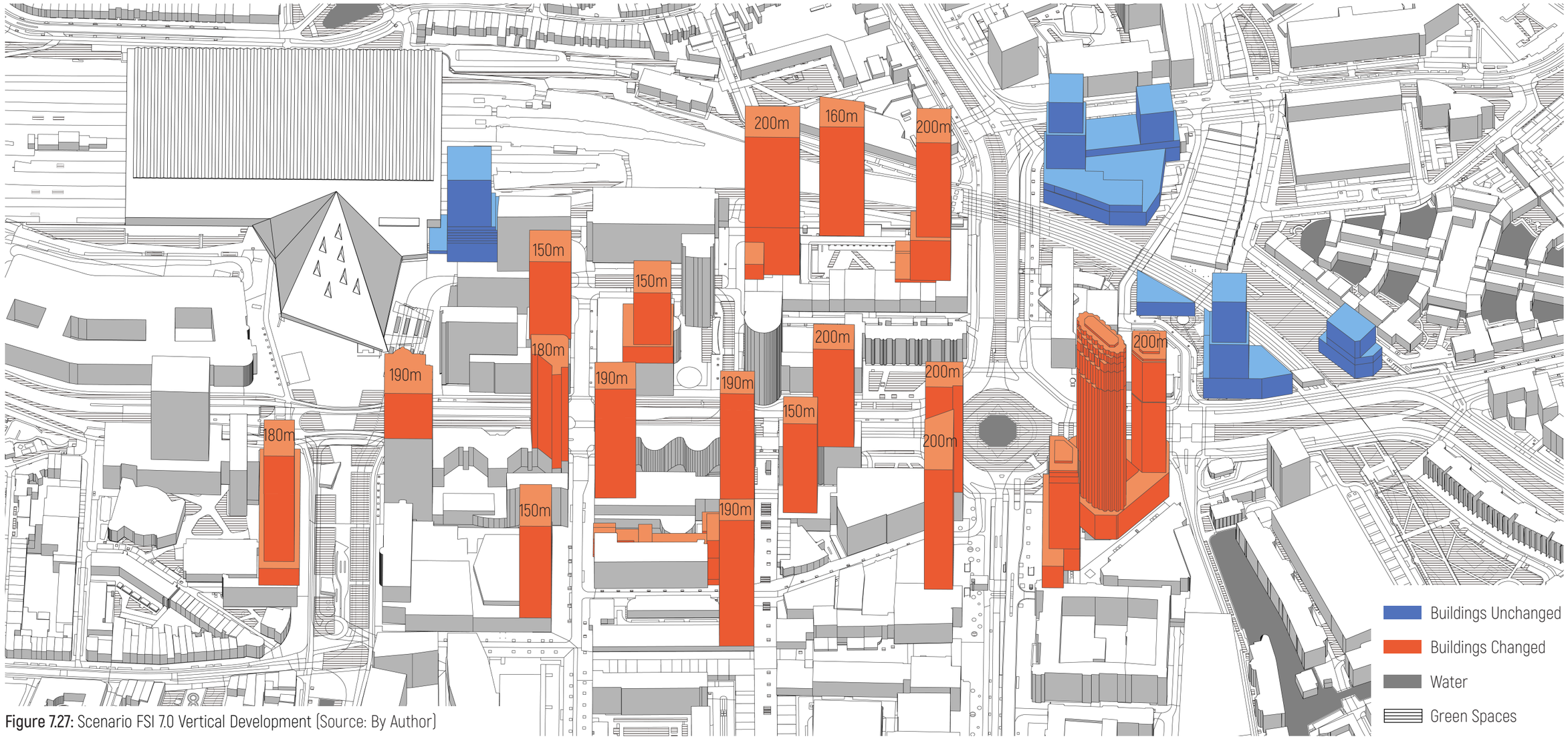



**Figure 7.27:** Scenario FSI 7.0 Vertical Development (Source: By Author)

## MRT Result

As FSI 7.0, vertical development leads to a reduction in average street-level MRT of 1.02 °C at 13:00 and 0.85 °C at 16:00. Compared to the lower-density arrangement, the higher density of high-rise towers creates a more continuous and overlapping pattern of shading, especially in the afternoon, leading to a stronger cooling effect in the late afternoon (After 16:00).

For windless night conditions, the increase in MRT is moderate, ranging from 0.25 to 0.34 °C, with local peaks up to 0.41 °C. Compared to horizontal development, vertical development resulted in a smaller increase in nighttime temperature, especially in narrow streets, indicating poor insulation.

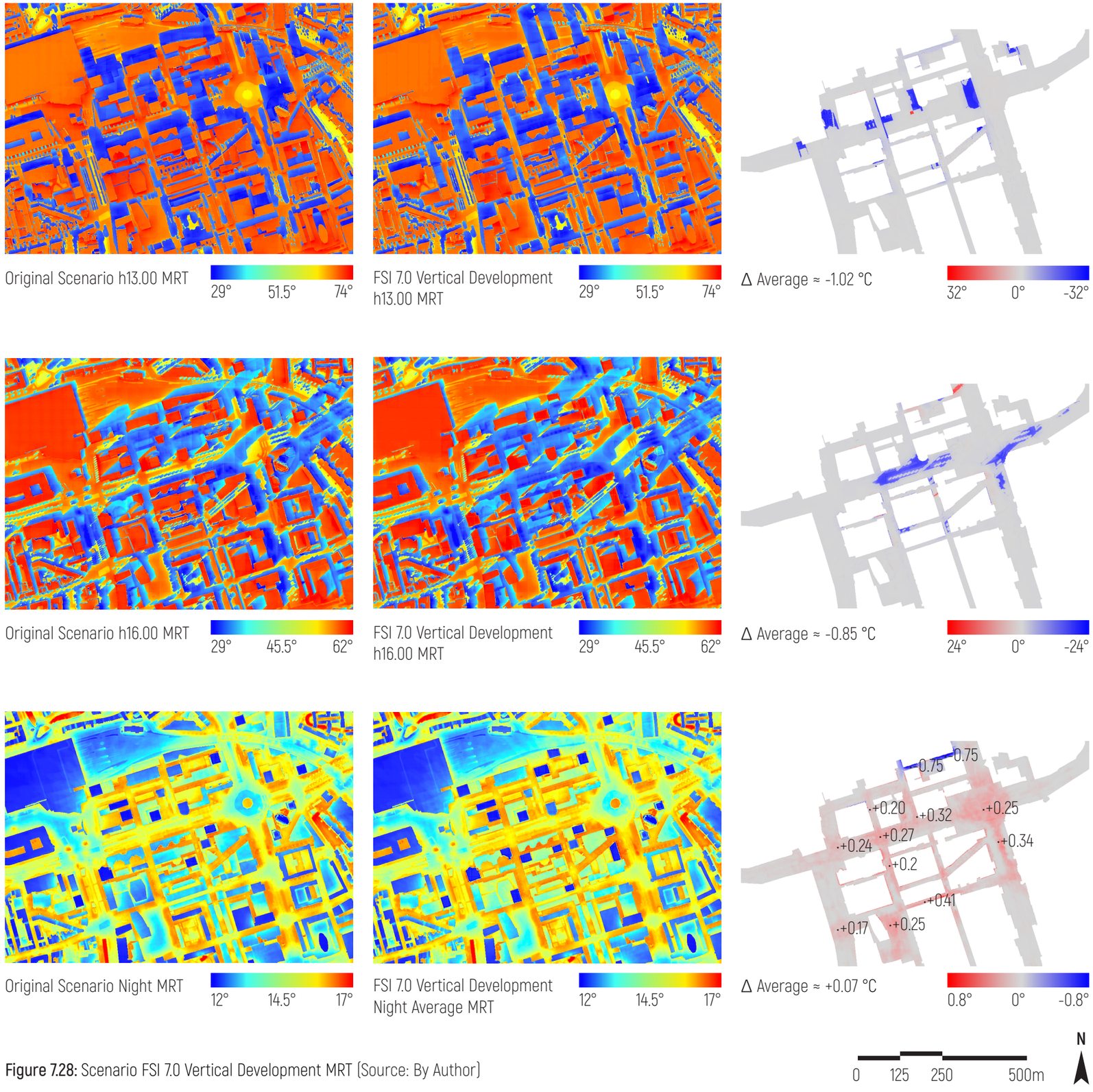



**Figure 7.28:** Scenario FSI 7.0 Vertical Development MRT (Source: By Author)

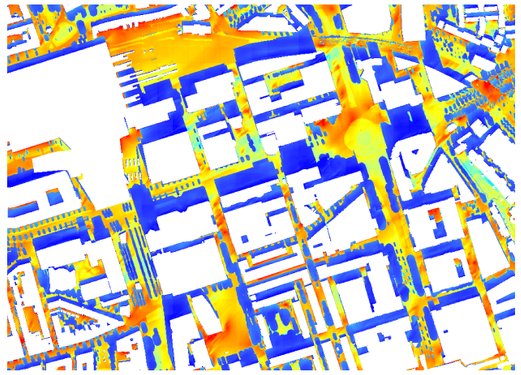
## PET Result

As shown in FSI 7.0, vertical development leads to a consistent reduction in daytime PET values. As compared to the original scenario, the average street level PET values reduce by 0.77°C at 13:00 and 0.52°C at 16:00.

On wider streets, under windy nighttime conditions, PET values experience localized increases and decreases in response to the redistribution of airflow caused by the vertical development.

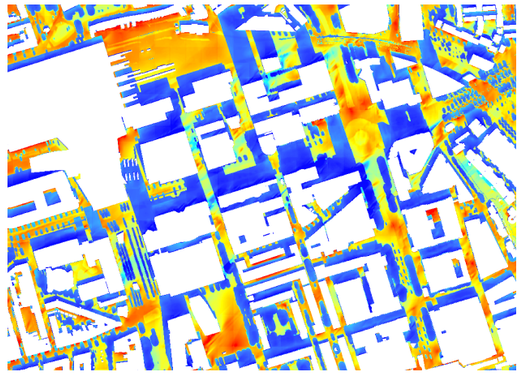
In narrower streets, vertical development increase localized airflow in some areas, which causes a greater reduction in PET values. The PET values reduce by as much as 3.2°C in some areas.

On diagonal streets, the increased height of the towers on both sides of the street enhances the wind corridor effect, especially when compared to horizontal development scenario at the same FSI. This causes a reduction in PET values by 2.57°C.



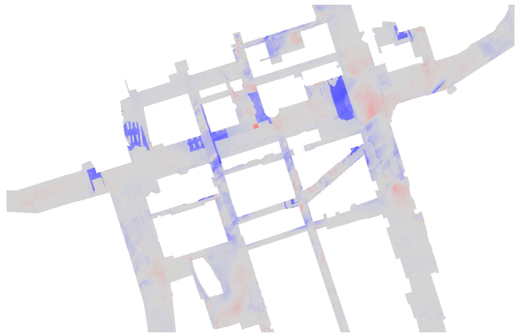
Original Scenario h13.00 PET

29° 44° 59°



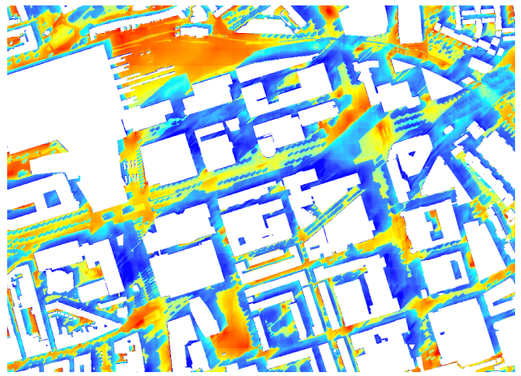
FSI 7.0 Vertical Development h13.00 PET

29° 44° 59°



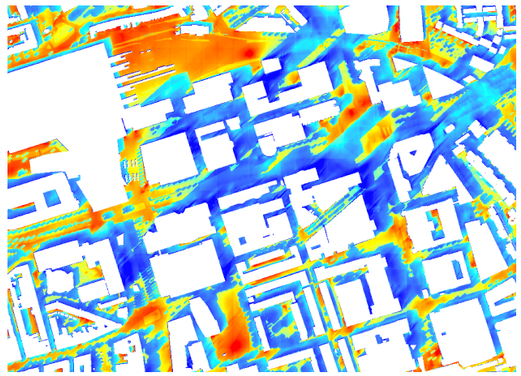
Δ Average ≈ -0.77 °C

-24° 0° 24°



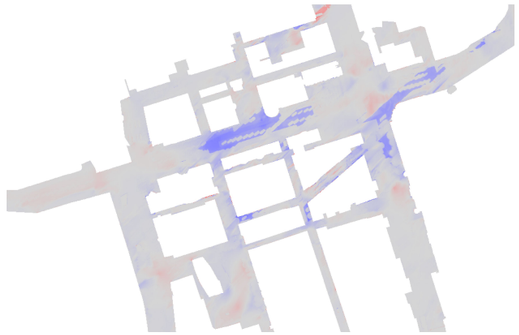
Original Scenario h16.00 PET

27° 38° 49°



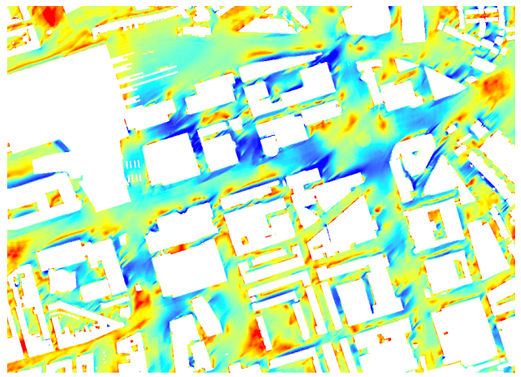
FSI 7.0 Vertical Development h16.00 PET

27° 38° 49°



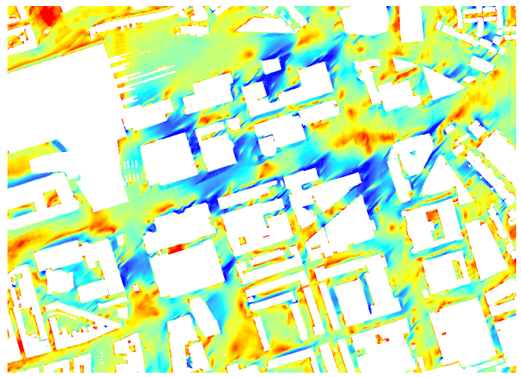
Δ Average ≈ -0.52 °C

20° 0° -20°



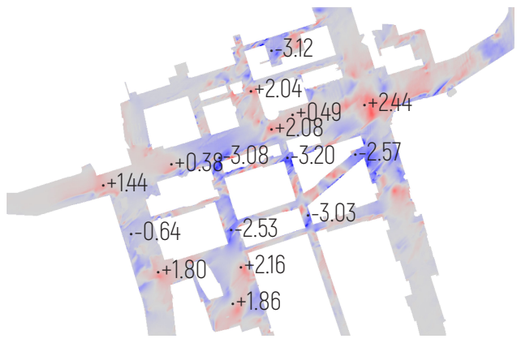
Original Scenario Night PET

9° 13° 17°



FSI 7.0 Vertical Development Night Average PET

9° 13° 17°




Δ Average ≈ -0.13 °C

5° 0° -5°

0 125 250 500m

N

**Figure 7.29:** Scenario FSI 7.0 Vertical Development PET (Source: By Author)

### 7.3.9 FSI =7.0 Combination

In Scenario 9, the FSI is improved to 7.0 to as an extreme density condition. This scenario combines the strategies proposed in Scenarios 7 and 8 by developed horhorizontally around the wider streets and adding more towers in the intersection areas. Additionally, horizontal development on the sides of narrower streets are also raised to assess the thermal performance in highly intensified density conditions.

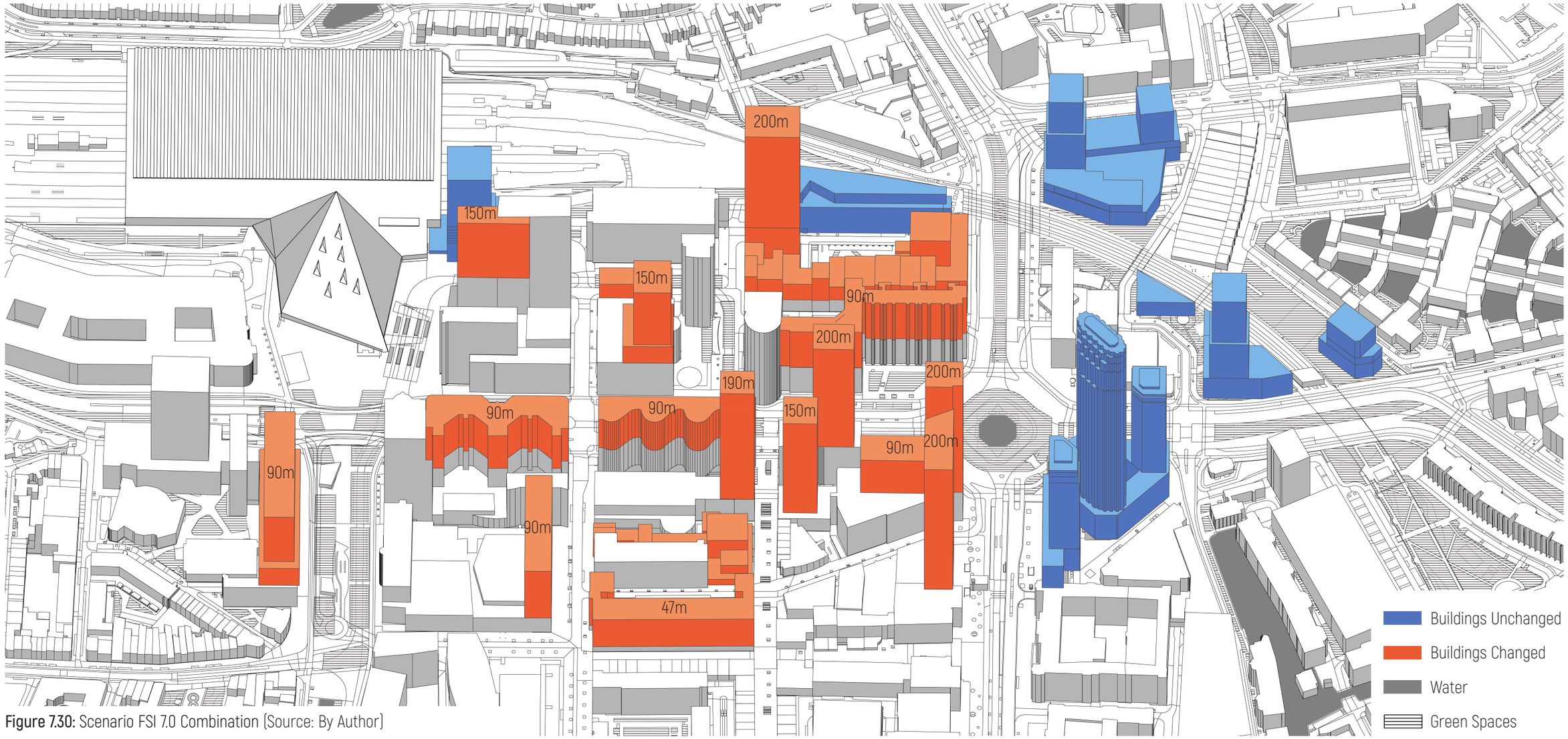



**Figure 7.30:** Scenario FSI 7.0 Combination (Source: By Author)

## MRT Result

Under FSI 7.0, the horizontal development and vertical development also significantly reduces the average MRT at street level, decreasing by 1.52 °C at 13:00 and 0.93 °C at 16:00. The similar MRT performance during these two time periods indicates that the combination of these factors can provide effective shading at different times of the day.

Under windless nighttime conditions, the MRT still shows a significant increase compared to lower-density scenarios. On main streets, the increase in street level temperature is between 0.25 and 0.39 °C; while in narrow streets, the increase is even greater due to the increased podium height, reaching 0.45 to 0.55 °C, which is larger than the vertical development under the same FSI. At street intersections, the MRT increase is 0.51 °C.

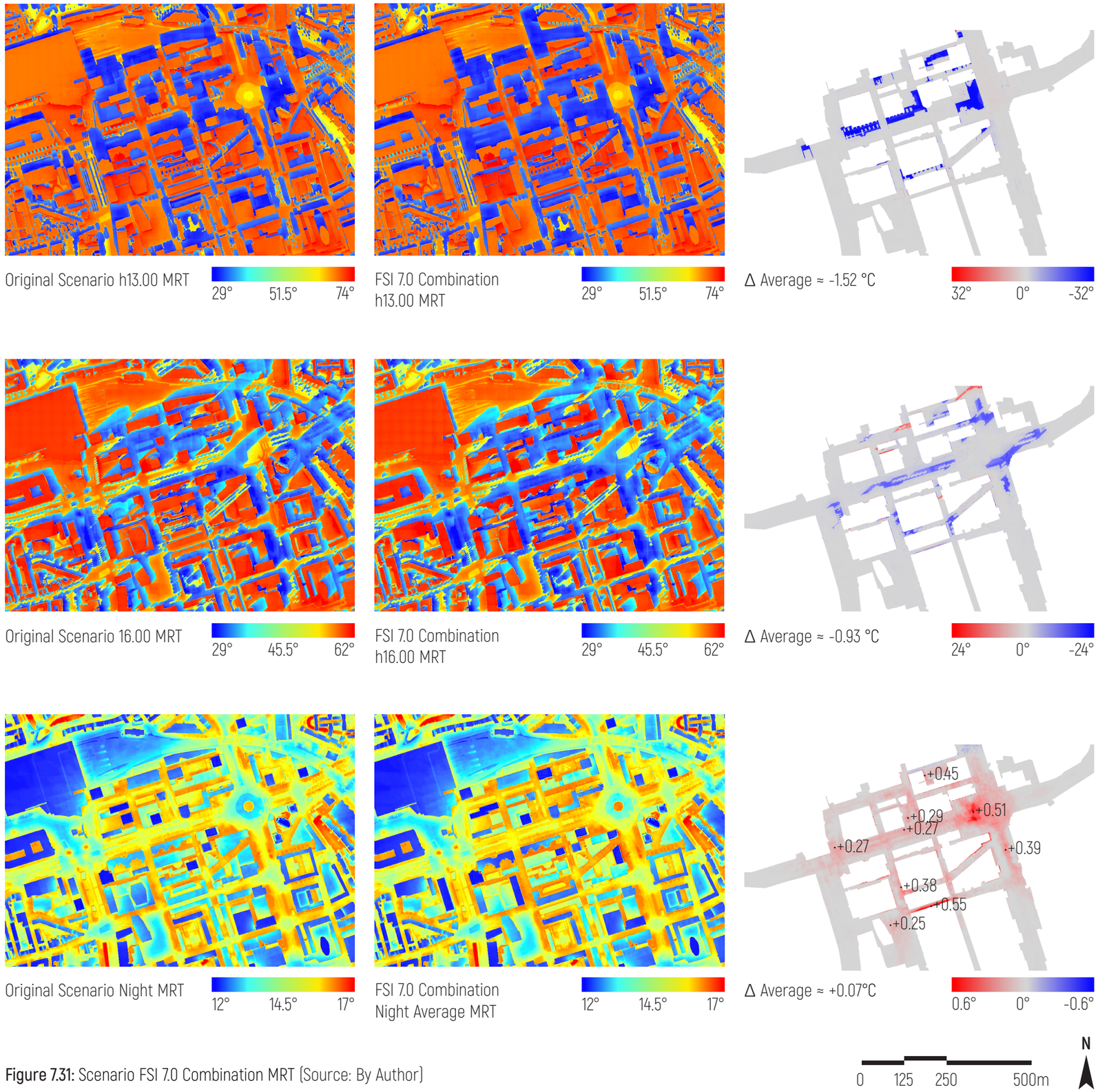



**Figure 7.31:** Scenario FSI 7.0 Combination MRT (Source: By Author)

## PET Result

For FSI 7.0, the overall combination of horizontal development and vertical development achieves the largest reduction in PET during the daytime. Compared to the original scenario, the reduction in PET averaged over streets reaches a maximum of approximately 0.88 °C at 13:00 and 0.53 °C at 16:00.

During windy nights, the overall pattern is similar to the combined strategy at FSI 6.5. For wider streets, there is a small change in PET values. Horizontal development cannot effectively deepen canyons on wider streets, and it also obstructs wind. As a result, PET increases on wider streets.

In narrower streets, increased building heights effectively deepened the street canyon, causing a more dramatic reduction in PET compared to the FSI 6.5 case. Along diagonal streets, a similar phenomenon occurs, where strengthened wind corridor conditions cause PET to be reduced by up to approximately 3.05 °C.

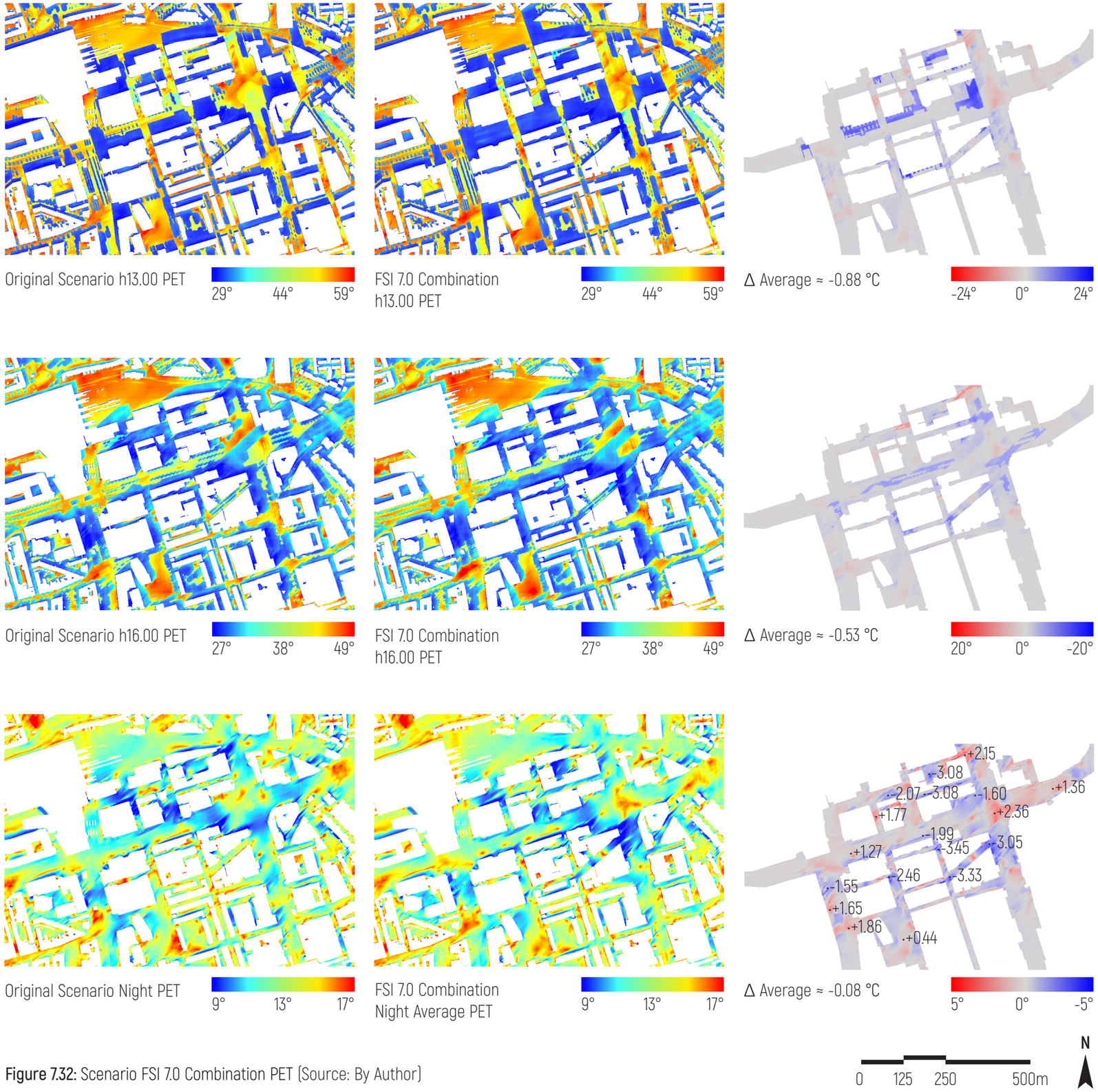



**Figure 7.32:** Scenario FSI 7.0 Combination PET (Source: By Author)

### 7.3.10 Conclusion

**Effect of FSI**: It was observed that there is an obvious ruduction on the daytime MRT and PET while FSI increasing due to its shading effect. However, the magnitude of temperature reduction gradually decreases especially for horizontal development because of the shadows on the street are becoming saturated. During windless night, local temperature increases due to the reduce of SVF, leading to more heat retention, but on average, the temperature growth is very slight. Under windy night conditions, localized wind speeds tend to increase with higher FSI, leading to a reduction in PET (Figure 7.33, Figure 7.34).

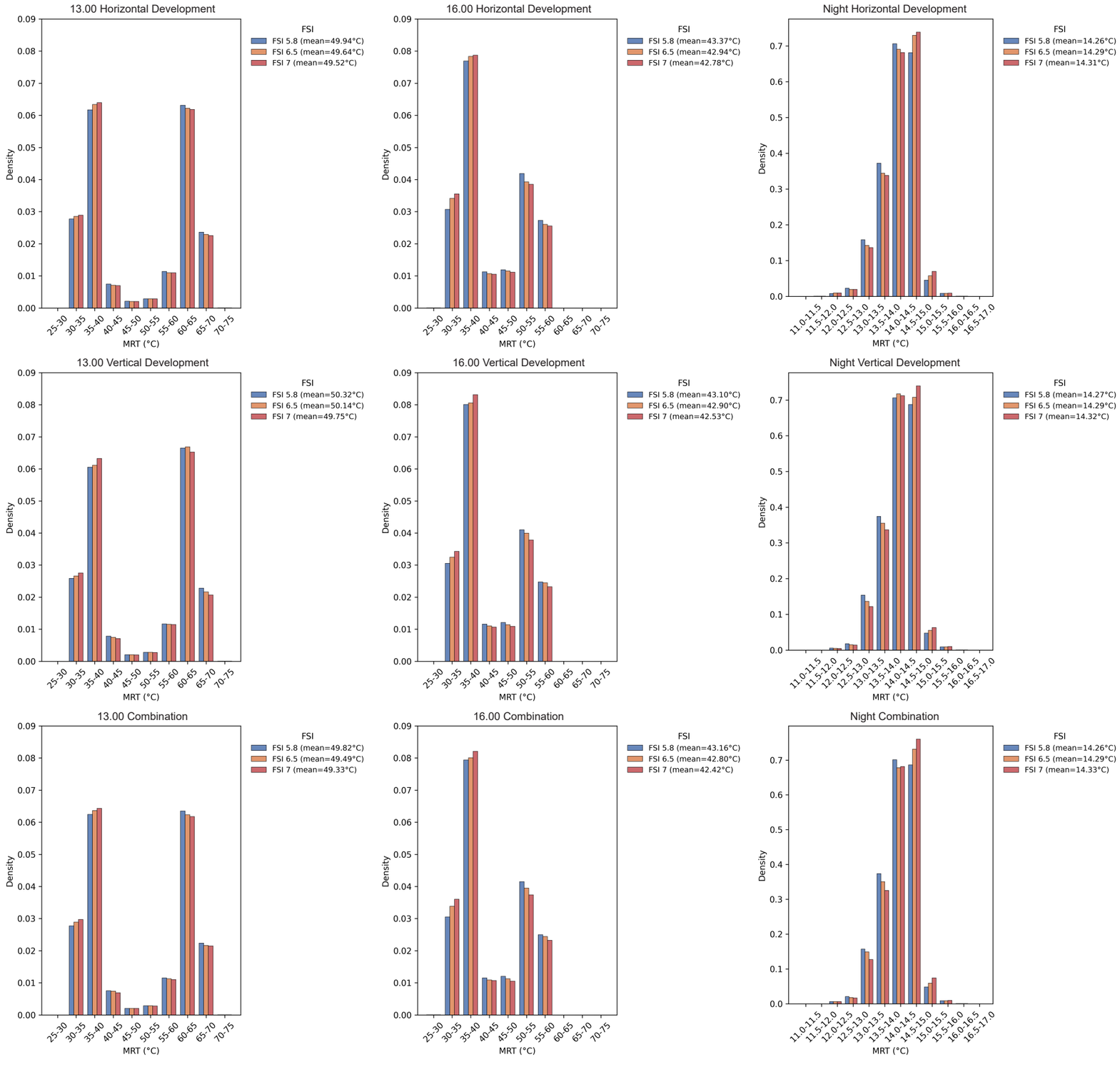
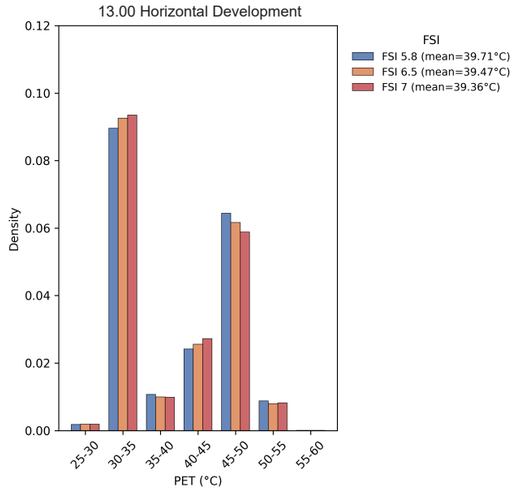
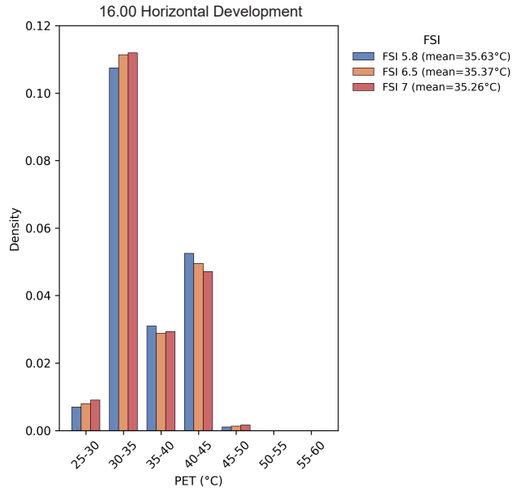
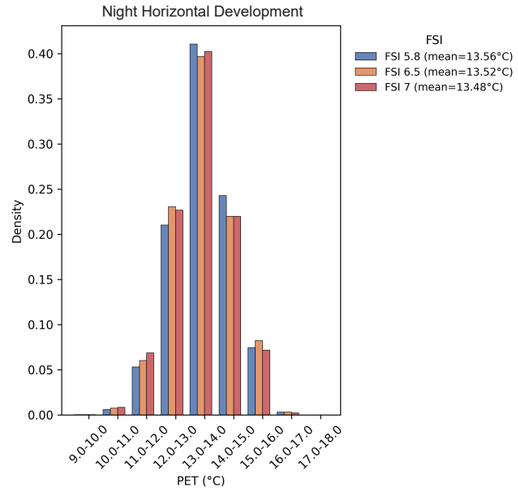
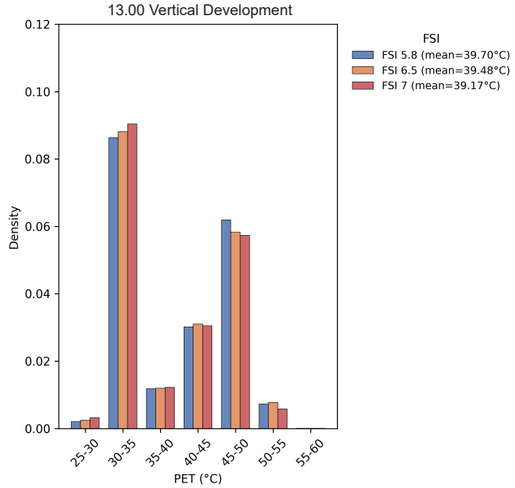


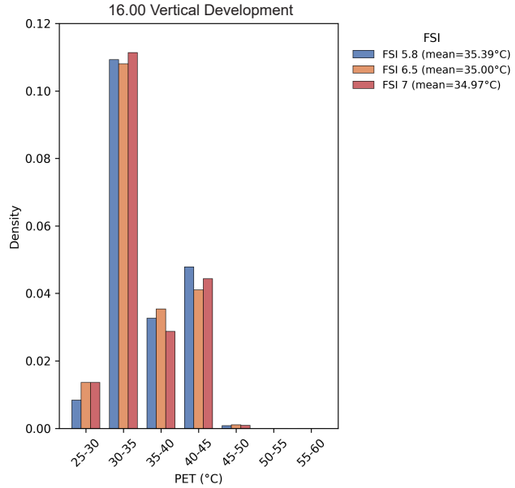

**Figure 7.33:** Distribution of MRT under Different FSI and Configurations (Source: By Author)

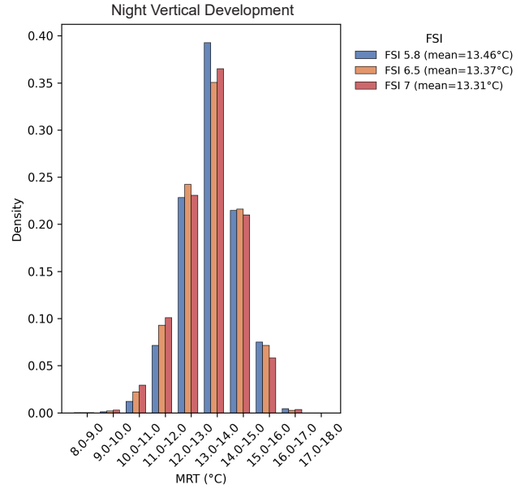


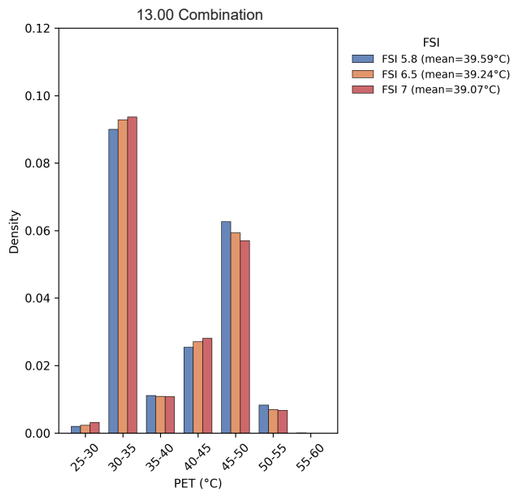



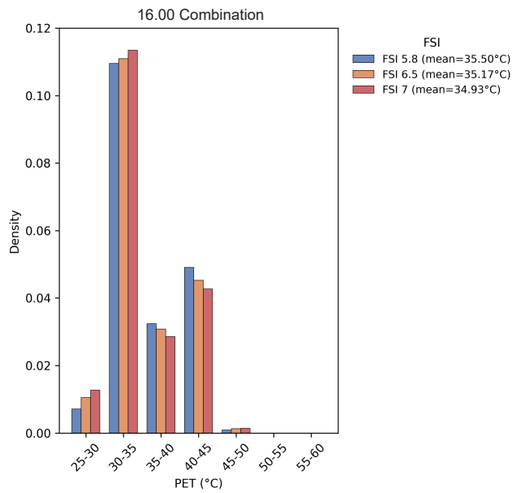



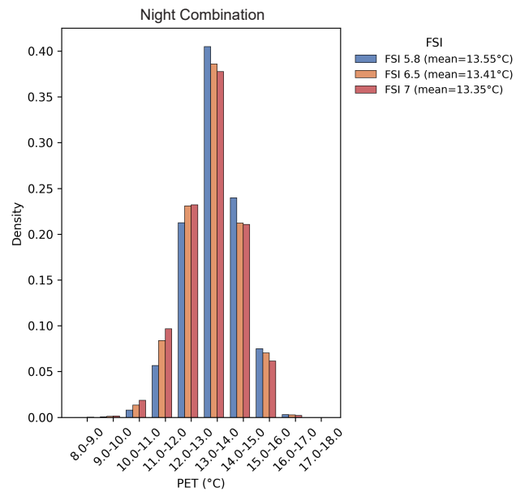




**Figure 7.34:** Distribution of PET under Different FSI and Configurations (Source: By Author)

**Horizontal Development vs. Vertical development:** Considering the issue of building form, the horizontal development has a greater effect in providing continuous shade in the street compared to the vertical development, but it is time-dependent, meaning that it becomes less effective after midday. Vertical development have a larger shadowing area in wide streets than horizontal development. Conversely, horizontal development provide better shading than vertical development on narrow streets (Figure 7.35). The same phenomenon was also observed at other times, such as 14:00 and 15:00, but under higher solar altitude conditions, for instance at around noon (13.00 and 14.00), the shading effect produced by vertical development is less efficient than horizontal development (Figure 7.36).

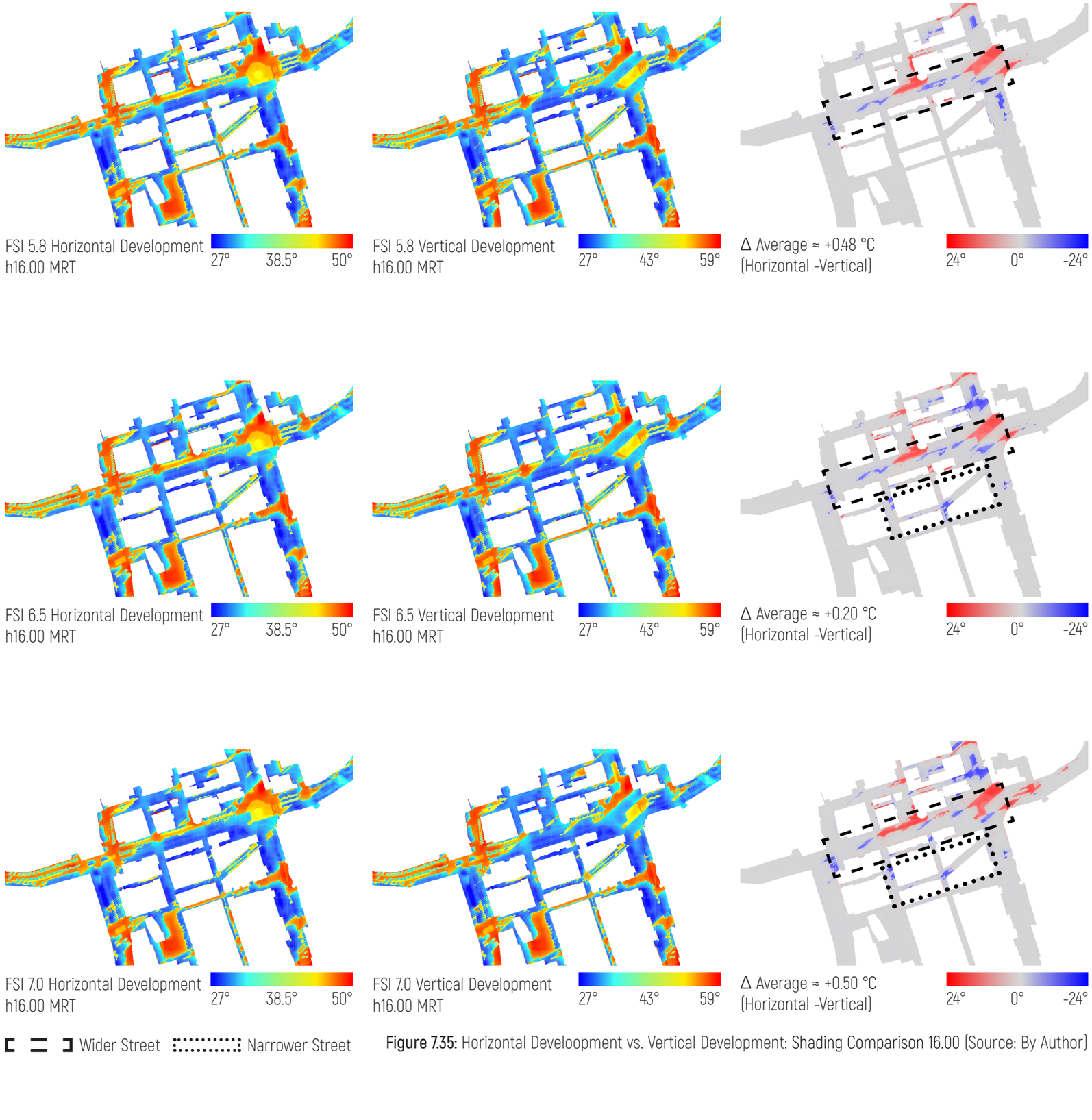
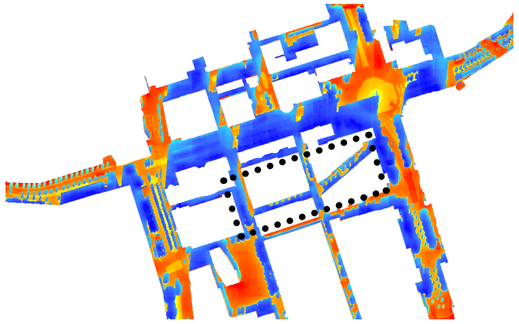
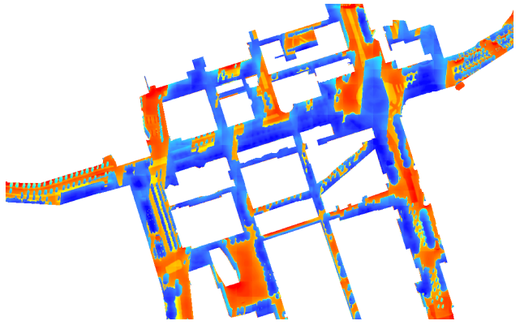



**Figure 7.35:** Horizontal Developoment vs. Vertical Development: Shading Comparison 16.00 (Source: By Author)



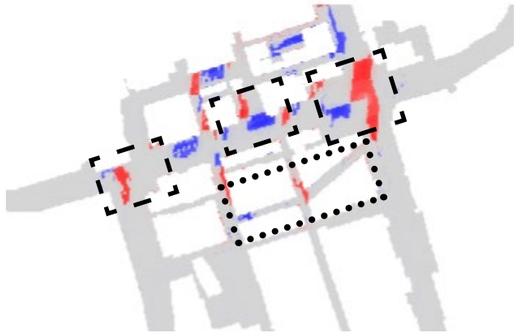
FSI 7.0 Horizontal Development
h14.00 MRT

28° 48° 68°



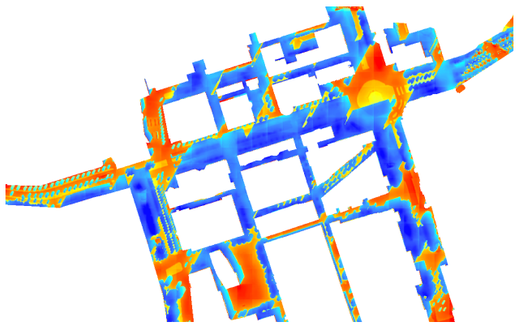
FSI 7.0 Vertical Development
h14.00 MRT

28° 48° 68°



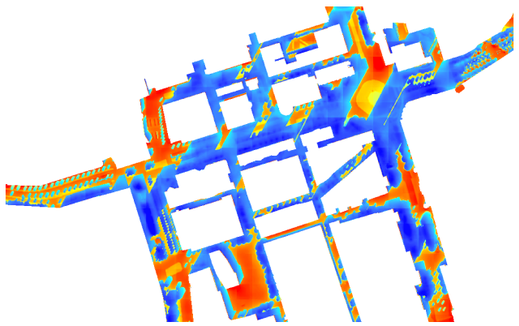
Δ Average ≈ +0.15 °C
(Horizontal -Vertical)

30° 0° -30°



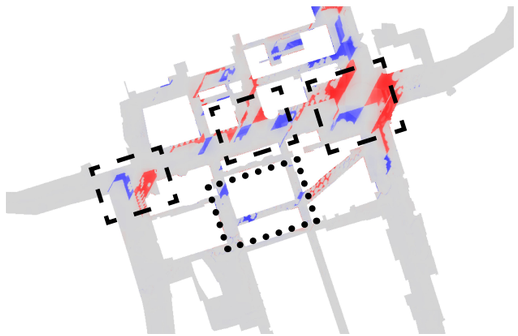
FSI 7.0 Horizontal Development
h15.00 MRT

28° 45.5° 63°



FSI 7.0 Vertical Development
h15.00 MRT

28° 45.5° 63°



Δ Average ≈ +0.34 °C
(Horizontal -Vertical)

27° 0° -27°

**Figure 7.36:** Horizontal Develoopment vs. Vertical Development: Shading Comparison 14.00 and 15.00 (Source: By Author)

Wider Street  Narrower Street

During windless nights, the urban form becomes significant in influencing the temperature. The horizontal development causes more heat retention compared to the vertical development, and this phenomenon is more prominently in narrower streets. This effect is less significant on the  wider streets and open spaces. Nevertheless, when the heights of the podiums are increasing around these wider streets or open areas, which creates a more enclosed urban context, the drop of SVF will also increase the heat retention obviously (Figure 7.37).

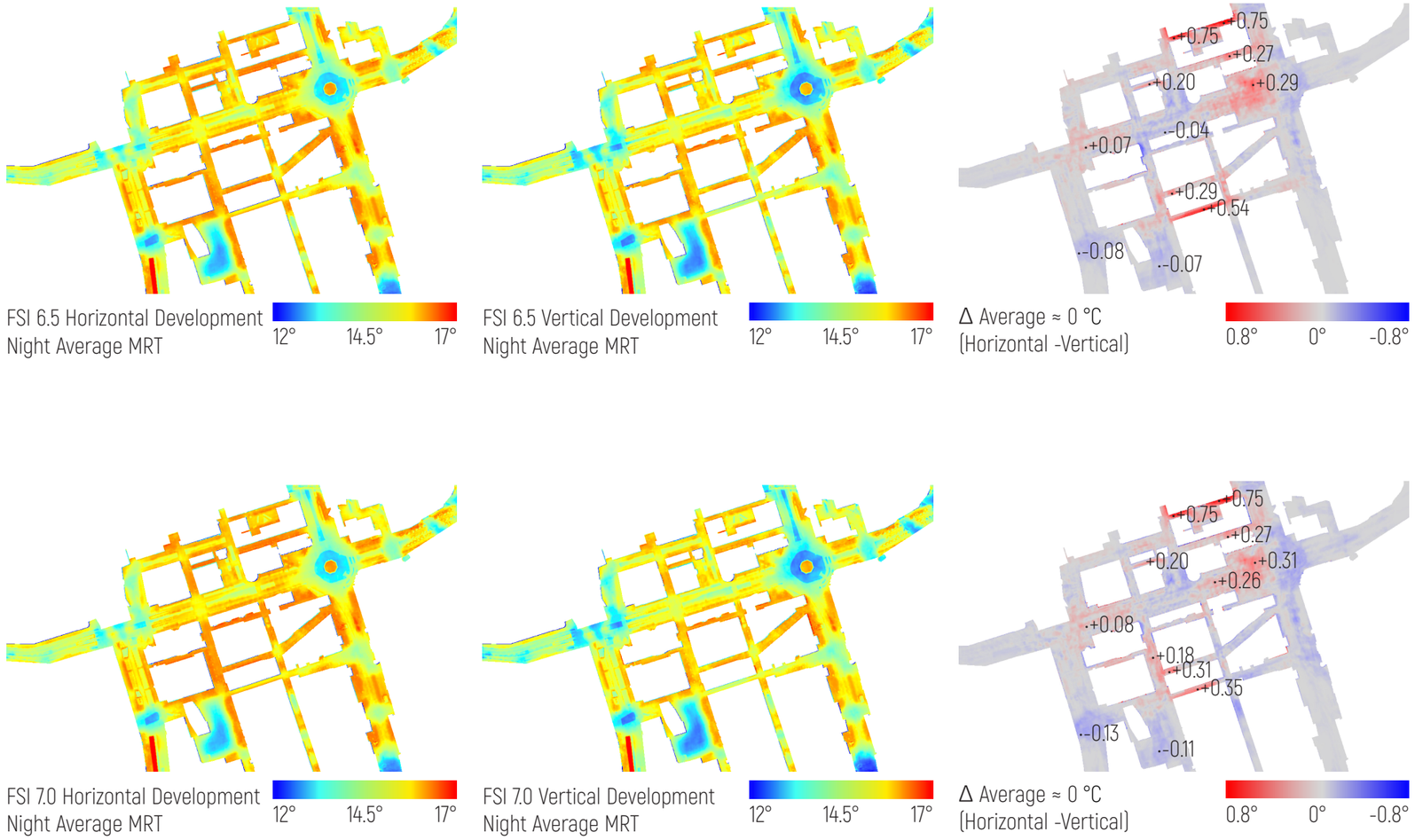



**Figure 7.37:** Horizontal Development vs. Vertical Development: Heat Retention Comparison (Source: By Author)

The impacts of wind are highly variant among different types of buildings. As indicated by Figure 7.38, the effect of horizontal development on wind and thermal comfort depends on the width of streets. Along wider streets, continuous podium forms tend to block airflow, reducing ventilation and increasing nighttime PET. In contrast, in narrower streets, podiums deepen the street canyon, which can enhance wind speeds through channeling effects and lead to lower nighttime PET.

By comparison, tower configurations generate localized wind acceleration through downwash effect, bringing higher-level airflow down to the pedestrian level. This increases wind speeds in surrounding areas and contributes to lower PET.

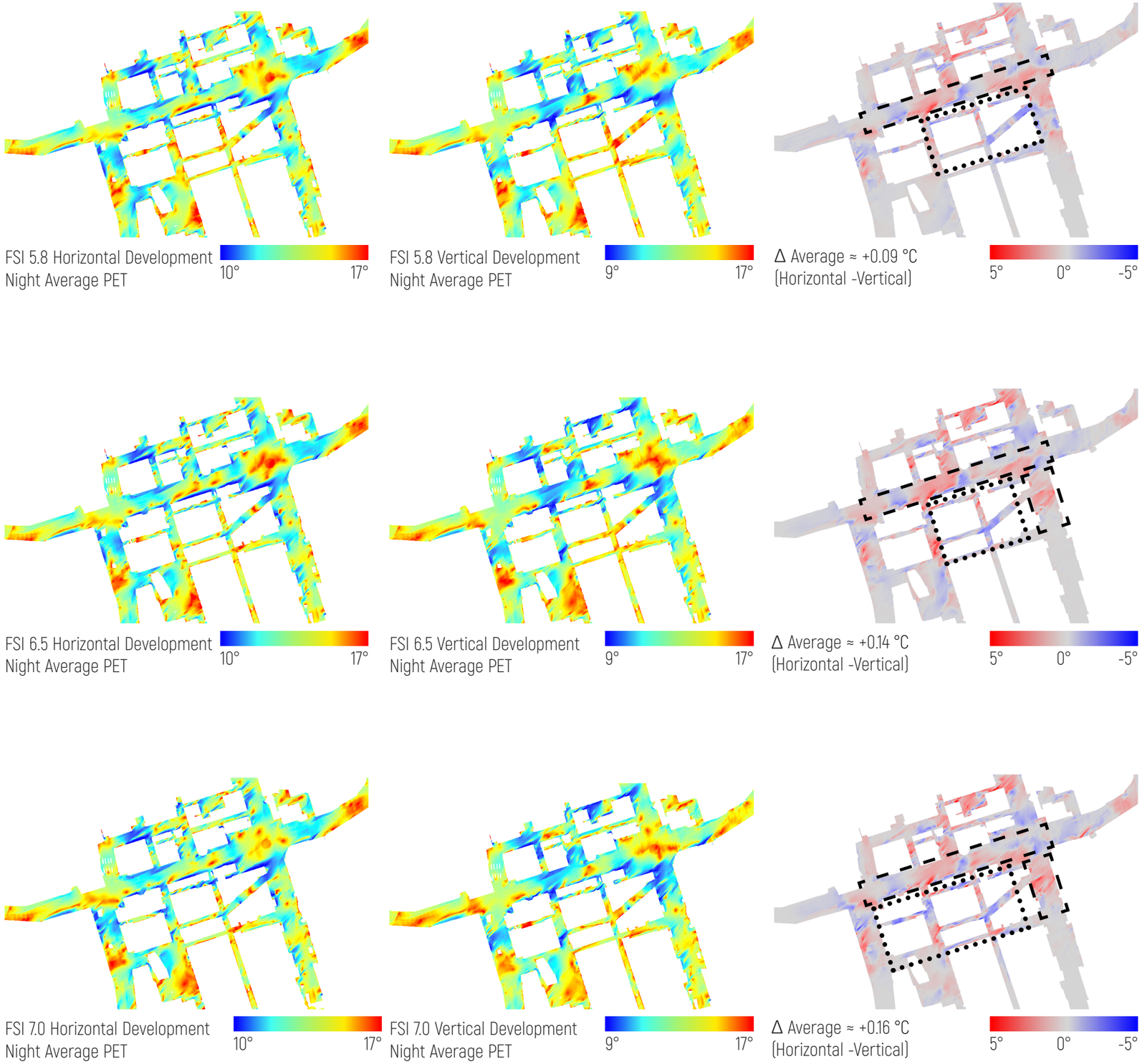



**Figure 7.38:** Horizontal Development vs. Vertical development: PET Comparison (Source: By Author)

## 7.4 Building Morphology Exploration

Despite providing better shading areas than vertical development in a narrow street during the daytime, horizontal development may result in greater heat retention at night. In order to solve this problem, additional experiments are conducted to investigate the effect that different shapes of podiums have on nighttime thermal environment.

The testing procedure revolves around narrow street canyons, focusing on the morphology of FSI 7, podium type. Based on this setup, four podium variations are examined while keeping the FSI as a constant: (1) a setback podium positioned 12-15m away from the street edge; (2) a stepped podium with vertically articulated massing; (3) a height-varied podium with non-uniform roof profiles; and (4) a hybrid configuration that combines podiums and towers.

### 7.4.1 Setback Podium

In the case of the setback podiums configuration, there is a slight decrease in nighttime heat gain in the absence of wind conditions, amounting to about 0.2°C. While considering about the wind, the setback podiums cause the wind speed to reduce because of the wider street canyon. On the contrary, because of the moving back and elevation of some podiums, parts of the street canyons are also deepened, thus increasing wind speed. In general, the PET remains unchanged.

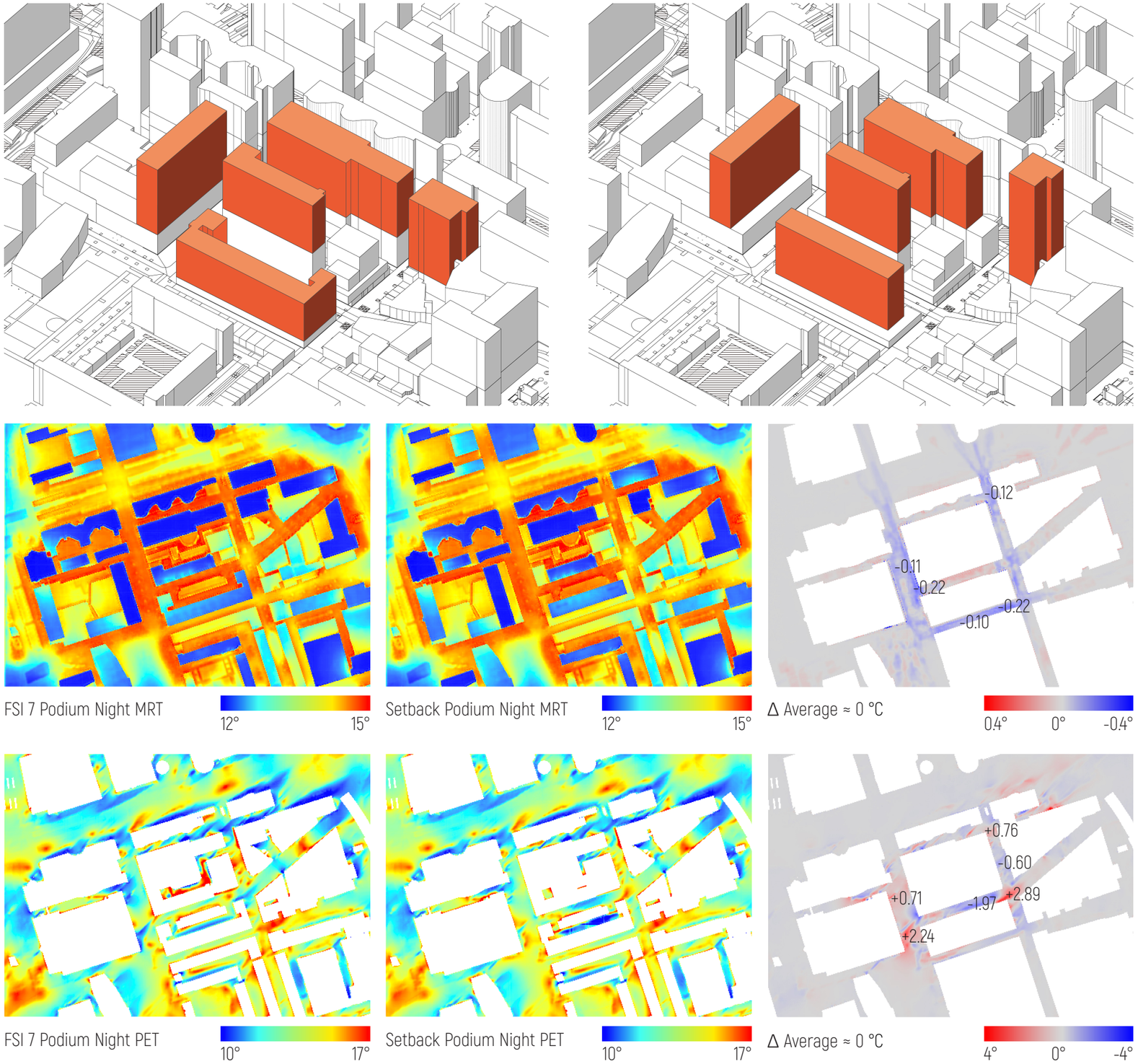



**Figure 7.38:** Building Morphology Comparison: Setback Podium (Source: By Author)

### 7.4.2 Stepped Podium

The stepped podium configuration also shows a slight change in nighttime heat retention under windless conditions, with a reduction of around 0.1°C compared to the baseline scenario, which is basically unnoticeable to pedestrians. Under the windy condition, same as the setback podium scenario, the wind speed within the street canyon decreases due to reduced enclosure and a weaker channeling effect, leading to an increase in nighttime PET. Meanwhile, in order to keep the FSI the same, some podiums are heightened which also deepens the street canyons, causing a decrease of wind speed and a rise in PET.

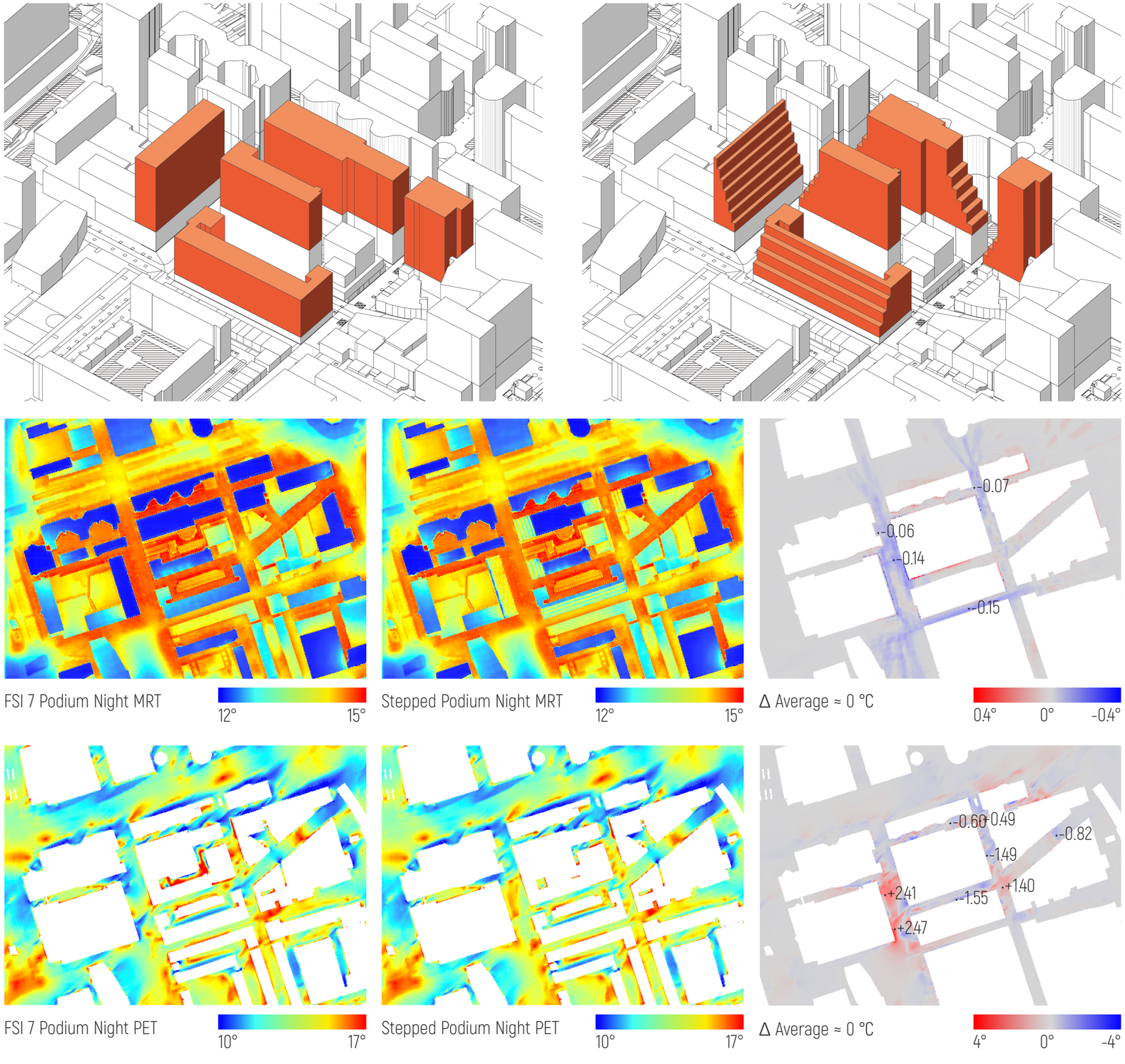



**Figure 7.39:** Building Morphology Comparison: Stepped Podium (Source: By Author)

### 7.4.3 Height-varied Podium 1

The height-varied podium layout does not demonstrate a significant capability on reducing nighttime heat retention. Under windy conditions, the result indicate that variations in podium height do not obviously increase wind speed at the pedestrian level. Instead, they alter airflow patterns within the street canyons due to the various heights of podiums, causing wind speeds to increase in some areas and decrease in others. In general, the overall PET still remains constant.

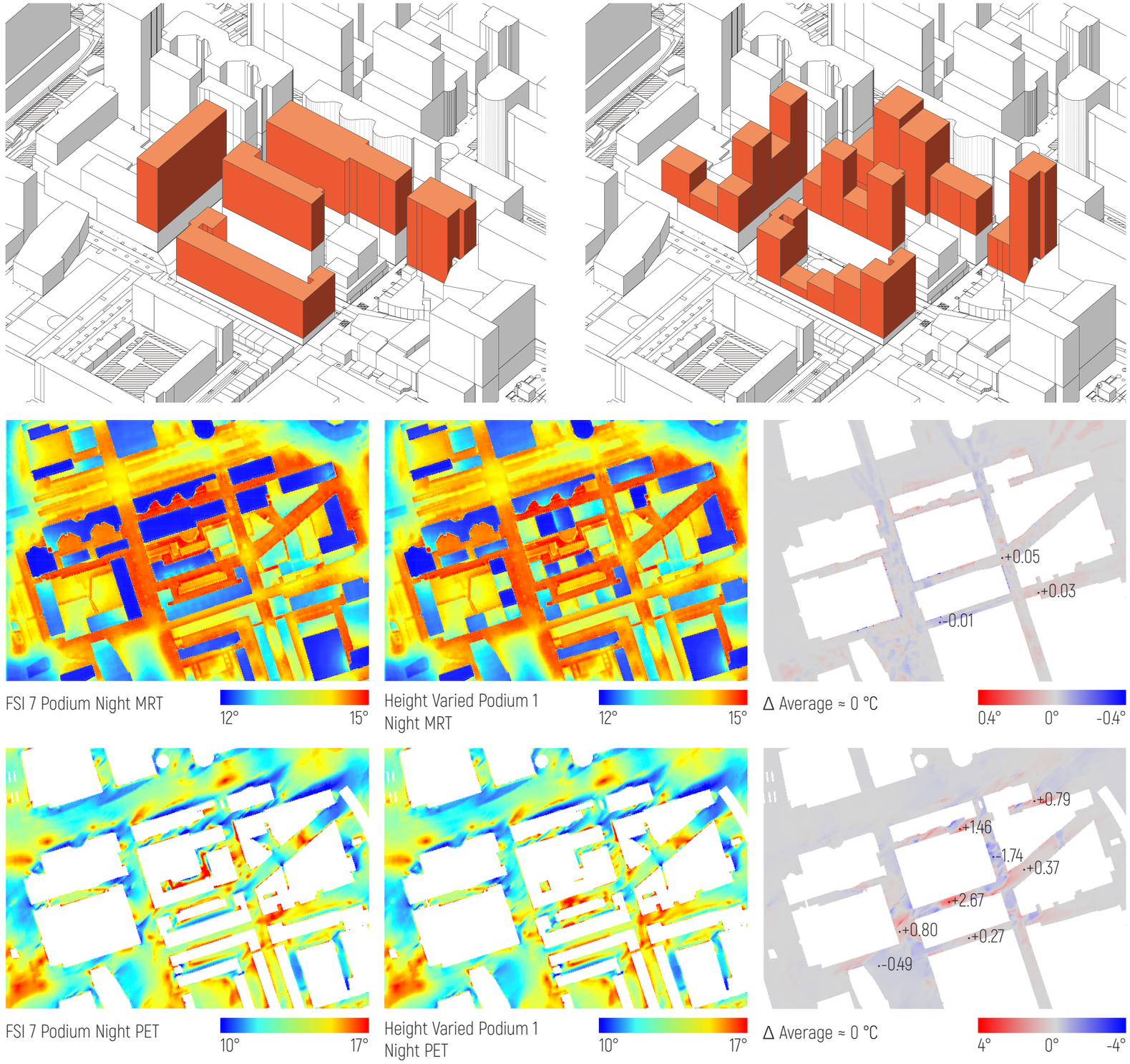



**Figure 7.40:** Building Morphology Comparison: Height-varied Podium 1 (Source: By Author)

### 7.4.4 Height-varied Podium 2

Similar to the configuration in 7.4.3, heat retention remains largely unchanged in this context. Under windy conditions, the average PET on the street level does not exhibit a clear increasing or decreasing trend. However, changes in the height of the podium also alter the local wind field, like the previous configuration. In general, Wind speed changes still depend on the depth of the street canyon.

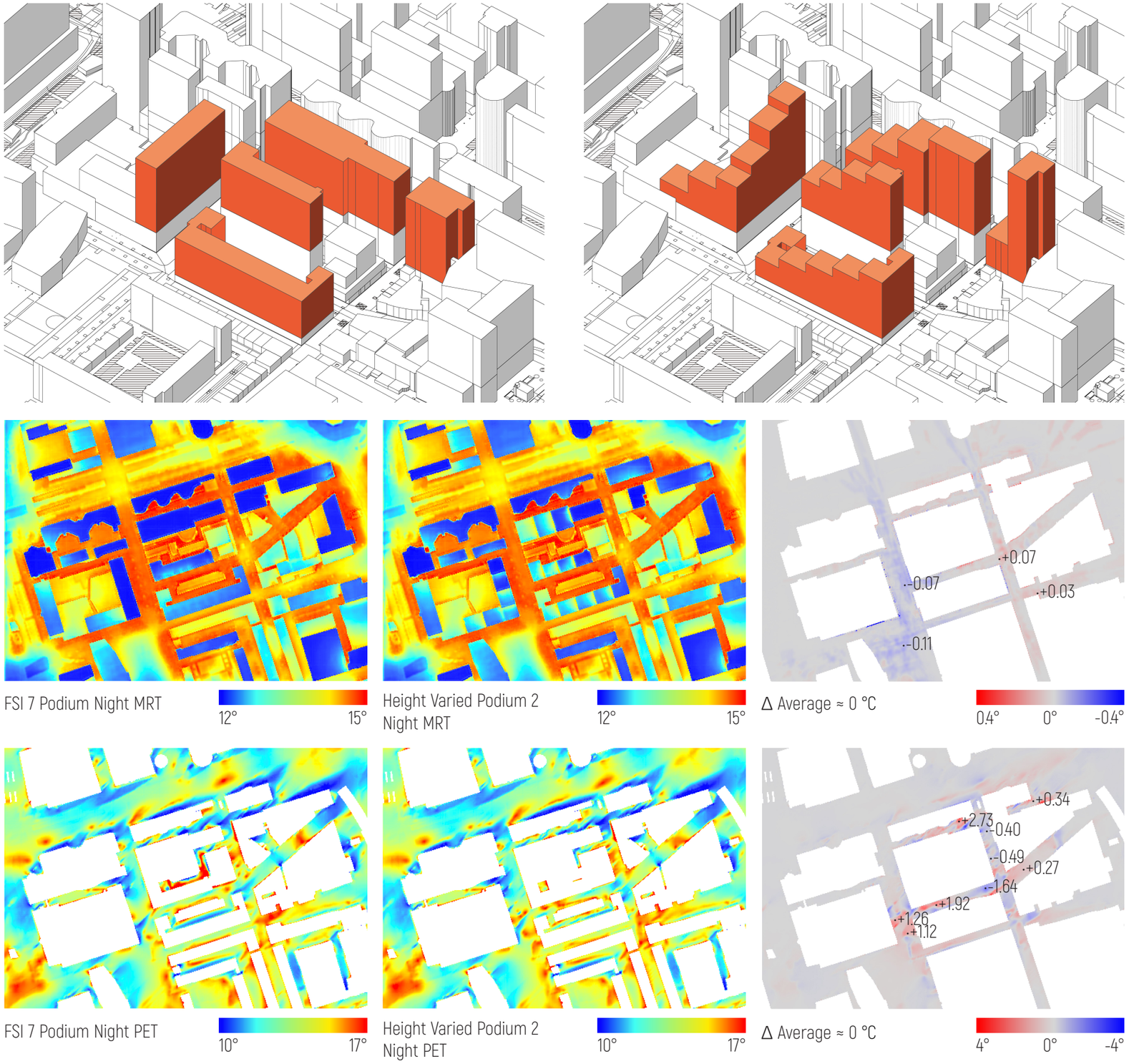



**Figure 7.42:** Building Morphology Comparison: Height-varied Podium 2 (Source: By Author)

### 7.4.5 Podium and Towers Combination

In terms of the podium-tower configuration, under windless conditions, the nighttime heat retention in some areas decreased, by approximately 0.3°C. This is because the continuous podium is replaced with high-rise towers of the same FSI, which reduces the enclosure of the space and thus reducing heat retention.

Under the windy situation, spatial variations in wind speed are evident, with some areas having higher wind speed and the others having lower wind speed. In this regard, higher wind speed is caused by those places where the high-rise towers deepen the street canyon, thus increasing the channeling effect. On the other hand, lower wind speeds will occur at zones where podium height is lowered and the new towers do not create efficient channeling effect.

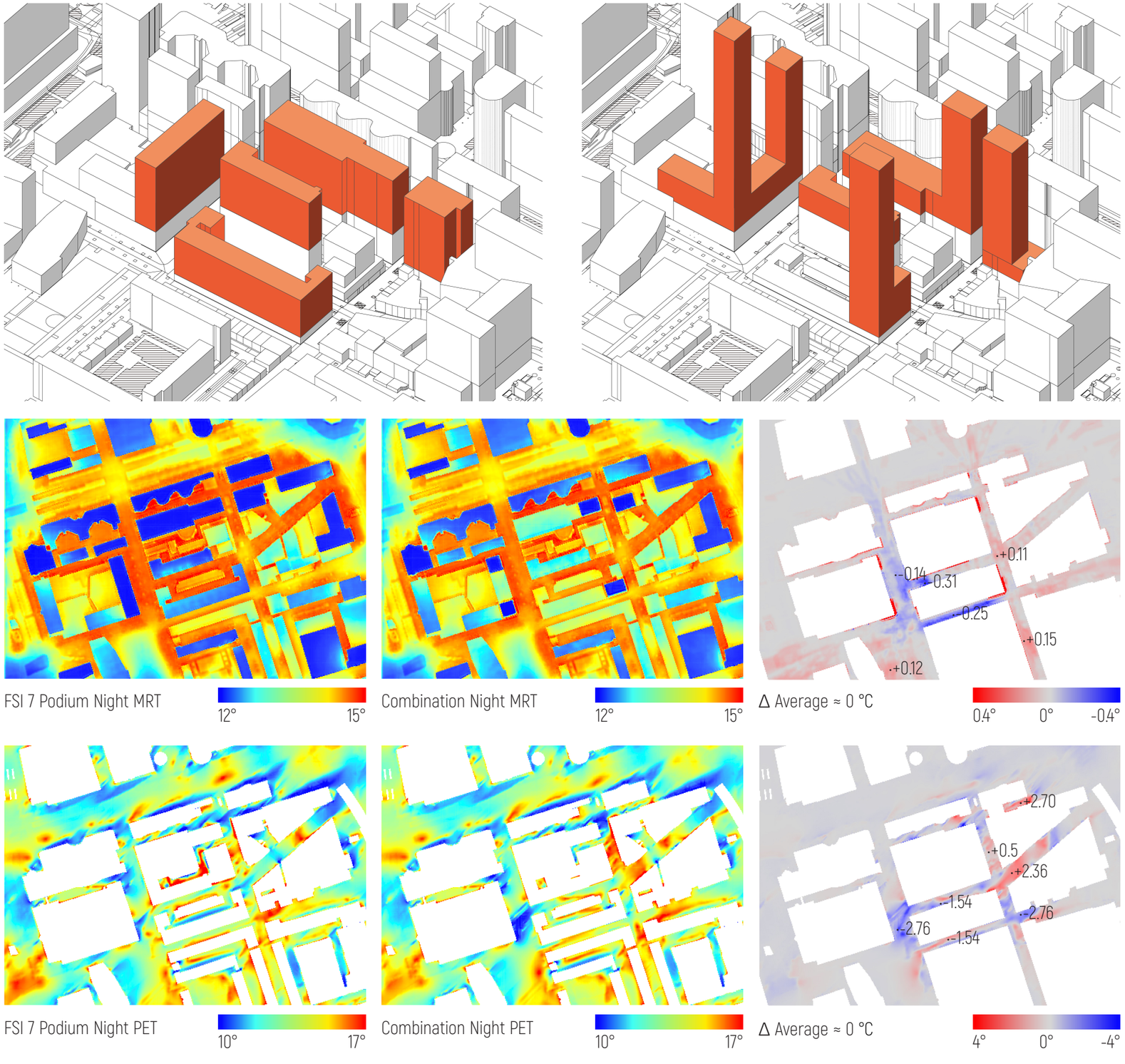



**Figure 7.43:** Building Morphology Comparison: Combination (Source: By Author)

### 7.4.6 Conclusion

The results suggest that, within narrow street canyons, only focus on building morphology alone has only a limited effect to reduce nighttime heat retention. Among these tests, setback and stepped podiums have better performance on reducing heat retention. The core mechanism of these two configurations is the increase of SVF, making the street canyon more open. However, the reduction remains small with the maximum around 0.3°C, which is unlikely to Significantsly improve pedestrian thermal comfort.

At narrow street level, continuous podium configurations are generally more effective on increasing wind speed because continuous podium can make street canyons deeper which strengthen the channeling effect under the tested wind conditions. Therefore, despite setback and stepped podiums slightly reducing heat retention, these two configurations may also weaken ventilation and lead to higher nighttime PET. Besides, the podium–tower combination also does not significantly reduce nighttime PET compared with continuous podium forms, since isolated towers are unable to generate a continuous channeling effect along the street canyon.

The height-varied podium configurations are particularly notable. In contrast to some previous studies, the wind speed does not show a noticeable increase at pedestrian level. Instead, variations in podium height mainly altered local airflow distribution, producing localized increases and decreases in wind velocity. This difference may be due to the fact that the URock model simplifies the simulation of airflow. The wind environment is highly complex, and the simulation used in this study is relatively simple, it may not be possible to capture all wind environment mechanisms. As a result, more specialized software is needed for further research on the wind environment. Nevertheless, previous research suggests that height variation can improve urban ventilation and pollutant dispersion. Therefore, Height-varied Podium might be a possible solution to reduce temperature.

Overall, under the tested conditions, increasing street canyon depth can be one of the more effective morphological strategies for reducing temperature in narrow streets, but its effectiveness remains strongly dependent on street orientation and prevailing wind direction.

# 8. GUIDELINES

8.1 Introduction

8.2 Urban Development Guidelines

8.3 Buildings Layout Guidelines

8.4 Additional Thermal Mitigation Guidelines

## 8.1 Introduction

According to the conclusions of the previous research, the relationship between densification and outdoor thermal environment is complicated. Although raising FSI may have a positive effect of reducing daytime heat stress by adding more shading, it may still cause higher heat retention during nighttime which mainly depends on urban and architectural morphology. Consequently, the adoption of urban densification as a design strategy must not be regarded as a one-size-fits-all approach but a morphology-dependent process balancing shading, ventilation, and heat storage.

This section will translate the results into a series of design guidelines for achieving thermally responsive urban densification.

## 8.2 Urban Development Guidelines

### 8.2.1 Conduct Spatially Concentrated Densification

High-density development can be conducted in a relatively compact way since high-density development increases the coherence and the area of shading on the pedestrian level, which minimizes thermal stress during daytime hours. Even if high-density development results in higher heat retention at night due to more enclosed spaces, its impact is minimal (Maximum improvement of about 0.6°C when the FSI increases by 1) and can be offset through ventilation improving by proper building layout and morphology design (Figure 8.1).

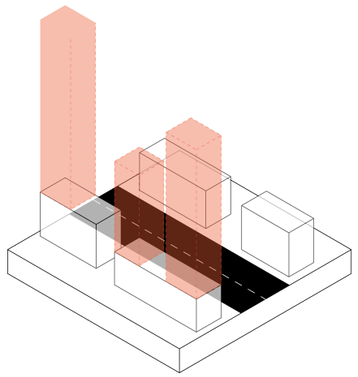
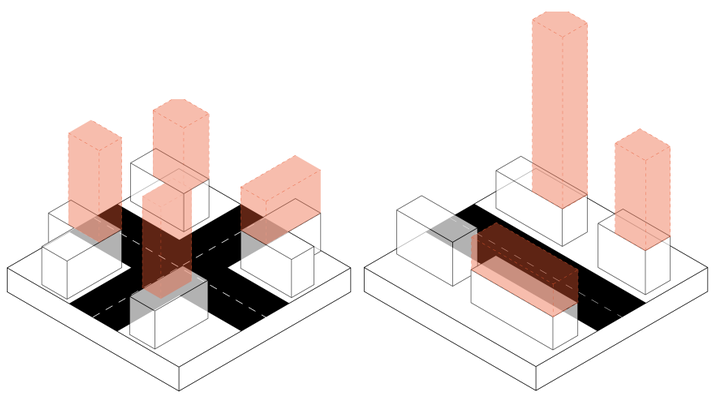


**Figure 8.1:** Spatially Concentrated Densification (Source: By Author)

### 8.2.2 Prioritize densification in wider streets and open spaces

Densification should be firstly considered to implement along broader streets, intersections, and large urban spaces (Figure 8.2). In these locations, higher building density can enhance shading for nearby open spaces during the daytime. On the other hand, since their sky view factors are relatively high and enclosures are low, there will not be stronger accumulation of heat at night. Figure 8.3 shows the wider streets and open areas which might prioritize to be developed.



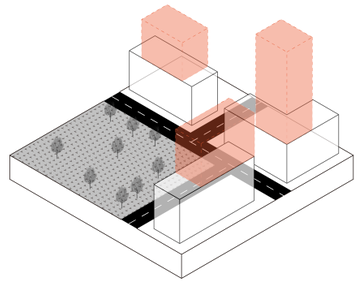
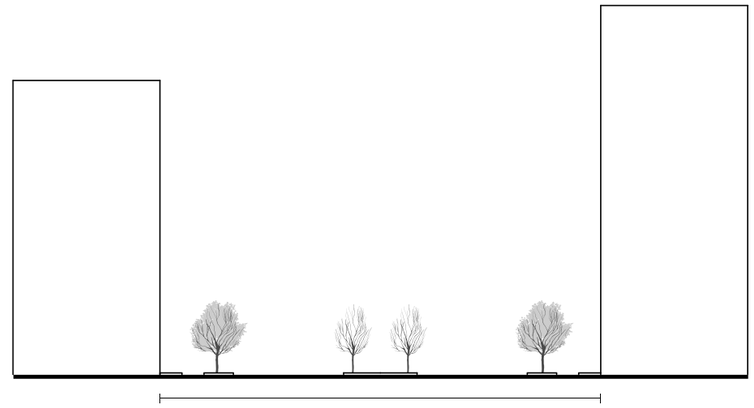


**Figure 8.2:** Prioritize densification in wider streets and open spaces (Source: By Author)

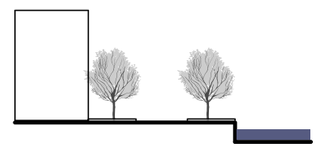



**Figure 8.3:** Priority Development Areas in Rotterdam City Center (Source: By Author)

In this research, streets are classified as wide when the distance between building façade on both sides exceeds 45 meters, whereas the distance between building façades on both sides is less than 20 meters are considered as narrow. Additionally, those streets that are adjacent to water, parks, or green spaces on one side can also be considered wider streets.



Wider Street: Width ≥ 40m



Open Areas: Adjacent to Water



Open Areas: Adjacent to Green



Narrower Street: Width ≤ 20m

### 8.2.3 Prioritize Vertical Densification

Vertical development provides more extensive and consistent shading than horizontal expansion, which can cover larger areas throughout the whole day. High-rise towers generally block airflow less than continuous podium structures and can locally accelerate wind through downwash effects, helping to reduce air stagnation. During windless nighttime, they retain less heat compared to horizontal development. In general, the results suggest that vertical development may be a more effective strategy for mitigating thermal risks in high-density urban development.

### 8.2.4 Consider densification in High Solar Exposure Areas

According to conclusions of this research, densification does not always trigger heat risk due to the higher building density can provide more shading at the pedestrian level, effectively reducing exposure to shortwave solar radiation during the daytime. As a result, areas with high solar exposure, may be considered as a priority locations for future densification. Based on figure 8.4, high exposure is more likely to occur along wide streets and open spaces with relatively low surrounding buildings or limited tree coverage. Besides, East–west oriented streets are also more vulnerable to solar exposure (Figure 8.5). Through appropriate building layout and morphological design, densification can potentially help mitigate thermal stress in these areas.




**Figure 8.4:** Solar Exposure of Rotterdam City Center (Source: By Author)

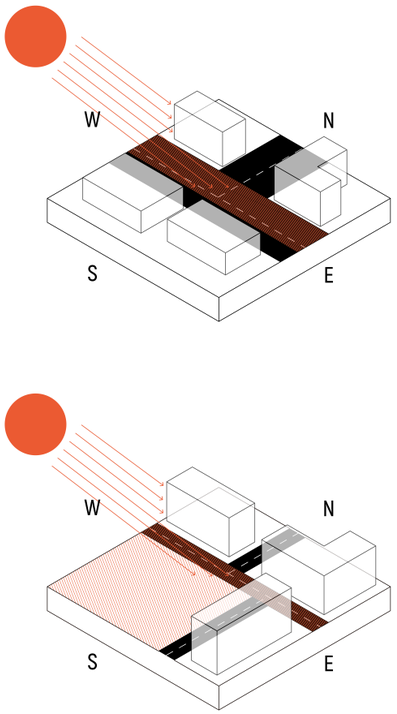



**Figure 8.5:** Potential High Exposure Areas (Source: By Author)

## 8.3 Building Layout Guidelines

### 8.3.1 Vertical Development Principles

#### 8.3.1.1 Prioritize Vertical Development in South and West sides of wider streets and open spaces

The vertical development should be prioritized for construction in wide streets and open spaces where the efficiency of their shade will be fully achieved. Besides, towers should be situated on the southern or western side of the streets and open spaces Because the strongest solar radiation in the afternoon can be blocked to form a cooler environment (Figure 8.6).

Though towers can be situated next to narrow streets, shading by towers is less efficient at street level. Since the height of the towers, much of the shadow falls on building façades and rooftops rather than on the ground. Therefore, their effectiveness in providing pedestrian-level shading in narrow streets is limited.

#### 8.3.1.2 Localize Vertical Development Along Street Edges

It is best not to place towers in the middle of urban blocks since their shadow will most probably be cast on rooftops instead of streets. Towers should rather be positioned closer to the street edge for greater street shading effects and enabling most of the downwash wind to reach the street level (Figure 8.6).

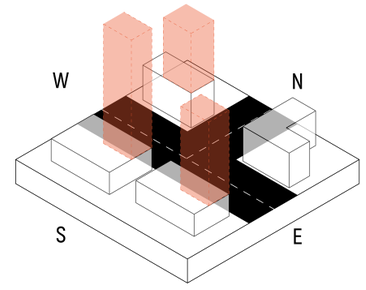



**Figure 8.6:** Vertical Development principle (Source: By Author)

### 8.3.2 Horizontal Development Principles

#### 8.3.2.1 Prioritize Horizontal Development in South and West sides of Narrower Streets

Podium-type buildings generally perform better in cooling narrower streets, where they can provide more effective street-level shading during the daytime. In addition, by increasing the street canyon aspect ratio, horizontal development can enhance airflow through channeling effects, potentially increasing wind speed and reducing PET.

South and western sides of areas should be prioritized since it will offer better shading in the afternoon, reducing the heat exposure (Figure 8.7). Horizontal development on the north side is also possible to consider, in that it can deepen the street canyon and improve the wind speed, which helps to decrease the PET. However, during the daytime, north side podiums cannot offer efficient shadow on the pedestrian level.

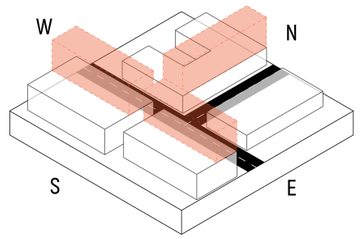



**Figure 8.7:** Horizontal Development principle (Source: By Author)

#### 8.3.2.2 Avoid Horizontal Development in Wider streets and Open Areas

Horizontal development is not recommended for wider streets or open spaces. In such contexts, continuous podium forms may obstruct airflow while offering less channeling effect and effective shading than high-rise towers, leading to higher MRT and PET than vertical development (Figure 8.8).

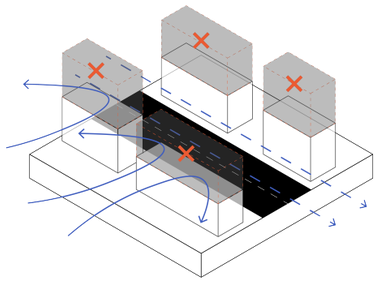


**Figure 8.8:** Avoid Horizontal Development in Open Areas (Source: By Author)

### 8.3.2.3 Avoid Horizontal Development on Both Sides

Placing podiums on both sides of a street should also be avoided. Even though it can lead to deeper streets canyon which tends to generate higher wind speeds, it also cause more heat retention under the windless night because of higher enclosure. However, one-sided podium development can also improve airflow and minimize nighttime heat retention (Figure 8.9).

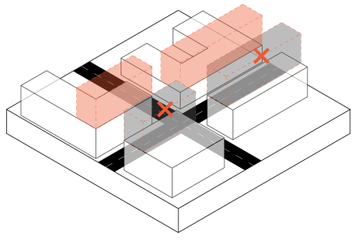


**Figure 8.9:** Avoid Horizontal Development on Both Sides (Source: By Author)

### 8.3.2.4 Implement Continuous Podium in Narrow Streets

Continuous podiums can actually be an effective configuration in narrow streets since they increase wind speeds by channeling effect, which lowers the PET. Despite this type of form retaining more heat at night on account of greater enclosure, the overall amount of retained heat remains relatively limited and can be offset by improved ventilation (Figure 8.10).

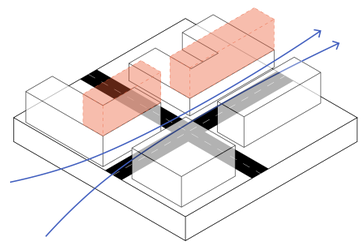


**Figure 8.10:** Implement Continuous Podium in Narrow Streets (Source: By Author)

## 8.4 Additional Thermal Mitigation Guidelines

This research mainly focus on the influence of the urban and building morphology on the thermal environment of outdoor areas. It is obvious, though, that apart from the form, there are other elements affecting thermal conditions. Besides, the findings of this research also demonstrate the limited impact of the morphological approaches to heat mitigation in some cases. The following chapter suggests a range of design measures based on scientific literature reviews.

### 8.4.1 Vegetation Guidelines

#### 8.4.1.1 Prioritize planting in Less Shading Areas

Figure 8.4 shows areas which have higher solar exposure. From the observation, it can be seen that the less shading areas especially northern edge of east–west oriented streets is difficult to shade using buildings. Although high-rise buildings can provide shading areas, it is often discontinuous and insufficient at the pedestrian level. In this case, planting trees along the northern side can provide more continuous shading and improve thermal comfort.

#### 8.4.1.2 Use large-canopy trees cautiously in narrow streets

The planting of large-canopy trees in narrow street canyons should be carefully considered, as a dense canopy cover will exacerbate nighttime heat retention due to low SVF and block the wind, leading to the increase of nighttime temperature (Wang et al., 2022). Given that shading and ventilation can already be effectively achieved through building morphology, such as continuous podium configurations, extensive tree canopy may offer limited daytime benefits while restricting airflow and increasing heat accumulation at night.

### 8.4.2 Materials Guidelines

#### 8.4.2.1 Avoid High Albedo Materials in High-density Urban Area

In high-density urban environments, material selection should balance solar radiation, heat capacity, and emissivity. Materials with moderate albedo are preferable rather than highly reflective ones to avoid intensifying MRT (Alchapar et al., 2025; Lopez-Cabeza et al., 2022). Materials with low heat capacity and high emissivity should be prioritized to consider to reduce heat storage and enhance nighttime cooling (Peluso et al., 2022).

#### 8.4.2.2 Prioritize Using Low Albedo Pavements for Pedestrians

Low albedo pavements absorb more solar

radiation and reduce the reflected shortwave radiation. For pedestrians, low albedo materials can reduce MRT and improves daytime thermal comfort. Although these materials may increase surface temperatures, the reduction in reflected radiation generally outweighs this effect in terms of human thermal perception (Erell et al., 2014).

#### 8.4.2.3 Prioritize Low Albedo Materials in Less Shading Areas

Low albedo materials with higher emissive are recommended in less shading places showing in figure 8.4 because these materials reflect less shortwave radiation during daytime and they are more effective on heat releasing during the night.

# 9. CONCLUSION

9.1 Answer of Research Questions

9.2 Academic Relevance

9.3 Urbanism Relevance

9.4 U-Net Model

9.5 Thermal Environment Research

9.6 Transferability

## 9.1 Answer of Research Questions

### 9.1.1 How could Rotterdam develop heat-sensitive densification strategies with the support of deep-learning technologies?

Heat-sensitive densification strategies for Rotterdam can be supported through deep-learning technologies that combine rapid prediction with different urban morphologies. In this study, deep learning models were trained using UMEP simulation results during heatwaves in Rotterdam.

In this study, Mean Radiant Temperature (MRT) and Physiological Equivalent Temperature (PET) are chosen as the primary indicators of temperature because outdoor thermal environment are mainly influenced by solar radiation and wind. The research takes both daytime and nighttime into account, as the mechanisms shaping the thermal environment are different between day and night. For the test scenarios, a parametric design approach is adopted to investigate larger scale and small scale spatial configuration by keeping FSI constant. At larger scale, the purpose is to understand the impact of spatial layout on the thermal environment. At smaller scale, it aims to investigate whether optimizing building form can improve the thermal environment.

The deep learning models are used while testing all those scenarios. When providing relatively accurate results, deep learning models significantly reduce the time required to calculate the MRT and PET of these scenarios, facilitating subsequent analysis and research.
Based on these results, the study proposes heat-sensitive densification strategies for Rotterdam aiming to balance shading, ventilation, and heat retention within high-density urban environments.

### 9.1.2 What kinds of urban, environmental and morphological factors contribute to urban outdoor temperature?

The urban thermal environment is affected by a number of physical factors including radiation, landcover, urban morphology, blue-green infrastructure, materials and human activities.

Solar radiation predominates the source of heat. During the day, urban surfaces absorb the shortwave radiation and transform it as heat. At night, the stored heat will be released as longwave radiation, contributing to rise nighttime temperatures.

Landcover plays an important role in thermal environment, as surfaces such as roads, buildings, water, and vegetation differ in albedo, meaning they reflect or absorb solar radiation to varying degrees. These surfaces also vary in their capacity to store heat and release heat, which causes temperature differences in day and night.

Urban morphology has a complex relationship with thermal environment. The arrangement of buildings affects both shortwave radiation during the day and the release of longwave radiation during nighttime. This can be described using the sky view factor (SVF), which mainly reflect building height and building density. Higher SVF increases daytime solar exposure, while lower SVF can restrict nighttime heat release. Additionally, urban morphology also impacts on wind field. Buildings can both block wind, causing localized temperature increases, and guide wind, thus lowering localized temperatures.

Blue and green infrastructure contribute to temperature reduction through evapotranspiration and shading. Depending on the area, blue-green infrastructure can reduce the temperature by up to 1-2 °C within a certain range.

Materials also have complex impacts on thermal environment. High-albedo materials reflect more shortwave radiation, meaning less heat is absorbed by the surface which releases less heat during nights, but they may increase reflected radiation and increase the thermal stress. On the contrary, low-albedo materials absorb more heat, leading to greater heat storage and potentially higher nighttime temperatures.

Finally, human activities also contribute to heat to urban environment. Those activities such as traffic, air conditioning, and other energy uses release anthropogenic heat, which can further elevate temperatures, particularly in densely built areas.

### 9.1.3 How can technology helps simplify and strengthen the prediction of urban outdoor temperature?

Deep learning models simplify the computational process compared to traditional simulation methods. Urban researchers only need to prepare the relevant raster datasets as input, without performing complex simulation procedures.

Under the support of deep learning model, a large amount of computation time can also be reduced. For instance, using a model like SOLWEIG to simulate MRT for a 2 km × 1 km area at 1 m resolution over 24 hours can take around 1.5 hours to calculate temporally continuous results. In contrast, the deep learning model can generate each raster in approximately 1–2 seconds.

The calculation of PET also has similar improvement. UMEP normally requires 10–15 minutes for one raster, but the deep learning model can produce each raster within 1–2 seconds.

As a result, urban researchers and planners can conduct thermal environment assessments on more design scenarios in a shorter time, supporting faster exploration and decision-making in urban design and planning.

Most importantly, the model developed in this study is not the most advanced one. Some recent studies have suggested that input data can be further simplified without compromising on accuracy. This implies that this method will make the process more simple and time-efficient along with the technology development.

### 9.1.4 Which types of spatial configurations are most effective on reducing heat during both day and night in high density urban area in Rotterdam?

In general, no single urban context can achieve the best cooling effect under all conditions. Each approach has its advantages and disadvantages depending on the specific climate situation, urban morphology, and street type.

Typically, FSI can lower daytime temperatures by increasing shading. However, under windless conditions, it may lead to higher nighttime temperatures due to greater heat retention. Under windy conditions, taller buildings and deeper street canyons can also promote airflow, which may help reduce temperatures.

Vertical development generally perform well across majority scenarios. High-rise towers create larger shaded areas during the day especially at wider streets and open areas, reducing solar exposure on pedestrian level, while the more open structure of high-rise towers allows heat to release more easily during nighttime. In addition, towers can enhance wind flow and improve local ventilation, which is effective on reduce temperature.

Horizontal development are relative effective in narrow street canyons. Under this situation, podiums provide more continuous street-level shading than high-rise towers, meaning less solar exposure during the day. Although podiums may increase nighttime heat retention, wind flow can also be enhanced due to the deeper street canyon, which partly offsets heat accumulation.

When it comes to the heat retention brought by podium on narrow street, modifications to building form can make slightly improve on thermal conditions. For example, setting back podium structures can slightly reduce heat retention, although this may also decrease wind speed. Generally speaking, it is not an effective way to deal with the heat retention.

In contrast, horizontal development are less effective in wider streets and open spaces. The shading effect of podiums is limited than high-rise towers, and podiums may block airflow, leading to localized temperature increase.

### 9.1.5 What guidelines can the municipality provide to developers to ensure a heat-sensitive densification?

Based on the conclusions, guidelines are formulated from the perspectives of urban development and buildings layout. These guidelines mainly consider reducing daytime solar

radiation, nighttime heat retention, and improving ventilation. Guidelines are as following:
1. Conduct Spatially Concentrated Densification

2.Prioritize densification in wider streets and open spaces

3. Prioritize Vertical Densification

4. Consider densification in High Solar Exposure Areas

5. Prioritize Vertical Development in South and West sides of wider streets and open spaces

6. Localize Vertical Development Along Street Edges

7. Prioritize Horizontal Development in South and West sides of Narrower Streets

8. Avoid Horizontal Development in Wider street and Open Areas

9.Avoid Horizontal Development on Both Sides

10. Implement Continuous Podium in Narrow Streets

11. Prioritize planting on the in Less Shading Areas

12. Use large-canopy trees cautiously in narrow streets

13. Avoid High Albedo Materials in High-density Urban Area
14. Prioritize Using Low Albedo Pavements for Pedestrians

15. Prioritize Low Albedo Materials in Less Shading Areas

### 9.2 Academic Relevance

This study explores how different levels of urban density and urban morphology influence the urban outdoor temperature under the background of densification.

In addition, the study introduces deep learning as a main methodological approach, aiming to replace the physical model which is complex to operate and time consuming. Under the help of deep learning model, the time spending on stimulation has been significantly reduced and it can support urban planners identify the most suitable scenarios with high efficiency.

Previous research has demonstrated the strong potential of deep learning in urban thermal studies, particularly for predicting temperature and thermal comfort. However, its application in practical design contexts remains limited, and relatively few studies assess whether such models are sufficiently reliable for decision-making. Meanwhile, in the field of thermal environment research, although a large number of literatures have studied the impact of urban morphology, vegetation and other elements on the thermal environment, there is a lack of systematic research on how different density strategies and building types affect the daytime and nighttime thermal environment at the pedestrian level.

This study attempts to fill this gap by using deep learning methods to test the thermal impact of different densification scenarios. While providing feasible suggestions for densification, it also explores the advantages and disadvantages of deep learning in practice.

### 9.3 Urbanism Relevance

The connection between this research and urbanism lies in the background of Dutch "One Million Housing" policy, which aims to deliver one million new homes to meet the needs of growing population. The study examines how future high-density development may influence the urban thermal environment.

A morphology-based approach is applied to investigate heat-sensitive densification, focusing on how different FSI, building forms and spatial configurations affect thermal conditions. The findings provide guidelines that can inform future urban planning and design practices to create a more heat-sensitive urban environment.

Simultaneously, the study reflects a possible shift within urbanism in the future, as urban challenges become increasingly complex and

require new analytical approaches. Researchers are now using AI to support both analysis and decision-making. In this study, deep learning is integrated with GIS tools to evaluate different scenairos with different FSI values and building forms, significantly reducing evaluation time and allowing planners to compare a wider range of design options within limited time. Apart from the conclusion on densification development, the study also points to a possible direction for future urbanism, demonstrating how AI can support complex analysis by providing reliable information. It frees planners from repetitive and time-consuming tasks, allowing them to spend more time on meaningful research and design.

## 9.4 U-Net Model

### 9.4.1 Conclusion

The results show that there is an obvious improvement of efficiency using the deep learning approach. The deep learning models are capable of simulating MRT and PET maps within 2 or 3 seconds, compared with the physical simulation models, such as SOLWEIG, which take much longer to calculate MRT maps. For instance, to calculate hourly MRT over a full day based on meteorological data, SOLWEIG model requires 1.5 to 2 hours for a 2 km × 1 km study area, and PET simulation takes approximately 10 to 15 minutes. This improvement on efficiency allows for rapid scenario simulations, which means that various design scenarios can be evaluated within a feasible time.

Moreover, the deep learning model allows for the simulation of fine spatial details under high speed, which are critical in simulating MRT and PET of both day and night thermal conditions. This provides a clearer understanding of the comflict thermal effects associated with urban densification, for instance, daytime shading benefits and nighttime heat retention. In addition, the model enables systematic comparisons between different urban morphological conditions, such as variations in density, building height, street canyon geometry, and spatial enclosure.

### 9.4.2 Limitations

First things first, the U-Net model is trained for a specific case, focusing on the city center of Rotterdam under heatwave conditions. The dataset is limited to this area and its immediate surroundings, with meteorological data covering only five days during the heatwave in 2022. As a result, the model currently has limited generalisation capability.

Second, the workflow still relies on current simulation tools (UMEP). Although the deep learning model significantly reduces the time required to compute MRT and PET, key inputs such as SVF and wind field are still generated using UMEP, which still wastes a large amount of time. Additionally, this model cannot predict the thermal performance of the detailed architectural design like elevated buildings, connecting corridor and materials.

Third, the model is trained on simulated data rather than real-world measurements. While it shows high accuracy when compared with UMEP outputs, the extent to which these results reflect actual conditions is still uncertain.

Finally, PET predictions depend on MRT outputs, meaning that errors in MRT estimation may propagate and accumulate in the PET results.

### 9.4.3 Future Research suggestions

Firstly, future research can expand the training dataset to improve model generalisation. The current model is developed based on a limited urban context. Future datasets could include a broader range of urban forms, such as compact areas, open low-rise blocks, high-rise clusters, and dense mixed-use developments.In addition, incorporating cities with different climatic conditions–such as coastal locations like The Hague, as well as inland or warmer cities–would help the model adapt to a wider variety of environmental contexts.

Secondly, future work could move toward more integrated modelling approaches. The current workflow still relies on external tools for certain inputs like SVF and Wind Field. Future models may embed physical equations directly into the deep learning framework, reducing dependence on simulation tools while improving computational efficiency. This would also help ensure that the model adheres to fundamental physical principles.

Finally, future studies could incorporate projected climate data into the modelling process. The current model relies on historical weather data, whereas recent research has used machine learning to predict future climate data. Integrating such data with deep learning models would enable simulation of thermal conditions under future climates, supporting more forward-looking urban planning.

## 9.5 Thermal Environment Research

### 9.5.1 Limitations

This research mainly focuses on urban morphology, including building form and spatial configuration, but there are still many other factors also influence the urban thermal environment including landcover composition, the distribution of blue and green infrastructure, planting strategies, material properties and human activities. Such factors are not incorporated into the simulation framework of this study but significantly contribute to the thermal environment. While the findings of this study identify several strategies for reducing temperature, they do not account for how people might perceive or respond to these interventions. For instance, higher density may help reduce thermal stress, but it may result in a more oppressive environment urban environment. Likewise, increasing shading can lower temperatures, yet it may not be conducive to healthy plant growth.

Additionally, this research is based on SOLWEIG model and URock in UMEP plugin. SOLWEIG model uses relatively simple surface parameter inputs and therefore does not represent the thermal condition of different materials. Consequently, the effects of material properties and detailed surface heat storage on the thermal environment may be simplified in the simulations.

In addition, URock applies a simplified airflow modelling approach rather than detailed CFD simulation. Although it is efficient for large-scale urban wind analysis, it has limitations in capturing detailed turbulence, vertical airflow exchange, and local vortex structures around complex building forms. At the same time, urban wind environments are highly complex under real-world conditions. This study only simulates the prevailing southwesterly summer wind in Rotterdam, meaning that the applicability of the findings under different wind directions still need further research. In addition, the wind analysis mainly focuses on the relationship with thermal conditions, while pedestrian-level wind comfort is not addressed. Although increased wind speed can help reduce thermal stress, it can also generate localized strong wind conditions that decrease pedestrian comfort. Overall, the investigation of urban wind environments in this research remains relatively limited, and more detailed wind-oriented studies are needed in the future.

In the guideline section, suggestions related to vegetation and materials are provided based on general thermal principles and existing literature. However, these strategies are not specifically tested within the Rotterdam context. As a result, their actual cooling performance may differ from the expected outcomes.

### 9.5.2 Future Suggestions

The future research may further focus on the following aspects:

Firstly, future research could adopt an approach by incorporating multiple factors—such as landcover, vegetation, materials, and urban morphology—and examining how interactions shape the thermal environment.

Secondly, the balance between human perspective and high-density city should be taken into account. The research could take more concentrations on the human perspective, in order to explore how to balance thermal comfort, urban density, and people's psychological experience within urban areas.

Thirdly, future work could focus on landscape research, particularly investigating the relationship between shading and urban greenery, and how different shading strategies influence plant growth and ecological quality. Water can also be another important element. A research from Jacobs and colleague has shown that small water bodies are basically ineffective on surrounding thermal environment. Meanwile, under extreme heat wave,

water bodies can become heat sources which address the urban heat problem during the night (Zeng et al., 2026).

### 9.6 Transferability

From the perspective of transferability, this study can be discussed in terms of both the conclusion of thermal environemntal study and the deep learning model.

Firstly, regarding the thermal environmental findings, the study indicates a certain degree of transferability. The fundamental physical processes dominate urban thermal environments–such as solar radiation, shading, and heat retention–are consistent across different locations. Therefore, the general relationships identified here may also be applicable in other parts of the Netherlands or in different countries. However, the specific outcomes are likely to vary depending on local climate conditions, urban morphology, and material properties.

In contrast, the transferability of the deep learning model is very limited. The model is trained using data from the city centre of Rotterdam, within a specific spatial context and under heatwave conditions. As a result, its performance may be reduced when applied to different cities, climates, or typical weather scenarios. To extend its applicability, additional training data and model adaptation would be necessary. However, the general method of using deep learning model to study thermal environment can be transferable in different situations.

# 10. REFLECTION

10.1 Personal Growth and Experience

10.2 Relationship Between Research and Design

10.3 Relation Between Urbanism

10.4 Values and Future Application of the Project

## 10.1 Personal Growth and Experience

As a student in urban planning, I have always been interested in technical methods such as GIS, parametric tools, and data analysis. This interest motivated me to incorporate deep learning into my graduation project.

Initially, I was inspired by studies that used deep learning to predict land surface temperatur (LST), because I noticed that these approaches were limited, as they relied on existing satellite data and could not be used to evaluate new urban design scenarios. I firstly attempted to build a dataset using GIS-based indicators, such as vegetation and water density, in order to test new design scenario. Later, I recognized that LST is not directly linked to human thermal comfort, and that indicators such as mean radiant temperature (MRT) and Physiological equivalent temperature (PET) are more relevant. This led me to revise my original LST based approach.

Compared with the original LST based approach, the new research on MRT and PET proved to be significantly more complex and time-consuming in terms of implementation. The most difficult part lies in modifying the deep learning code and tuning the parameters. Although it may seem like simply changing the training metric from LST to MRT, the entire model structure needed to be adjusted to ensure a high degree of fit. In addition, large amounts of time also went into learning UMEP, data preparation and simulations. Consequently, the model training process became highly iterative rather than linear, and several aspects of the methodology had to be revised multiple times throughout the project. Despite these challenges, the experience provided me with a much deeper understanding of deep learning.

In the research on urban thermal environments, I used to think that high-density urban areas were more prone to trigger heat risks because hard paving and dense buildings tend to trap heat. Certain LST related studies also appear to support this assumption, as dense urban areas often exhibit higher surface temperatures than surrounding rural environments. However, my research on MRT and PET, and testing them with my deep learning model, revealed otherwise. This initially puzzled me, as high-density urban areas can actually provide cooler daytime thermal environments. This conclusion contradicted some findings from LST studies and even made me question whether my model was flawed. To explain this, I read more literature and finally discovered that this is indeed the case. More shadows at the pedestrian level can block shortwave solar radiation, a key factor contributing to high-temperature risks. In some urban forms, deeper street canyons can also enhance wind speed through channel effects, further reducing temperature.

Through my graduation project, I not only explored new disciplinary knowledge but also gained a deeper understanding of the research process. I gradually realized that the conclusions in the literature are not necessarily applicable to all urban environments, and that research on urban issues needs to be based on rigorous experiments, data analysis, and repeated verification.

## 10.2 Relationship Between Research and Design

Despite having studied Urbanism, this project was primarily research-based, as it sought to develop guidance for design via comprehensive environmental research instead of developing an actual design proposal for the urban environment. In the early stages of the project, I focused on a literature review, including research on thermal environment and deep learning. The aim of this work was to better understand the mechanisms of the urban thermal environment and to train deep learning models based on these mechanisms for further exploration.

Chapter 7 involved a systematic exploration of various urban design scenarios. In this context, I regarded design as a method of research and experimentation instead of a solution or result, which is Design For Research approach. Based on different parametric design scenario, I controlled parameters like FSI, building heights, building forms, and street canyon geometry to examine their thermal effects. Ultimately, from this experiment, certain urban design principles that might contribute to urban cooling and heat-sensitive densification were identified.

The disciplines derived from the exploration of different urban design scenarios were converted into several guidelines to create a heat-sensitive densification on chapter 8. At this point, the project shifted to a Research For Design approach, wherein results from environmental simulations and comparative tests are converted into spatial designs for heat sensitive urban growth.

### 10.3 Relation Between Urbanism

In my view, urbanism is not purely a design or social science subject, but a comprehensive discipline that combines knowledge from multiple fields including environment, technology, data, society, and space. This interdisciplinary nature was one of the main reasons that I chose to combine my graduation project with deep learning. At the same time, thermal environmental issues are closely related to various factors such as urban space, social activities, ecosystems, and human health. Although I have almost no experience on deep learning and only little knowledge on thermal environment, urbanism provided a platform that connected these different aspects, allowing me to conduct interdisciplinary exploration and research, because urbanism not only focuses on the space itself but also integrates technological, environmental, and social issues into a single research and design framework.

This understanding also influenced the methodology used for the project, moving towards a more scientific, rigorous, and data-driven approach. Currently, urban planning and design relies heavily on the subjective observations and judgments of designers, which are truely important parts of the design process, however, such subjective judgments can sometime lead to erroneous or unscientific planning schemes. As a result, urbanism also requires rigorous research and data support, in order to make urban planning schemes will become more reliable. Therefore, in my project, I tested and evaluated the thermal performances of design scenarios through a series of controlled experiments, variables such as FSI and building height, in order to ensure the rigor of the conclusions.

From the perspective of the urbanism discipline, the project is also trying to explore the possible uses of artificial intelligence technology in the future process of urban planning and design. The appearance of AI does not mean that traditional urban researchers will be replaced, conversely, urban researchers can use their knowledge to enable AI to provide efficient assistance, which allows the future urbanism to become more iterative, transparent, and evidence-based, particularly when dealing with more complex urban challenges.

### 10.4 Values and Future Implementation

#### 10.4.1 Values

The values of this project are from three aspects. First, the research provides a set of heat-sensitive densification guidelines for the Rotterdam municipality, which are able to support future densification development to create a cooler urban outdoor environment. These guidelines are derived from systematic comparisons between different urban morphologies and their thermal performance, rather than relying solely on intuitive design decisions.

Second, the project proposes a deep learning workflow capable of rapidly simulating MRT and PET under different urban morphological scenarios with relatively high accuracy. Compared with conventional physical simulation methods, the framework has potential to make the simulation process easier and substantially improves computational efficiency, making it feasible to evaluate multiple urban design scenarios within the limited timeframe of planning processes.

Third, the project can also be a research framework for future urbanism. It is neither purely scientific research nor a conventional urban design project, but instead adopts a real urban sites as experimental conditions and explored different design solutions based on these conditions. In this sense, the framework may also serve as a potential pre-design research process for future urban design and planning projects.

#### 10.4.2 Benefits for Municipality

Firstly, the results from this research could give municipalities a better understanding of how

urban densification is related to the thermal environment and prove that high density does not always mean increased vulnerability to heat stress. Secondly, the research methodology could also contribute to a better understanding among planners of how urban morphology, including FSI, building height, tower locations, and street canyon configuration, affects outdoor temperatures for pedestrians. Thirdly, the developed guidelines might assist in developing future heat-resistant densification designs and help cities alleviate the negative effects of heat waves in terms of their societal impact through climate-resilient urban designs. Lastly, an efficient workflow based on deep learning can be proposed for urban designers to evaluate different scenarios using this new approach.

### 10.4.3 Future Implementation

Nevertheless, the results of this study mainly provide guidelines of the morphological development. However, mitigating thermal risks solely by building morphology is still not sufficient. Further research needs to be carried out into the impact of vegetation, water bodies, and materials. More importantly, such mitigation approaches must not be applied based on assumptions, which are overly simplistic and subjective, since vegetation and water bodies can exacerbate thermal risk in certain conditions, especially during the night.

The human factor remains a crucial unpredictable element in the urban thermal environment. Areas which have a high density of human activities might still face thermal risks, due to heat generation and carbon-induced heating of anthropogenic origin that might lead to higher heat storage at night.

Apart from the research on other factors, municipality will need a richer local meteorological database regarding environmental parameters and monitoring data to enhance the credibility of heat-sensitive planning schemes. In addition, future research should also include empirical data from the field, climatic seasonal variability, and enhanced wind environment modeling to confirm the thermal performance of various urban forms.

# 11. REFERENCE

Ahmad, M. W., Mourshed, M., Mundow, D., Sisinni, M., & Rezgui, Y. (2016). Building energy metering and environmental monitoring – A state-of-the-art review and directions for future research. Energy and Buildings, 120, 85–102. https://doi.org/10.1016/j.enbuild.2016.03.059

Alchapar, N., Giancola, E., Pérez, G., Terraza, M., & Pezzuto, C. (2025). Façade Strategies for Climate Resilience: The Impact of Thermal Mass and Albedo on Urban Microclimates Across Different Climatic Zones. Urban Science, 9(10), 428. https://doi.org/10.3390/urbansci9100428

Alizadeh, S. (2025). Revitalizing urban spaces: Rooftop architecture and its potential applications in Turin, Italy [Master's thesis, Politecnico di Torino].

Attia, S. (n.d.). OVERVIEW AND RECOMMENDATION ON URBAN DENSIFICATION POTENTIAL IN LIÈGE, BELGIUM.

Beurden, J. B., Doepel, D., & Tillie, N. (n.d.). Sustainable Densification and Greenification in the Inner City of Rotterdam.

Bezemer, D., van der Krabben, E., Barendregt, E., & van der Vlugt, G. (2022, May 30). Zonder baksteen aan de bak. (M. Janssen Groesbeek, Interviewer) AT5. Amsterdam. Retrieved May 26, 2024, from https://dezwijger.nl/programma/zonder-baksteen-aan-de-bak

Briegel, F., Makansi, O., Brox, T., Matzarakis, A., & Christen, A. (2023). Modelling long-term thermal comfort conditions in urban environments using a deep convolutional encoder-decoder as a computational shortcut. Urban Climate, 47, 101359. https://doi.org/10.1016/j.uclim.2022.101359

Cao, Z., Wu, Z., Liu, L., Chen, Y., & Zou, Y. (2019). Assessing the relationship between anthropogenic heat release warming and building characteristics in Guangzhou: A sustainable development perspective. Science of The Total Environment, 695, 133759. https://doi.org/10.1016/j.scitotenv.2019.133759

Chen, Q., Cheng, Q., Chen, Y., Li, K., Wang, D., & Cao, S. (2021). The Influence of Sky View Factor on Daytime and Nighttime Urban Land Surface Temperature in Different Spatial-Temporal Scales: A Case Study of Beijing. Remote Sensing, 13(20), 4117. https://doi.org/10.3390/rs13204117

Copernicus Climate Change Service. (2026, January 14). Copernicus: 2025 was the third hottest year on record. https://climate.copernicus.eu/copernicus-2025-was-third-hottest-year-record

Dirksen, M., Ronda, R. J., Theeuwes, N. E., & Pagani, G. A. (2019). Sky view factor calculations and its application in urban heat island studies. Urban Climate, 30, 100498. https://doi.org/10.1016/j.uclim.2019.100498

Erell, E., Pearlmutter, D., Boneh, D., & Kutiel, P. B. (2014). Effect of high-albedo materials on pedestrian heat stress in urban street canyons. Urban Climate, 10, 367–386. https://doi.org/10.1016/j.uclim.2013.10.005

Grimmond, C. S. B., & Oke, T. R. (1999). Evapotranspiration rates in urban areas.

Hashemi, F., Najafian, P., Salahi, N., Ghiasi, S., & Passe, U. (2025). The Impact of the Urban Heat Island and Future Climate on Urban Building Energy Use in a Midwestern U.S. Neighborhood. Energies, 18(6), 1474. https://doi.org/10.3390/en18061474

He, R., Wang, J., & Liu, D. (2025). Assessing the Impact of Urban Spatial Form on Land Surface Temperature Using Random Forest–Taking Beijing as a Case Study. Land, 14(8), 1639. https://doi.org/10.3390/land14081639

Hoang, N.-D. (2025). Machine Learning Approaches for Geospatial Modeling of Urban Land Surface Temperature: Assessing Geographical Compactness, Interpretability, and Causal Inference. Sensors, 25(17), 5380. https://doi.org/10.3390/s25175380

Hoang, N.-D., Tran, V.-D., & Huynh, T.-C. (2025). From Data to Insights: Modeling Urban Land Surface Temperature Using Geospatial Analysis and Interpretable Machine Learning. Sensors, 25(4), 1169. https://doi.org/10.3390/s25041169

Höppe, P. (1999). The physiological equivalent temperature–A universal index for the biometeorological assessment of the thermal environment. International Journal of Biometeorology, 43(2), 71–75. https://doi.org/10.1007/s004840050118

Hulley, G. C., Ghent, D., Göttsche, F. M., Guillevic, P. C., Mildrexler, D. J., & Coll, C. (2019). Land Surface Temperature. In Taking the Temperature of the Earth (pp. 57–127). Elsevier. https://doi.org/10.1016/B978-0-12-814458-9.00003-4

Iodice, S., Arbau, L. C., Maistrali, A., Marando, F., Melchiorri, M., Proietti, P., Sulis, P., Tainguy, O., & Vandecasteele, I. (2024). EU cities and heat extremes (JRC137891). European Commission, Joint Research Centre.

Jacobs, C., Klok, L., Bruse, M., Cortesão, J., Lenzholzer, S., & Kluck, J. (2020). Are urban water bodies really cooling? Urban Climate, 32, 100607. https://doi.org/10.1016/j.uclim.2020.100607

Jiang, Y., & Menz, S. (2025). Urban Densification and Outdoor Thermal Comfort: Scenario-Based Analysis in Zurich's Altstetten–Albisrieden District. Land, 14(8), 1516. https://doi.org/10.3390/land14081516

Joshi, K., Khan, A., Anand, P., & Sen, J. (2024). Understanding the synergy between heat waves and the built environment: A three-decade systematic review informing policies for mitigating urban heat island in cities. Sustainable Earth Reviews, 7(1), 25. https://doi.org/10.1186/s42055-024-00094-7

Kim, J., Lee, D.-K., Brown, R. D., Kim, S., Kim, J.-H., & Sung, S. (2022). The effect of extremely low sky view factor on land surface temperatures in urban residential areas. Sustainable Cities and Society, 80, 103799. https://doi.org/10.1016/j.scs.2022.103799

King, M. D. (1999). EOS Science Plan: The State of Science in the EOS Program. NASA, Washington, DC 397 pp.

Kuo, C.-Y., Wang, R.-J., Lin, Y.-P., & Lai, C.-M. (2020). Urban Design with the Wind: Pedestrian-Level Wind Field in the Street Canyons Downstream of Parallel High-Rise Buildings. Energies, 13(11), 2827. https://doi.org/10.3390/en13112827

Kustura, K., Conti, D., Sammer, M., & Riffler, M. (2025). Harnessing Multi-Source Data and Deep Learning for High-Resolution Land Surface Temperature Gap-Filling Supporting Climate Change Adaptation Activities. Remote Sensing, 17(2), 318. https://doi.org/10.3390/rs17020318

Lai, A., Maing, M., & Ng, E. (2017). Observational studies of mean radiant temperature across different outdoor spaces under shaded conditions in densely built environment. Building and Environment, 114, 397–409. https://doi.org/10.1016/j.buildenv.2016.12.034

Lindberg, F., Grimmond, C. S. B., Gabey, A., Huang, B., Kent, C. W., Sun, T., Theeuwes, N. E., Järvi, L., Ward, H. C., Capel-Timms, I., Chang, Y., Jonsson, P., Krave, N., Liu, D., Meyer, D., Olofson, K. F. G., Tan, J., Wästberg, D., Xue, L., & Zhang, Z. (2018). Urban Multi-scale Environmental Predictor (UMEP): An integrated tool for city-based climate services. Environmental Modelling & Software, 99, 70–87. https://doi.org/10.1016/j.envsoft.2017.09.020

Lopez-Cabeza, V. P., Alzate-Gaviria, S., Diz-Mellado, E., Rivera-Gomez, C., & Galan-Marin, C. (2022). Albedo influence on the microclimate and thermal comfort of courtyards under Mediterranean hot summer climate conditions. Sustainable Cities and Society, 81, 103872. https://doi.org/10.1016/j.scs.2022.103872

Mansourmoghaddam, M., Rousta, I., Ghafarian Malamiri, H., Sadeghnejad, M., Krzyszczak, J., & Ferreira, C. S. S. (2024). Modeling and Estimating the Land Surface Temperature (LST) Using Remote Sensing and Machine Learning (Case Study: Yazd, Iran). Remote Sensing, 16(3), 454. https://doi.org/10.3390/rs16030454

Mats, A., Mitryasova, O., Salamon, I., & Kochanek, A. (2025). Atmospheric air temperature as an integrated indicator of climate change. Ecological Engineering & Environmental Technology, 26(3), 352–360. https://doi.org/10.12912/27197050/200307

Morini, E., Touchaei, A., Castellani, B., Rossi, F., & Cotana, F. (2016). The Impact of Albedo Increase to Mitigate the Urban Heat Island in Terni (Italy) Using the WRF Model. Sustainability, 8(10), 999. https://doi.org/10.3390/su8100999

Müller, N., Kuttler, W., & Barlag, A.-B. (2014). Counteracting urban climate change: Adaptation measures and their effect on thermal comfort. Theoretical and Applied Climatology, 115(1–2), 243–257. https://doi.org/10.1007/s00704-013-0890-4

Muniz-Gäal, L. P., Pezzuto, C. C., Carvalho, M. F. H. D., & Mota, L. T. M. (2020). Urban geometry and the microclimate of street canyons in tropical climate. Building and Environment, 169, 106547. https://doi.org/10.1016/j.buildenv.2019.106547

Nederlandse Arbeidsinspectie. (2024). Heat stress study (Verkenning hittestress). Nederlandse Arbeidsinspectie.
Nekkers, M. (2025). Mapping stakeholder dynamics in brownfield redevelopment: A case study of Arnhem-Nijmegen region, Netherlands [Master's thesis, Radboud University].

Oke, T. R. (1987). Boundary layer climates (Second edition). Methuen & Co. https://doi.org/10.4324/9780203407219

Pattnaik, N., Rahman, M. A., & Pauleit, S. (2025). From Ground to Crown: Analyzing shade provision and thermal comfort benefits of multilayered vegetation structures, 12th International Conference on Urban Climate, Rotterdam, The Netherlands, 7–11 Jul 2025, ICUC12-598, https://doi.org/10.5194/icuc12-598, 2025.

Peluso, P., Persichetti, G., & Moretti, L. (2022). Effectiveness of Road Cool Pavements, Greenery, and Canopies to Reduce the Urban Heat Island Effects. Sustainability, 14(23), 16027. https://doi.org/10.3390/su142316027

Possega, M., Aragão, L., Ruggieri, P., Santo, M. A., & Di Sabatino, S. (2022). Observational evidence of intensified nocturnal urban heat island during heatwaves in European cities. Environmental Research Letters, 17(12), 124013. https://doi.org/10.1088/1748-9326/aca3ba

Ramachandra, T. V., Rana, R. S., Vinay, S., & Aithal, B. H. (n.d.). Urban heat island linkages with the landscape morphology.

Rashtian, Z., Tabatabaei Manesh, M., Tahsildoost, M., & Zomorodian, Z. S. (2025). Data-driven real-time visualization of urban heat islands using mean radiant temperature for urban design. Energy and Buildings, 333, 115470. https://doi.org/10.1016/j.enbuild.2025.115470

Rijksinstituut voor Volksgezondheid en Milieu. (2025). Jaarplan RIVM 2025: De zorg voor morgen begint vandaag. Rijksinstituut voor Volksgezondheid en Milieu (RIVM).

Ronneberger, O., Fischer, P., & Brox, T. (2015). U-Net: Convolutional Networks for Biomedical Image Segmentation. In N. Navab, J. Hornegger, W. M. Wells, & A. F. Frangi (Eds), Medical Image Computing and Computer-Assisted Intervention – MICCAI 2015 (Vol. 9351, pp. 234–241). Springer International Publishing. https://doi.org/10.1007/978-3-319-24574-4_28

Roshan, G., Moghbel, M., & Attia, S. (2020). Evaluating the wind cooling potential on outdoor thermal comfort in selected Iranian climate types. Journal of Thermal Biology, 92, 102660. https://doi.org/10.1016/j.jtherbio.2020.102660

Santamouris, M., & Osmond, P. (2020). Increasing Green Infrastructure in Cities: Impact on Ambient Temperature, Air Quality and Heat-Related Mortality and Morbidity. Buildings, 10(12), 233. https://doi.org/10.3390/buildings10120233

Sirenko, M., Comes, T., & Verbraeck, A. (2026). Urban heatwaves reverse vulnerability-resilience relationships throughout the day. Npj Urban Sustainability, 6(1), 22. https://doi.org/10.1038/s42949-025-00327-4
Sobstyl, J. M., Emig, T., Qomi, M. J. A., Ulm, F.-J., & Pellenq, R. J.-M. (2018). Role of City Texture in Urban Heat Islands at Nighttime. Physical Review Letters, 120(10), 108701. https://doi.org/10.1103/PhysRevLett.120.108701

Tax, S., Vlaun, N., Fahner, T., Terry, E., Pelkmans, D., Bink, J., & Maas, R. (2024). Wind as an opportunity: Mapping urban air systems in Rotterdam – A pilot study. Municipality of Rotterdam & Actiflow.

Thorsson, S., Lindberg, F., Eliasson, I., & Holmer, B. (2007). Different methods for estimating the mean radiant temperature in an outdoor urban setting. International Journal of Climatology, 27(14), 1983–1993. https://doi.org/10.1002/joc.1537

Thorsson, S., Rocklöv, J., Konarska, J., Lindberg, F., Holmer, B., Dousset, B., & Rayner, D. (2014). Mean radiant temperature – A predictor of heat related mortality. Urban Climate, 10, 332–345. https://doi.org/10.1016/j.uclim.2014.01.004

Wallenberg, N., Lindberg, F., Holmer, B., & Thorsson, S. (2020). The influence of anisotropic diffuse shortwave radiation on mean radiant temperature in outdoor urban environments. Urban Climate, 31, 100589. https://doi.org/10.1016/j.uclim.2020.100589

Wang, L., Tian, W.-X., Zhao, X.-Y., & Huang, C.-Q. (2022). Numerical simulation of the effects of canopy properties on airflow and pollutant dispersion in street canyons. Indoor and Built Environment, 31(2), 466–478. https://doi.org/10.1177/1420326X211005174

Watson, I. D., & Johnson, G. T. (1987). Graphical estimation of sky view-factors in urban environments. Journal of Climatology, 7(2), 193–197. https://doi.org/10.1002/joc.3370070210

Wu, Z., & Zhang, Y. (2019). Water Bodies' Cooling Effects on Urban Land Daytime Surface Temperature: Ecosystem Service Reducing Heat Island Effect. Sustainability, 11(3), 787. https://doi.org/10.3390/su11030787

Yang, X., & Li, Y. (2015). The impact of building density and building height heterogeneity on average urban albedo and street surface temperature. Building and Environment, 90, 146–156. https://doi.org/10.1016/j.buildenv.2015.03.037

Zeng, X., Luo, Q., Liu, M., Chu, Y., Rong, J., & Zhou, J. (2026). Revealing the nighttime warm effects of urban water bodies: Evidence from Wuhan, China. Environmental Impact Assessment Review, 118, 108303. https://doi.org/10.1016/j.eiar.2025.108303

Zhan, W., Bechtel, B., Du, H., Chakraborty, T., Kotthaus, S., Scott, E., Martilli, A., Naserikia, M., Nazarian, N., Roth, M., Stewart, I. D., & Voogt, J. (n.d.). Satellite-derived Land Surface Temperatures Strongly Mischaracterise Urban Heat Hazard.

Zhu, X. X., Tuia, D., Mou, L., Xia, G.-S., Zhang, L., Xu, F., & Fraundorfer, F. (2017). Deep Learning in Remote Sensing: A Comprehensive Review and List of Resources. IEEE Geoscience and Remote Sensing Magazine, 5(4), 8–36. https://doi.org/10.1109/MGRS.2017.2762307

# 12. APPENDIX

# FSI 5.8 Horizontal Development Dataset

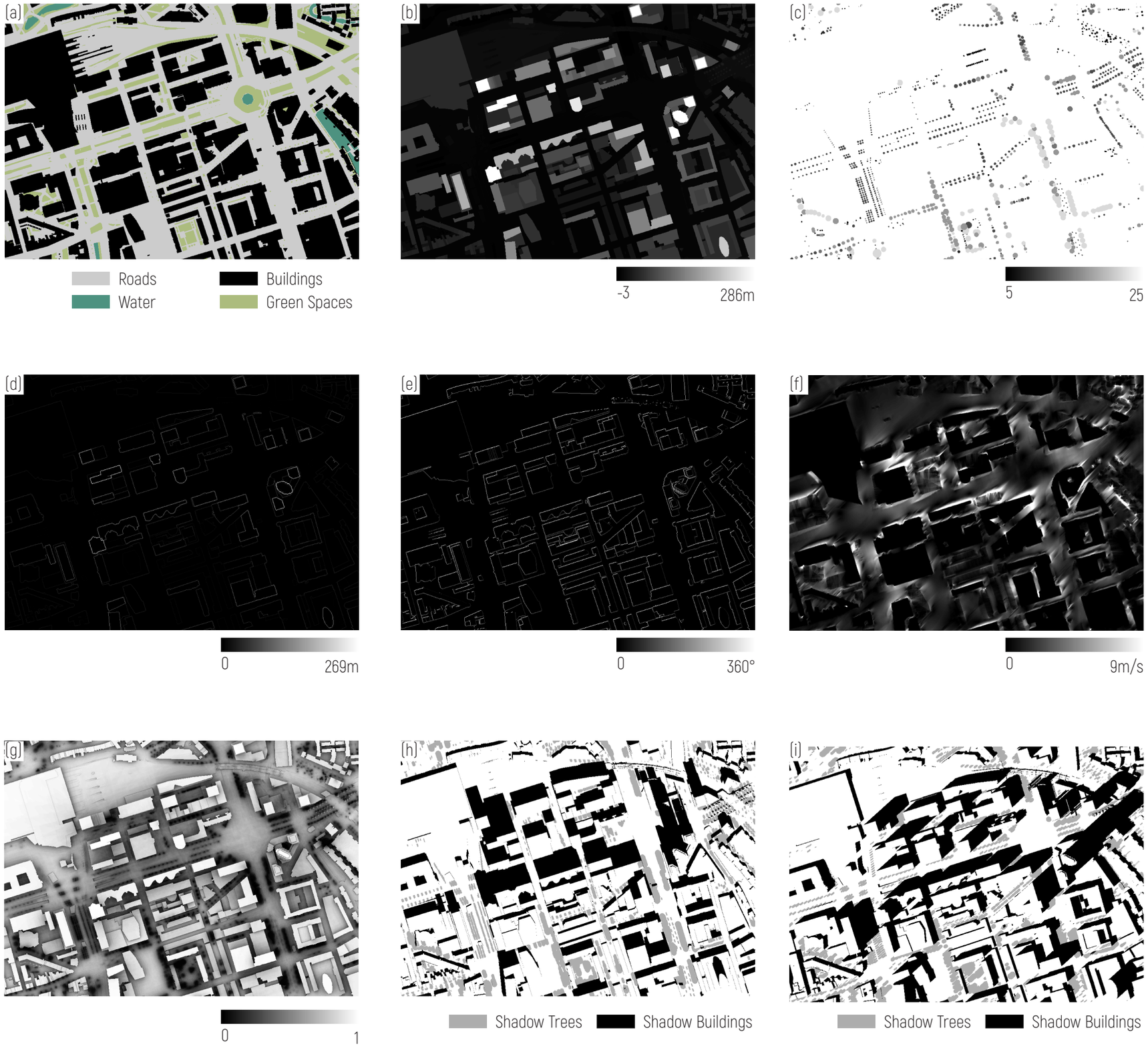



**Figure 12.1:** FSI 5.8 Horizontal Development Dataset
(a) Landcover. (b) DBSM. (C) DSM Vegetation. (D) Wall Height.
(e) Wall Aspect. (f) Wind Speed. (g) SVF. (h) Shadow h13.00.
(i) Shadow h16.00

# FSI 5.8 Vertical Development Dataset

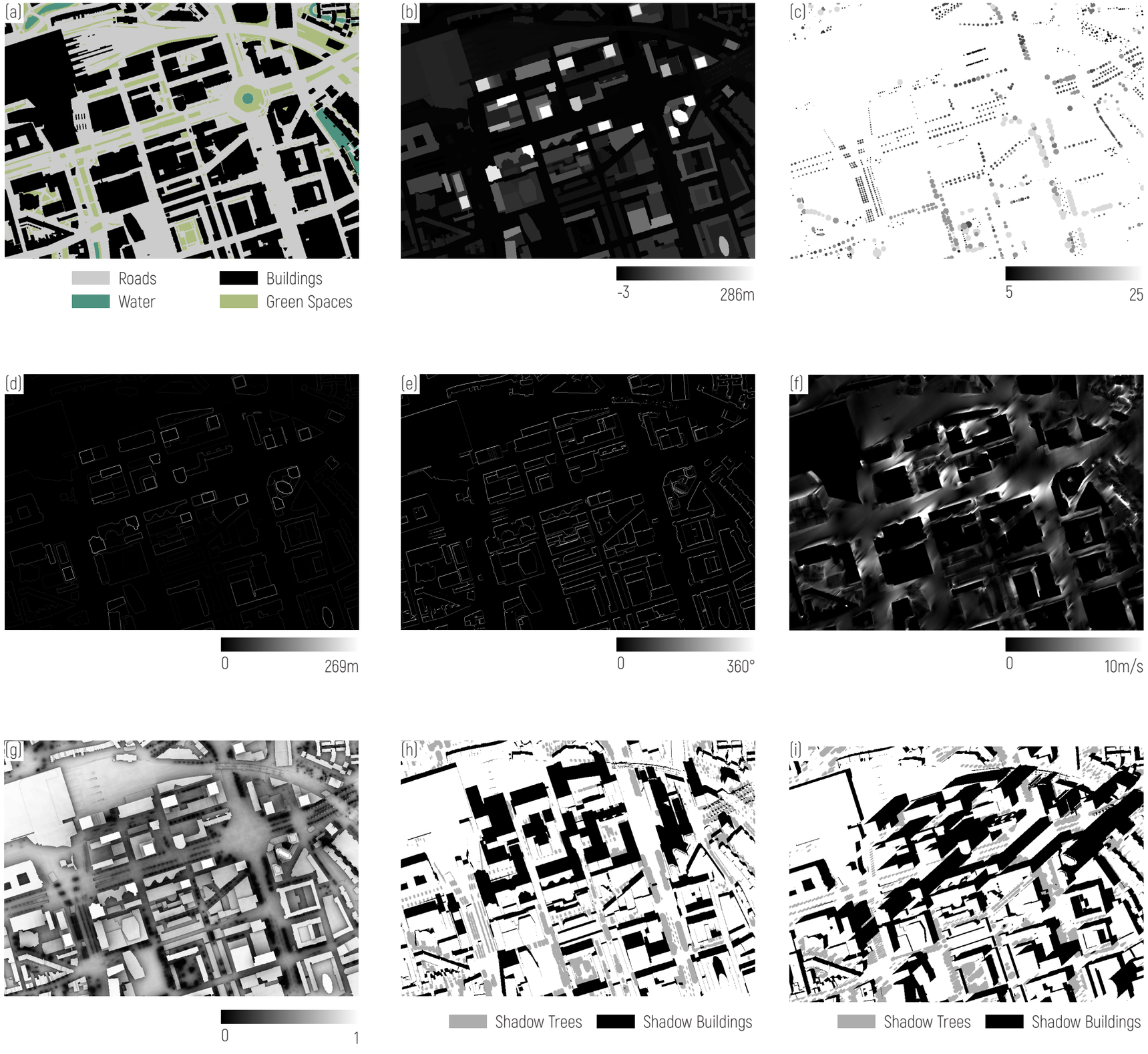



**Figure 12.2:** FSI 5.8 Vertical Development Dataset
(a) Landcover. (b) DBSM. (C) DSM Vegetation. (D) Wall Height. (e) Wall Aspect. (f) Wind Speed. (g) SVF. (h) Shadow h13.00. (i) Shadow h16.00

## FSI 5.8 Combination Dataset

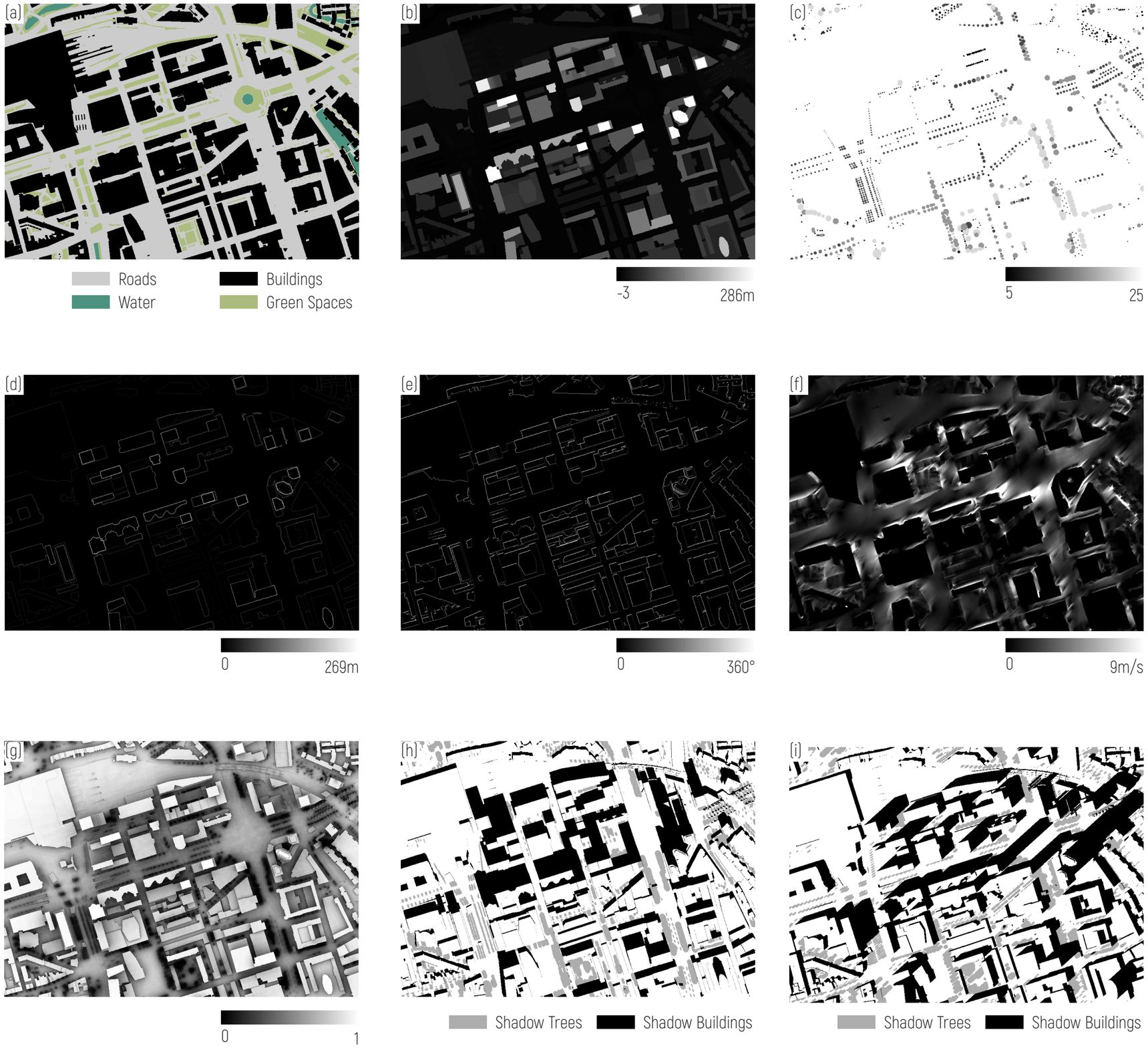



**Figure 12.3:** FSI 5.8 Combination Dataset
(a) Landcover. (b) DBSM. (C) DSM Vegetation. (D) Wall Height. (e) Wall Aspect. (f) Wind Speed. (g) SVF. (h) Shadow h13.00. (i) Shadow h16.00

## FSI 6.5 Horizontal Development Dataset

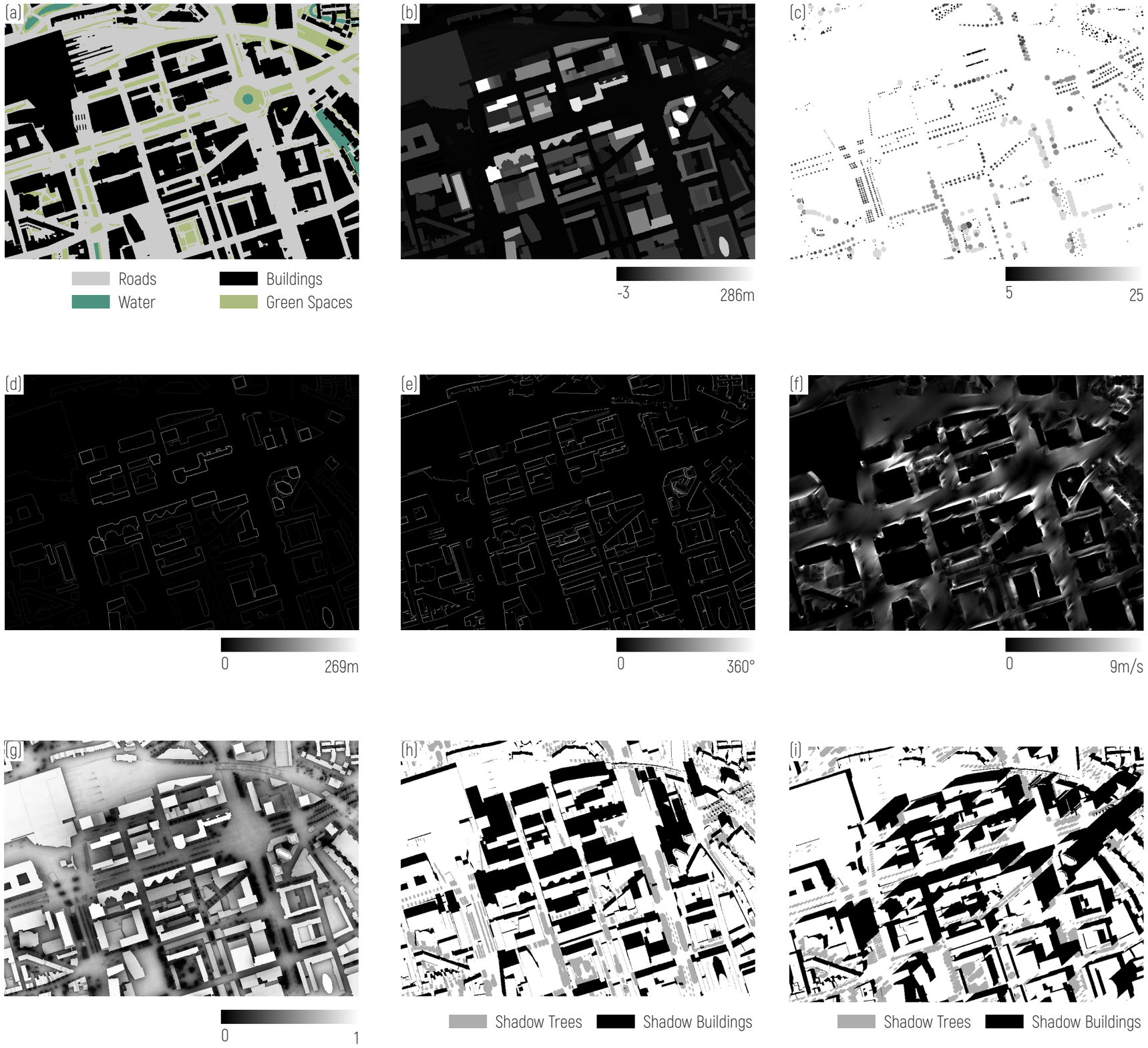



**Figure 12.4:** FSI 6.5 Horizontal Development Dataset
(a) Landcover. (b) DBSM. (C) DSM Vegetation. (D) Wall Height.
(e) Wall Aspect. (f) Wind Speed. (g) SVF. (h) Shadow h13.00.
(i) Shadow h16.00

## FSI 6.5 Vertical Development Dataset

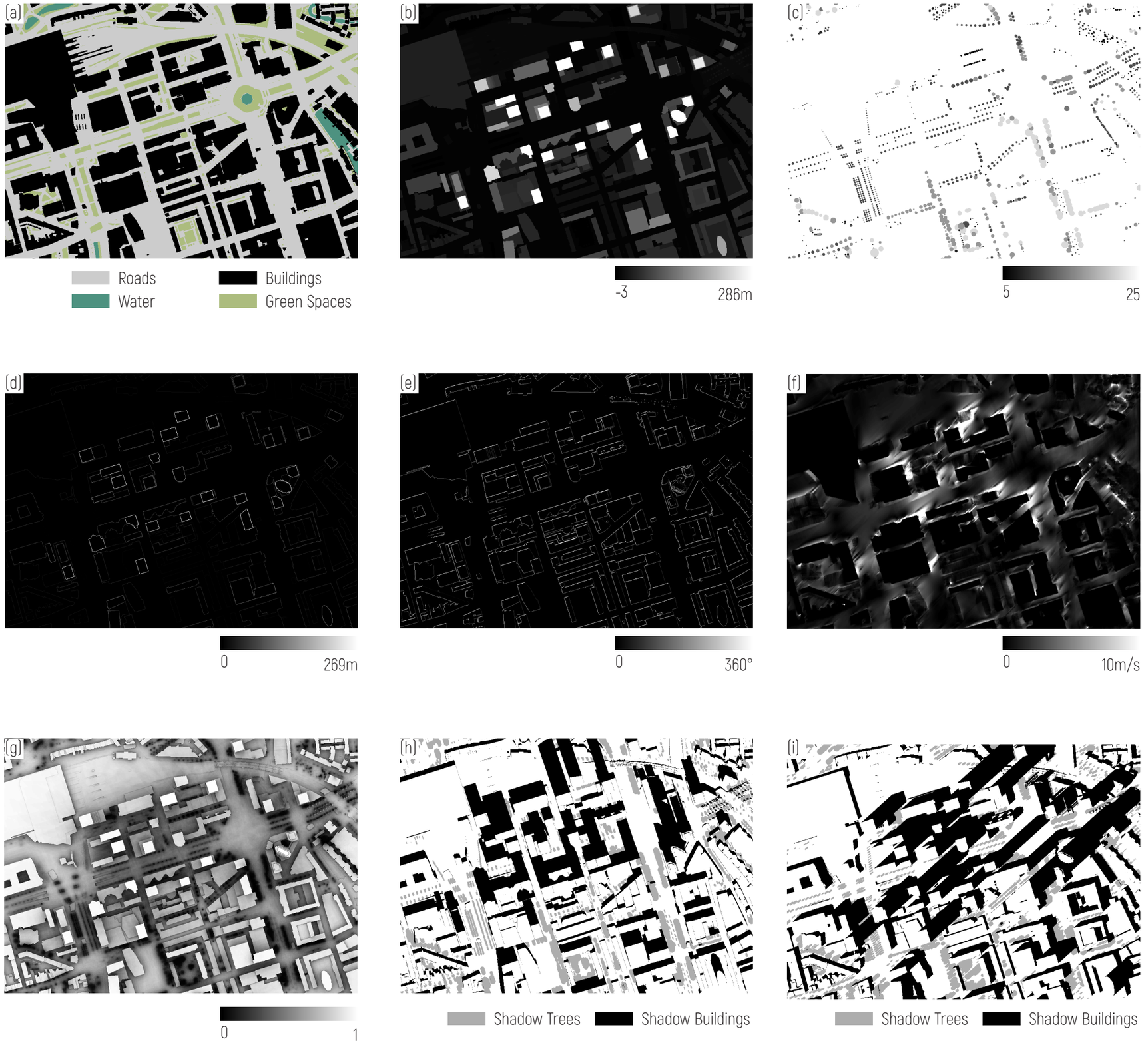



**Figure 12.5:** FSI 6.5 Vertical Development Dataset
(a) Landcover. (b) DBSM. (C) DSM Vegetation. (D) Wall Height.
(e) Wall Aspect. (f) Wind Speed. (g) SVF. (h) Shadow h13.00.
(i) Shadow h16.00

## FSI 6.5 Combination Dataset

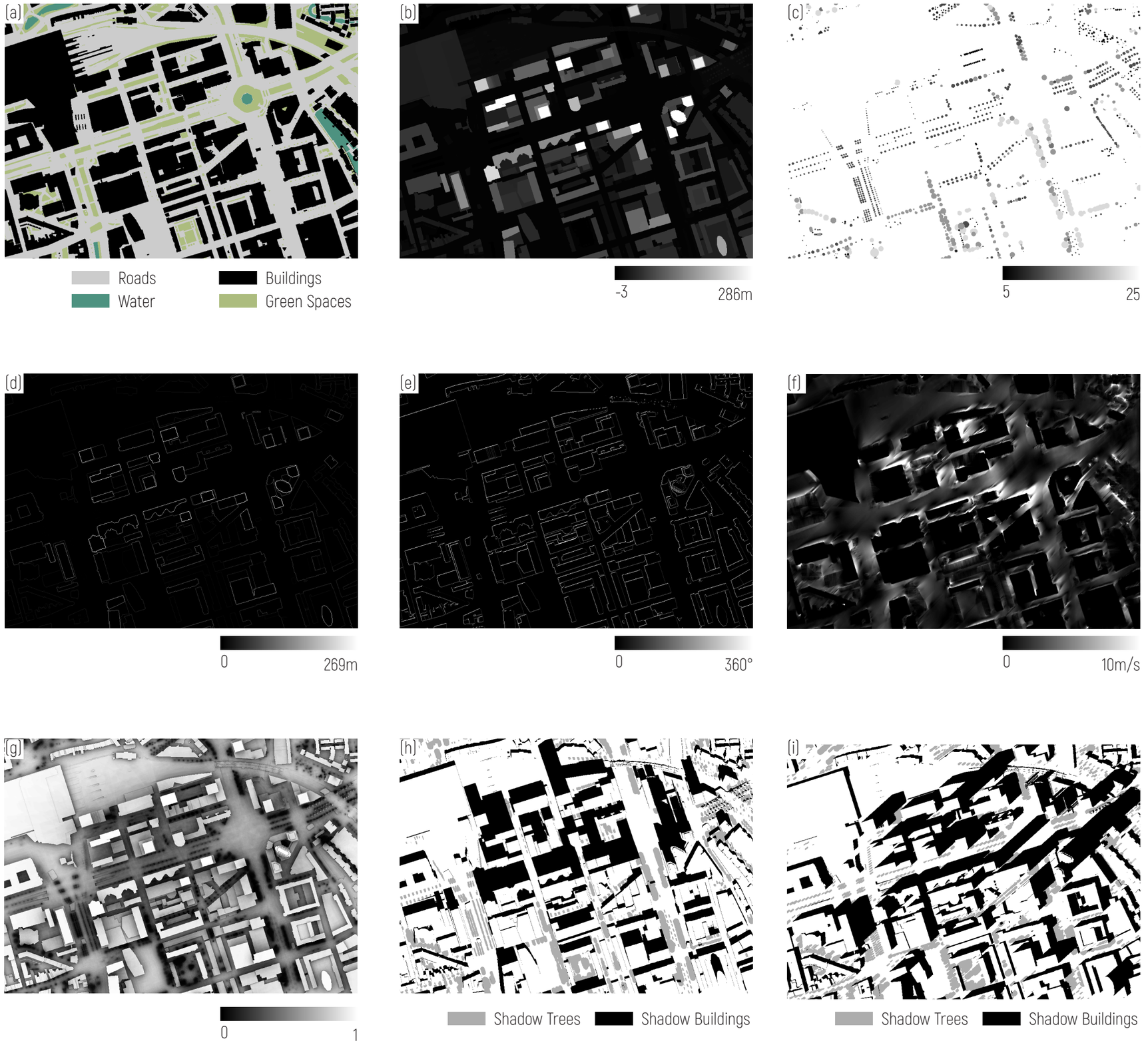



**Figure 12.6:** FSI 6.5 Combination Dataset
(a) Landcover. (b) DBSM. (C) DSM Vegetation. (D) Wall Height. (e) Wall Aspect. (f) Wind Speed. (g) SVF. (h) Shadow h13.00. (i) Shadow h16.00

## FSI 7.0 Horizontal Development Dataset

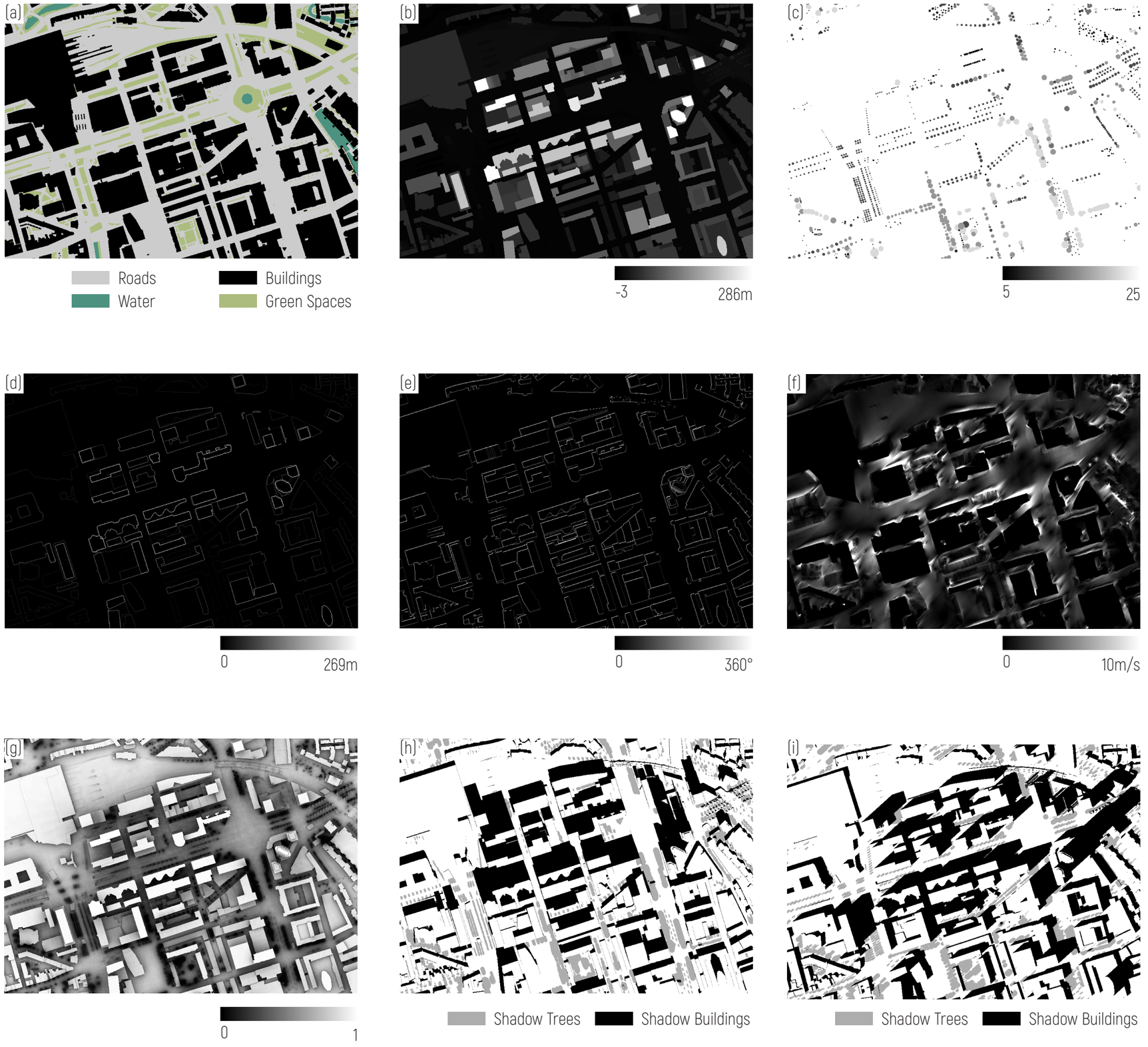



**Figure 12.7:** FSI 7.0 Horizontal Development Dataset
(a) Landcover. (b) DBSM. (C) DSM Vegetation. (D) Wall Height. (e) Wall Aspect. (f) Wind Speed. (g) SVF. (h) Shadow h13.00. (i) Shadow h16.00

# FSI 7.0 Vertical Development Dataset

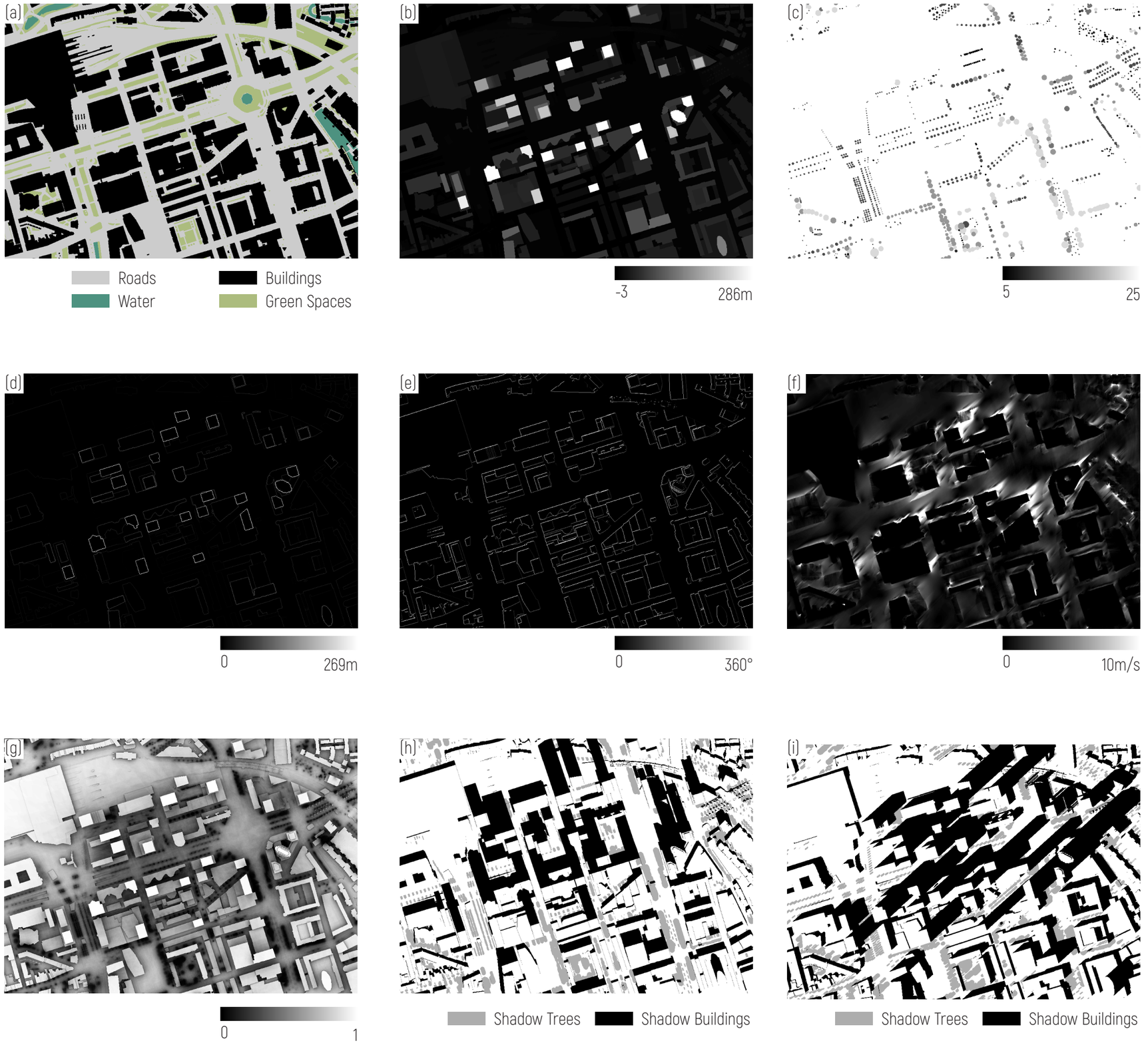



**Figure 12.8:** FSI 7.0 Vertical Development Dataset
(a) Landcover. (b) DBSM. (C) DSM Vegetation. (D) Wall Height. (e) Wall Aspect. (f) Wind Speed. (g) SVF. (h) Shadow h13.00. (i) Shadow h16.00

## FSI 7.0 Combination Dataset

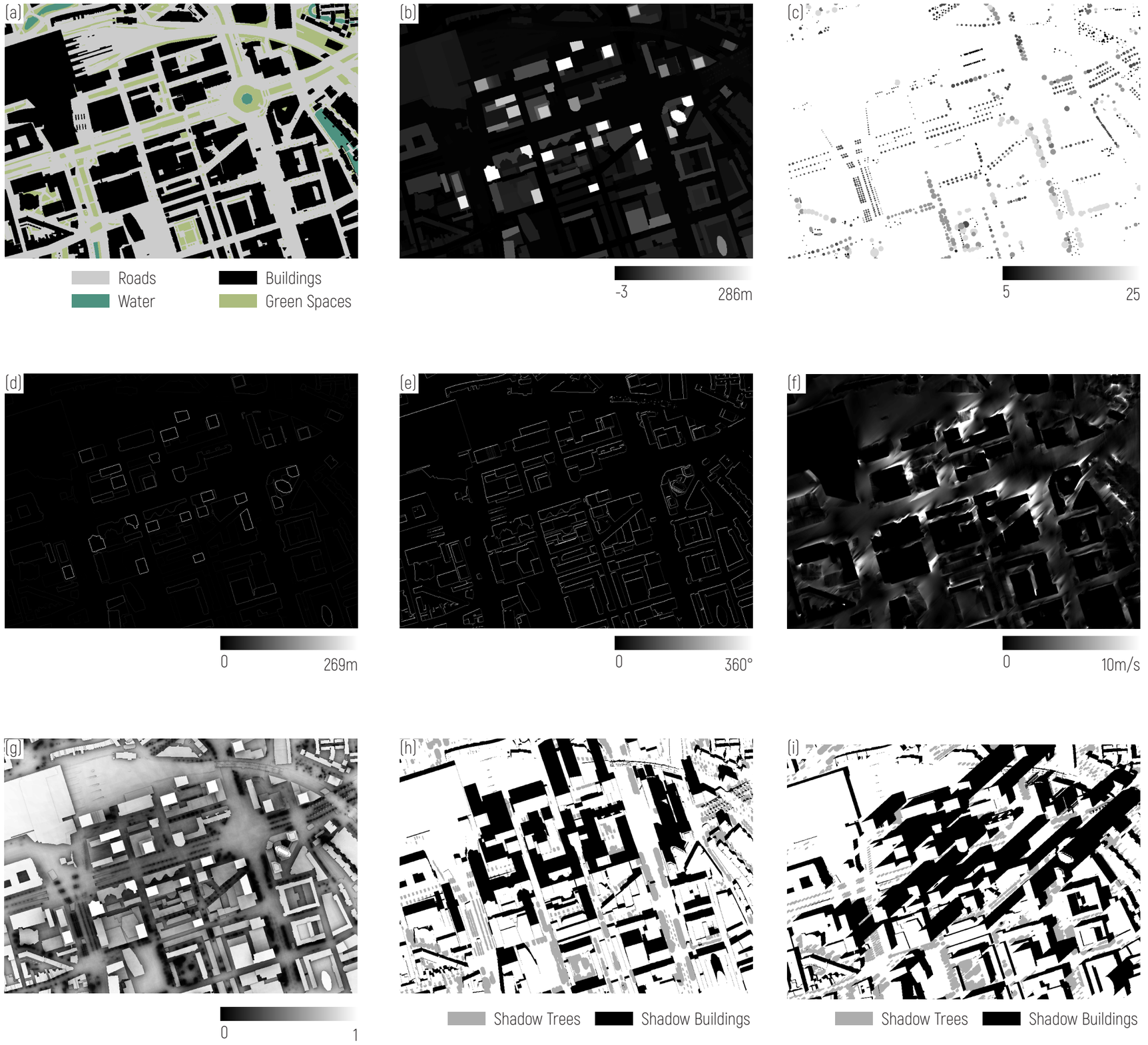



**Figure 12.9:** FSI 7.0 Combination Dataset
(a) Landcover. (b) DBSM. (C) DSM Vegetation. (D) Wall Height. (e) Wall Aspect. (f) Wind Speed. (g) SVF. (h) Shadow h13.00. (i) Shadow h16.00